

INFORMATION TO USERS

This manuscript has been reproduced from the microfilm master. UMI films the text directly from the original or copy submitted. Thus, some thesis and dissertation copies are in typewriter face, while others may be from any type of computer printer.

The quality of this reproduction is dependent upon the quality of the copy submitted. Broken or indistinct print, colored or poor quality illustrations and photographs, print bleedthrough, substandard margins, and improper alignment can adversely affect reproduction.

In the unlikely event that the author did not send UMI a complete manuscript and there are missing pages, these will be noted. Also, if unauthorized copyright material had to be removed, a note will indicate the deletion.

Oversize materials (e.g., maps, drawings, charts) are reproduced by sectioning the original, beginning at the upper left-hand corner and continuing from left to right in equal sections with small overlaps. Each original is also photographed in one exposure and is included in reduced form at the back of the book.

Photographs included in the original manuscript have been reproduced xerographically in this copy. Higher quality 6" x 9" black and white photographic prints are available for any photographs or illustrations appearing in this copy for an additional charge. Contact UMI directly to order.

UMI

A Bell & Howell Information Company
300 North Zeeb Road, Ann Arbor MI 48106-1346 USA
313/761-4700 800/521-0600

Evaluation and Improvement of Frost Durability of Clay Bricks

Surej R. Koroath

A Thesis

in

The Centre

for

Building Studies

Presented in Partial Fulfilment of the Requirements
for the Degree of Doctor of Philosophy at
Concordia University
Montreal, Quebec, Canada

April 1997

© Surej Koroath, 1997



National Library
of Canada

Acquisitions and
Bibliographic Services

395 Wellington Street
Ottawa ON K1A 0N4
Canada

Bibliothèque nationale
du Canada

Acquisitions et
services bibliographiques

395, rue Wellington
Ottawa ON K1A 0N4
Canada

Your file *Votre référence*

Our file *Notre référence*

The author has granted a non-exclusive licence allowing the National Library of Canada to reproduce, loan, distribute or sell copies of this thesis in microform, paper or electronic formats.

The author retains ownership of the copyright in this thesis. Neither the thesis nor substantial extracts from it may be printed or otherwise reproduced without the author's permission.

L'auteur a accordé une licence non exclusive permettant à la Bibliothèque nationale du Canada de reproduire, prêter, distribuer ou vendre des copies de cette thèse sous la forme de microfiche/film, de reproduction sur papier ou sur format électronique.

L'auteur conserve la propriété du droit d'auteur qui protège cette thèse. Ni la thèse ni des extraits substantiels de celle-ci ne doivent être imprimés ou autrement reproduits sans son autorisation.

0-612-25926-9

Canada

ABSTRACT

Evaluation and Improvement of Frost Durability of Clay Bricks

Surej R. Koroath, Ph.D.
Concordia University, 1997

In cold regions like Canada, frost action was reported to be the major cause of disintegration of brick veneer. Two approaches to ensure frost durability of clay bricks were studied in this research. One involved the evaluation of durability, while the other studied the improvement of durability through impregnation. In order to carry out these studies, three major objectives were set out for this research. They were:

- to develop an index to evaluate frost durability,
- to investigate the feasibility of using nondestructive methods to evaluate durability, and
- to study the effect of impregnation with different materials on improving durability.

It was intended in this research to develop a general durability index for clay bricks, irrespective of the manufacturing process adopted. The performance of the brick was studied using laboratory freeze-thaw test. As the time and facility requirements necessary for the unidirectional freezing test were beyond the constraints which existed in this research, an accelerated omnidirectional freeze-thaw test was used. This fact must be considered while interpreting the results from the freeze-thaw test.

The study carried out to compare the performance of existing durability indices showed that they had limitations in reliably assessing durability. Therefore new durability indices were developed based on water absorption properties of bricks. These indices were found to overcome the limitations of existing indices.

The feasibility study on nondestructive evaluation of durability was carried out using ultrasonic pulse velocity. New durability provisions were derived based on pulse velocity, using ASTM C216 specifications. At this stage it can be used only along with the ASTM method but it can avoid the time consuming ASTM procedure in many cases.

Studies on impregnated bricks showed that there was a general shifting of pore sizes towards lower diameter region. Paraffin impregnated brick showed excellent freeze-thaw performance. The bond between brick and mortar was found to have been adversely affected due to impregnation. But more studies using brick wall component are recommended before final conclusions are drawn on brick-mortar bond strength. Paraffin was found to be the most cost effective among the impregnating materials studied.

Acknowledgements

The author wishes to express his sincere gratitude to *Dr. Paul Fazio* for his supervision, encouragement, and the financial support during the course of this research. His effort and time in reviewing this thesis are gratefully acknowledged. The author is also grateful to *Dr. Dorel Feldman* for his supervision, encouragement, help at various stages of the research, and for reviewing this thesis and giving suggestions to improve it.

Thanks are due to *Dr. Richard Guy* for his suggestions on ultrasonic pulse measurements and *Dr. Srinivasa Reddy Mallidi* for his help at various occasions during the course of this research, especially in the initial stages of porosimetry test. Special appreciation is due to *Mrs. Dorina Banu* for her help in the laboratory.

The author is also thankful to the technical staff of the Centre for Building Studies, namely, *Mr. J. Payer*, *Mr. J. Hrib*, *Mr. H. Obermeir*, and *Mr. J. Zilka* for their help in the fabrication of experimental set-up and the running of experiments. The friendship and help provided by the rest of the *Staff* and fellow *Graduate Students* at the Centre for Building Studies are also acknowledged.

Last but not least, the author expresses his sincere gratitude to his wife, *Usha*, for her help, love, understanding, and patience and to his *Parents* for their encouragement and support.

Table of Contents

LIST OF FIGURES	x
LIST OF TABLES	xvi
NOMENCLATURE	xix
Chapter 1 INTRODUCTION	1
1.1 Frost Durability	2
1.2 Need for the Research	4
1.2.1 Evaluation of Durability	4
1.2.2 Improvement of Durability	7
1.3 Objectives of the Research	8
1.4 Scope of the Research	8
1.5 Organization of the Thesis	11
Chapter 2 REVIEW OF PREVIOUS STUDIES	12
2.1 Frost Durability of Bricks	12
2.1.1 Factors Affecting Durability	13
2.1.2 Evaluation of Durability	14
2.1.2.1 Freeze-Thaw Testing	15
2.1.2.2 Evaluation using Standards	18
2.1.2.3 Durability Indices	19
2.2 Nondestructive Evaluation of Masonry	27
2.2.1 Nondestructive Testing Methods	27

	2.2.2	Ultrasonic Pulse Velocity Method	29
	2.2.3	Evaluation of Masonry using UPV Method	29
2.3		Impregnation of Porous Building Materials	30
	2.3.1	Impregnation with Polymers	31
	2.3.1.1	Monomers for Impregnation	31
	2.3.1.2	Monomer Loading	33
	2.3.1.3	Polymerization Process	33
	2.3.1.4	Properties of Polymer Impregnated Building Materials	35
	2.3.2	Impregnation with Sulphur	37
	2.3.3	Impregnation with Paraffin	39
	2.3.4	Sealers and other Hydrophobic Materials for Treatment	40
2.4		Summary of the Review	41
Chapter 3		RESEARCH METHODOLOGY	43
	3.1	Research Overview	43
	3.1.1	Development of Durability Index	43
	3.1.2	Nondestructive Evaluation of Durability	44
	3.1.3	Effect of Impregnation on Durability	47
	3.2	Selection of Materials	47
	3.2.1	Bricks	49
	3.2.2	Impregnating Materials	49
	3.3	Preparation of Specimens	52
	3.4	Impregnation Procedure	55
	3.4.1	Impregnation with Polymer	55
	3.4.1.1	Soaking of Specimen	55
	3.4.1.2	Polymerization	56
	3.4.2	Impregnation with Paraffin	56
	3.4.3	Impregnation with Acrylic Sealer	58
	3.5	Test Procedures	58
	3.5.1	Water Absorption Tests	58
	3.5.1.1	Capillary Absorption Test	58
	3.5.1.2	Submersion Test	59
	3.5.1.3	Boiling Absorption Test	59
	3.5.1.4	Vacuum Saturation Test	60
	3.5.2	Mercury Intrusion Porosimetry	62
	3.5.3	Ultrasonic Pulse Velocity Test	65
	3.5.4	Freezing and Thawing Test	66

	3.5.5	Compressive Strength Test	67
	3.5.6	Brick-Mortar Bond Strength Test	67
	3.6	Summary	69
Chapter 4		ANALYSIS OF BRICK PROPERTIES	71
	4.1	Experimental	71
	4.2	Pore Properties	72
	4.3	Water Absorption Properties	84
	4.4	Compressive Strength	98
	4.5	Ultrasonic Pulse Velocity	101
	4.6	Freeze-thaw Performance	101
	4.7	Summary	103
Chapter 5		DEVELOPMENT OF DURABILITY INDEX	104
	5.1	Comparative Study of Durability Indices	104
	5.1.1	Indices Selected	105
	5.1.2	Experimental	107
	5.1.3	Discussion of Results	107
	5.1.4	Summary of the Comparative Study	113
	5.2	Development of Durability Index	114
	5.2.1	Method Adopted	114
	5.2.2	Relation between <i>PV</i> and Water Absorption Property . . .	115
	5.2.3	Relation between <i>P3</i> and Water Absorption Property . . .	116
	5.2.4	Derivation of New Durability Index	119
	5.2.5	Validation	123
	5.3	Summary	125
Chapter 6		NONDESTRUCTIVE EVALUATION OF DURABILITY	128
	6.1	Research Procedure	128
	6.2	Pulse Velocity Vs. Brick Properties	129
	6.3	Relation between Brick Properties	131
	6.4	Derivation of Durability Provisions	134
	6.5	Validation	136
	6.6	Summary	137

Chapter 7	EFFECT OF IMPREGNATION	138
7.1	Research Procedure	138
7.2	Loading of Impregnating Materials	140
7.3	Effect on Pore Properties	142
7.3.1	Pore Volume and Porosity	142
7.3.2	Median and Average Pore Diameters	146
7.3.3	Pore Size Distribution	148
7.3.4	Summary	154
7.4	Effect on Water Absorption Properties	159
7.4.1	Vacuum Saturation	159
7.4.2	Submersion Absorption	163
7.4.3	Capillary Absorption	164
7.4.4	Summary	172
7.5	Effect on Compressive Strength	172
7.6	Effect on Pulse Velocity	176
7.7	Effect on Freeze-Thaw Performance	176
7.8	Effect on Brick-Mortar Bond Strength	183
7.9	Economic Aspects of Impregnation	187
7.10	Comparison of Impregnation Types	188
Chapter 8	CONCLUSION	191
8.1	Conclusions from the Study	191
8.1.1	Conclusions from the Review of Previous Studies	191
8.1.2	Conclusions from the Present Study	192
8.2	Recommendations for Further Study	196
	REFERENCES	197
Appendix A	PORE SIZE DISTRIBUTION TABLES AND CURVES	202
Appendix B	WATER ABSORPTION TABLES	208
Appendix C	TABLES OF PROPERTIES FOR DURABILITY INDICES	214
Appendix D	PORE SIZE DISTRIBUTION TABLES FOR IMPREGNATED BRICKS	219

List of Figures

Figure 3.1	Research procedure adopted for the development of durability index	45
Figure 3.2	Research procedure for feasibility study on nondestructive evaluation of durability	46
Figure 3.3	Research procedure for studies on effect of impregnation on brick properties	48
Figure 3.4	The different types of bricks used in this research	53
Figure 3.5	The desiccator used for cooling and storing dried specimens	53
Figure 3.6	The vacuum chamber used for impregnation and vacuum saturation	57
Figure 3.7	The constant temperature bath used for paraffin impregnation	57
Figure 3.8	The experimental set-up used for the capillary absorption test	61
Figure 3.9	The boiling water absorption test set-up used in this study	61
Figure 3.10	The Mercury Intrusion Porosimeter: PoreSizer 9320 (Micromeritics Instrument Corporation, Norcross, U.S.A)	64
Figure 3.11	The core drilling machine (right) and the fine cutting saw (left) used for making specimens for mercury intrusion porosimetry	64
Figure 3.12	The pulse velocity testing equipment (PUNDIT) and test set-up (C N S Electronics Ltd., London, U.K.)	68
Figure 3.13	The Environmental Chamber used for the freezing and thawing test	68
Figure 3.14	The specimen (in inset) and the loading set-up for bond strength test	69

Figure 4.1	The pore properties of the bricks	74
Figure 4.2	Distribution of relevant pore size ranges of the bricks expressed as cumulative intrusion in ml/g	78
Figure 4.3	Distribution of relevant pore size ranges of the bricks expressed as cumulative intrusion in % of pore volume (<i>PV</i>)	79
Figure 4.4A	Pore size distribution curves for bricks A, B, C, and D expressed as cumulative intrusion in ml/g	80
Figure 4.4B	Pore size distribution curves for bricks E, F, G, H, and J expressed as cumulative intrusion in ml/g	81
Figure 4.5A	Pore size distribution curves for bricks A, B, C, and D expressed as cumulative intrusion in % of total pore volume (% of <i>PV</i>)	82
Figure 4.5B	Pore size distribution curves for bricks E, F, G, H, and J expressed as cumulative intrusion in % of total pore volume (% of <i>PV</i>)	83
Figure 4.6	Absorption properties of the bricks	86
Figure 4.7A	Submersion absorption curves for bricks A, B, C, and D expressed as % of dry weight (<i>Cx</i>)	88
Figure 4.7B	Submersion absorption curves for bricks E, F, G, H, and J expressed as % of dry weight (<i>Cx</i>)	89
Figure 4.8A	Submersion absorption curves for bricks A, B, C, and D expressed in % of 5 hr. boiling water absorption (<i>Cx/B</i>)	90
Figure 4.8B	Submersion absorption curves for bricks E, F, G, H, and J expressed in % of 5 hr. boiling water absorption (<i>Cx/B</i>)	91
Figure 4.9A	Capillary absorption curves for bricks A, B, C, and D expressed as % of dry weight (<i>Sx</i>)	92
Figure 4.9B	Capillary absorption curves for bricks E, F, G, H, and J expressed as % of dry weight (<i>Sx</i>)	93
Figure 4.10A	Capillary absorption curves for bricks A, B, C, and D expressed in absorption per unit area (<i>Sx/A</i>)	94
Figure 4.10B	Capillary absorption curves for bricks E, F, G, H, and J expressed in absorption per unit area (<i>Sx/A</i>)	95

Figure 4.11A	Capillary absorption curves for bricks A, B, C, and D expressed in % of 5 hr. boiling water absorption (Sx/B)	96
Figure 4.11B	Capillary absorption curves for bricks E, F, G, H, and J expressed in % of 5 hr. boiling water absorption (Sx/B)	97
Figure 4.12	Compressive strength (gross) of the bricks	100
Figure 4.13	Bulk density of the bricks	100
Figure 4.14	Ultrasonic pulse velocity of the bricks	100
Figure 4.15	Freeze-thaw cycles resisted by the bricks	100
Figure 5.1	The different durability indices for the bricks	109
Figure 5.2	Relation between the different durability indices and frost resistance of the bricks	112
Figure 5.3	Relation between pore volume (PV) and 5 hr. boiling water absorption (B)	116
Figure 5.4	Relation between $P3$ and $(1-CI/B)100$	118
Figure 5.5	Relation between $P3$ and $(1-S4/B)100$	118
Figure 5.6	Relation between $DIAP(C)$ and frost resistance	120
Figure 5.7	Relation between $DIAP(S)$ and frost resistance	120
Figure 5.8	Relation between DIM and $DIAP(C)$	122
Figure 5.9	Relation between DIM and $DIAP(S)$	122
Figure 5.10	Relation between $DIM-I(C)$ and frost resistance	124
Figure 5.11	Relation between $DIM-I(S)$ and frost resistance	124
Figure 5.12	Validation of $DIAP(C)$	127
Figure 5.13	Validation of $DIAP(S)$	127
Figure 6.1	Relation between ultrasonic pulse velocity (V_u) and 5 hr. boiling water absorption (B)	130

Figure 6.2	Relation between ultrasonic pulse velocity (V_u) and 24 hr. water absorption (C)	130
Figure 6.3	Relation between ultrasonic pulse velocity (V_u) and compressive strength (CS)	131
Figure 6.4	Relation between 24 hr. water absorption (C) and 5 hr. boiling water absorption (B)	133
Figure 6.5	Relation between compressive strength and 5 hr. boiling water absorption (B)	133
Figure 6.6	Derivation of limiting values for pulse velocity to evaluate durability	135
Figure 7.1	Intruded pore volume (PV) of the impregnated bricks	145
Figure 7.2	Porosity (P) of the impregnated bricks	145
Figure 7.3	Median pore diameter of the impregnated bricks	145
Figure 7.4	Average pore diameter of the impregnated bricks	147
Figure 7.5	Pore volume of the impregnated bricks $> 3 \mu\text{m}$ in diameter, expressed in ml/g	147
Figure 7.6	Pore volume of the impregnated bricks in the pore diameter range 3-1 μm , expressed in ml/g	147
Figure 7.7	Pore volume of the impregnated bricks in the pore diameter range 1-0.1 μm , expressed in ml/g	151
Figure 7.8	Pore volume of the impregnated bricks $< 0.1 \mu\text{m}$ in diameter, expressed in ml/g	151
Figure 7.9	Pore volume of the impregnated bricks $> 3 \mu\text{m}$ in diameter, expressed in % of total pore volume (PV)	151
Figure 7.10	Pore volume of the impregnated bricks in the pore diameter range 3-1 μm , expressed in % of total pore volume (PV)	153
Figure 7.11	Pore volume of the impregnated bricks in the pore diameter range 1-0.1 μm , expressed in % of total pore volume (PV)	153
Figure 7.12	Pore volume of the impregnated bricks $< 0.1 \mu\text{m}$ in diameter, expressed in % of total pore volume (PV)	153

Figure 7.13A	Pore size distribution curves for the impregnated bricks A4, B4, C4, and F3, expressed as cumulative intrusion in ml/g	155
Figure 7.13B	Pore size distribution curves for the impregnated bricks A5, B5, and C5, expressed as cumulative intrusion in ml/g	156
Figure 7.14A	Pore size distribution curves for the impregnated bricks A4, B4, C4, and F3, expressed as cumulative intrusion in % of total pore volume (<i>PV</i>)	157
Figure 7.14B	Pore size distribution curves for the impregnated bricks A5, B5, and C5, expressed as cumulative intrusion in % of total pore volume (<i>PV</i>)	158
Figure 7.15	Vacuum saturation (<i>V</i>) of the impregnated bricks	162
Figure 7.16	24 hr. water absorption (<i>C</i>) of the impregnated bricks	162
Figure 7.17	Saturation coefficient (<i>C/V</i>) of the impregnated bricks	162
Figure 7.18	10 minute submersion absorption of the impregnated bricks expressed in % of dry weight (<i>CIOM</i>)	167
Figure 7.19	10 minute submersion absorption of the impregnated bricks expressed in % of vacuum saturation (<i>CIOM/V</i>)	167
Figure 7.20	1 hour submersion absorption of the impregnated bricks expressed in % of dry weight (<i>CI</i>)	167
Figure 7.21	1 hour submersion absorption of the impregnated bricks expressed in % of vacuum saturation (<i>CI/V</i>)	168
Figure 7.22	10 minute capillary absorption of the impregnated bricks expressed in % of dry weight (<i>SIOM</i>)	168
Figure 7.23	10 minute capillary absorption of the impregnated bricks expressed in % of vacuum saturation (<i>SIOM/V</i>)	168
Figure 7.24	1 hour capillary absorption of the impregnated bricks expressed in % of dry weight (<i>SI</i>)	171
Figure 7.25	1 hour capillary absorption of the impregnated bricks expressed in % of vacuum saturation (<i>SI/V</i>)	171
Figure 7.26	Compressive strength of the impregnated bricks	175

Figure 7.27	Bulk density of the impregnated bricks	175
Figure 7.28	Ultrasonic pulse velocity of the impregnated bricks	175
Figure 7.29	Frost resistance of the impregnated bricks	180
Figure 7.30	Durability index by Maage (<i>DIM</i>) of the impregnated bricks	180
Figure 7.31	Durability index based on absorption properties [<i>DIAP(S)</i>] of the impregnated bricks	180
Figure A.1A	Pore size distribution curves for brick A, B, C, and D, expressed as cumulative intrusion in % of sample volume (% of <i>SV</i>)	206
Figure A.1B	Pore size distribution curves for brick E, F, G, H, and J, expressed as cumulative intrusion in % of sample volume (% of <i>SV</i>)	207

List of Tables

Table 2.1	Physical requirements for durability [ASTM 1992a]	18
Table 2.2	Equations for indirect evaluation of frost susceptibility [Nakamura 1988a]	23
Table 2.3	Durability index based on strength [Arnott 1990]	25
Table 2.4	Durability index based on visual distress [Arnott 1990]	26
Table 2.5	Physical properties of common monomers [ACI 1977]	32
Table 2.6	Various properties of PIC [ACI 1977]	36
Table 2.7	Effects of polymerization on properties of bricks [Fowler et al 1974]	37
Table 3.1	Details of brick types selected	50
Table 3.2	Properties of paraffin used [Stochem 1994]	52
Table 3.3	Absorption ranges for brick group classification	54
Table 3.4	Comparison of vacuum saturation with boiling water absorption	62
Table 4.1	Pore properties of the bricks	73
Table 4.2	Distribution of relevant pore size ranges of the bricks Expressed as cumulative intrusion in ml/g	76
Table 4.3	Distribution of relevant pore size ranges of the bricks Expressed as cumulative intrusion in % of total pore volume (<i>PV</i>)	77
Table 4.4	Absorption properties of the bricks	85

Table 4.5	Density, strength, and pulse velocity of the bricks	99
Table 4.6	Freeze-thaw performance of the bricks	102
Table 5.1	Durability indices of the bricks	108
Table 5.2	Limiting values for the indices	123
Table 5.3	Properties of brick types K, L, and M	126
Table 6.1	Details of test data used in this study	132
Table 6.2	Limiting values for pulse velocity (V_u) to evaluate durability	136
Table 6.3	Validation of durability provisions based on pulse velocity	137
Table 7.1	Impregnation type designation and brick groups studied	139
Table 7.2	Loading of impregnating material	141
Table 7.3	Pore properties of impregnated bricks	143
Table 7.4	Distribution of relevant pore size ranges of impregnated bricks	149
Table 7.5	Water absorption properties of impregnated bricks	160
Table 7.6	Submersion absorption properties of impregnated bricks	165
Table 7.7	Capillary absorption properties of impregnated bricks	169
Table 7.8	Strength, density, and pulse velocity of impregnated bricks	173
Table 7.9	Freeze-thaw performance of impregnated bricks	177
Table 7.10	Durability indices for impregnated bricks	181
Table 7.11	Effect of impregnation on brick-mortar bond strength	185
Table 7.12	Additional material cost of impregnation	188
Table 7.13	Comparison of impregnation types	189
Table A.1	Pore size distribution of bricks expressed in terms of cumulative intrusion in ml/g	203
Table A.2	Pore size distribution of bricks expressed as cumulative intrusion in % of total pore volume	204

Table A.3	Pore size distribution of bricks expressed as cumulative intrusion in % of sample volume	205
Table B.1	Submersion absorption of bricks expressed as % of dry weight (Cx)	209
Table B.2	Submersion absorption of bricks expressed as % of boiling water absorption (Cx/B)	210
Table B.3	Capillary absorption of bricks expressed as % of dry weight (Sx)	211
Table B.4	Capillary absorption of bricks expressed as absorption per unit area (Sx/A)	212
Table B.5	Capillary absorption of bricks expressed as % of boiling water absorption (Sx/B)	213
Table C.1	Physical properties used for calculating DIR	215
Table C.2	Physical properties used for calculating DIM	216
Table C.3	Physical properties used for calculating DIN	217
Table C.4	Physical properties used for calculating DIA	218
Table D.1	Pore size distribution of impregnated bricks expressed as cumulative intrusion in ml/g	220
Table D.2	Pore size distribution of impregnated bricks expressed as cumulative intrusion in % of total pore volume	222

Nomenclature

A_p	Specific pore volume in the pore radius range 5-10 nm
A_v	% of total sample volume represented by pores greater than 2.8 μm
ACI	American Concrete Institute
AiBN	Azobisisobutyronitrile
AN	Acrylonitrile
AP	Apparent Porosity
APD	Average Pore Diameter
ASTM	American Society for Testing & Materials
A45	Adsorbed water in adsorption at 45% rh
A98	Adsorbed water at 98% rh
B	5 hr. boiling water absorption as percentage of dry weight
B_p	Specific pore volume in the pore radius range 10-50 nm
B_s	168 day cold soak as a percentage of total pore volume filled
B_v	30 minute IRA based on net area of sample face exposed to water
BD	Bulk Density
BP	Benzoyl Peroxide
C	24 hr. cold water absorption as percentage of dry weight

C_p	Specific pore volume in the pore radius range 0.05-0.1 μm
C_s	Percentage of total sample volume greater than 1.1 microns
C_v	Ratio of weight % 5 hr. boiling absorption divided by weight % vacuum saturation
COC	Cleveland Open Cup
CP	Difference in Adsorbed water, ie A98-A45
CS	Compressive Strength (gross area)
CS	Chlorostyrene
CSA	Canadian Standards Association
C/B	Saturation Coefficient (based on boiling absorption)
C/V	Saturation Coefficient (based on vacuum saturation)
CI	1 hr. cold water absorption as percentage of dry weight
CIOM	10 minute cold water absorption as percentage of dry weight
D	Pore diameter
D_p	Specific pore volume in the pore radius range 0.1-0.4 μm
D_s	4 hr. cold soak as percentage of total pore volume filled
D_v	Ratio of weight % 4 hr. soak divided by weight % 5 hr. boiling absorption
DIA	Durability Index by Arnott
DIAP(C)	Durability Index based on Water absorption Properties (Submersion absorption)
DIAP(S)	Durability Index based on Water absorption Properties (Capillary absorption)
DIM	Durability Index by Maage
DIM-I(C)	Improved Maage's Index based on submersion absorption property
DIM-I(S)	Improved Maage's Index based on capillary absorption property
DIN	Durability Index by Nakamura
DIR	Durability Index by Robinson

<i>DIS</i>	Durability Index based on Strength (Arnott)
<i>DIV</i>	Durability Index based on Visual Distress (Arnott)
<i>DS</i>	Degree of Saturation
<i>D45</i>	Adsorbed water in Desorption at 45% rh
<i>E_p</i>	Specific pore volume in the pore radius range 0.4-0.7 μm
<i>E_v</i>	Ratio of weight % 56 day cold soak divided by weight % 5 hr.boiling absorption
<i>EB</i>	Linear expansion at WA
<i>ED</i>	Linear expansion at A98
<i>F_c</i>	Frost resistance number (Maage)
<i>F_p</i>	Specific pore volume in the pore radius range 0.7-1.0 μm
<i>F_v</i>	% of total pore volume filled in a 15 minute IRA test
<i>FIDX</i>	Calculated frost susceptibility (Nakamura)
<i>G_p</i>	Specific pore volume in the pore radius range 1.0-7.5 μm
<i>G_v</i>	Modulus of rupture based on net area of fracture
<i>H_v</i>	True specific gravity of brick material
<i>H45</i>	Difference in Adsorbed Water, ie. A45-D45
<i>I_v</i>	% of total sample volume represented by pores greater than 4.4 μm
<i>IRA</i>	Initial Rate of Absorption
<i>J_v</i>	% of total pore volume filled in a 2 minute IRA test
<i>K_v</i>	120 minute IRA based on net area of sample face exposed to water
<i>L</i>	Distance between transducers in UPV test.
<i>L_v</i>	Compressive strength based on net area
<i>MMA</i>	Methyl methacrylate
<i>MPD</i>	Median Pore Diameter

<i>n</i>	Number of factors considered (in the equations developed by Nakamura)
<i>P</i>	Porosity
<i>p</i>	Pressure applied
<i>PA</i>	Pore Area
<i>PIC</i>	Polymer Impregnated Concrete
<i>PMMA</i>	Polymethyl methacrylate
<i>PSD</i>	Pore Size Distribution
<i>PUNDIT</i>	Portable Ultrasonic Nondestructive Digital Indicating Tester
<i>PV</i>	Intruded Pore Volume
<i>P3</i>	% of pores with diameter larger than 3 μm (% of PV)
<i>rh</i>	relative humidity
<i>S</i>	Styrene
<i>SUS</i>	Saybolt Universal Seconds
<i>S1</i>	1 hr. capillary absorption as percentage of dry weight
<i>S10M</i>	10 minute capillary absorption as percentage of dry weight
<i>S4</i>	4 hr. capillary absorption as percentage of dry weight
<i>t_u</i>	Ultrasonic pulse transit time
<i>TBS</i>	Tert-butyl Styrene
<i>TMPTMA</i>	Trimethylol propane trimethacrylate
<i>T1A</i>	Impregnation using MMA at atmospheric pressure
<i>T1B</i>	Impregnation using MMA under vacuum
<i>T2A</i>	Impregnation using UNICERE 62 paraffin
<i>T2B</i>	Impregnation using PARAFLINT H1 paraffin
<i>T3</i>	Impregnation using Acrylic Sealer

UPV	Ultrasonic Pulse Velocity
V	Vacuum Saturation as a percentage of dry weight
V_u	Ultrasonic pulse velocity
VAc	Vinyl Acetate
WA	Water absorption
Y	Relative index of durability (Robinson et al)
γ	Surface tension of mercury
θ	Contact angle of mercury
ρ	Density

Introduction

Clay brick is one of the oldest building materials and in fact the first to be manufactured by man. It is still popular as a construction material mainly because of its structural properties, easy availability, relatively low cost, and architectural reasons. Traditionally clay brick is considered to be a strong and durable material under normal weather conditions. Where clay deposit is available, brick can be manufactured locally, thus making it easily available at relatively low cost. Clay brick has pleasing color and can be made with different surface textures, which makes it architecturally more acceptable. It is widely used for the envelope of buildings and quite commonly it forms part of the brick veneer wall system adopted for the facade of buildings. Many failures in building envelope are associated with the disintegration of the brick veneer. Therefore, durability is one of the major requirements to be considered in the design and construction of building envelope. Failure due to deterioration may be of concern for safety. In some cases it may result in expensive repairs and there is no assurance that deterioration will not recur.

All building components and materials are designed and constructed to perform certain functions. Durability refers to the capability of successfully performing these functions over a

specified period called the service life of the building. Various factors may adversely affect the performance during this period. They include: material properties, design considerations, construction techniques, environmental conditions, and maintenance. Even though all these factors may act together, some of them may be more predominant than others. The cause of deterioration is usually attributed to these predominant factors. Since the factors that govern deterioration vary from material to material and from location to location, identification of the predominant factors is the first step in the design of durable building materials and components. In the case of brick masonry, frost action and salt crystallisation are found to be the major causes of deterioration. In cold regions like Canada, frost action is reported to be the principal cause.

Frost action is produced when the temperature falls below freezing and the water in the pores of the material starts freezing. The expansion of the ice in the pores results in pressure development inside the material. The extent of pressure developed during freezing will depend upon the amount of pores in the material and the degree of saturation of the material. Larger the amount of pores, greater will be the pressure developed. When the pressure exceeds material strength, it results in frost damage. In the case of low degree of saturation the pressure development will be negligible, as the free space in the pores accommodates the expansion of the freezing water. In places where the temperature fluctuates about freezing, the material is subjected to cyclic freezing and thawing. The damage, in such cases, may be caused not just by a single frost action but by a number of cycles during the course of time.

1.1 Frost Durability

The performance of materials against frost action is commonly referred to as frost

durability, freeze-thaw durability, or frost resistance. Frost durability is a function of both the material characteristics and the environment to which they are exposed. The major properties that affect durability are strength, porosity and pore size distribution. Frost action causes internal stress which is resisted by the material. The material strength, usually expressed as compressive strength, refers to the maximum strength that the material can offer in resisting the stress due to frost action. Presence of water in the pores during freezing is the major cause for frost action. The amount of water that is absorbed by a brick, while in contact with water, depends on porosity and pore size distribution of bricks. Therefore, they are critical factors in deciding the freeze-thaw durability of bricks. An increase in porosity is normally accompanied by a decrease in compressive strength.

The exposure conditions that affect the durability include: the temperature range, rate of freezing, and the extent of wetting of the surface and/or the contact with sources of dampness. When the temperature falls below 0°C, the freezing of water in the pores starts with larger pores. Since the water in the smaller pores are held by capillary force, they freeze only at much lower temperature. Therefore the temperature range to which the bricks are exposed is important in deciding the total force exerted by the frost action. The rate of freezing also has a controlling effect on the frost action. Usually when the water freezes in the pores, the expanding force squeezes the unfrozen water into unsaturated pore spaces, thus relieving pressure. But under high rate of freezing, there would not be enough time for the unfrozen water to move to empty pores, causing sudden increase in pressure. Also, when the rate of freezing is low, it may cause "ice lensing" phenomenon to occur, resulting in large accumulation of ice within the material and subsequent spalling of bricks.

The degree of saturation attained by bricks in an envelope also depends upon the exposure conditions. The major source of saturation is the water falling on the surface due to driving rain. Normally water gets into the pores of bricks through capillary suction. Both the intensity of rain and its duration are important in this case. Contact with other sources of dampness like accumulated water or melting of snow and leakage in drainage system can also cause increased saturation level.

1.2 Need for the Research

In cold regions where alternate freezing and thawing cycles exist, clay bricks used for the envelope of buildings are susceptible to damage due to frost action. This problem is more severe in the case of envelopes that are exposed to driving rain, where bricks may get saturated prior to undergoing freezing. In order to avoid frost damage, durable bricks should be used so that it can withstand the adverse effects of severe weather during the course of time. Therefore there should be some techniques for ensuring that bricks to be used for the envelope are durable. In this research two approaches to achieve this are studied. The first approach involves testing the bricks to evaluate their durability under the expected weathering conditions and selecting the durable bricks. This requires that suitable methods are either available or needed to be developed for fast and reliable evaluation of durability. The second approach is to improve the durability of poor bricks using suitable methods.

1.2.1 Evaluation of Durability

The most reliable test for evaluating durability of building materials is actual exposure to the natural environment. Since such a test is highly time consuming, laboratory exposure to

accelerated freeze-thaw cycles is being practised as the most widely accepted test for assessing durability. The potential durability of clay bricks is generally assessed using specifications and test methods mentioned in current American and Canadian standards [ASTM 1992a; ASTM 1993a; CSA 1987; CSA 1978].

The evaluation method suggested in current standards specify physical requirements for water absorption properties and compressive strength of bricks, and the durability is assessed based on whether these requirements are satisfied or not. They also specify a freezing and thawing test, when the bricks do not meet the water absorption requirements. The freezing and thawing test consists of 50 cycles and takes at least 50 days to complete. Therefore it cannot be used for quick evaluation. The durability assessment is based on whether the brick completes the 50 cycles of freezing and thawing without any failure or not, and so the performance of bricks cannot be compared in this procedure. Some researchers have criticized the standard requirements as unreliable in certain cases [Bortz et al 1990; Gazzola 1992; Marusin 1990]. Nevertheless, being the method suggested in standard, they continue to be used for assessing durability.

The standard evaluation method requires facilities for freezing and thawing test and takes considerable time for completion. Therefore testing of commercially available bricks prior to selection is not always possible and the selection is usually done based on the technical data provided by manufacturers. It is normally observed that within a single type of brick the properties may vary over a wide range. So the evaluation method used for durability assessment should be capable of giving the limits of performance level of the bricks rather than the average assessment as durable or not durable. This cannot be done using the standard evaluation method. Hence there is a need for developing other techniques for durability assessment.

A better method of assessment would be to develop a durability index rather than using a set of physical requirements. Such an index should be developed using properties that are critical to durability and which can be quickly measured. Durability index has the advantage that it can be used for comparing brick types. It can also be used to specify the upper and lower limits of performance level that are expected of a brick type. Having an index will also facilitate the designers to specify it as a construction requirement for selecting the proper type of brick. A few indices have already been developed by other researchers [Robinson et al 1977; Maage 1984; Nakamura 1988a; Arnott 1990]. They are not being widely used either because they have not been validated against field performance or they need relatively expensive equipments for measurements. Hence there is a real need for developing a durability index based on easily measurable physical properties of bricks so that reliable assessment of durability can be made in short time. The evaluation method using index should specify limiting values for durable and nondurable bricks. Then the durability index of a given type of brick can be compared against these limiting values to determine its durability.

The standard method for evaluating the durability of bricks is based on laboratory tests and is basically destructive in nature. Certain nondestructive methods are widely used for evaluating the quality and properties of some materials like metals, concrete, etc. Not much research work has been done on nondestructive evaluation of bricks or brick masonry. Hence a feasibility study is needed to find whether nondestructive method can be used for evaluating the properties of bricks and thereby possibly their durability. Such a method has a potential for in situ evaluation of durability.

1.2.2 Improvement of Durability

Certain areas in a building facade like parapets may be subjected to high levels of wetting due to snow or water accumulation. Bricks that are normally durable may fail when used in such areas because of the high degree of saturation attained. This warrants the need for bricks of improved durability. Improvements in durability can be achieved either by modification at the production process or by suitable process after production.

Clay bricks are made in factories by firing bricks at high temperature in kilns. The quality of bricks depends upon the raw materials, forming process, and the firing temperature. There is no established direct relation between these production parameters and the frost resistance of bricks. For commercially marketed bricks these details are usually not available. Improvements in durability can be observed with increased firing temperature but it is at the expense of more fuel. More over, not all bricks in a given production run might be subjected to uniform firing temperature because of their different positions in the kiln and therefore they may have varying properties. Unlike concrete, the use of admixtures in raw materials for improvement of frost durability of clay bricks has not been successfully accomplished, probably because of the firing stage involved in the production process. Therefore a better control on the durability of bricks can be expected if the improvement methods are carried out after the firing stage in the production.

Bricks that are found nondurable can still be used if their durability is improved by suitable means. The method used for improving the durability should retard the impact of those factors that adversely affect durability. Since the degree of saturation attained prior to freezing is a major factor affecting the durability of bricks in a given environment, improvement in durability can be achieved by lowering the degree of saturation. This can be accomplished by impregnation

of the pore space of brick with suitable materials, which can reduce the porosity of brick. Currently there is insufficient research information regarding the effect of impregnation on the pore structure, water absorption characteristics, and the performance of bricks under freeze-thaw environment.

1.3 Objectives of the Research

The major objectives of this research can be outlined as follows:

- * To develop an index to evaluate the frost durability of bricks based on easily measurable physical properties.
- * To investigate the feasibility of using nondestructive method to evaluate the frost durability of bricks.
- * To study the effect of impregnation with different materials on frost durability of bricks.

1.4 Scope of the Research

In this research commercially available clay bricks were used, so that results from the study could be extended to bricks used in practice. Both extruded and dry pressed brick types were included in the study. Most of the bricks that are used these days are of extruded type. But dry pressed brick are also available in the market. The selection of the brick types for this research was not based on a statistical survey regarding the percentage of each brick type made or used in construction. The efforts to get information from the manufacturers regarding the bricks produced by them did not succeed and therefore the research had to depend on the bricks obtained from local vendors, with very limited information about their source and properties. Some of the

bricks in existing buildings may contain pressed bricks, especially in locations like parapets which are most exposed to severe weather. The durability index should be capable of evaluating the durability of bricks in existing structures as well. It was intended in this research to develop a general durability index, irrespective of the production process used for manufacturing the brick. Therefore it was considered necessary to include pressed bricks also in this study.

One of the objectives of this study was to develop a durability index based on easily measurable physical properties of the brick, so that durability evaluation involved simple and fast procedure, without the need for any expensive equipments. Therefore, factors such as raw materials and their chemical composition, forming process, and the firing temperature used for making the bricks were not considered in developing the index. This information is usually difficult to obtain and therefore developing indices based on these factors may complicate the evaluation procedure. It is presumed that the effect of these factors is reflected in the various physical properties of the bricks produced.

The freeze-thaw test used in this research consisted of accelerated omnidirectional freezing with four cycles per day. The current American and Canadian standard freeze-thaw tests are also omnidirectional, with one cycle per day [ASTM 1993a; CSA 1978]. To study the performance of the index in evaluating durability, the freeze-thaw test must provide the number of cycles at which the brick would fail, so that it could give a data point for plotting. As the brick must fail, there was a need for the accelerated freeze-thaw test with more severe conditions than used in the standard procedure. In this study, the freeze-thaw test results were used only for observing the relative performance of the brick types and they were not used for deriving the durability index. It was presumed that a brick, which resisted a higher number of laboratory freeze-thaw cycles

before failure, was expected to be more durable under the actual field conditions than a brick, which resisted a relatively lower number of cycles.

There is a trend now to use unidirectional freezing test to evaluate the freeze-thaw performance of brick. It is observed that the failure patterns (delamination and surface spalling) in such a test were similar to that found in actual field conditions. But the unidirectional freezing test has not yet been accepted as a standard procedure in Canada and US. The time and facility requirements necessary for the unidirectional test were beyond the constraints which existed in this research. Therefore, for the reasons discussed above, the accelerated omnidirectional freezing test was used in this research. This fact must be considered while interpreting the result from the freeze-thaw test and while studying the performance of the durability index. For the freeze-thaw test all the specimens were initially saturated to a level corresponding to 24 hr. water absorption and this level was maintained during the test. The effect of varying degrees of saturation and varying rates of freezing on durability are beyond the scope of this study. It is recommended that further work might be carried out to study the performance of the durability index using the unidirectional freezing test.

In this research, the impregnation process was used only as a technique for modifying the pore structure. The studies on impregnated bricks were limited to the extent of observing improvements in pore size distribution, compressive strength, water absorption properties, and freeze-thaw behaviour and the effect on bond between mortar and bricks. A detailed analysis of economic aspects of impregnation process and the viability of using impregnation at the manufacturing stage are beyond the scope of this study

1.5 Organization of the Thesis

An extensive review of literature was carried out in the above mentioned research area. The relevant results and summary of the review are provided in Chapter 2. The research methodology and the test procedures recommended to meet the objectives of this research are described in Chapter 3. The various physical properties of the clay bricks used in this study are analyzed and discussed in Chapter 4. Chapter 5 provides the derivation of a new index for assessing durability. The results of the feasibility study on nondestructive evaluation of durability are given in Chapter 6. Chapter 7 discusses the effect of impregnation on various properties of clay bricks. Finally, the conclusions drawn from this study and the recommendations for future work are explained in Chapter 8.

Review of Previous Studies

A review of literature was undertaken to find out the extent of work already carried out in the area of the proposed research. The review basically consisted of three topic areas: frost durability of bricks and its evaluation, nondestructive evaluation of masonry, and impregnation of porous building materials. The relevant results and conclusions from the previous studies are discussed in this chapter.

2.1 Frost Durability of Bricks

The durability of brick is usually measured in terms of its resistance to freezing and thawing cycles. The performance of bricks depends upon their properties. As mentioned in the previous chapter, a major objective of this research is to develop an index to evaluate the durability based on easily measurable physical properties. Therefore it is necessary to understand the various factors that may influence the properties of bricks and thereby their durability. This review is aimed at identifying those factors that are critical to durability of bricks. The existing methods for evaluating durability of bricks are also reviewed.

2.1.1 Factors Affecting Durability

The properties of burnt bricks and thus their frost durability depend upon the raw materials, the forming process, and the firing temperature used for manufacturing the bricks [Hauck et al 1990; Herget et al 1992; Kung 1987b; Kung 1987c]. Within the normal brick firing temperature range, the water absorption and the porosity of the burnt bricks increase with increasing calcium carbonate or limestone content in the raw materials [Kung 1987c]. The manufacturing technique has an effect on the relationship between the absorption and the chemical composition of bricks. In general, a higher proportion of fine particles (less than 20 μm) in the raw materials contributes to a higher saturation coefficient in burnt bricks, and coarse particles help to decrease the saturation coefficient [Kung 1987c].

It has long been known that high strength and low porosity of bricks increase the frost resistance. Firing temperature in the kiln affects the strength, porosity, and pore size distribution of brick (Kung 1987b; Maage 1984; May and Butterworth 1962; Robinson 1984). Increasing the temperature and duration of burning normally results in higher strength, lower porosity, and bigger pores, thus contributing to frost resistance.

Recent studies have proved that pore size distribution is also an important factor affecting the frost durability of materials [Maage 1984; Nakamura 1988a; Robinson 1984]. Robinson [1984] found that brick of poor durability showed a preponderance of pores smaller than 1 μm , while good brick exhibited a majority of pores larger than 2 μm . Kung [1985] explained that coarse pores were rarely filled with water during freezing, because although they were easily filled with water, it drained out quickly and therefore were not harmful to frost durability. Since small pores did not fill or dry easily and water in small pores did not freeze until very low temperatures were

reached, it had very little effect on the frost susceptibility of bricks. Intermediate pores (1-0.1 μm), on the other hand, were most susceptible to frost action because they were most frequently filled with water and the water dried more slowly than in larger pores.

Maage [1984] found that frost resistance was inversely proportional to the intruded pore volume and was directly proportional to the volume percentage of pores with diameter bigger than 3 μm . Based on correlation analysis between specific pore volume and freeze-thaw results Nakamura [1988a] concluded that pores with diameter less than 0.2 μm were harmful to frost durability of bricks. From studies on freeze-thaw durability of clay bricks, Arnott [1990] found that pores greater than 1-3 microns correlated well to brick with high durability as assessed by laboratory freeze-thaw testing.

Nakamura et al [1991] studied the frost susceptibility of inorganic porous building materials and its relation to internal pore structure using two dimensional pore size distribution and three dimensional pore connecting texture. They found that frost susceptibility showed excellent correlations with factors obtained by the quantitative analysis of pore connecting texture such as shape factor.

2.1.2 Evaluation of Durability

It is often necessary to know in advance whether the bricks to be used in a construction have adequate durability. In certain cases the durability of bricks in existing buildings needs to be evaluated. So there should be some means of predicting the durability. Laboratory freeze-thaw tests are widely used for assessing the durability of brick. The American and Canadian standards [ASTM 1992a; ASTM 1993a; CSA 1987; CSA 1978] specify physical requirements and a freezing

and thawing test to assess the durability of bricks. Some researchers [Robinson et al 1977; Maage 1984; Nakamura 1988a; Arnott 1990] have developed indices meant to predict the durability of bricks. These indices are expected to evaluate the durability in a short time based on certain physical properties.

2.1.2.1 Freeze-Thaw Testing

The American and Canadian standard freeze-thaw tests [ASTM 1993a; CSA 1978] consist of cyclic freezing in air and thawing in water with one cycle per day. Each cycle includes submerging the specimen in the water of the thawing tank at 24°C for 4 hours and then freezing them in a freezing chamber, with the temperature of air not exceeding -9°C, for 20 hours, followed by the thawing process of the next cycle. The test is continued for 50 cycles. Half brick specimens are used for testing. For freezing, the specimens are placed in a tray with 12.7 mm (1/2 in.) of water at the base. A specimen is considered to have passed the test if there is no visible crack or breakage and the weight loss is not greater than 0.5 %. The standard procedure for freezing and thawing is omnidirectional, where all faces of the brick are exposed to the same conditions. In the case of omnidirectional freezing, the test specimens seldom showed delamination, as was observed in practice. Most of the time they simply broke into a few pieces [West et al 1984; Van Der Klugt 1988]

Now there is a trend to use unidirectional freezing to evaluate the frost durability of brick. It consists of removing heat through only one face of the sample. Unidirectional freeze-thaw test usually produces a mode of failure similar to that observed in walled bricks in a building [West et al 1984]. It has not yet been accepted as a standard procedure in Canada and US. Some of the unidirectional freeze-thaw test procedures are reviewed here.

West et al [1984] at the British Ceramic Research Association Ltd. developed a unidirectional brick panel freezing test to assess the resistance of bricks to freeze-thaw conditions. The method was designed to test a panel of brickwork consisting of 10 courses of 3 bricks laid in half-bond. The panel was soaked in water for 7 days before exposing one face to repeated cycles of freezing and thawing. The other face and the top and the sides of the panel were enclosed in a close fitting jacket of 25 mm expanded polystyrene. The panels were built on steel channel bases using mortar and they were cured for at least 28 days. The apparatus automatically subjected the wall to a cycle of freezing and thawing consisting of 132 min freezing at an air temperature of -15°C ; 20 min thawing with rapid heaters to a maximum air temperature of 25°C ; 2 min spraying with water to replace that lost by evaporation; and finally 3 min to drain away the water in the system. The cycle was repeated and after 50 cycles the test was halted and the panel allowed to thaw out completely before being removed from the apparatus for careful examination. If no damage had occurred, the panel was replaced in position and tested for up to a further 50 cycles. After the completion of 100 cycles, the panel was removed and dismantled. Each brick was carefully examined for surface damage and any incipient separation of the surface layers. Results on over 200 test panels had demonstrated that the method placed bricks in a ranking order of frost resistance which broadly agreed with that based on the experience of the manufacturers who supplied the samples.

Van Der Klugt [1988] developed the "sand tray test" in which brickwork was simulated by placing loose bricks in a metal tray on a layer of sand, with sand between the bricks to simulate the mortar. To achieve unidirectional freezing in the test the tray was insulated on the inside by means of 30 mm polystyrene foam. The thawing took place in water at 20°C , and the freezing in air at -15°C . The freezing phase lasted until a thermocouple in one brick 30 mm

beneath the surface measured -10°C , and the thawing phase lasted until 10°C was measured. The specimens were saturated by 4 days immersion in tap water at 20°C . The test results showed that all bricks known as vulnerable to frost were damaged.

Nakamura [1988b] recommended a newly developed automatic unidirectional freeze-thaw test apparatus controlled by personal computer for evaluating the frost durability of building materials. For the unidirectional freeze-thaw test, rectangular samples $2.0 \times 2.5 \times 1.8$ cm were cut from a brick and the top and bottom surfaces were polished parallel to each other. They were saturated by immersion in water for 5 hours. The freeze-thaw schedule for the test was a modification of the German standard DIN 52252. Each cycle consisted of freezing from $+20^{\circ}\text{C}$ to -20°C (in about 7.5 hours) and thawing from -20°C to $+20^{\circ}\text{C}$ (in about 5.5 hours). The freeze-thaw cycle was repeated 15 times. The residual linear expansion of the specimen was employed as the degree of frost susceptibility. Based on the test results from 33 kinds of brick, Nakamura concluded that the unidirectional test method has promised to be a reliable test for mimicking actual frost deterioration of building materials.

Arnott [1990] used unidirectional freeze-thaw test, based on the Dutch standard NEN 2872, to assess the freeze-thaw performance of brick. The test was based on the method developed by TNO Netherlands. The test incorporated three levels of saturation (low, medium, and high) in the test procedure and two rates of freezing. The heat was removed at 150 watts/m^2 with the final temperature of -5°C and 300 watts/m^2 with the final temperature of -15°C . For low saturation level, the brick specimens were soaked in water at 20°C for 48 hours before placing in the testing machine. In the case of medium saturation level, specimens were soaked in 80°C water for 48 hours, followed by 24 hours in 20°C . High saturation level was achieved by vacuum saturation

of the specimens. A cycle consisted of 8 hours of thawing and 16 hours of freezing. A brick was considered to have passed the test if it had no visible crack or spalling after 24 cycles of freezing and thawing.

The various standard and non-standard freeze-thaw test methods to assess the frost resistance of clay bricks were reviewed by Stupart [1989].

2.1.2.2 Evaluation using Standards

The requirements for durability of facing bricks are specified in American Standard ASTM C216 [ASTM 1992a] and in Canadian Standard CAN/CSA-82.1 [CSA 1987]. The physical requirements, to be satisfied to qualify as durable brick, are given Table 2.1.

TABLE 2.1
Physical Requirements for Durability
[ASTM 1992a; CSA 1987]

Designation	Min. Compressive Strength MPa (Psi), gross area		Max. Water Absorption by 5 hr Boiling, %		Maximum Saturation Coeff.	
	Av. of 5	Individual	Av. of 5	Individual	Av. of 5	Individual
Grade SW (Severe Weathering)	20.7 (3000)	17.2 (2500)	17.0	20.0	0.78	0.80
Grade MW (Moderate Weathering)	17.2 (2500)	15.2 (2200)	22.0	25.0	0.88	0.90

The saturation coefficient requirement given in Table 2.1 shall be waived provided the average 24 hr. cold water absorption does not exceed 8%. The 50 cycle freezing and thawing test

as per ASTM C67 [ASTM 1993a] and CAN3-82.2 [CSA 1978] is specified only as an alternative when bricks do not conform to the requirements given in Table 2.1. Those specified for 5 hr. boiling water absorption and saturation coefficient shall be waived provided a sample of 5 bricks meeting all the other requirements passes the freezing and thawing test with no breakage and not greater than 0.5% loss in dry weight of any individual brick.

Marusin [1990] found that low value of 24 hr. water absorption needed for ASTM C216 waiver condition and the ASTM C67 freeze-thaw criteria were not sufficient requirements to achieve brick durability under severe weather conditions. Marusin concluded that the ASTM C67 freeze-thaw test procedure needed substantial revision to be useful in the prediction of brick durability. Also, new satisfactory criteria for durability need to be developed [Bortz et al 1990]. The current American and Canadian freeze-thaw test is regarded inadequate because the 50 cycles of freezing and thawing for the test is considered too few [Gazzola 1992]. It is also considered unrealistic and time consuming because it subjects specimens to omnidirectional freezing and thawing and takes about 10 weeks to complete.

2.1.2.3 Durability Indices

A brick has many physical properties associated with it and each property contributes positively or negatively to durability. Durability is the sum of these attributes [Amott 1990]. Attempts had been made by various researchers to relate the physical properties of the bricks and their frost resistance in order to develop indices for predicting durability . Their works are reviewed here.

(i) Robinson et al (1977)

Robinson et al carried out tests on 5,217 commercially marketed bricks to establish relation between different physical properties of the bricks and their resistance to freezing and thawing. The bricks were tested according to ASTM C67 to determine initial rate of absorption, cold water absorption, boiling water absorption, saturation coefficient, compressive strength, and resistance to freezing and thawing. The statistical analysis of the test results failed to show any acceptable relation between individual properties or combinations of properties and the resistance of the bricks to freezing and thawing. The best formula developed (converted to SI units) from the test results for the durability index of brick was :

$$Y = \left[\frac{IRA}{10(1 - C/B)} \right] - \left[\frac{145 CS - 6000}{1000} \right] + [C - 10] \quad [2.1]$$

where,

- Y = a relative index of durability
- IRA = initial rate of absorption, (g/min.193.55cm²)
- C = 24 hr. cold water absorption (%)
- B = 5 hr. boiling water absorption (%)
- CS = compressive strength (MPa) , and
- C/B = Saturation Coefficient

The lower the value of Y , the higher the durability with values of 7 or less indicating that less than 10% of the bricks would fail.

The durability index suggested by Robinson et al is based on brick properties mentioned in ASTM C67 and does not consider the effect of pore size distribution, which is found to have significant influence on frost durability.

(ii) Maage (1984)

Maage studied the correlation between frost resistance, porosity and pore size distribution of bricks. Thirteen different types of bricks were included in the study. Nine of them were produced at different factories in Norway and four were produced in Indiana, USA. The frost resistance of the different types of bricks was characterized by four different methods, including exposure to natural environment. The porosity and the pore size distribution of the bricks were determined by mercury intrusion porosimetry. Based on statistical analysis of the results, he suggested a mathematical correlation to calculate a frost resistance number for a brick from its pore structure. The frost resistance number, F_c is given by :

$$F_c = \frac{3.2}{PV} + 2.4 P3 \quad [2.2]$$

where, PV = intruded pore volume in ml/gram, and
 $P3$ = % of pores with diameters larger than 3 μm (% of PV)

Maage found that when $F_c > 70$, the brick was frost resistant and when $F_c < 55$, the brick was not frost resistant. According to his method, the assessment of potential frost durability is made not merely on the total pore volume, but also on how that volume is distributed among the possible pore sizes in the brick.

Winslow et al [1988] collected about 78 samples of bricks removed from walls of existing buildings, that had been exposed to wet and freezing environments at 53 different sites in USA. They studied the correlation between the observed performance of the bricks and the durability

index calculated using Maage's method. It was found that all bricks with an index greater than 70 exhibited no frost durability problems, thus validating Maage's equation. They concluded that Maage's method was more reliable and faster than ASTM method for assessing the potential frost durability of a brick. Smalley et al [1987] applied Maage's method to bricks made from 43 different clay mixes with additives. They found that the equation suggested by Maage for frost resistance was valid but the values for identifying frost resistant bricks were wrong. They concluded from their research that if $F_c > 45$, the brick was frost resistant and if $F_c < 35$, the brick was not frost resistant. The discrepancies in their values for evaluation might be due to the fact that the bricks were made in the laboratories with saw dust as an additive.

(iii) Nakamura (1988a)

Nakamura studied the frost susceptibility of 33 kinds of building bricks in order to develop indirect evaluation equations. The frost susceptibility data used for deriving the equations were obtained by the freeze-thaw test under unidirectional heat flow conditions, which resembled natural climatic conditions. The indirect evaluation equations were derived by multivariate regression analysis using two different data sets, one from physical characteristic factors and the other from pore size distribution of bricks. The equations suggested by Nakamura, with increasing number of factors and the corresponding R^2 values, are given in Table 2.2.

The equations suggested by Nakamura do not give any idea whether the bricks are durable or not. They can only be used for finding the relative durabilities. Some of the characteristic factors mentioned cannot be easily measured and therefore prediction of frost susceptibility is not simple.

TABLE 2.2
Equations for Indirect Evaluation of Frost Susceptibility
 [Nakamura 1988a]

(A) Evaluation by Physical Characteristic Factor of Sample

$FIDX (n=1) = 0.85 + 1.34\ln(A45)$	$(R^2 = 0.6287)$	[2.3]
$FIDX (n=2) = 1.80 + 0.50\ln(EB) + 0.79\ln(D45)$	$(R^2 = 0.6611)$	[2.4]
$FIDX (n=3) = 4.02 + 0.50\ln(AP) + 0.54\ln(ED) + 0.82\ln(D45)$	$(R^2 = 0.6952)$	[2.5]
$FIDX (n=7) = 6.95 - 1.20\ln(DS) - 0.61\ln(AP) + 0.54\ln(ED) - 2.80\ln(A98)$ $+ 1.34\ln(CP) + 0.26\ln(H45) + 2.14\ln(A45)$	$(R^2 = 0.7161)$	[2.6]
$FIDX (n=10) = 7.82 + 0.47\ln(WA) - 1.10\ln(DS) - 1.14\ln(AP) + 0.71\ln(ED)$ $- 0.23\ln(EB) - 2.75\ln(A98) + 1.24\ln(CP) + 0.43\ln(H45)$ $- 0.43\ln(D45) + 2.49\ln(A45)$	$(R^2 = 0.7179)$	[2.7]

(B) Evaluation by Specific Pore Volume * in a Specified Pore Size

$FIDX (n=1) = -0.24 + 0.15(B_p)$	$(R^2 = 0.7683)$	[2.8]
$FIDX (n=2) = -0.06 + 0.15(B_p) - 0.01(G_p)$	$(R^2 = 0.7751)$	[2.9]
$FIDX (n=3) = -0.04 - 0.06(A_p) + 0.17(B_p) - 0.01(G_p)$	$(R^2 = 0.7799)$	[2.10]
$FIDX (n=4) = -0.25 - 0.09(A_p) + 0.15(B_p) + 0.08(C_p) - 0.01(D_p)$	$(R^2 = 0.7876)$	[2.11]
$FIDX (n=5) = -0.11 - 0.09(A_p) + 0.15(B_p) + 0.07(C_p) - 0.01(D_p)$ $- 0.01(G_p)$	$(R^2 = 0.7914)$	[2.12]
$FIDX (n=6) = -0.05 - 0.09(A_p) + 0.15(B_p) + 0.07(C_p) - 0.01(D_p)$ $- 0.01(E_p) - 0.01(F_p)$	$(R^2 = 0.7941)$	[2.13]
$FIDX (n=7) = -0.12 - 0.09(A_p) + 0.15(B_p) + 0.08(C_p) - 0.01(D_p)$ $- 0.01(E_p) - 0.01(F_p) - 0.01(G_p)$	$(R^2 = 0.7950)$	[2.14]

*Specific pore volume expressed in $10^{-3}\text{cm}^3/\text{g}$

Pore Size Ranges: $A_p = 5\text{-}10 \text{ nm}$; $B_p = 10\text{-}50 \text{ nm}$; $C_p = 0.05\text{-}0.1 \text{ }\mu\text{m}$; $D_p = 0.1\text{-}0.4 \text{ }\mu\text{m}$;
 (Pore Radius) $E_p = 0.4\text{-}0.7 \text{ }\mu\text{m}$; $F_p = 0.7\text{-}1.0 \text{ }\mu\text{m}$; $G_p = 1.0\text{-}7.5 \text{ }\mu\text{m}$.

where, $FIDX =$ Calculated Frost Susceptibility

$n =$ Number of Factors Considered

<i>WA</i>	=	Water Absorption
<i>DS</i>	=	Degree of Water Saturation
<i>AP</i>	=	Apparent Porosity
<i>A45</i>	=	Adsorbed Water in Adsorption at 45% rh
<i>D45</i>	=	Adsorbed Water in Desorption at 45% rh
<i>H45</i>	=	Difference in Adsorbed Water, ie. A45-D45
<i>A98</i>	=	Adsorbed Water at 98% rh
<i>CP</i>	=	Difference in Adsorbed Water, ie A98-A45
<i>ED</i>	=	Linear Expansion at A98, and
<i>EB</i>	=	Linear Expansion at WA.

(iv) Arnott (1990)

A research program to investigate the frost durability of clay bricks was carried out by Arnott at National Research Council, Canada. Bricks collected from six plants from across Canada were used for the study. All the bricks were manufactured using high vacuum extrusion techniques and were selected to reflect the normal range of bricks which a plant would produce and ship to the customers. Based on the results of the laboratory freeze-thaw tests, he developed relationships, using multiple regression approach, which could be used to relate brick properties to its relative durability. Two types of durability indices were developed, one based on loss of strength and the other based on the first visible sign of distress during freeze-thaw cycling.

(a) Durability Index Based on Strength

This durability index used loss in strength as determined by ultrasonic pulse transit time readings taken before and after a freeze-thaw test to establish the durability level of the bricks.

The index was developed using stepwise multiple regression approach with increasing correlation coefficient values. The indices are given in Table 2.3.

TABLE 2.3
Durability Index Based on Strength
[Amott 1990]

<i>DIS1</i>	$= -160.3C/B + 213.4$	$(R^2 = 0.70)$	[2.15]
<i>DIS2</i>	$= -151.2C/B + 0.3694B_s + 174.2$	$(R^2 = 0.83)$	[2.16]
<i>DIS3</i>	$= -132.0C/B + 0.3670B_s + 0.4200C_s + 154$	$(R^2 = 0.86)$	[2.17]
<i>DIS4</i>	$= -66.72C/B + 0.8039B_s + 0.7686C_s - 0.6509D_s + 102.1$	$(R^2 = 0.90)$	[2.18]
<i>DIS5</i>	$= -40.92C/B + 1.392B_s + 0.4409C_s - 1.0826D_s + 1.6068C + 77.1$	$(R^2 = 0.91)$	[2.19]

where,

- DIS* = Durability Index Based on Strength
- C/B* = Saturation coefficient
- B_s* = 168 day cold soak as a percentage of total pore volume filled
- C_s* = Percentage of total sample volume greater than 1.1 microns
- D_s* = 4 hour cold soak as percentage of total pore volume filled, and
- C* = 24 hour cold soak as a percentage of dry sample weight.

(b) Durability Index Based on Visual Distress

In this, the number of unidirectional freeze-thaw cycles required to produce the first crack or other sign of distress was used to establish the durability level of the bricks. The number of cycles to failure was then compared to the brick properties and a relationship was developed. In this case also, the statistical analysis was performed using a stepwise multiple regression approach. The indices with the corresponding R^2 values are given in Table 2.4.

TABLE 2.4
Durability Index Based on Visual Distress
[Arnott 1990]

<i>DIV1</i>	$= 15.37A_v + 39.7$	$(R^2 = 0.76)$	[2.20]
<i>DIV2</i>	$= 14.97A_v - 0.5946B_v + 119.6$	$(R^2 = 0.91)$	[2.21]
<i>DIV3</i>	$= 11.50A_v - 0.6481B_v + 292.6C_v - 131.2$	$(R^2 = 0.93)$	[2.22]
<i>DIV4</i>	$= 9.187A_v - 0.4870B_v + 423.8C_v - 2.408D_v - 84.5$	$(R^2 = 0.95)$	[2.23]
<i>DIV5</i>	$= 8.220A_v - 0.6131B_v + 599.7C_v - 3.492D_v + 3.253E_v - 452.3$	$(R^2 = 0.96)$	[2.24]
<i>DIV6</i>	$= 5.498A_v - 1.4241B_v + 355.3C_v - 5.084D_v + 5.584E_v - 4.468F_v - 306.9$	$(R^2 = 0.97)$	[2.25]
<i>DIV7</i>	$= 6.720A_v - 1.1518B_v + 429.5C_v - 5.144D_v + 5.331E_v + 3.714F_v + 0.0171G_v + 5.591H_v - 411.0$	$(R^2 = 0.98)$	[2.26]
<i>DIV8</i>	$= 13.14A_v - 2.1580B_v + 441.0C_v - 5.894D_v + 5.089E_v + 9.268F_v + 0.0189G_v + 7.208H_v - 7.274I_v - 4.127J_v - 0.4386K_v + 0.00198L_v - 454.0$	$(R^2 = 0.98)$	[2.27]

- where,
- DIV* = Durability Index Based on Visual Distress
 - A_v = % of total sample volume represented by pores greater than 2.8 μm
 - B_v = 30 minute IRA based on net area of sample face exposed to water
 - C_v = Ratio of 5 hour boiling absorption (%) to vacuum saturation (%)
 - D_v = Ratio of weight % 4 hour soak divided by weight % 5 hour boil
 - E_v = Ratio of weight % 56 day cold soak divided by weight % 5 hour boil
 - F_v = % of total pore volume filled in a 15 minute IRA test
 - G_v = Modulus of rupture based on net area of fracture in psi
 - H_v = Specific gravity of brick material in g/cc (without considering pores)
 - I_v = % of total sample volume represented by pores greater than 4.4 μm
 - J_v = % of total pore volume filled in a 2 minute IRA test
 - K_v = 120 minute IRA based on net area of sample exposed to water, and
 - L_v = Compressive strength based on net area in psi

For the above indices developed by Arnott, higher number indicates better durability for the brick. These indices have a drawback in that they can only be used for comparing the frost durabilities of bricks and cannot be used for evaluating whether a brick is frost resistant or not. Arnott found that these indices did not relate well with that of Robinson. But Maage's durability index compared much better with both of the indices developed by Arnott.

2.2 Nondestructive Evaluation of Masonry

A major problem in determining the durability of building materials is the difficulty in assessing the deterioration and the identification of proper criterion for evaluating failure. The current ASTM standard freeze-thaw test for durability of bricks specifies a failure criterion based on visual distress and/or percentage loss of weight [ASTM 1993a]. This criterion may not truly represent the actual deterioration of a brick. From his research Arnott [1990] found that bricks could experience significant losses in strength and cracking due to laboratory freeze-thaw cycling while having no appreciable weight. Also, loss in brick strength due to freeze-thaw cycling was not always accompanied by visual distress. Certain nondestructive testing methods have been found to be useful in assessing deterioration of masonry materials [Abrams and Matthys 1991].

2.2.1 Nondestructive Testing Methods

Most of the earlier works on nondestructive testing of building materials were carried out for concrete. Of the various nondestructive methods, Resonant Frequency Method and Ultrasonic Pulse Velocity Method are commonly used for assessing strength and durability aspects of concrete. The resonant frequency of vibration of a material is related to its dynamic modulus of elasticity. Changes in dynamic modulus of elasticity with the deterioration of concrete, subjected

to repeated cycles of freezing and thawing, had been reported by various researchers [Malhotra and Sivasundaran 1991]. The ASTM Test Method C666 [1992b] specifies resonant frequency method for studying the deterioration of concrete specimens subjected to freeze-thaw cycles. The standard requires the calculation of the relative dynamic modulus of elasticity and durability factor. A major disadvantage of this method is that it is purely a laboratory one with no possibility of field application. Other nondestructive evaluation methods for assessing damage, which can be recommended for masonry, include Sonic Pulse Velocity Method, Acoustic Emission Method and Impact Echo Method [Abrams and Matthys 1991].

Sonic testing consists of generating a mechanical pulse with a calibrated impact hammer, and measuring the arrival time of the stress wave with an accelerometer at a distant point. This method can be used to detect delamination as well as the quality of bond between mortar and brick. Acoustic emission method involves listening to a specimen with a very sensitive microphone. Extremely small amounts of released energy can be detected with equipment that is sensitive enough to discern differences in sound patterns. This method has proven useful for detection of cracking in concrete beams. The impact echo method consists of subjecting a structure to a mechanical pulse, and measuring reflected waves with a transducer. The reflection of stress waves off discontinuities within a material can be detected with a sensitive accelerometer. This method can be used for detection of cracks, delamination, and voids.

For studying the pore structure of bricks, ultrasonic method seems to be better suited. In this method, the frequency of pulse can be controlled by selecting the proper transducers. Longer wave lengths for the other methods make them less sensitive to minor voids or fluctuations in material properties. It is also suitable for in situ evaluation of structures.

2.2.2 Ultrasonic Pulse Velocity Method

The Ultrasonic Pulse Velocity (UPV) method has been used successfully to evaluate the quality of concrete for over 50 years [Naik and Malhotra 1991]. Pulse velocity method is an excellent means for investigating the uniformity of concrete. Various researchers had attempted to correlate compressive and flexural strengths of concrete with pulse velocity. Some researchers had established relations between pulse velocity and compressive strength [Malhotra 1976; Naik and Malhotra 1991]. Durability of concrete under freeze-thaw action and under aggressive environments had been studied by various investigators using pulse velocity method. It was found that, in general, there was a reduction in the value of longitudinal pulse velocity, the magnitude of reduction depending on the degree of damage sustained by the specimens.

Ultrasonic pulse velocity method is very simple and easy to carry out. The equipment basically consists of a pulse generator, transmitting and receiving transducers, and a time measuring circuit and display unit. The transducers are used to send and receive pulse through the material to be evaluated. The frequency of the pulse can be varied by changing the transducers. The equipment measures and displays the pulse transit time taken to travel from the transmitting transducer to the receiving transducer. Knowing the length of the path and the transit time, the velocity of pulse can be calculated.

2.2.3 Evaluation of Masonry using UPV Method

So far nondestructive evaluation of masonry has been essentially an adaptation of available methods which have been used for evaluation of concrete [Kingsley et al 1987; Noland et al 1990]. Ultrasonic pulse velocity method has only recently been applied to masonry. These were

mostly exploratory studies, evaluating the feasibility of using nondestructive evaluation methods on masonry structures [Kingsley et al 1987]. A review of earlier studies by Noland et al [1990] showed that ultrasonic pulse velocity measurements could be correlated to masonry prism compressive strength but no generalised relationships were developed. These correlations must be developed for individual structures being assessed. It was found that UPV method was better suited to the detection of flaws than the prediction of compressive strength. Arnott [1990] used UPV method to assess loss in strength of brick subjected to freeze-thaw cycles, for developing durability indices. The loss in strength was determined from the pulse transit time readings taken before and after the freeze-thaw test. Arnott's approach was based on the premise that, brick which lost more strength during freezing and thawing were not as durable as other bricks and would be prone to failure earlier.

The signal strength of the ultrasonic pulse deteriorates rapidly during passage through low density materials, hence limiting their usefulness. Pulse velocity is only a single descriptive parameter of the pulse transmission and that attenuation or frequency analysis may reveal more about material condition than the velocity alone [Noland et al 1990; Sayers 1981]. Since pulse transit time and its attenuation depend upon the porous nature of the material through which it passes, study of correlations between pulse measurements and the properties that are related to pore characteristics seems to be worth attempting.

2.3 Impregnation of Porous Building Materials

Impregnation of porous building materials is mainly carried out to improve the strength and durability aspects. Most of the early studies were on the improvement of concrete properties.

Low viscosity of the impregnating materials is the major factor in deciding the effectiveness of impregnation process. Polymers and sulphur were successfully used for impregnating concrete and mortar specimens. In general, the various materials which may be used for impregnating porous bodies can be broadly classified into three types:

- (i) Polymer based materials which are polymerized after impregnation with the monomer,
- (ii) Materials which melt at reasonable temperature to low viscosity liquids, and
- (iii) Solvent based sealers and other hydrophobic impregnating materials (which are solutions based on polymers).

2.3.1 Impregnation with Polymers

Large scale research on polymer impregnated concrete (PIC) commenced in the United States in 1966 [ACI 1977]. PIC showed significant improvements in strength, absorption characteristics, and resistance against aggressive media. Polymer impregnated specimens are produced by polymerizing the monomer in the monomer saturated specimens. The polymer impregnation process includes: drying the specimens, impregnating them with a selected monomer, and polymerizing the monomer saturated specimens using suitable technique.

2.3.1.1 Monomers for Impregnation

The monomers that have been investigated for impregnation by various researchers include Methyl methacrylate (MMA), Styrene (S), Acrylonitrile (AN), Chlorostyrene (CS), Tert-butyl Styrene (TBS), and Vinyl Acetate (VAc) [ACI 1977; Ramachandran et al 1981]. Viscosity and vapour pressure of the monomers are two important considerations in their selection for

impregnation. The physical properties of common monomers used in polymer impregnated concrete is shown in Table 2.5 [ACI 1977]. In addition, copolymer systems developed by combining different monomers and cross-linking agents (for example, trimethylolpropane-trimethacrylate-TMPTMA) are also used for impregnation. Out of all the monomers, MMA has proved to be one of the most popular impregnants due to its low cost, low viscosity and best results [Ramachandran et al 1981]. Styrene has a relatively higher viscosity compared to MMA but its vapour pressure and solubility in water are low.

TABLE 2.5
Physical Properties of Common Monomers
[ACI 1977]

Monomer	Viscosity at 25°C cP	Density g/cc	Vapour Pressure at 20°C mm of Hg	Boiling Point °C	Solubility in Water at 25°C %
AN	0.34	0.81	85	77	7.4
MMA	0.57	0.94	35	100	1.5 (30°C)
S	0.76 (20°C)	0.91	2.9	135	0.070
CS	1.04	1.11	0.68	180	0.0064
TBS	1.46	0.88	1.0 (46°C)	218	0.0005
VAc	0.43 (20°C)	0.93	115 (25°C)	73	2.5 (20°C)

2.3.1.2 Monomer Loading

Specimens are usually pre-dried to facilitate maximum impregnation. Oven drying at 150°C for 24 hours is recommended to produce high quality product [ACI 1977]. In addition to monomer viscosity and dryness of specimens, the method and duration of soaking also influence the rate and amount of impregnation. Vacuum, pressure and simple soaking methods have been studied to optimize conditions for maximum impregnation in the minimum time [Ramachandran et al 1981; Kukacka et al 1973]. The effect of vacuum and pressure on monomer loading is in the following order: vacuum and pressure > vacuum > simple soaking [Ramachandran et al 1981]. ACI [ACI 1977] recommends the following procedure for monomer impregnation to produce good quality PCI:

- (i) Evacuate oven dry specimens at about 101 KPa (760 mm of Hg) and maintain for about 30 minutes.
- (ii) Introduce monomer under vacuum and subsequently pressurize to about 68.9 KPa (10 psig).
- (iii) Pressure soak for about 60 minutes before removal of specimens for polymerization.

2.3.1.3 Polymerization Process

Polymerization of the monomers can be initiated by radiation, thermal catalysis using chemical initiators and heat, or by the use of promoter-catalyst systems. The radiation process uses gamma rays emitted by cobalt-60 for the production of free radicals necessary for initiating polymerization [ACI 1977; Ramachandran et al 1981]. Radiation polymerization of monomer is practical at room temperature and can occur without the addition of catalysts. But expensive facilities needed limit its use in large scale production.

The simplest method of polymerization is through the addition of small amounts of initiators (or catalysts) which will generate free radicals on heating. The initiators are dissolved in the monomers prior to impregnation. The various initiators that are commercially available include : benzoyl peroxide (BP), azobisisobutyronitrile (AIBN), tert-butyl perbenzoate, α -tert-butyl azoisobutyronitrile [ACI 1977; Ramachandran et al 1981]. These initiators decompose at relatively elevated temperatures to initiate polymerization. BP is well suited for most vinyl monomers such as MMA and Styrene because it decomposes, producing radicals, well below their boiling point.

Polymerization process can also be initiated at ambient temperatures by the use of catalysts in conjunction with certain promoters. Promoters which have been used in PIC systems include: methyl aniline, dimethyl-p-toluidine and cobalt naphthenate [ACI 1977]. Polymerization starts immediately after the promoter and the initiator are added to the monomer. Therefore its use in polymer impregnated systems would be restricted to shallow impregnations.

Evaporation and drainage losses of monomer from the specimens is a major problem during the polymerization process. The various methods that have been studied for reducing these losses include [ACI 1977]:

- (i) Wrapping monomer saturated specimens in polyethylene sheet or aluminium foil.
- (ii) Encapsulation of the specimen in a form during impregnation and polymerization.
- (iii) Polymerization with the monomer saturated specimen immersed in water.
- (iv) Impregnation with monomer followed by a pre-polymer dip prior to wrapping the specimen.

Of the methods studied, under-water polymerization appears to be the most practical for large scale application [ACI 1977]. It is recommended for monomers with lower water solubility. This method has been used successfully in conjunction with radiation and thermal-catalytic polymerization. If the water is saturated with monomer prior to use, very little surface depletion is observed. Under-water polymerization does not have any detrimental effects on the properties of the impregnated specimens. Polymerization can be achieved by using pre-heated water, steam heating, or other methods of heating like keeping in an oven at the required temperature. The polymerization temperature will depend upon the type of monomer selected. For MMA a temperature of about 75°C was found to produce good results [Kukacka et al 1973].

2.3.1.4 Properties of Polymer Impregnated Building Materials

Polymer impregnation results in significant increases in compressive strength, decreases in absorption characteristics and considerable improvements in durability properties of concrete [ACI 1977; De Puy 1975]. Table 2.6 gives the typical properties of PIC specimens, made with different monomers thermal catalytically polymerized [ACI 1977].

The first known experimentation with polymer impregnated clay masonry took place at the University of Texas at Austin in 1969 [Fowler and Fraley 1974; Fraley 1971]. The study included the effect of polymerization of methyl methacrylate on the compressive and flexural strength of prisms made of both high and low strength bricks, and the effect of polymerization on the strengths of mortar and brick. Polymer impregnation improved the compressive strength of common brick prisms and mortar cubes by a factor of 3 to 4. Compressive strength and modulus of rupture of common brick were approximately doubled. The bond between brick and mortar was tested by producing tensile load on the joint. Polymerized specimens showed relatively

high adhesion than control specimens, with a bond strength ratio of 11.45. Table 2.7 shows the various properties of bricks impregnated with MMA monomer and thermal catalytically polymerized using 2% benzoyl peroxide as catalyst [Fowler et al 1974]. Chen et al [1976] also found that impregnation with polymethyl methacrylate (PMMA) could result in significant increases in strength and modulus of elasticity of masonry units.

TABLE 2.6
Various Properties of PIC
[ACI 1977]

Property	Control	Monomer used for PIC				
		MMA	MMA+ 10% TMPTMA	S	CS	AN
Compressive Strength, MPa (psi)	36.28 (5,260)	125.24 (18,160)	131.03 (19,000)	60.62 (8,790)	99.24 (14,390)	74.14 (10,750)
Flexural Strength MPa (psi)	4.59 (666)	5.79 (2,290)	---	7.31 (1,060)	10.90 (1,580)	4.28 (620)
Water Absorption, %	6.4	0.34	0.21	0.70	1.97	5.68
Freeze-Thaw # of Cycles % Wt. Loss	740 25	3,650 2	4,660 0	5,440 21	1,800 10	4,120 6
Sulphate Attack # of days % Expansion	480 0.522	720 0.006	630 0.003	690 0.030	300 0.009	540 0.032
Acid Resistance (15% H ₂ SO ₄) # of days % Wt. Loss	49 35	119 26	-- --	77 29	77 26	70 33

TABLE 2.7
Effects of Polymerization on Properties of Bricks
[Fowler et al 1974]

Property	Type of Brick					
	Common			High Strength		
	Control	Impreg-nated	Polymer Loading	Control	Impreg-nated	Polymer Loading
Compressive Strength, MPa (psi)	62.19 (9,018)	111.00 (16,095)	9.90	95.42 (13,836)	134.14 (19,450)	8.47
% increase		78.48			40.58	
Modulus of Rupture, MPa (psi)	4.66 (676)	11.19 (1,623)	11.10	9.03 (1,309)	15.11 (2,191)	3.32
% increase		140.00			60.50	
24 hr. Water Absorption, %	8.72	1.54	11.00	1.65	0.19	3.78
% reduction		82.34			88.48	
5 hr. Boiling Water Abs., %	11.20	2.68	11.00	2.39	0.38	3.78
% reduction		76.07			84.10	
Saturation Coefficient	0.780	0.620	11.00	0.694	0.407	3.78
% reduction		20.51			41.35	

2.3.2 Impregnation with Sulphur

The price of monomers and the relatively low viscosity of molten sulphur makes it a very

attractive substitute for polymers in impregnating porous bodies [Chen et al 1976]. There is the additional reduction in process cost with the elimination of the polymerization step required in the polymer impregnated materials. The process normally employed for sulphur impregnation is as follows [Ramachandran et al 1981; Al-Hadithi et al 1987; Chen et al 1976]. Samples are dried in an oven at about 150°C to constant weight to remove the evaporable water in the pores. They are then immersed in a vessel containing molten sulphur and maintained at about 150°C by suitable heating methods. At the end of the specified period of immersion, the samples are removed from the sulphur and air cooled.

Study by Shah et al [1978] showed that sulphur impregnation could increase the compressive strength, flexural strength, and modulus of elasticity of concrete specimens by about 2 to 5 times those of the corresponding control specimens. Based on a study on long term strength and durability of concrete impregnated with sulphur, Malhotra et al [1978] reported that sulphur impregnated concrete specimens performed excellently under exposure to repeated cycles of freezing in air and thawing in water. Impregnation of concrete with sulphur considerably increased its resistance to attack by acidic solutions, but not to attack by alkaline solutions.

Studies were also conducted to evaluate properties of bricks impregnated with sulphur [Al-Hadithi et al 1987; Chen et al 1976; Ravaglioli et al 1976]. It was found that impregnation could significantly increase the strength and modulus of elasticity. There was substantial reduction in water absorption for sulphur treated bricks as compared to untreated units. There was virtually no acid attack on sulphur treated blocks. Ravaglioli et al [1976] investigated the effect of sulphur impregnation on pore size distribution and frost resistance of fired ceramic bodies. They found that impregnation process improved the frost resistance of all the tested samples. A general

shifting of the pore classes towards smaller diameter classes was observed. It was also observed that impregnation resulted in decrease in pore diameter classes between 0.25 to 1.4 μm .

A major disadvantage with sulphur impregnation of bricks is the yellow colour imparted to the surface due to sulphur coating. This could be of concern for facing bricks unless certain treatments are carried out to remove or conceal this coating.

2.3.3 Impregnation with Paraffin

Paraffin is a macrocrystalline wax derived from petroleum and is a by-product of the oil refining process. Paraffin can be used for impregnating porous materials because of its low viscosity on melting. It is also an hydrophobic material. Petroleum paraffin waxes normally have melting point around 60°C. In addition to these waxes, high melting point synthetic waxes are also available in the market today. One such synthetic wax, by the trade name PARAFINT [Stochem 1994] has the melting point between 90 and 100°C and is synthesized from coal.

Hawes [1991] carried out studies on paraffin as a phase change material in concrete. He found that impregnation with paraffin resulted in significant reduction in water absorption of concrete specimen. He also observed that concrete specimens impregnated with paraffin showed better frost resistance and no change was found even after 560 cycles of freezing and thawing.

Impregnation procedure for paraffin is similar to sulphur impregnation. Paraffin is heated in a vessel until it melts, using suitable heating methods and the temperature of the system is maintained at 80 to 120°C depending on the type of paraffin used. Dried samples are kept immersed in the molten bath for the specified duration. At the end of the period, they are removed

from the bath and air cooled. Impregnation process is simple and relatively inexpensive. Unlike sulphur, paraffin does not affect the appearance of facing bricks. The only concern is the bond between brick and mortar.

2.3.4 Sealers and other Hydrophobic Materials for Treatment

Various types of sealers are commercially available for water repellent treatments on materials. Most of these sealers were initially developed for treatment on concrete surfaces. Materials that have been used as sealers on concrete surfaces include : epoxies, silicones, acrylics, linseed oil, polyurethanes, sodium silicate and silicofluorides of zinc and magnesium [Gabor et al 1991; Mailvaganam et al 1990; Marusin 1989].

Acrylic materials are polymers of esters based on acrylic or methacrylic acids, and are used with different types of solvents. Acrylic resins were found to be effective sealers. Some of the most effective and more widely used products for providing water repellency in concrete and masonry structures are the organosilicon compounds, collectively referred to as silicones. These materials are used as emulsions or as solutions to impart a colourless water repellent surface finish to concrete and masonry [Mailvaganam et al 1990]. Some studies had shown that silicone resins not only lowered freeze-thaw resistance, but also did not prevent the ingress of chlorides into the concrete. A recent study by Litvan [1992] on mortar specimens treated with sealers showed that even though water absorption was reduced, the freeze-thaw resistance was lowered due to the treatment.

As sealers may adversely affect the freeze-thaw durability, materials which can impregnate the pores are better suited for improving durability. A product information brochure by Wacker

Chemie, Germany [Wacker Chemie] introduces silicone micro emulsions as aqueous impregnating agents for masonry. These aqueous impregnating agents form hydrophobic zones in the masonry and promise to be effective in damp proofing.

2.4 Summary of the Review

The review has shown that, in addition to porosity, pore size distribution is also an important factor influencing the frost durability of bricks. It can be concluded that pores larger than 3 μm in diameter have no adverse effect on frost resistance of bricks whereas pores smaller than 1 μm are harmful. The current American and Canadian standard specifications and test methods for evaluating durability of clay bricks are time consuming and reported to be inadequate in certain cases. The criteria mentioned in the ASTM do not take into account the distribution of pore size. Thus there is a need for developing proper relationships between the properties of bricks and their frost resistance, so that indices can be derived which can be used for reliable assessment of durability in short time.

The durability index developed by Robinson et al [1977] is based on brick properties mentioned in ASTM C67 and does not consider the influence of pore size distribution. The indices suggested by Nakamura and Arnott can only be used for comparing the durabilities of bricks and thus have limited use. Maage's frost resistance number is simple and relatively fast to determine and has been validated by other researchers. It takes into consideration the effects of porosity and pore size distribution and is regarded as reliable for predicting the frost durability of bricks. Maage's method is based on mercury intrusion porosimetry and thus is an expensive and destructive test.

It was found from the review that nondestructive testing methods have been extensively used to assess the quality of concrete. Research on the use of these methods for the evaluation of brick masonry has been very limited. Of the various nondestructive testing methods, ultrasonic pulse velocity is better suited for studying those properties that are related to pore structure of bricks. Since the attenuation of pulse depends upon the porous nature of the material through which it passes, study of pulse characteristics might be used to evaluate certain brick properties. More studies are needed on the feasibility of using nondestructive methods for evaluating frost durability.

Most of the earlier studies on the effect of impregnation were carried out on concrete specimens. The review has shown that impregnation with polymers and sulphur resulted in increased strength, reduced water absorption, and improved freeze-thaw resistance for concrete and brick specimens. A major concern in the case of sulphur impregnation of facing bricks is the yellow colour imparted to the surface due to sulphur coating. Concrete specimens impregnated with paraffin also showed significant reduction in water absorption and improved frost resistance but the bond between brick and mortar is a concern. Impregnated bricks can be used for locations where high level of saturation and severe weather conditions are expected. In the absence of detailed studies on the effect of impregnation on water absorption properties, pore size distribution, and durability of clay bricks, more research work is needed in this regard.

Research Methodology

3.1 Research Overview

As mentioned earlier, this research primarily concentrates on three objectives. They are: to develop a durability index based on easily measurable physical properties of bricks, to study the feasibility of using nondestructive evaluation method for assessing frost durability, and to study the effect of impregnation on the properties of bricks. This chapter discusses the methodology adopted to achieve these objectives.

3.1.1 Development of Durability Index

The best method of developing a durability index is by relating the properties of bricks to their field performance. As it takes many years to collect data from field performance studies, development of index from such data is not attempted. Therefore the usual method involves subjecting the bricks to accelerated freezing and thawing test in laboratory and then relating the observed performance to the measured properties of the bricks using suitable statistical applications.

In order to determine the limiting values of an index for durable and nondurable bricks, the laboratory performance test should be able to identify durable and nondurable bricks or it should be related to field performance. If the laboratory test used cannot identify whether the bricks are durable or not, then the index developed from such a test can only be used for measuring the relative durabilities of bricks.

The research procedure adopted for the development of a new durability index is shown as a block diagram in Figure 3.1. The bricks were tested for various physical properties and accelerated freeze-thaw performance. A comparative study of the existing durability indices was carried out to determine the method to be used for deriving the new index. The results of the comparative study and the derivation of the new durability index are discussed in Chapter 5.

3.1.2 Nondestructive Evaluation of Durability

The different nondestructive testing methods that are currently in use for evaluating the properties of materials have been discussed in detail in Section 2.2.1. Out of these methods, ultrasonic pulse velocity method seems to be better suited for evaluating durability of bricks. This is due to the fact that brick durability is found to depend to a large extent on its porosity and pore size distribution and that changes in pore structure results in variations in pulse velocity through the material. Therefore pulse velocity measurements may be used to relate to properties of brick and thereby possibly to evaluate its durability.

The research procedure adopted for the feasibility study on nondestructive evaluation of durability is shown as a block diagram in Figure 3.2. The bricks were tested for compressive strength, water absorption properties, and pulse velocity. Using the test data and those available

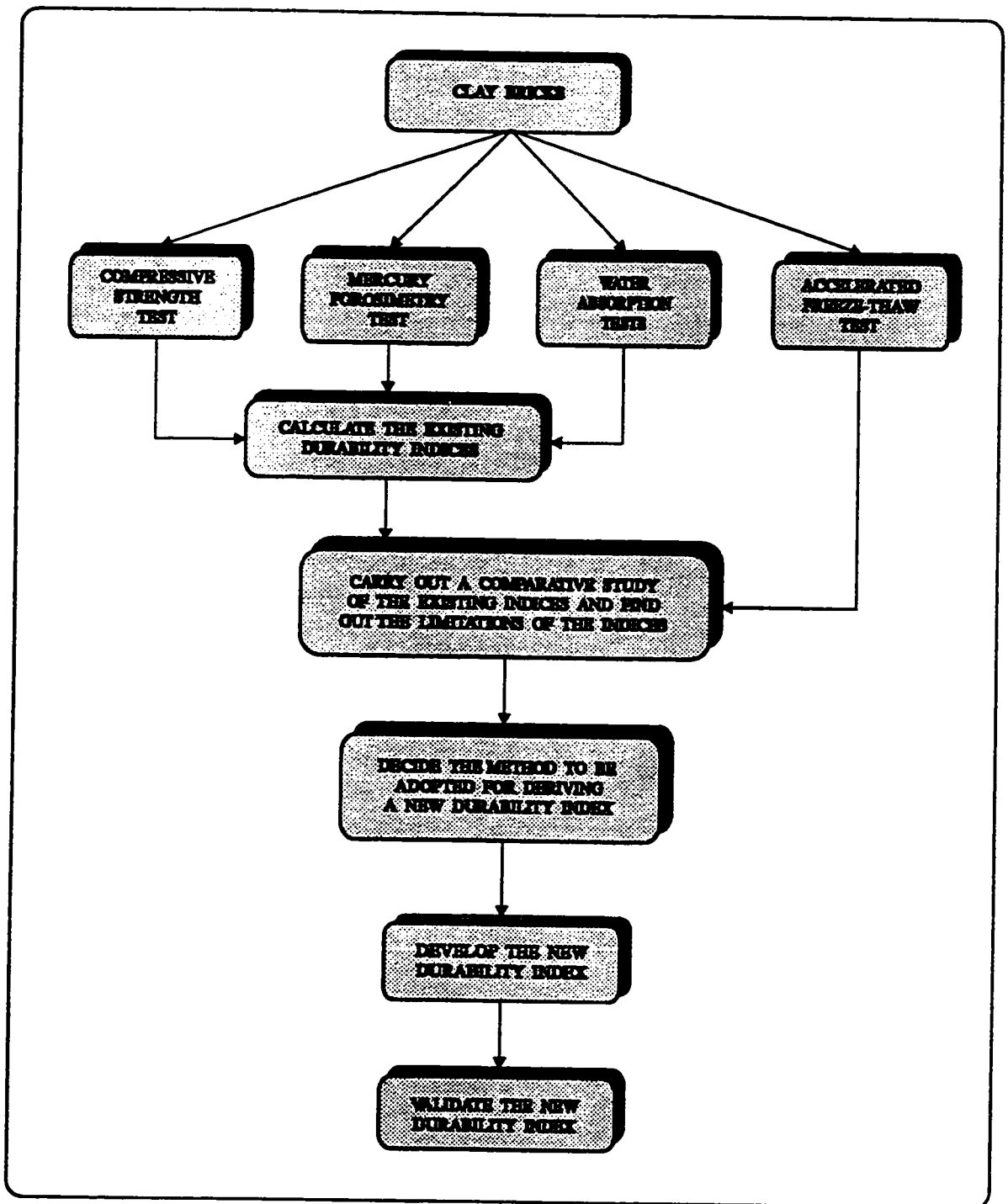


Figure 3.1 Research procedure adopted for the development of Durability Index

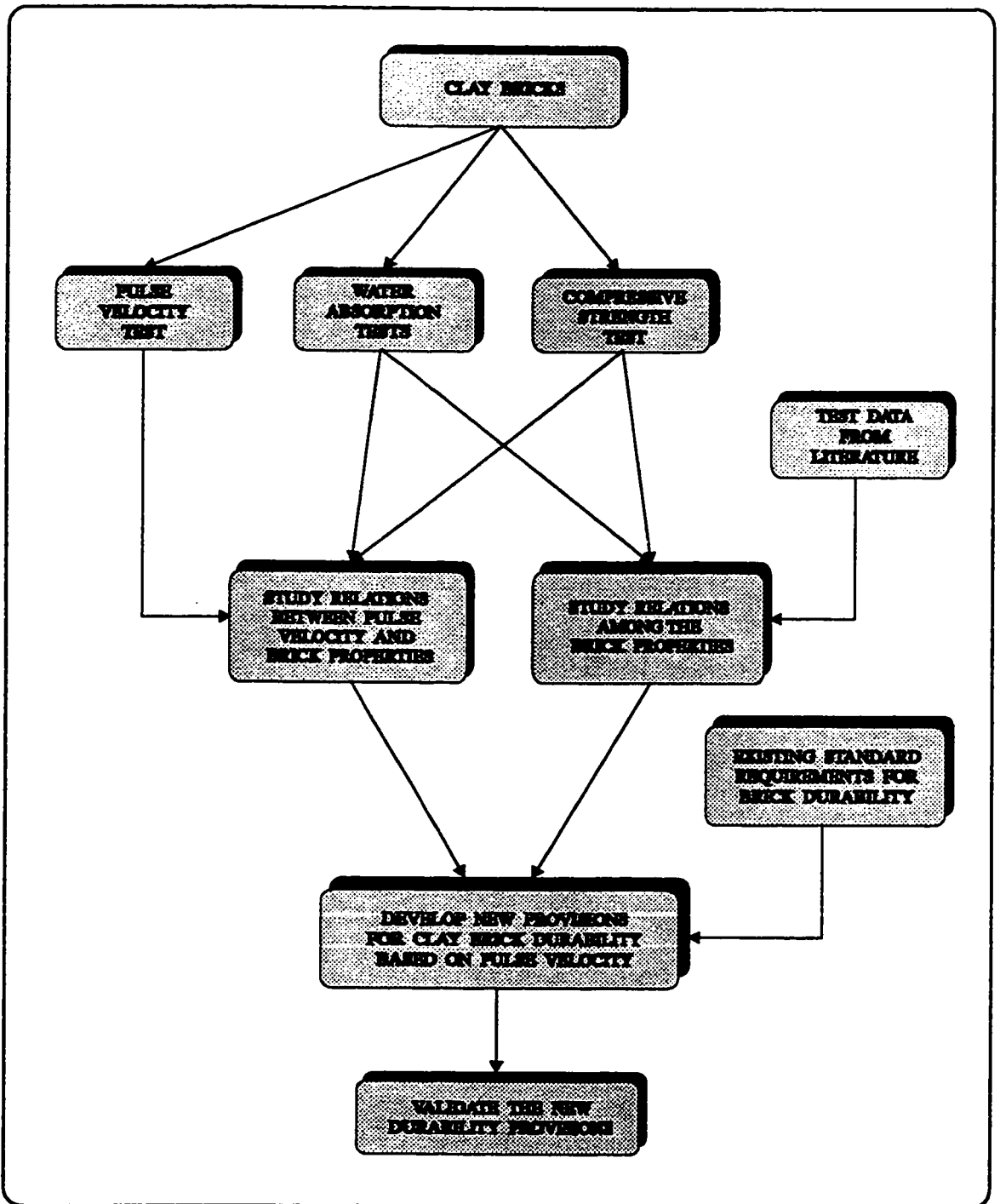


Figure 3.2 Research procedure for feasibility study on nondestructive evaluation of durability

from earlier studies, relations were developed between the properties of bricks. The new durability provisions based on pulse velocity were derived by using the above relations and the existing provisions for durability specified in American Standard ASTM C216 [ASTM 1992a]. The derivation of the provisions for nondestructive evaluation of durability is discussed in Chapter 6.

3.1.3 Effect of Impregnation on Durability

This part of the research studies the improvement of brick durability due to impregnation with different materials. Apart from frost resistance, the other properties that were studied include water absorption properties, pore size distribution, compressive strength and ultrasonic pulse velocity. The research procedure adopted for the studies on impregnated bricks is shown as a block diagram in Figure 3.3. In addition to impregnated bricks, one set of control bricks were also tested for each type of brick studied. Comparing the test results of control and impregnated bricks, the improvement in properties could be known. The results from the study are discussed in Chapter 7.

The bond between brick and mortar is important for satisfying the performance requirements of a building envelope. In order to study whether impregnation with different materials would adversely affect the bonding, bond strength tests were also conducted on control and treated specimen.

3.2 Selection of Materials

Basically two materials are involved in this research, namely bricks and impregnating materials.

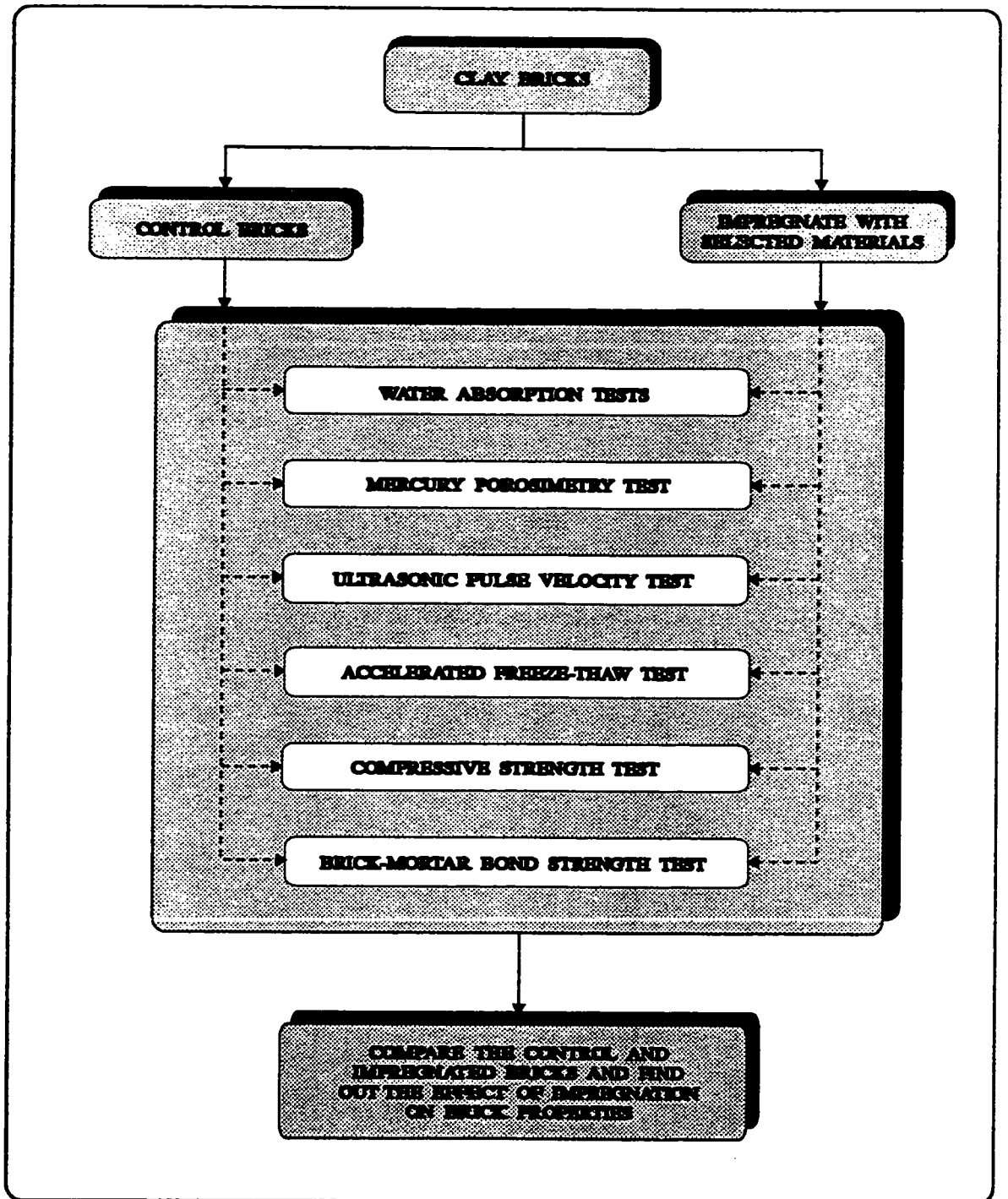


Figure 3.3 Research procedure for studies on effect of impregnation on brick properties

3.2.1 Bricks

Commercially marketed clay bricks were chosen for this research so that the results could be extended to bricks used in practice. The bricks were obtained from local vendors in Montreal, Quebec. Nine different types of bricks were selected for developing durability index and for the feasibility study on nondestructive evaluation of durability. Four types of bricks were used for studying the effect of impregnation on brick properties. In addition to these, 3 more types of bricks were used to validate the experimental results. Figure 3.4 shows the brick types used in this research. Details of the bricks are given in Table 3.1. The various properties of the bricks are discussed in detail in Chapter 4.

3.2.2 Impregnating Materials

Three broad categories of impregnating materials were discussed earlier in Section 2.3. The merits and demerits of different materials for impregnating brick were also discussed. The impregnating materials used in this research were selected based on those information. The materials were selected such that all the three categories were represented. The following materials were chosen in this research:

- (i) Methyl Methacrylate (a vinyl monomer)
- (ii) Paraffin, and
- (iii) Acrylic Sealer

Methyl methacrylate (MMA) falls under the first category of impregnating materials discussed in Section 2.3. MMA is one of the most popular monomers and has been used successfully for impregnating porous materials. MMA monomer used in this study was produced

TABLE 3.1
Details of Brick Types Selected

Brick Type	Method of Molding	Type of Study	Brick Types Used
A	Dry Pressed	1. Development of Durability Index	A,B,C,D,E,F,G,H,J
B	Dry Pressed		
C	Dry Pressed		
D	Extruded	2. Feasibility Study on Nondestructive Evaluation	A,B,C,D,E,F,G,H,J
E	Extruded		
F	Extruded		
G	Extruded	3. Studies on Impregnated Bricks	A,B,C,F
H	Dry Pressed		
J	Extruded		
K	Extruded	4. Validation of Experimental Results of 1 & 2	K,L,M
L	Extruded		
M	Dry Pressed		

by Fischer Scientific, New Jersey, USA and contained about 25 ppm of hydroquinone as inhibitor to prevent polymerization while storing. It was decided to use benzoyl peroxide (BP) as the catalyst for initiating polymerization. BP is widely used as initiator with MMA and it decomposes well below the boiling point of MMA. The amount of initiator required was decided based on review of earlier works and also a preliminary study carried out with MMA monomer. Different percentages of BP initiator were mixed with MMA and polymerized by keeping their mixture in

oven at about 75°C. Also small brick slices were dried and immersed in MMA with initiator for about 1 hour. The monomer saturated specimens were then polymerized by immersing in hot water at about 75°C. 0.5, 0.7, 1, 1.5, 2, and 3 % of initiator by weight of monomer were studied and it was found that 1 % of BP was just sufficient to cause successful polymerization. It was observed that when the amount of initiator was lower than 1 %, polymerization rate was very low and the loss of monomer was considerable. With higher amounts of initiators, there was brisk polymerization causing the monomer to foam.

Paraffin belongs to the second category of impregnating materials. Two types of paraffin were used in this research, which are known by their trade names as UNICERE 62 and PARAFLINT H1. They were supplied by Stochem Inc., Lachine, Quebec. UNICERE 62 is a fully refined paraffin wax having melting point around 62°C whereas PARAFLINT H1 is a high melting point synthetic wax having melting point around 98°C. The relevant properties of these two waxes are given in Table 3.2 [Stochem 1994].

Sealers are usually applied as water repellent coatings on surfaces. The present study will look in to the effect of sealers when used for impregnating bricks, rather than as surface coatings. A variety of different sealers are available in the market nowadays for application on concrete and brick surfaces. Among them Acrylic sealers are widely used and therefore in this research it was selected for impregnation. The sealer used in this study was Mastercraft Acrylic Sealer produced by Canadian Tire Corporation Limited, Toronto. This sealer is recommended for all concrete and masonry surfaces and has a coverage of up to 93 m² (1000 sq. ft) per 4 litres.

TABLE 3.2
Properties of Paraffin used
 [Stochem 1994]

Property	Typical Values	
	UNICERE 62	PARAFLINT H1
Melting Point, °C (ASTM D 87)	61.67	-
Congealing Point, °C (ASTM D938)	-	97.8
Color, Saybolt (ASTM D 156)	+ 28	+ 30
Viscosity	41 Saybolt @ 98.89 °C (SUS) (ASTM D88)	8 cP @ 135°C (ASTM D2669)
Needle Penetration at 25°C, mm/10 (ASTM D1321)	14	1
Flash Point (COC), °C (ASTM D92)	257.22	204.44

3.3 Preparation of Specimens

All tests in this study were done on half bricks because in such a case two destructive tests could be performed on a single brick. First of all, the bricks used for the experimental study were cut into two halves using a diamond saw. The bricks were cleaned with a wire brush and washed in water to remove loose particles. They were then dried in oven at 110°C for 24 hours and cooled to room temperature in a desiccator before subjecting to any tests or impregnation process. Figure 3.5 shows the desiccator that was fabricated for cooling and storing the brick specimens.

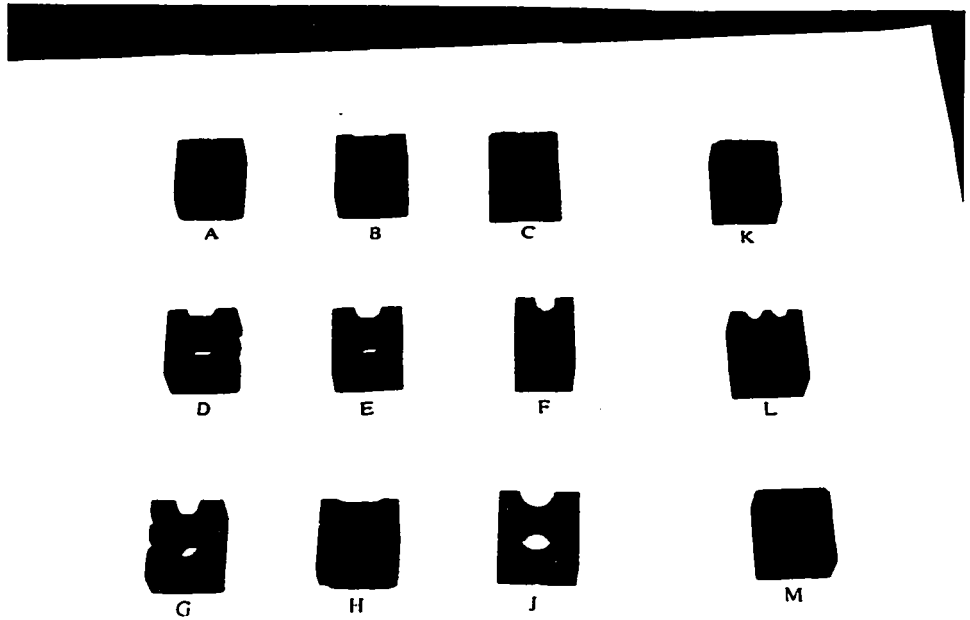


Figure 3.4 The different types of bricks used in this research

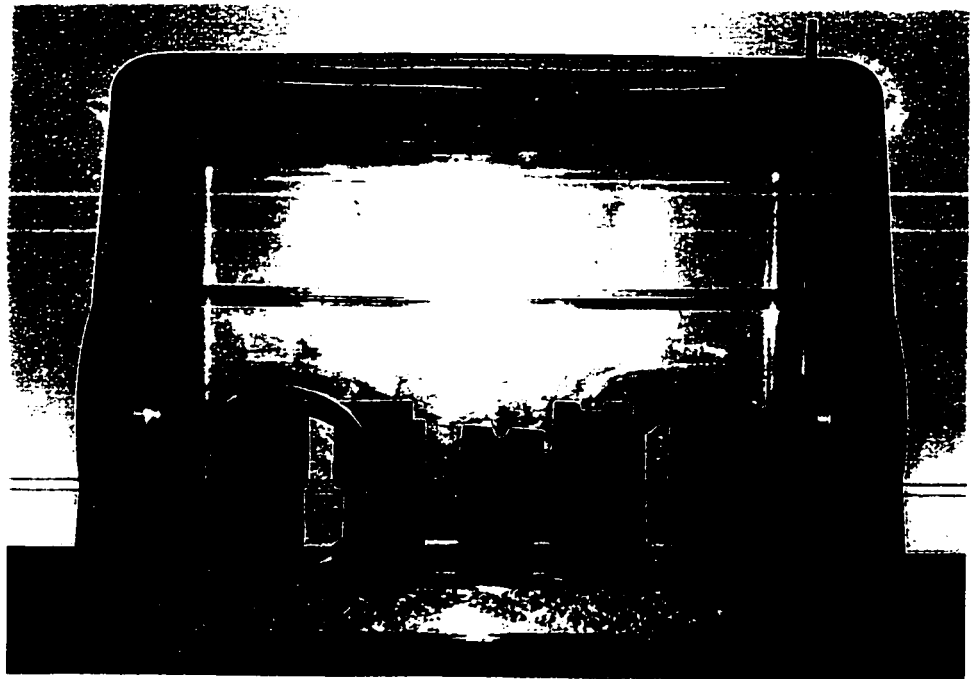


Figure 3.5 The desiccator used for cooling and storing dried specimens

The properties of bricks may vary widely within a brick type. In order to make sure that an average of 3 or 5 bricks represents the true average, it was decided to divide a brick type into small groups having a 24 hour water absorption interval of 2%. The different brick group designations and their corresponding absorption ranges are given in Table 3.3. Based on this classification a brick group designation of B4 refers to bricks of type B having 24 hr. water absorption between 6 and 8% and so on.

To group the bricks, clean dry specimens were immersed in cold water for 24 hours and their % absorptions after 24 hours were calculated. Based on the absorption values, the bricks were assigned the respective group designation. Tests were conducted on each brick group as if they were different brick types.

TABLE 3.3
Absorption Ranges for Brick Group Classification

Brick Group Designation	24 Hr. Absorption Range, %
1	0 - 2
2	2 - 4
3	4 - 6
4	6 - 8
5	8 - 10
6	10 - 12

3.4 Impregnation Procedure

3.4.1 Impregnation with Polymer

In general the polymer impregnation process involved 3 distinct stages: preparation of specimen, soaking, and polymerization of monomer saturated specimen.

3.4.1.1 Soaking of Specimen

Monomer saturation of specimens was achieved by soaking the specimens for the specified time in monomer. Prior to soaking, BP initiator was dissolved in MMA monomer. Two methods of soaking were studied: one simple soaking at atmospheric pressure and the other under vacuum. Impregnation under vacuum was expected to give higher monomer loading.

For soaking at atmospheric pressure, clean and dry specimens were weighed and kept in a vessel. MMA monomer was then poured into the vessel until the specimens were fully immersed. The specimens were kept immersed in the monomer for about 4 hours and were subsequently removed for polymerization.

The impregnation under vacuum was carried out in a chamber made by modifying an existing vacuum oven of internal dimensions 24W x 29D x 24H cm. Figure 3.6 shows the vacuum chamber used for impregnation. A tube with valve was fitted into the chamber to introduce liquids under vacuum. Evacuation of the specimens was carried out by using a vacuum pump attached to the chamber. The soaking procedure adopted for impregnation involved keeping the dry specimens, after finding their weights, in a vessel and evacuating them for 30 minutes at a vacuum of 740 mm of mercury. Then monomer was introduced into the vessel through the tube till the

specimens were completely submerged. The vacuum was then released and atmospheric pressure was maintained in the chamber. The specimens were kept immersed for 1 hour before being taken for polymerization.

3.4.1.2 Polymerization

Polymerization was carried out by subjecting the monomer saturated specimens to heat. In order to reduce monomer loss by evaporation, specimens were kept immersed in warm water in a vessel and heated in an oven at around 75°C. Polymerization was normally completed within 2 hours but the specimens were kept immersed in hot water overnight to make sure that all the impregnated monomer was fully polymerized. At the end, the specimens were removed from the hot water, dried at 100°C for 24 hours and weighed to determine the polymer loading.

3.4.2 Impregnation with Paraffin

Impregnation with paraffin involved heating the paraffin in a constant temperature bath until it melted to low viscosity. The temperature of the molten paraffin bath was maintained at around 80°C for UNICERE 62 and 120°C for PARAFINT H1 wax. Dry brick specimens were weighed, preheated at a temperature around that of molten paraffin bath and then kept immersed in it for about 4 hours. After the specified period of soaking, impregnated specimens were removed from the bath, allowed to cool at room temperature for solidification of paraffin and weighed to determine paraffin loading. Figure 3.7 shows the constant temperature bath used for paraffin impregnation.

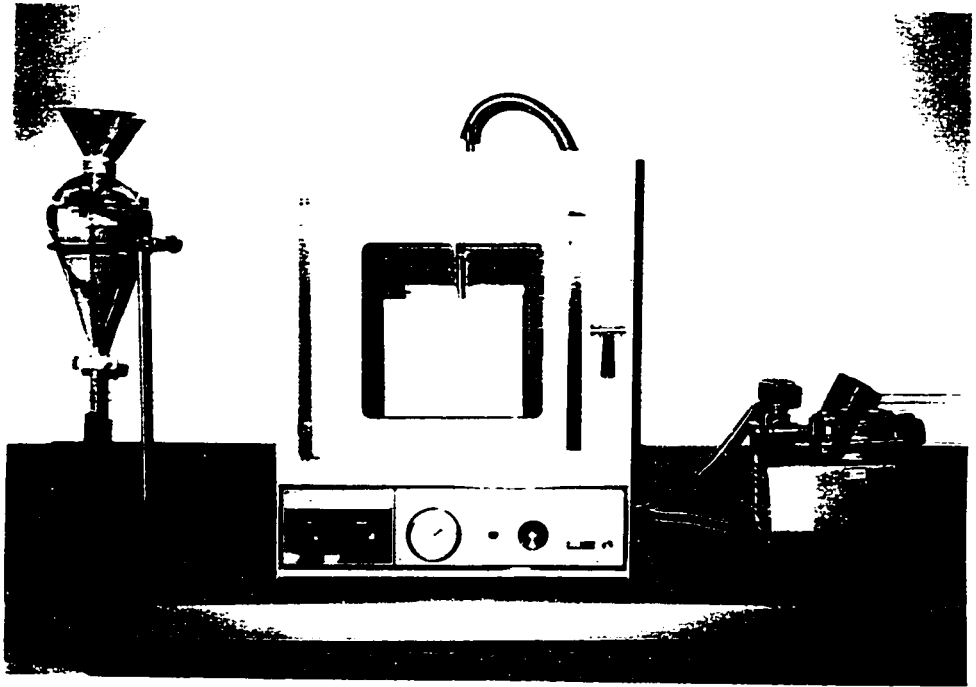


Figure 3.6 The vacuum chamber used for impregnation and vacuum saturation

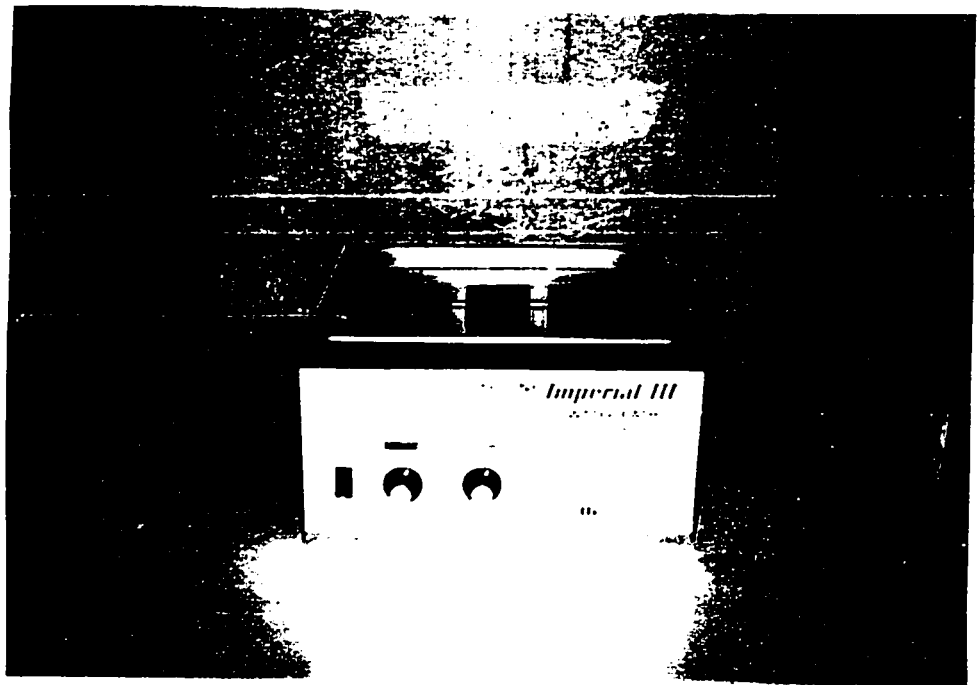


Figure 3.7 The constant temperature bath used for paraffin impregnation

3.4.3 Impregnation with Acrylic Sealer

Dried specimens were weighed and kept in a vessel. Acrylic sealer was poured into the vessel until the specimens were fully immersed. The soaking was continued for 4 hours, at the end of which, the specimens were taken out and dried in air for 3 days. The impregnated specimens were then dried in an oven at 60°C for 24 hours and weighed.

3.5 Test Procedures

The procedures adopted for the various tests used for the experimental study in this research work are discussed in detail in this section.

3.5.1 Water Absorption Tests

Absorption tests provide a rough estimate of the porosity of the bricks and the degree of saturation attained by the specimens. Four different absorption tests were performed to obtain the absorption characteristics of the specimens. They were capillary absorption test, submersion test, boiling absorption test, and vacuum saturation test.

3.5.1.1 Capillary Absorption Test

Capillary absorption test measures the amount of water absorbed by the brick specimens through capillary action. In a typical wall exposed to rain, the major mechanism of water absorption is capillary suction. With more capillary pores the chance of brick getting saturated increases, there by affecting frost durability.

The test was carried out in a rectangular tank of size 48L x 38W x 29H cm, specially designed and fabricated for it. The specimens were supported on level supports at a height of 25 mm from the bottom of the tank. Water level in the tank was maintained at a height of 3 mm above the top of the supports with an overflow mechanism. This level was maintained for the entire duration of test by connecting it to water supply line. Figure 3.8 shows the experimental set-up used for the capillary absorption test. Dry specimens were brought into contact with the water surface and the increases in weights after 1, 2, 4, 5, 8, 10, 15, 30 minutes, 1, 2, 4, 8, and 24 hrs. were noted. Knowing the amount of water absorbed and the base area of the bricks in contact with water, the capillary absorption by the bricks can be calculated for the specified time intervals. The amount of absorption was expressed as % of dry weight, % of 5 hr. boiling water absorption, and also as absorption per unit area.

3.5.1.2 Submersion Test

24 hr. absorption value is commonly used and it gives a rough estimate of the maximum amount of water that is possibly absorbed by a brick under normal circumstances. This test was carried out in a similar way as mentioned in ASTM C67. Dried specimens were immersed in water at room temperature and increases in weights were noted after 1, 2, 4, 5, 8, 10, 15, 30 minutes, and 1, 2, 4, 8, and 24 hrs. and expressed as % of dry weight. The test was carried out in the same tank that was used for capillary absorption test.

3.5.1.3 Boiling Absorption Test

This test was carried out as per ASTM C67. Dried specimens were kept immersed in boiling water for 5 hours. The specimens along with the hot water were allowed to cool overnight and the increases in weights of the bricks were noted and expressed as percentage of the

corresponding dry weights. The boiling water absorption test set-up used in this study is shown in Figure 3.9.

3.5.1.4 Vacuum Saturation Test

The ASTM C216 specifies 5 hr. boiling water absorption as one of the criteria for assessing durability of bricks. In the case of impregnated bricks, most of the impregnants will be damaged when subjected to the boiling test. Hence it was found necessary to develop an alternative test. Vacuum saturation was carried out to replace the boiling water absorption.

The test was performed in the same chamber used for impregnation (see Figure 3.6). Dry specimens were evacuated at a vacuum of 740 mm of Hg. for 30 minutes. Then water was introduced into the chamber under vacuum till the specimens were completely immersed. Vacuum was then released and the specimens were kept immersed in water for 1 hour. At the end of absorption period, specimens were taken out, surface water removed with a wet cloth and weighed.

A preliminary study was conducted to compare the vacuum saturation and boiling absorption tests. The results of the study are given in Table 3.4. It could be seen that the vacuum saturation process mentioned above gave almost the same absorption values as the 5 hr. boiling test. In the experimental methodology used for this research, the 5 hr. boiling water absorption test was replaced with the vacuum saturation test for the impregnated specimens and the saturation coefficient was calculated based on vacuum saturation value as:

$$\text{Saturation Coefficient} = \frac{24 \text{ hr. Water Absorption}}{\text{Vacuum Saturation}}$$



Figure 3.8 The experimental set-up used for the capillary absorption test

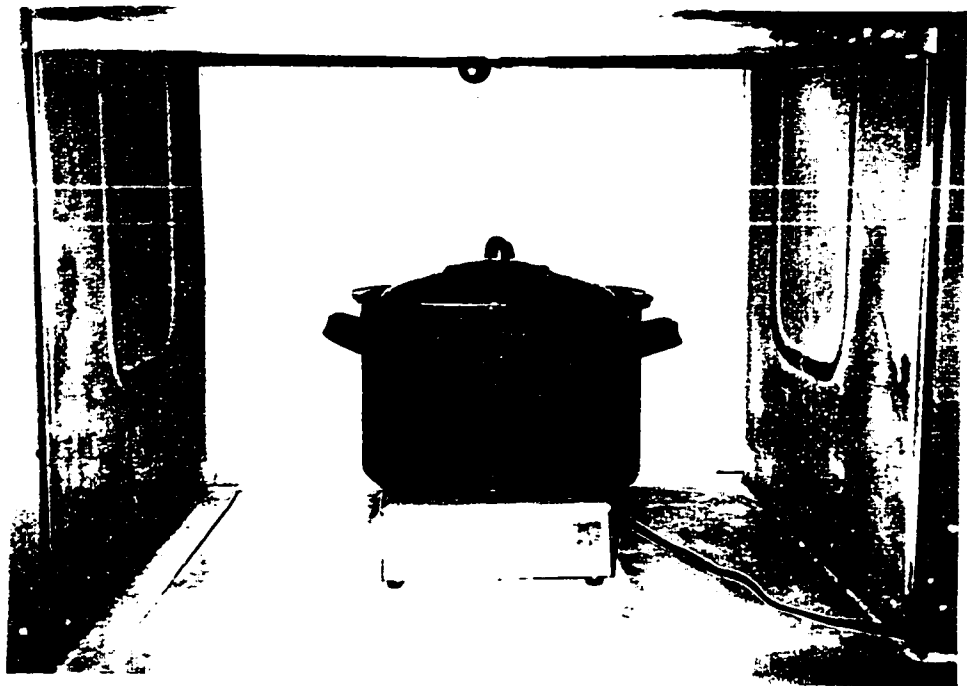


Figure 3.9 The boiling absorption test set-up used in this study

TABLE 3.4
Comparison of Vacuum Saturation with
Boiling Water Absorption

Brick Type	24 hr. Water Absorption (C) %	5 hr. Boiling Water Absorption (B) %	Vacuum Saturation (V) %	Saturation Coefficient (Boiling) (C/B)	Saturation Coefficient (Vacuum) (C/V)
A	5.12	9.59	9.54	0.53	0.54
B	4.52	9.47	9.71	0.48	0.47
C	7.17	11.88	11.96	0.60	0.60
D	4.05	5.35	5.38	0.76	0.75

3.5.2 Mercury Intrusion Porosimetry

The porosity and pore size distribution of bricks were determined using high pressure mercury intrusion porosimetry. The instrument used for the study was PoreSizer 9320 manufactured by Micromeritics Instrument Corporation, Norcross, U.S.A. The porosimeter used in this research is shown in Figure 3.10.

PoreSizer 9320 is a 207 MPa (30,000 psi) mercury porosimeter covering pore diameter range from approximately 360 to 0.006 μm . The unit has two built-in low pressure ports and one

high pressure chamber. Data collection, data reduction and data display are processed by the control module. The PoreSizer measures the volume distribution of pores in materials by mercury intrusion or extrusion [Micromeritics 1993].

Mercury porosimetry is based on the capillary law governing liquid penetration into small pores. In the case of a non-wetting liquid like mercury and cylindrical pores, the relationship between pressure and size of pore is given by the Washburn equation [ASTM 1984]:

$$D = \frac{-4 \gamma \cos\theta}{p} \quad [3.1]$$

where, D = pore diameter
 p = applied pressure
 γ = surface tension, and
 θ = contact angle (all in consistent units).

The volume v of mercury penetrating the pores is measured directly as a function of applied pressure, p . This p - v information serves as a unique characterization of pore structure [Micromeritics 1993]. In this study, values of $\gamma = 485$ dynes/cm and $\theta = 124^\circ$ were used based on review of earlier works [Kayyali 1985; Maage 1984; Metz and Knofel 1992; Micromeritics 1993; Muresan 1973; Winslow 1978; Winslow and Diamond 1970].

Samples approximately 15 mm in diameter and about 24 mm in length were used for testing. They were cored out from the middle of the brick samples using a core drilling machine and then cut into the specified length with a cutting saw. The core drilling machine and the fine cutting saw used for preparing the specimens are shown in Figure 3.11. The porosimeter was run

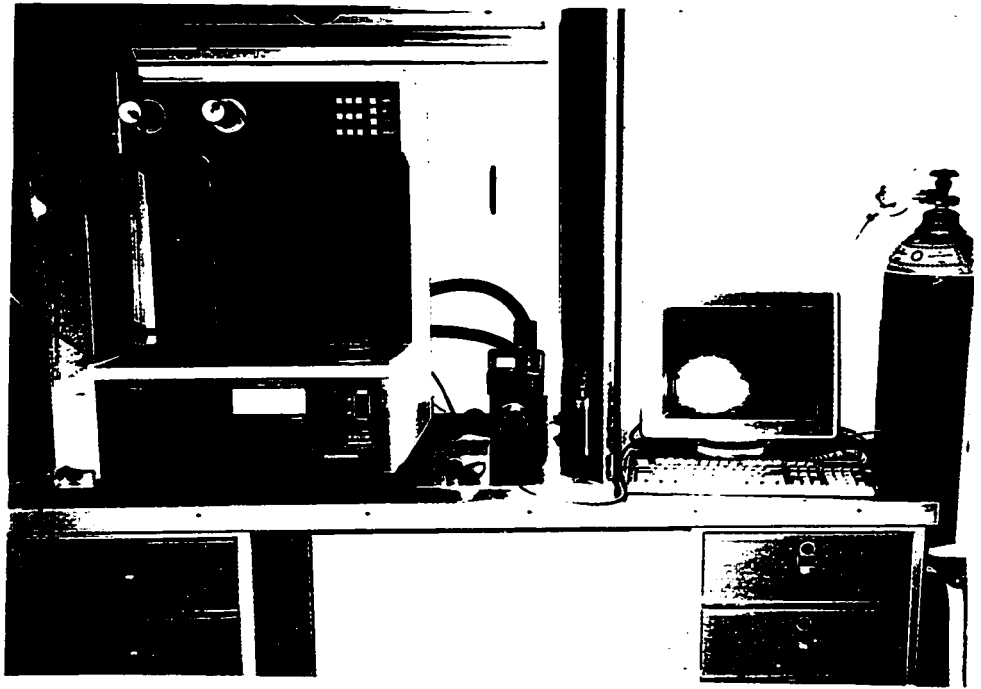


Figure 3.10 The Mercury Intrusion Porosimeter: PoreSizer 9320
(Micromeritics Instrument Corporation, Norcross, U.S.A)

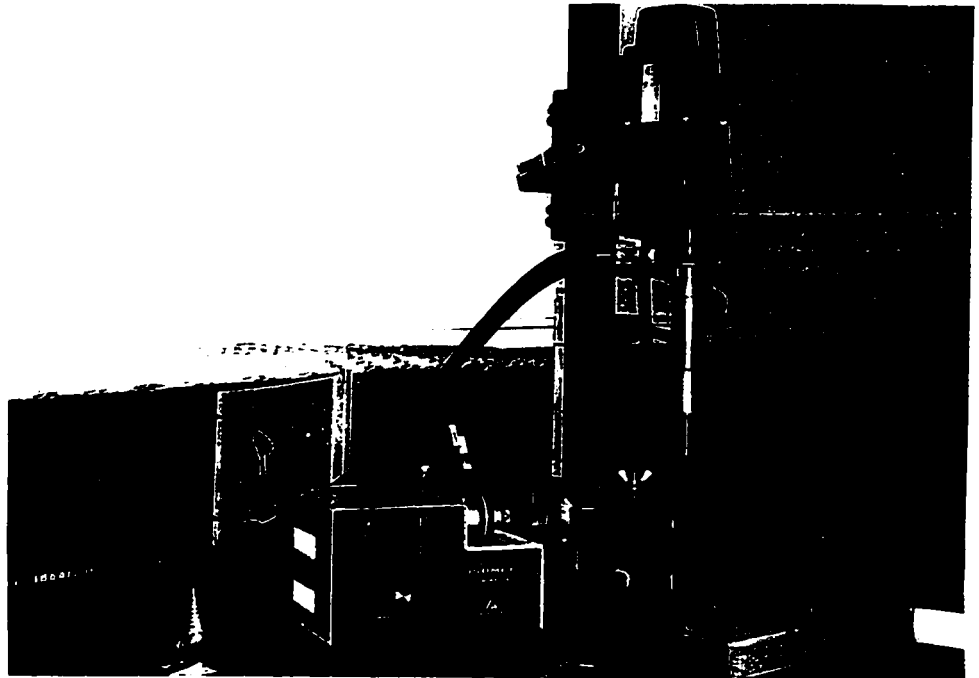


Figure 3.11 The core drilling machine (right) and the fine cutting saw (left) used
for making specimens for mercury intrusion porosimetry

automatically using a control module. The test results provided by the instrument included: bulk density (*BD*), porosity (*P*), average pore diameter (*APD*), median pore diameter (*MPD*), pore area (*PA*), intrusion volume (*PV*), and pore size distribution (*PSD*).

3.5.3 Ultrasonic Pulse Velocity Test

Ultrasonic testing method is adopted in this study mainly to find relations between brick properties and the velocity of the transmitted pulse coming through the material. The instrument used for the test was a Portable Ultrasonic Nondestructive Digital Indicating Tester (PUNDIT) manufactured by C.N.S. Electronics Ltd., London, U.K. It consists of a pulse generator, transmitting and receiving transducers, a receiver amplifier, time measuring circuit, and a time display unit. The pulse velocity testing equipment and test set-up is shown in Figure 3.12.

The PUNDIT instrument measures the ultrasonic pulse transit time along the shortest path through the material. Knowing the shortest path length of the pulse (for direct transmission of pulse, shortest path length is the distance between transmitting and receiving transducers), the pulse velocity can be calculated as [ASTM 1983; ASTM 1992c]:

$$V_u = \frac{L}{t_u} \quad [3.2]$$

where, V_u = pulse velocity (m/s)
 L = distance between transducers (m), and
 t_u = transit time (s).

For dense materials the transit time will be comparatively less, and therefore velocity will be faster.

In order to keep proper contact between transducers and brick surface during testing, a frame was fabricated. Using it, the transducers could be tightened against brick and this helped in maintaining uniformity in test procedure. Based on review of earlier works [CNS Electronics 1993; Malhotra 1976; Naik and Malhotra 1991; Noland et al. 1990], transducers having a frequency of 37 KHz were found suitable and were therefore used in the present study, for pulse measurements on brick specimens. Higher frequency can not be used as it causes significant attenuation of signal strength due to the porous structure of bricks.

For rough material surfaces, the ASTM standards and the PUNDIT manual recommend the use of coupling agents for proper contact. Water pump grease was used as coupling agent and pulse velocity measurements were taken with it.

3.5.4 Freezing and Thawing Test

The freezing and thawing test was carried out to compare the performance of impregnated and control specimens. The freezing and thawing test specified in ASTM C67 takes about 70 days for completion. To reduce the time taken by the test, it was found necessary to adopt a faster freeze-thaw test. With the existing facilities, a test with 4 cycles of freezing and thawing per day was found suitable.

The testing was done in an Environmental Chamber, where the temperature of air was set to vary between -30°C and $+30^{\circ}\text{C}$. A lower temperature of -30°C was used to make sure the freezing of water in the capillary pores. Since thawing was done in air, a temperature of $+30^{\circ}\text{C}$ was chosen to allow for the melting of all the frozen water in the pores. Specimens were soaked in water for 24 hours before being taken for the test. To maintain the degree of saturation of the

specimens during testing, the saturated specimens were kept in a tray with 3 mm of water at bottom. Absorption measurements taken during the test showed that this method helped in maintaining the degree of saturation during test. Specimens were removed from the chamber after cracks or other visible distress were noticed. The number of freeze-thaw cycles resisted before removal was noted. Removed specimens were weighed, dried in oven and their weight loss determined. Figure 3.13 shows the Environmental Chamber with the specimens.

3.5.5 Compressive Strength Test

Compressive strength of brick specimens was determined as per ASTM C67. All the specimens were capped using sulphur prior to testing. Knowing the maximum load at failure and the gross area of the specimen, the compressive strength was calculated.

3.5.6 Brick-Mortar Bond Strength Test

The bond strength test was carried out to find whether the impregnation processes had any adverse effect on the bond between brick and mortar. The test was performed as per ASTM C952 [ASTM 1991] using crossed brick couplet.

Test specimens were made by cutting half bricks into two equal pieces and then bonding them together at right angles to each other (one over the other) using mortar. Based on ASTM C270 [ASTM 1992d] specifications, cement-lime mortar of type N was used for making the brick couplet. Also bond strength using cement mortar (1:3) with out lime was studied. A w/c ratio of 0.5 was used for the mortar. After curing for 28 days, the specimens were tested in the testing machine. A special testing set-up was fabricated to produce tensile load at the mortar joint. The

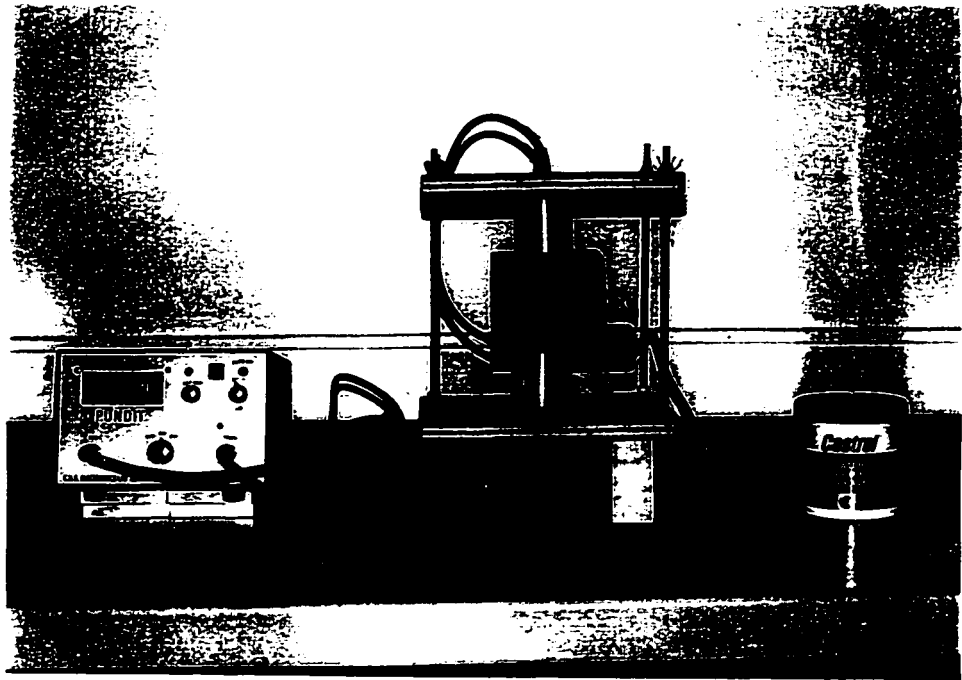


Figure 3.12 The pulse velocity testing equipment (PUNDIT) and test set-up (C N S Electronics Ltd., London, U.K.)

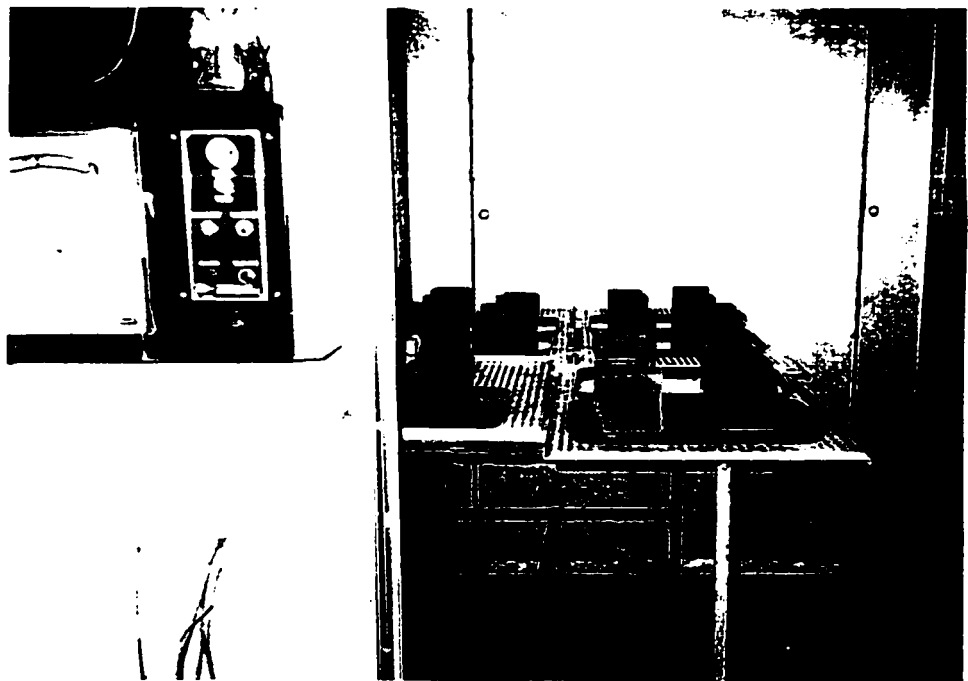


Figure 3.13 The Environmental Chamber used for the freezing and thawing test

test set-up is shown in Figure 3.14. Knowing the load at failure and the cross sectional area in bond, the tensile bond strength was calculated. Both control and treated specimens were tested.

3.6 Summary

The research procedures to be adopted to achieve the three major objectives of the research were decided and described in this chapter. Nine different types of commercially available clay bricks were selected for the experimental study. In addition, three more types of bricks were used to validate the experimental results. Based on the review of various impregnating materials, methyl methacrylate, paraffin, and acrylic sealer were chosen for impregnation of bricks. For polymer impregnation two methods of soaking were studied: one simple soaking and the other under vacuum. Impregnation with paraffin and acrylic sealer were carried out by simple soaking.



Figure 3.14 The specimen (in inset) and the loading set-up for bond strength test

The various tests to be carried out on the bricks for the experimental study were decided and their procedures explained in this chapter. They included water absorption tests, mercury intrusion porosimetry, ultrasonic pulse velocity test, freezing and thawing test, compressive strength test, and brick-mortar bond strength test. The experimental results are discussed in Chapters 4 and 7.

Analysis of Brick Properties

The different brick types that were selected for the experimental study in this research were already discussed in Section 3.2. The performance of bricks depend upon their various properties and therefore proper understanding of properties is essential for reliable evaluation of performance. This chapter analyzes the measured properties of these brick types in order to characterize them. They included pore properties, water absorption properties, compressive strength, pulse velocity, and freeze-thaw performance. Also, these properties were used for the derivations in Chapters 5 and 6. The properties of impregnated bricks are discussed separately in Chapter 7.

4.1 Experimental

As shown in Table 3.1, a total of 9 brick types (A, B, C, D, E, F, G, H, and J) were used for the development of durability index and the feasibility study on nondestructive evaluation of durability. These brick types were further divided into groups, based on their 24 hr. water absorption values, as explained in Section 3.3. Using this classification, a total of 23 brick groups were available for the study. They were: A3, A4, A5; B2, B3, B4, B5, B6; C3, C4, C5; D2, D3;

E1, E2; F2, F3; G2; H3, H4, H5, H6; and J5. These brick groups were tested for the various properties of the bricks according to the test procedures explained in Section 3.5. The tests carried out included mercury intrusion porosimetry, water absorption, ultrasonic pulse velocity, compressive strength, and freezing and thawing. As some of the tests were destructive, 3 sets of specimens were used for each brick group. One set was used for water absorption, pulse velocity, and porosimetry tests. The second and third sets were used for compressive strength and freeze-thaw tests respectively. Each set consisted of 5 brick specimens for brick types A, B, C, D, E, and F and 3 brick specimens for brick types G, H, and J.

4.2 Pore Properties

The pore properties of the bricks were measured using mercury intrusion porosimetry as explained in Section 3.5.2. The properties studied were: pore volume (*PV*), porosity (*P*), median pore diameter (*MPD*), average pore diameter (*APD*), and the distribution of pore sizes. *PV* is the total volume of pore space intruded, expressed in ml/g and *P* is the total pore volume expressed as % of sample volume. *MPD* is the pore size corresponding to 50% of *PV*. *APD* is calculated from *PV* and total pore area (*PA*) as $4PV/PA$, *PV* and *PA* being in consistent units. *APD* refers to the size of a uniform pore which will give the same *PV* and *PA* as the measured quantities. The pore properties of the bricks are given in Table 4.1. Figure 4.1 shows them in a graphical form.

Brick types D and E had lower pore volumes compared to other bricks whereas brick J had the highest value. The porosity of the bricks ranged from as low as about 7 % for E1 to about 28 % for J5. As already mentioned under review of literature in Chapter 2, pores bigger than 3 μm contribute to frost durability while pores smaller than 1 μm are not desirable. Bricks A, B, C,

TABLE 4.1
Pore Properties of the Bricks

Brick Type	Intruded Pore Volume (PV)	Porosity (P)	% of Pores > 3 μm (P3)	Median Pore Diameter (MPD)	Average Pore Diameter (APD)
	ml/g	%	% of PV	μm	μm
A3	0.0828	17.63	67.32	10.57	1.19
A4	0.0986	20.49	57.81	5.79	1.12
A5	0.1185	23.84	43.46	1.84	0.81
B2	0.0739	16.09	76.71	6.22	1.42
B3	0.0822	17.63	71.53	4.43	1.61
B4	0.0999	20.48	65.54	3.92	1.79
B5	0.1171	23.31	58.43	3.46	1.63
B6	0.1237	24.16	49.23	2.98	1.42
C3	0.0829	17.70	53.09	3.24	1.33
C4	0.1140	23.16	52.81	3.16	1.56
C5	0.1241	24.87	47.17	2.91	1.47
D2	0.0514	11.91	41.67	1.21	0.44
D3	0.0577	13.18	33.60	0.72	0.41
E1	0.0297	7.01	3.90	0.53	0.21
E2	0.0408	9.77	3.09	0.83	0.35
F2	0.0734	15.54	24.50	0.58	0.09
F3	0.0836	17.54	18.53	0.63	0.12
G2	0.0851	18.12	18.13	0.65	0.16
H3	0.0864	18.09	72.69	5.38	1.79
H4	0.0947	19.52	69.28	4.74	1.48
H5	0.1110	22.23	49.61	2.99	1.17
H6	0.1303	25.52	52.72	3.18	1.37
J5	0.1430	27.91	0.73	0.70	0.53

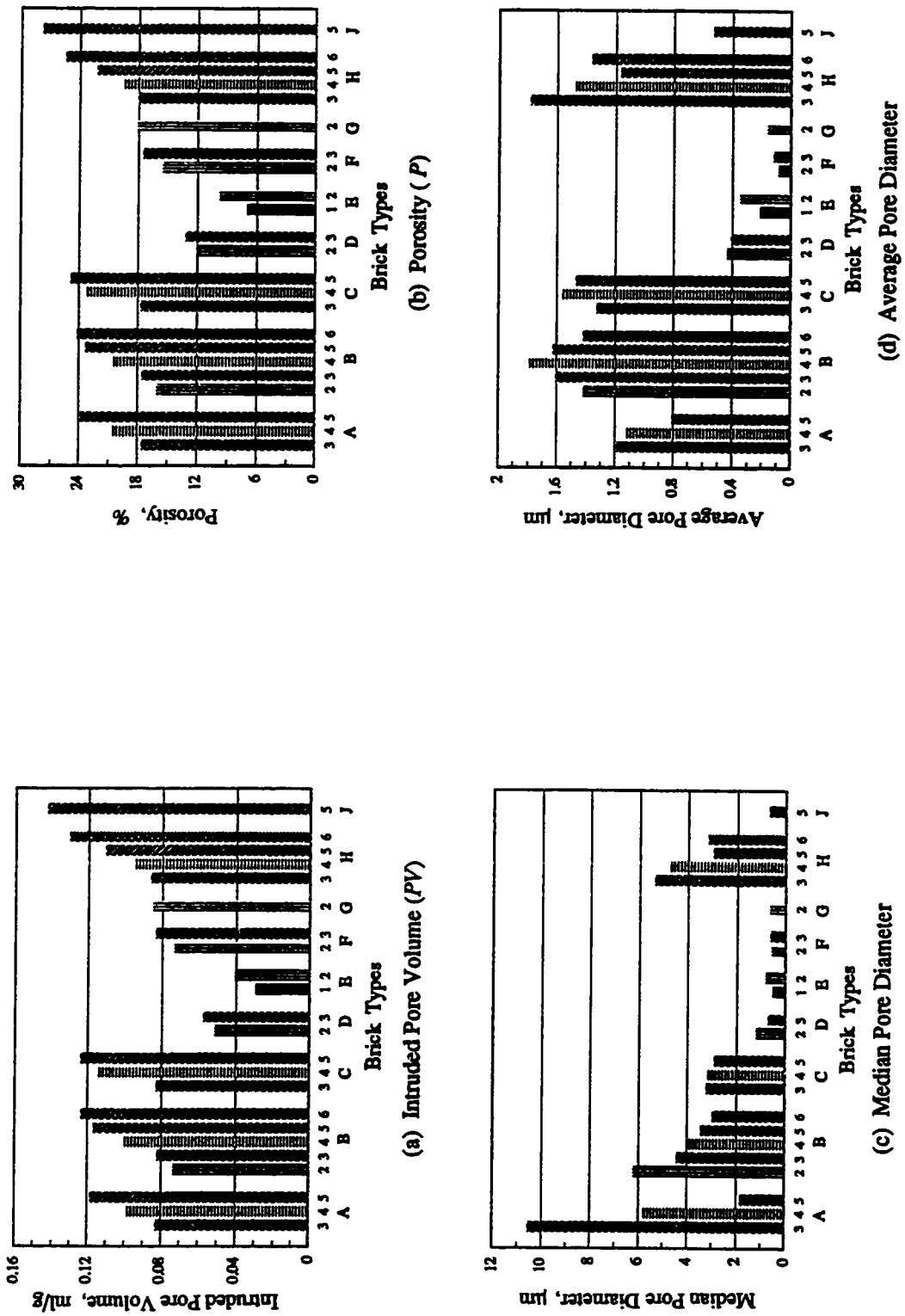


Figure 4.1 Pore Properties of the Bricks

and H, with the exception of A5, had median pore diameters close to 3 μm or above. Brick types D3, E1, E2, F2, F3, G2, and J5 had median pore diameters less than 1 μm . So for these bricks the majority of pore sizes were shifted towards low pore size range of < 1 μm . The average pore diameters were also lower for these bricks with values less than 0.6 μm .

The distribution of relevant pore size ranges are shown in Figures 4.2 and 4.3. The cumulative intrusion values for these pore size ranges are given in Tables 4.2 and 4.3. In Figure 4.2 the distribution is expressed as cumulative intrusion in ml/g and in Figure 4.3 the distribution is expressed as % of total pore volume. Bricks A, B, C, and H had significantly large number of pores bigger than 3 μm and all the groups in these brick types except A5 had more than 80 % of their pores bigger than 1 μm . From Table 4.3 it could be seen that brick A had about 30-50 % of their pores larger than 10 μm . Brick type D had around 30-40 % of the pores larger than 1 μm and around 40-50 % between 1 μm and 0.1 μm . Brick E had most of its pores smaller than 3 μm with about 60 % of the pores in the 1-0.1 μm range. Brick type F had only around 20 % of pores larger than 3 μm . Around 60 % of the pores for F were below 1 μm . Brick G also had more than 60 % of the pores smaller than 1 μm and only around 20 % bigger than 3 μm . Brick J5 had a significantly large amount of about 95 % of its pores in the range 1-0.1 μm .

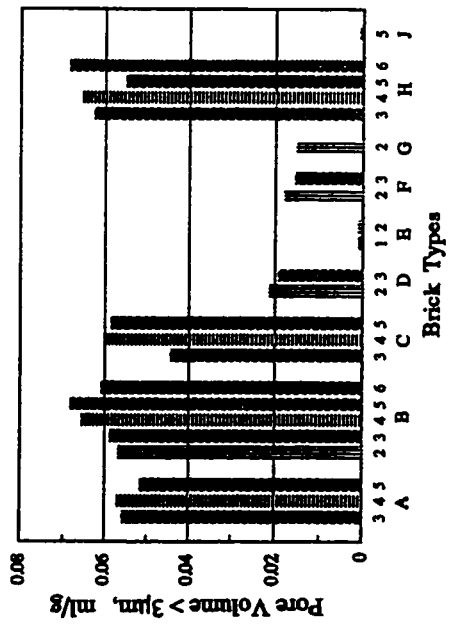
The pore size distribution curves for the bricks are shown in Figures 4.4A&B and 4.5A&B. In Figures 4.4A and 4.4B the curves are expressed in terms of cumulative intrusion in ml/g and in Figures 4.5A and 4.5B they are expressed in % of total pore volume. The pore size distribution may also be expressed as % of sample volume. The distribution curves expressed in % of sample volume are shown in Appendix A. The cumulative intrusion values used for plotting the curves are also given in Appendix A. From these curves the following observations could be

TABLE 4.2
Distribution of Relevant Pore Size Ranges of the Bricks
Expressed as Cumulative Intrusion in ml/g

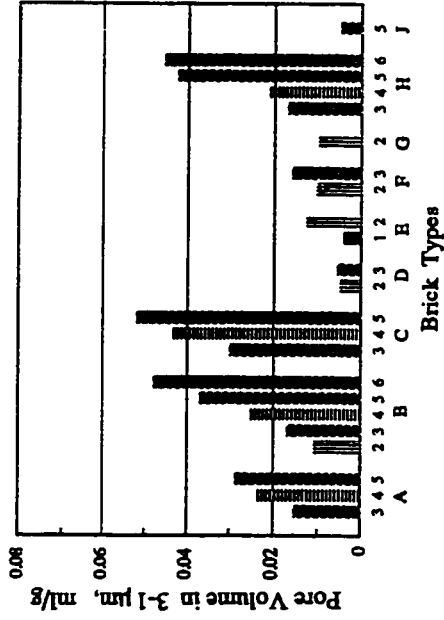
Brick Type	Pore Size Distribution : Cumulative Intrusion in ml/g					
	Pore Diameter Range					
	> 10 μm	> 3 μm	10 - 3 μm	3 - 1 μm	1 - 0.1 μm	< 0.1 μm
A3	0.0419	0.0557	0.0138	0.0154	0.0102	0.0015
A4	0.0419	0.0569	0.0150	0.0234	0.0167	0.0016
A5	0.0368	0.0515	0.0147	0.0286	0.0360	0.0024
B2	0.0218	0.0567	0.0349	0.0108	0.0054	0.0010
B3	0.0129	0.0589	0.0577	0.0169	0.0056	0.0008
B4	0.0159	0.0657	0.0498	0.0252	0.0083	0.0007
B5	0.0167	0.0685	0.0518	0.0371	0.0108	0.0007
B6	0.0180	0.0609	0.0429	0.0478	0.0141	0.0009
C3	0.0135	0.0444	0.0309	0.0300	0.0074	0.0011
C4	0.0151	0.0600	0.0449	0.0433	0.0099	0.0008
C5	0.0133	0.0585	0.0452	0.0520	0.0126	0.0010
D2	0.0128	0.0214	0.0086	0.0051	0.0228	0.0021
D3	0.0098	0.0193	0.0095	0.0057	0.0304	0.0023
E1	0.0007	0.0011	0.0004	0.0041	0.0189	0.0056
E2	0.0008	0.0012	0.0004	0.0126	0.0244	0.0026
F2	0.0066	0.0180	0.0114	0.0103	0.0277	0.0174
F3	0.0064	0.0155	0.0091	0.0160	0.0364	0.0157
G2	0.0065	0.0153	0.0088	0.0100	0.0476	0.0122
H3	0.0194	0.0628	0.0434	0.0169	0.0060	0.0007
H4	0.0120	0.0656	0.0536	0.0211	0.0072	0.0008
H5	0.0119	0.0551	0.0432	0.0424	0.0124	0.0011
H6	0.0126	0.0688	0.0562	0.0455	0.0148	0.0012
J5	0.0005	0.0010	0.0005	0.0051	0.1355	0.0014

TABLE 4.3
Distribution of Relevant Pore Size Ranges of the Bricks
Expressed as Cumulative Intrusion in % of Total Pore Volume (PV)

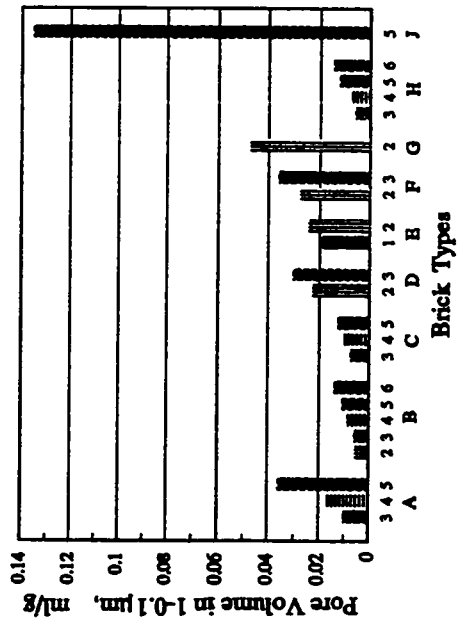
Brick Type	Pore Size Distribution : Cumulative Intrusion in % of PV					
	Pore Diameter Range					
	> 10 μm	> 3 μm	10 - 3 μm	3 - 1 μm	1 - 0.1 μm	< 0.1 μm
A3	50.67	67.32	16.65	18.53	12.33	1.82
A4	42.53	57.81	15.28	23.79	16.81	1.59
A5	31.05	43.46	12.41	24.18	30.31	2.05
B2	29.72	76.71	46.99	14.53	7.28	1.48
B3	15.95	71.53	55.75	20.53	6.86	1.08
B4	15.78	65.54	49.76	25.44	8.31	0.71
B5	14.30	58.43	44.13	31.73	9.17	0.67
B6	14.50	49.23	34.73	38.65	11.36	0.76
C3	16.56	53.09	36.53	36.57	9.01	1.33
C4	13.43	52.81	39.38	37.79	8.62	0.78
C5	10.60	47.17	36.57	41.88	10.17	0.78
D2	24.93	41.67	16.24	9.74	44.38	4.21
D3	17.01	33.60	16.59	9.74	52.60	4.06
E1	2.48	3.90	1.42	13.07	64.16	18.87
E2	2.04	3.09	1.03	30.61	59.90	6.40
F2	8.91	24.50	15.59	14.03	37.75	23.72
F3	7.74	18.53	10.79	19.13	43.53	18.81
G2	7.75	18.13	10.38	11.78	55.80	14.29
H3	22.59	72.69	50.10	19.53	6.97	0.81
H4	12.88	69.28	56.40	22.34	7.54	0.84
H5	10.70	49.61	38.91	38.21	11.17	1.01
H6	9.59	52.72	43.13	35.02	11.38	0.88
J5	0.35	0.73	0.38	3.56	94.75	0.96



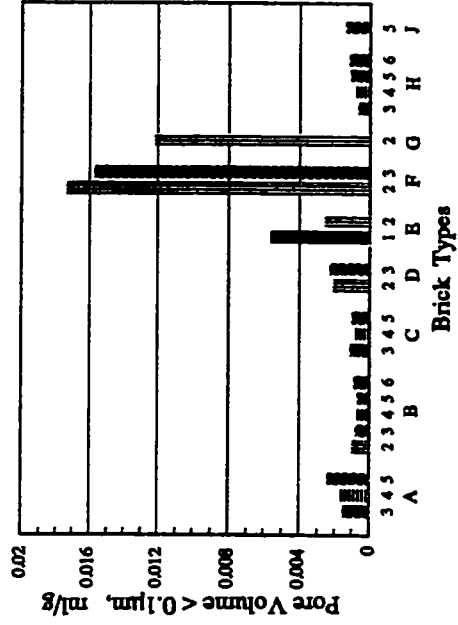
(a) Pore Size Range > 3 µm



(b) Pore Size Range 3-1 µm

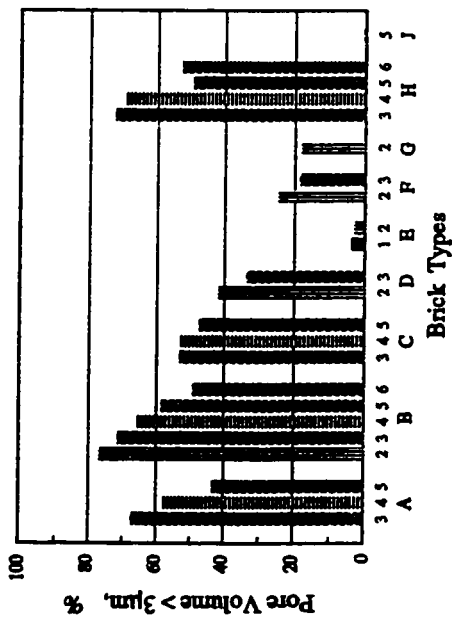


(c) Pore Size Range 1-0.1 µm

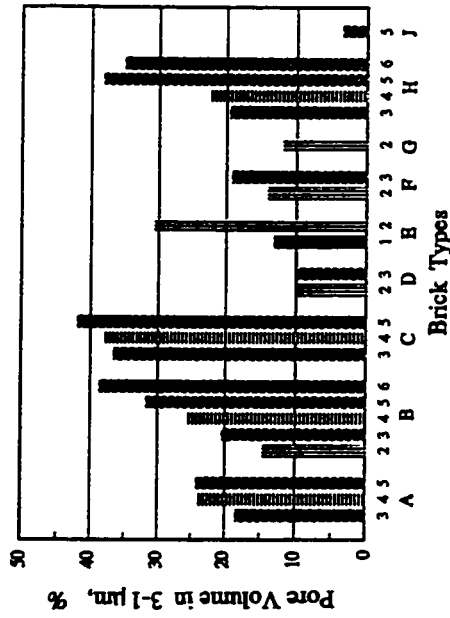


(d) Pore Size Range < 0.1 µm

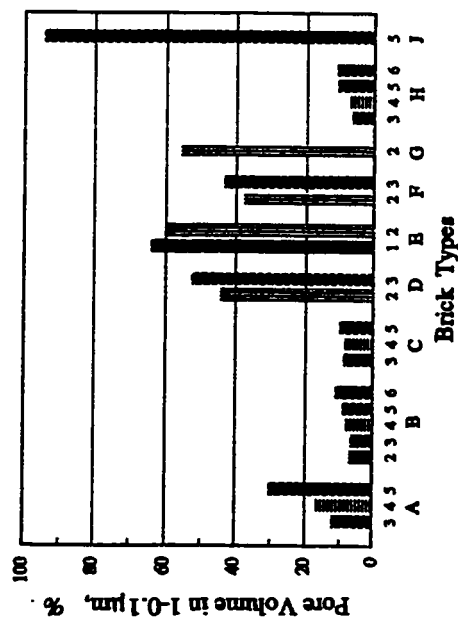
Figure 4.2 Distribution of relevant pore size ranges of the bricks expressed as cumulative intrusion in ml/g



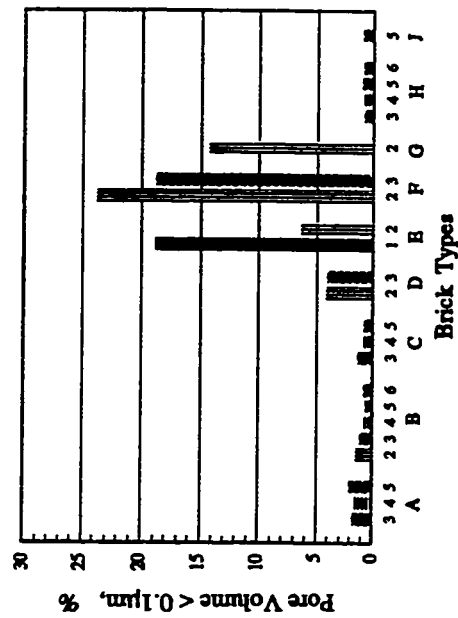
(a) Pore Size Range > 3 µm



(b) Pore Size Range 3-1 µm



(c) Pore Size Range 1-0.1 µm



(d) Pore Size Range < 0.1 µm

Figure 4.3 Distribution of relevant pore size ranges of the bricks expressed as cumulative intrusion in % of Pore Volume (PV)

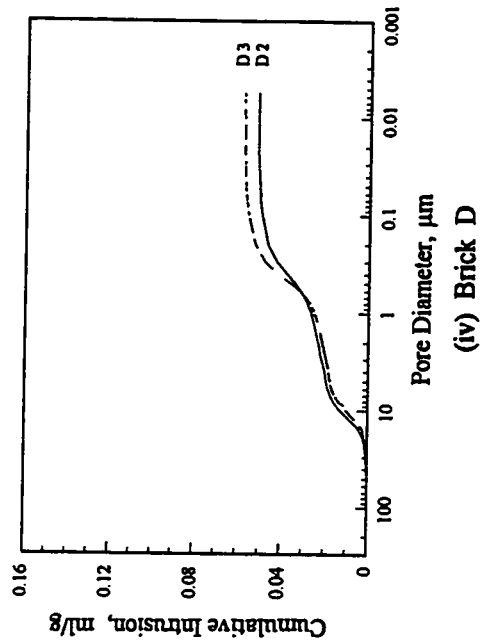
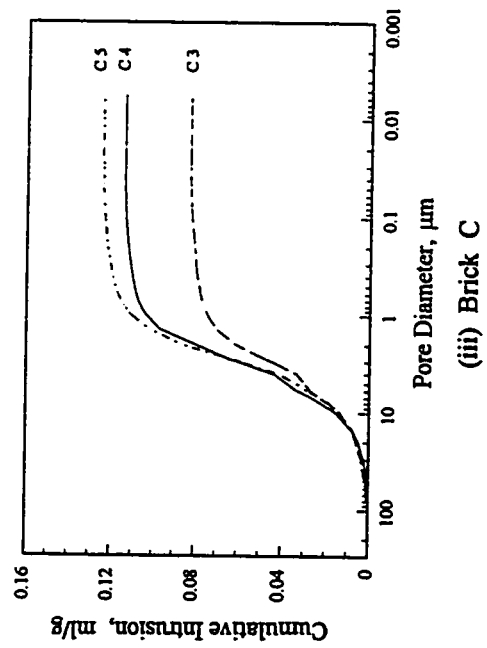
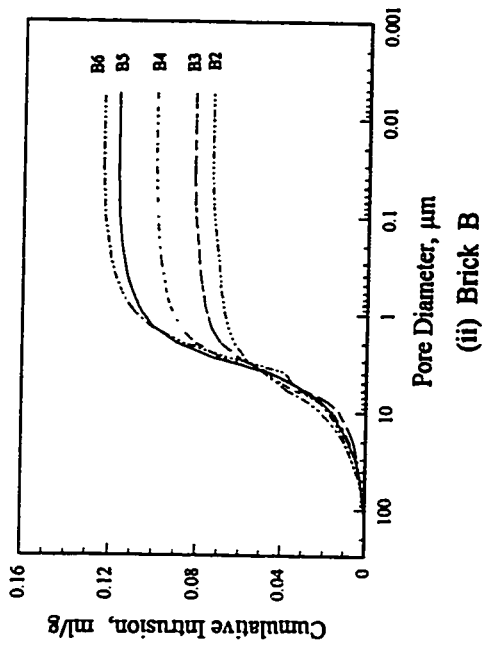
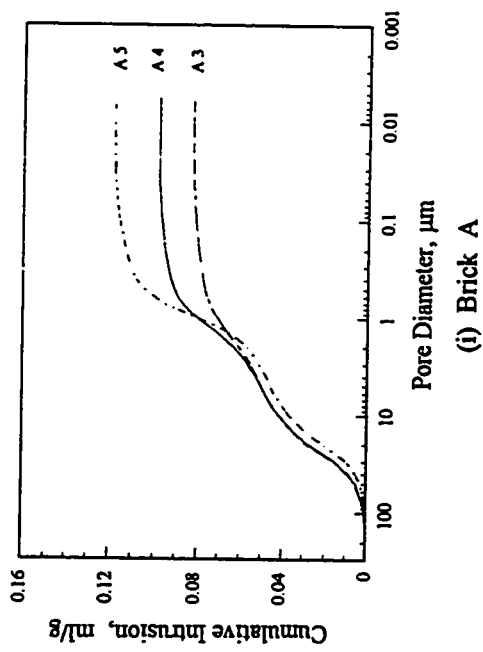


Figure 4.4A Pore Size Distribution Curves for bricks A, B, C, and D expressed as cumulative intrusion in ml/g

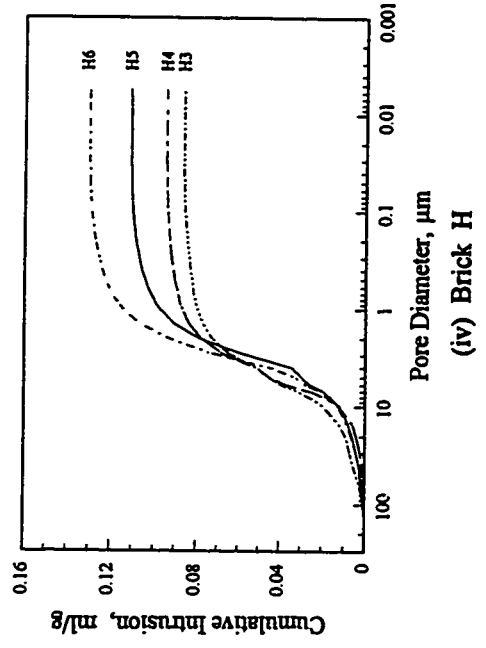
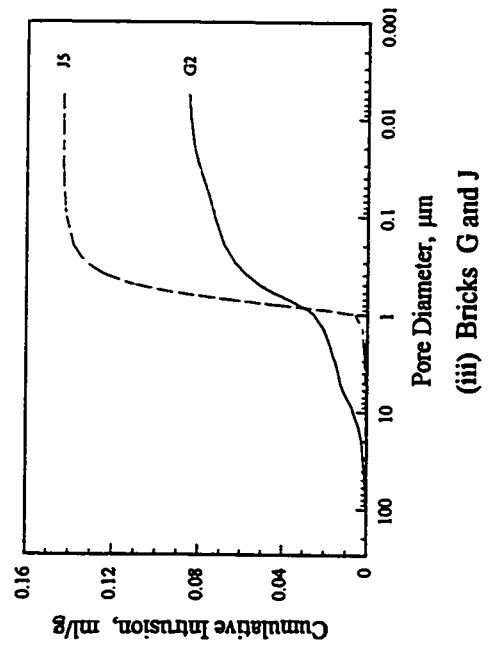
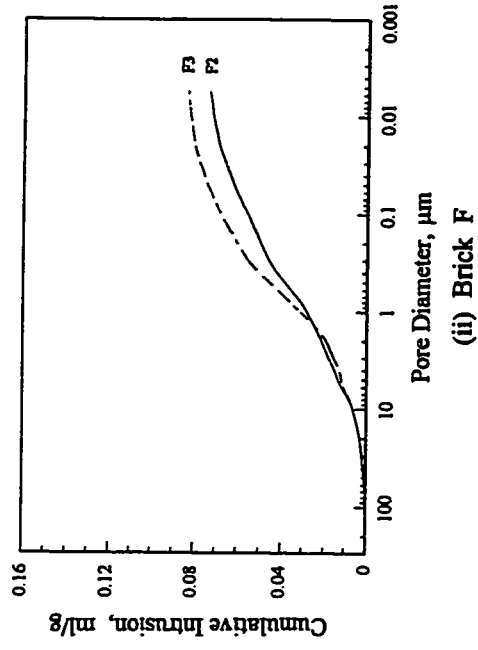
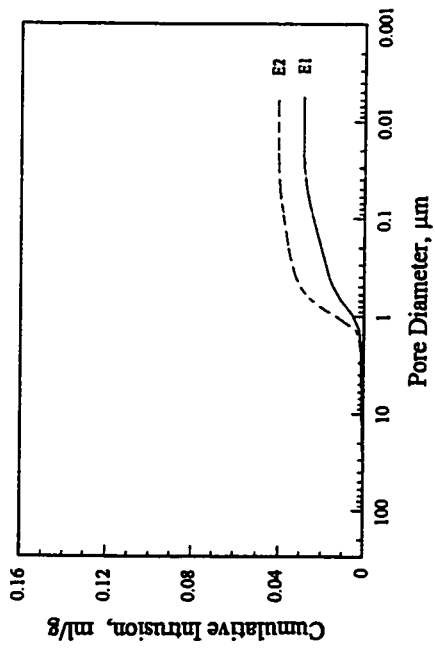


Figure 4.4B Pore Size Distribution Curves for bricks E, F, G, H, and J expressed as cumulative intrusion in ml/g

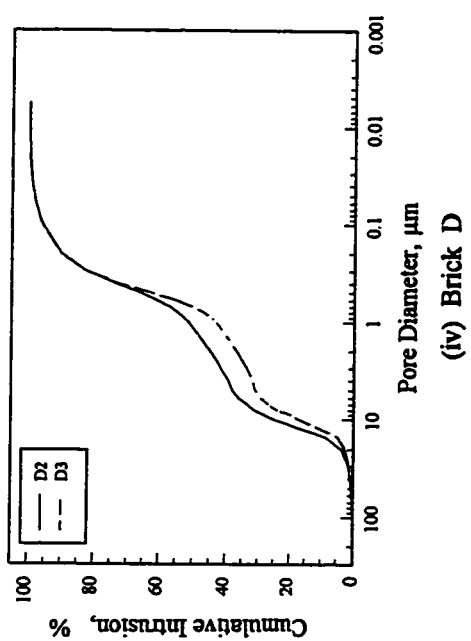
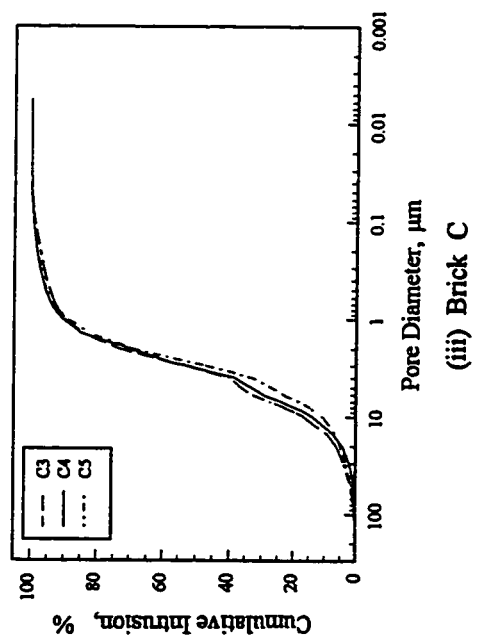
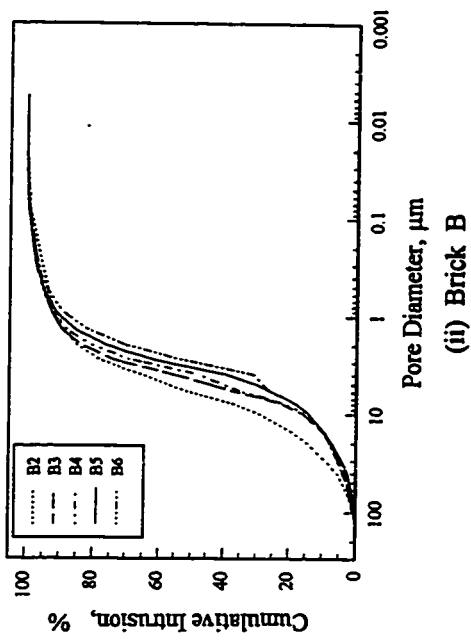
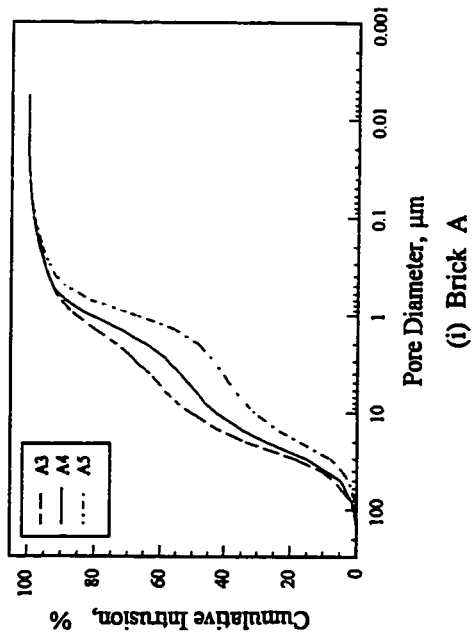


Figure 4.5A Pore Size Distribution Curves for bricks A, B, C, and D expressed as cumulative intrusion in % of total Pore Volume (% of PV)

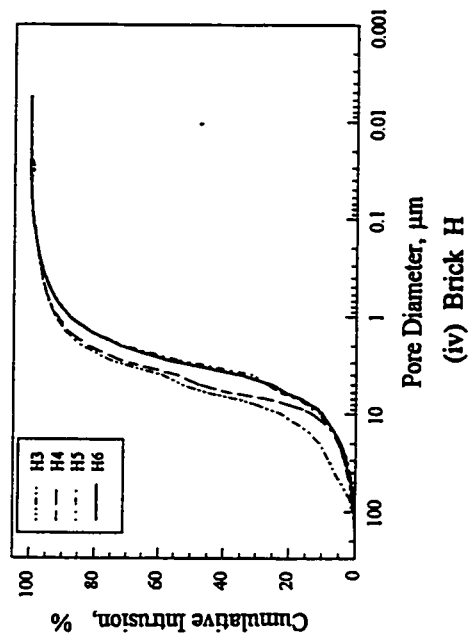
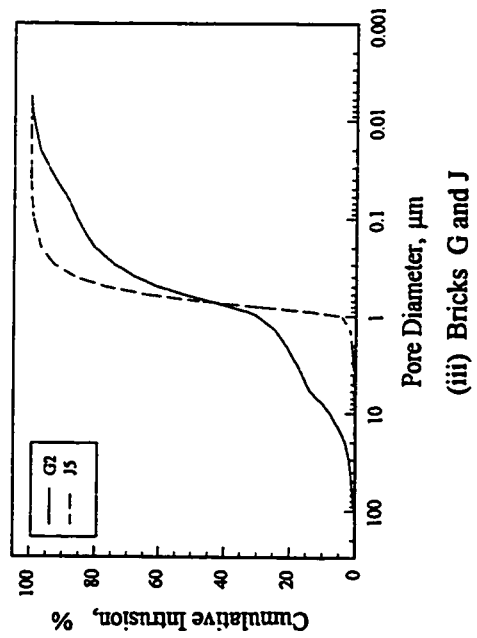
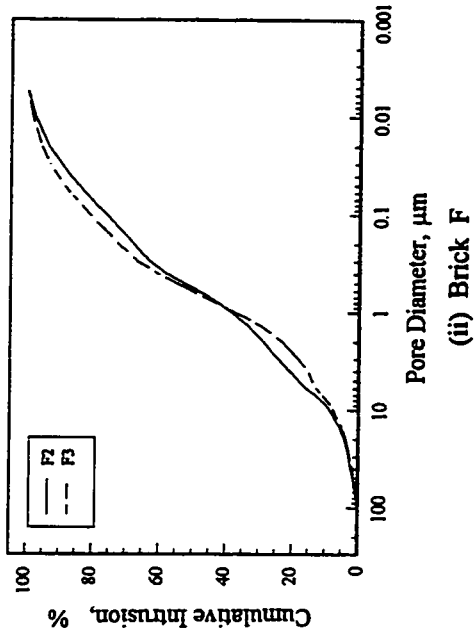
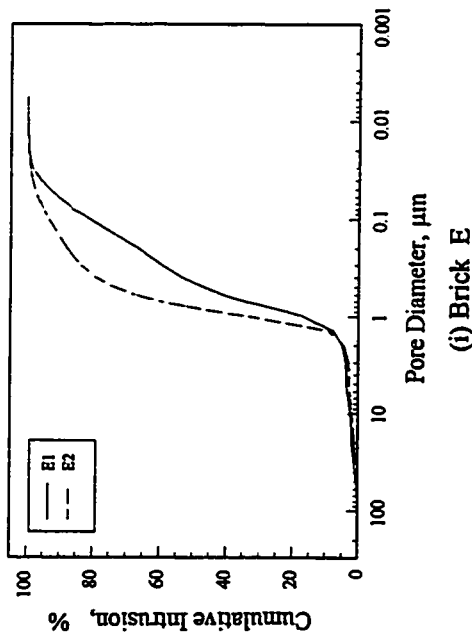


Figure 4.5B Pore Size Distribution Curves for bricks E,F,G,H, and J expressed as cumulative intrusion in % of total Pore Volume (% of PV)

drawn. For brick A there were two prominent pore size ranges, one 40-10 μm and the other 1-0.1 μm . For bricks B, C, and H most of the pores fell between 10 μm and 1 μm . D type also had two major pore size ranges, 20-5 μm and 0.7-0.08 μm . For brick E the pore sizes were mostly between 1 μm and 0.04 μm . Brick type F had a rather uniform distribution of pore sizes with no particular pore size being predominant. Most of the pores for F were smaller than 10 μm . Brick type G had a uniform distribution between 10 μm and 1 μm and a predominant pore size range between 1 μm and 0.2 μm . Brick J had negligible amount of pore space larger than 1 μm and most of the pores fell in the range 1-0.3 μm . It was observed that, in general, within a brick type the pore size distribution shifted towards lower pore size range with increase in porosity.

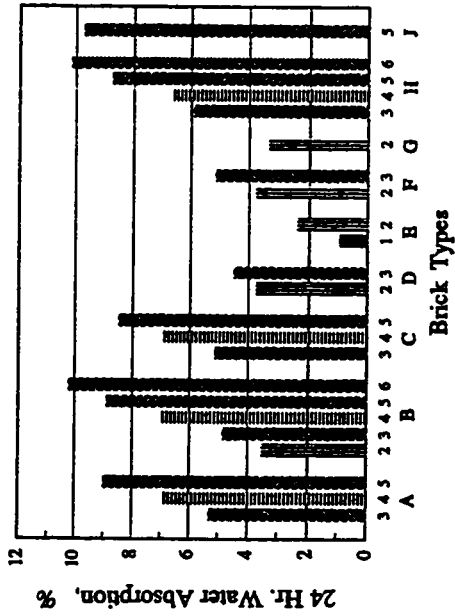
4.3 Water Absorption Properties

Basically three types of absorption tests were carried out: submersion absorption in cold water, capillary absorption in cold water, and boiling water absorption. Vacuum saturation was used only for studies on impregnated bricks. The commonly used absorption properties of the bricks are given in Table 4.4. In order to compare the brick types, these properties are shown in a graphical form in Figure 4.6

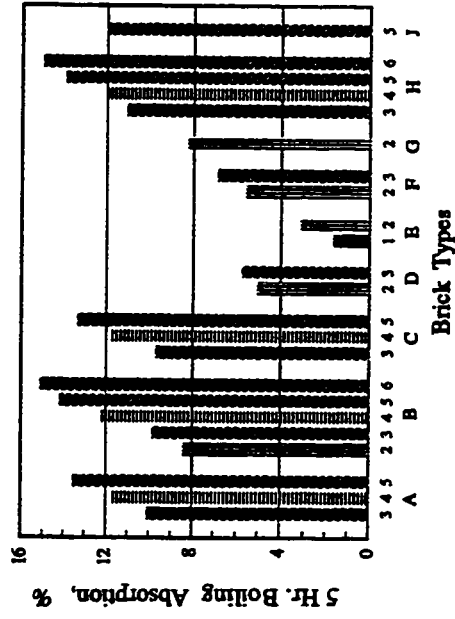
The 24 hr. water absorption values of the bricks ranged from as low as about 1 % (for E1) to about 10 % (for B6 and H6). All the bricks satisfied the ASTM C216 requirement (see Table 2.1) for maximum water absorption by 5 hr. boiling of 17 % for severe weathering. Brick types D, E, and F had much lower boiling absorption compared to other brick types. Therefore these brick types had somewhat higher saturation coefficients. Brick J5 with a C/B value of 0.81 was the only brick that did not satisfy the ASTM requirement for maximum saturation coefficient

TABLE 4.4
Absorption Properties of the Bricks

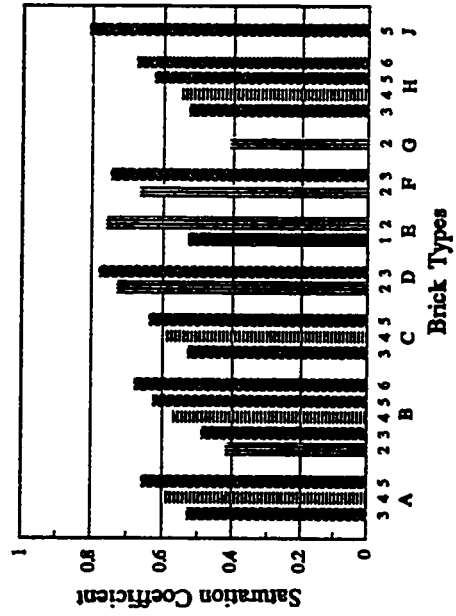
Brick Type	24 Hr. Water Absorption (C)	5 Hr. Boiling Absorption (B)	Saturation Coefficient (C/B)	Initial Rate of Absorption (IRA)	10 Minutes Extended IRA
	%	%		g/min./ 193.55cm ²	g/10min./ 193.55cm ²
A3	5.32	10.10	0.53	20.98	58.39
A4	6.89	11.67	0.59	26.90	76.26
A5	9.01	13.53	0.66	33.61	98.31
B2	3.53	8.41	0.42	11.29	23.86
B3	4.84	9.86	0.49	13.92	35.28
B4	6.95	12.24	0.57	24.92	76.73
B5	8.92	14.22	0.63	37.78	120.02
B6	10.25	15.11	0.68	45.22	146.06
C3	5.15	9.70	0.53	9.46	26.20
C4	6.90	11.75	0.59	15.54	55.93
C5	8.48	13.32	0.64	26.49	88.59
D2	3.73	5.07	0.73	7.69	18.15
D3	4.48	5.76	0.78	10.06	24.14
E1	0.93	1.64	0.53	0.81	1.34
E2	2.37	3.13	0.76	1.48	3.26
F2	3.75	5.59	0.67	6.06	12.48
F3	5.15	6.86	0.75	9.03	21.69
G2	3.35	8.22	0.41	7.91	13.77
H3	5.90	11.10	0.53	24.02	61.87
H4	6.63	12.00	0.55	25.70	75.07
H5	8.75	13.93	0.63	36.92	112.42
H6	10.17	15.03	0.68	42.29	139.32
J5	9.75	12.05	0.81	17.48	68.09



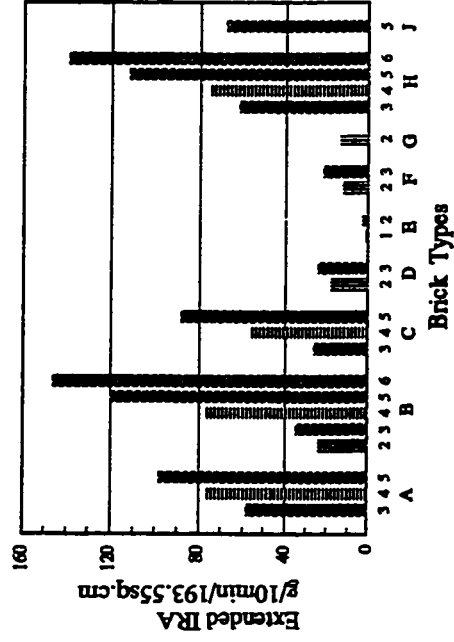
(a) 24 Hr. Water Absorption (C)



(b) 5 Hr. Boiling Water Absorption (B)



(c) Saturation Coefficient (C/B)



(d) Extended IRA for 10 minutes

Figure 4.6 Absorption Properties of the Bricks

of 0.78. The 1 minute initial rate of absorption (*IRA*) specified in ASTM C67 is not a qualifying condition or property to be considered in durability assessment. Excessive initial rates of absorption can adversely affect the strength and water tightness of the joints between mortar and masonry units. The *IRA* test also gives a measure of the capillary absorption rate of the bricks. The 1 minute period of measurement is considered too small for comparing the rates of absorption of bricks. Therefore in this study an extended *IRA* of 10 minutes was used. From Figure 4.6 it can be seen that brick types D, E, F, and G had very low capillary absorption rates compared to other brick types

The rates of submersion and capillary absorptions of the bricks are shown as absorption curves in Figures 4.7A&B to Figures 4.11A&B. The absorption values used for plotting these curves are given in Appendix B. In Figures 4.7A and 4.7B the submersion absorption values are expressed in percentage of the dry weight of brick and in Figures 4.8A and 4.8B they are expressed as % of 5 hr. boiling water absorption. Figures 4.9A and 4.9B show the capillary absorption curves expressed in % of dry weight. In Figures 4.10A and 4.10B the capillary absorption is expressed as absorption per unit area and in Figures 4.11A and 4.11B it is expressed in % of 5 hr. boiling water absorption.

The following observations were made from the absorption curves. Except for brick types E1 and E2 (in both submersion and capillary absorption), and F2 (in capillary absorption), all other bricks showed an initial period of high rate of absorption followed by a slow rate in both submersion and capillary absorptions. So the absorption curves for these bricks show an initial steep rise followed by a flattened curve. The initial rate at which water was absorbed by the bricks was faster in the case of submersion absorption compared to capillary absorption. Within a brick

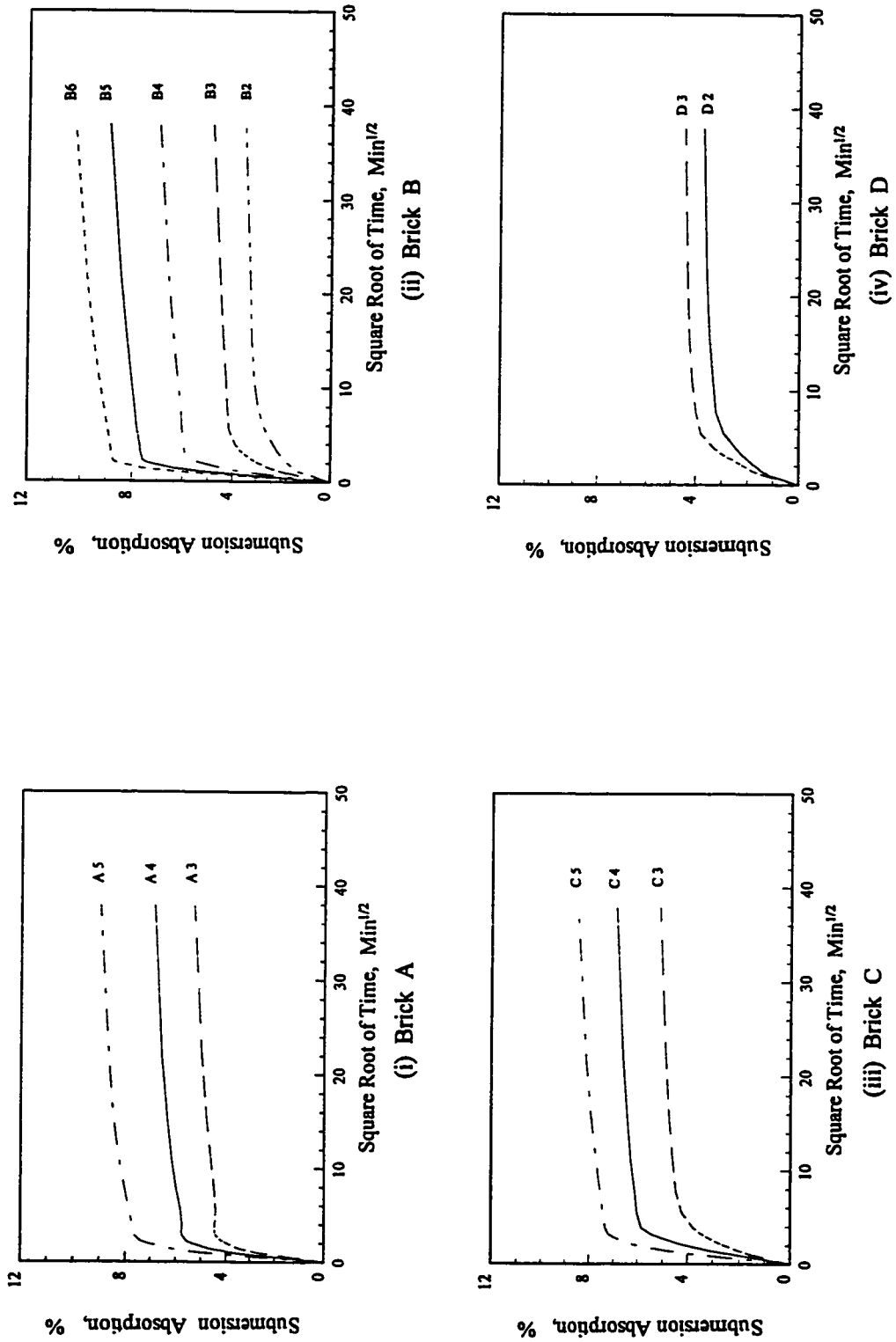


Figure 4.7A Submersion Absorption Curves for bricks A,B,C, and D expressed in % of dry weight (Cx)

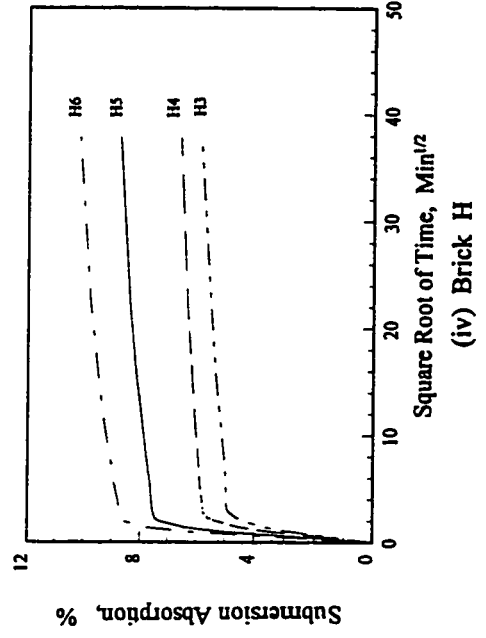
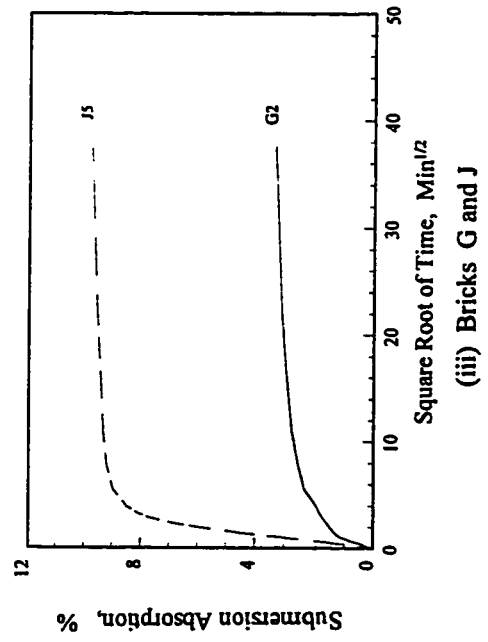
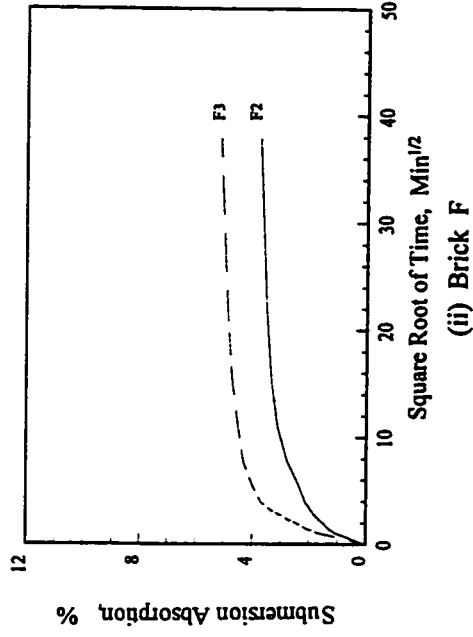
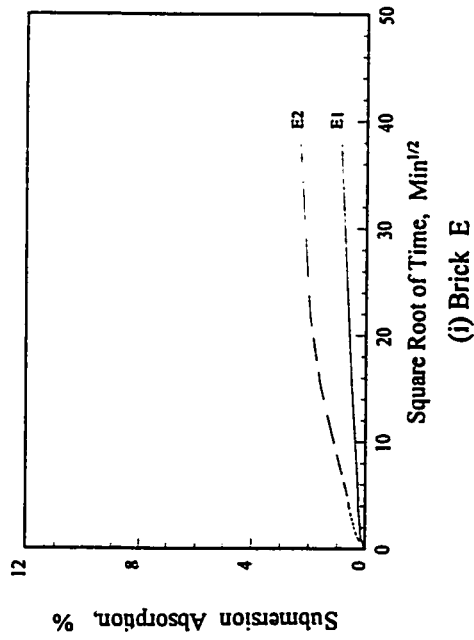


Figure 4.7B Submersion Absorption Curves for bricks E,F,G,H, and J expressed in % of dry weight (Cx)

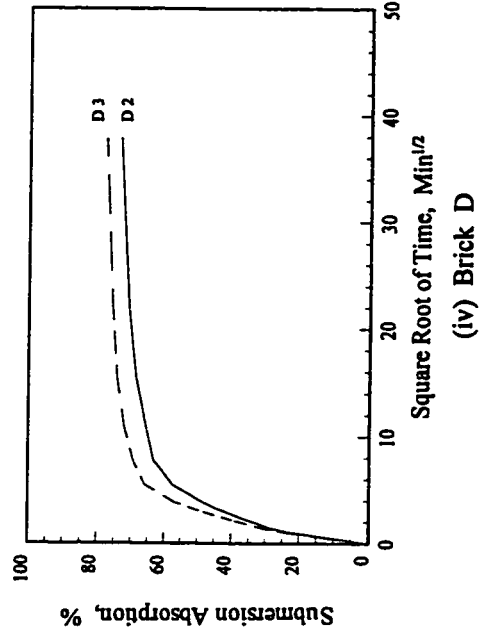
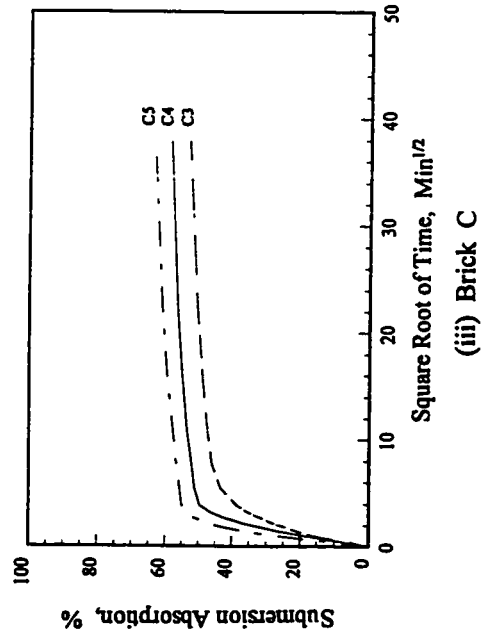
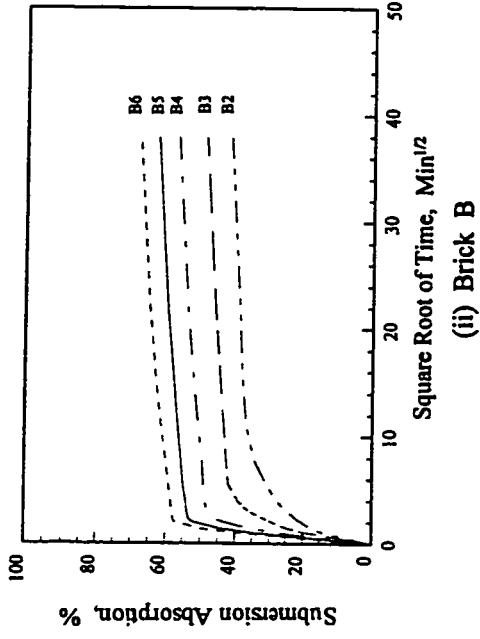
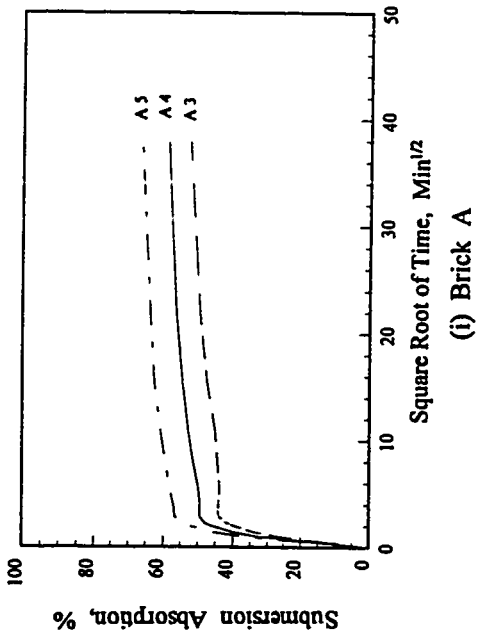


Figure 4.8A Submersion Absorption Curves for bricks A,B,C, and D expressed in % of 5 hr. Boiling Water Absorption (C_x/B)

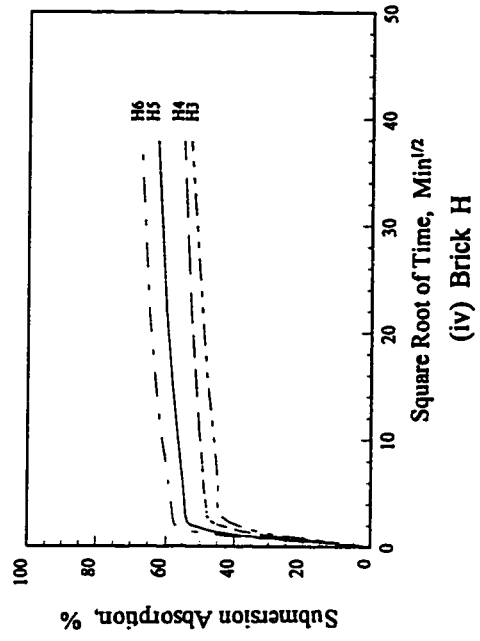
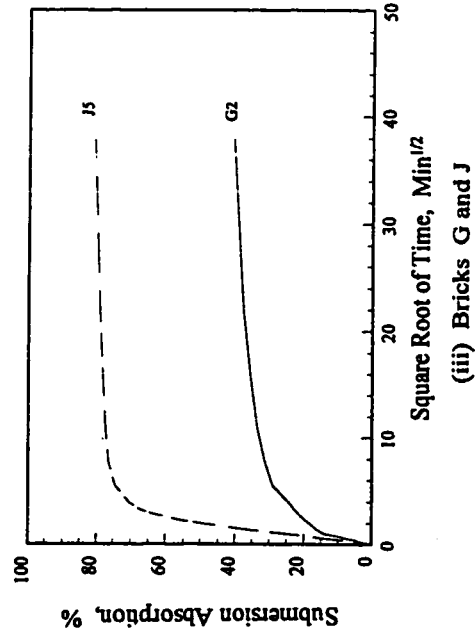
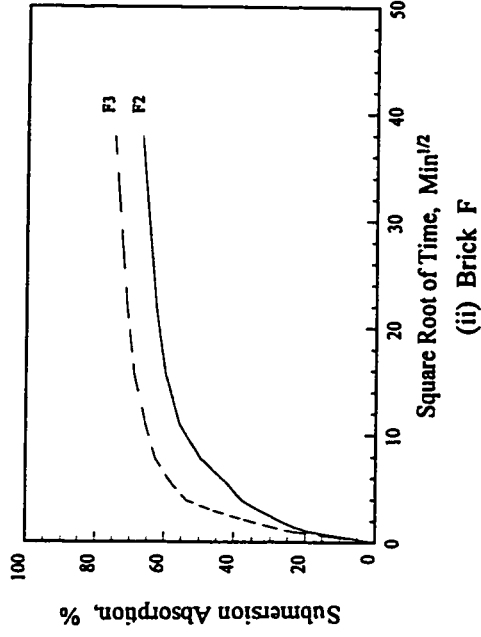
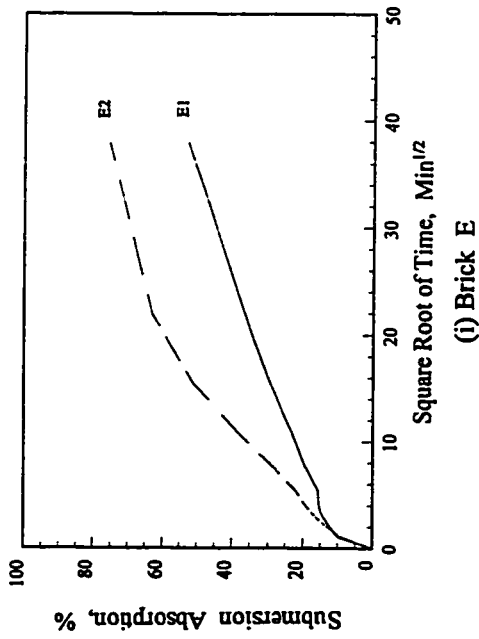


Figure 4.8B Submersion Absorption Curves for bricks E,F,G,H, and J expressed in % of 5 hr. Boiling Water Absorption (C_x/B)

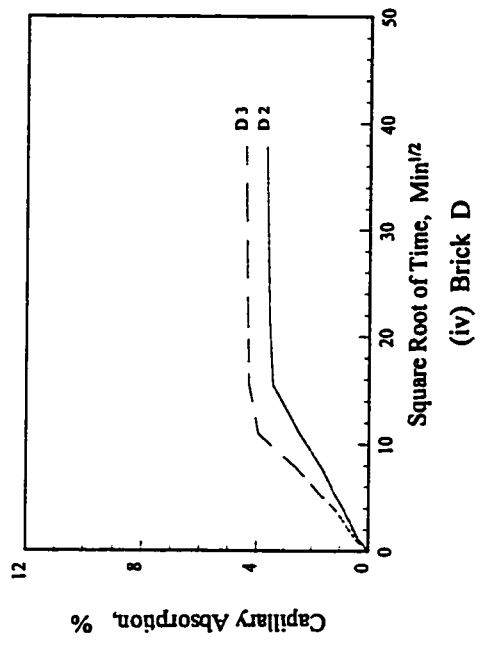
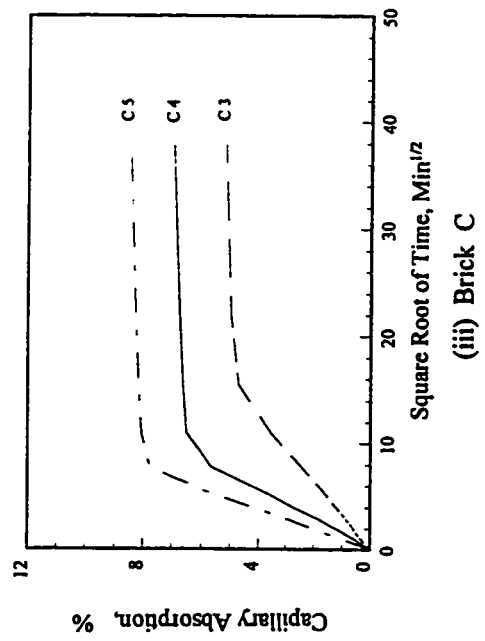
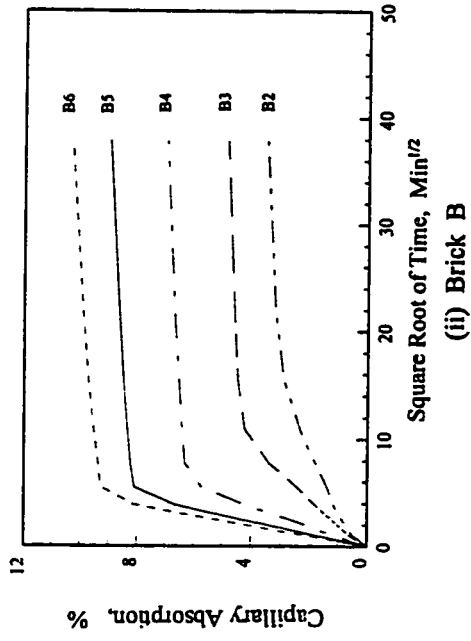
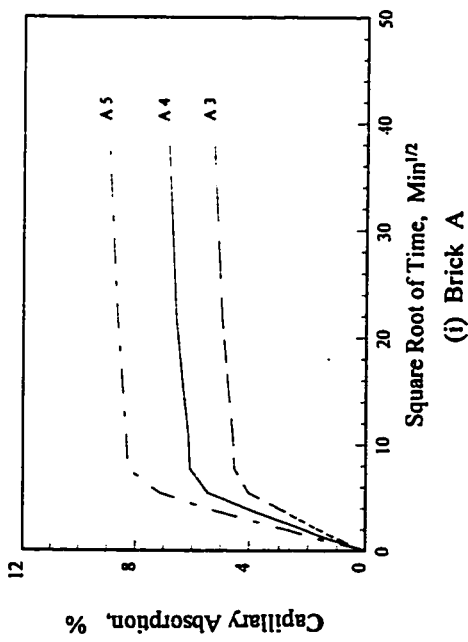


Figure 4.9A Capillary Absorption Curves for bricks A,B,C, and D expressed in % of dry weight (S_x)

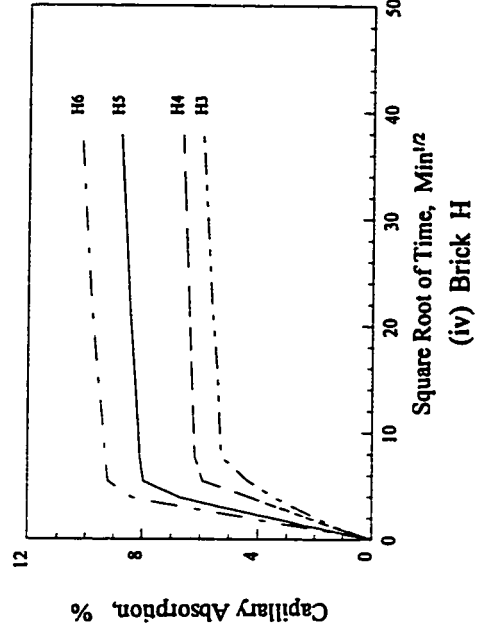
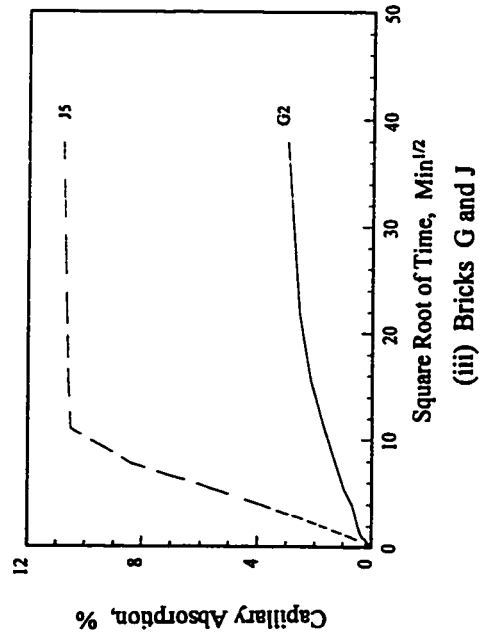
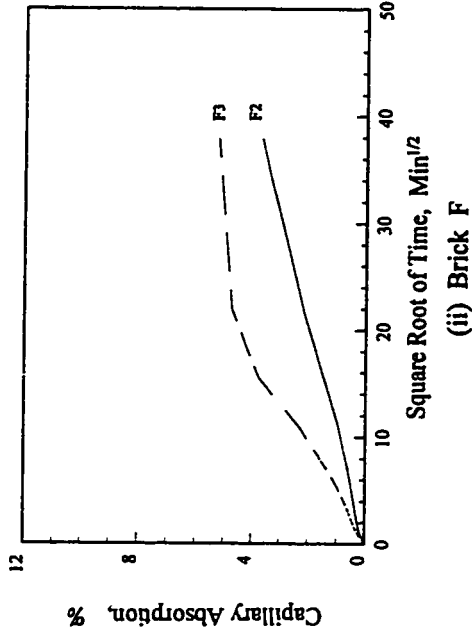
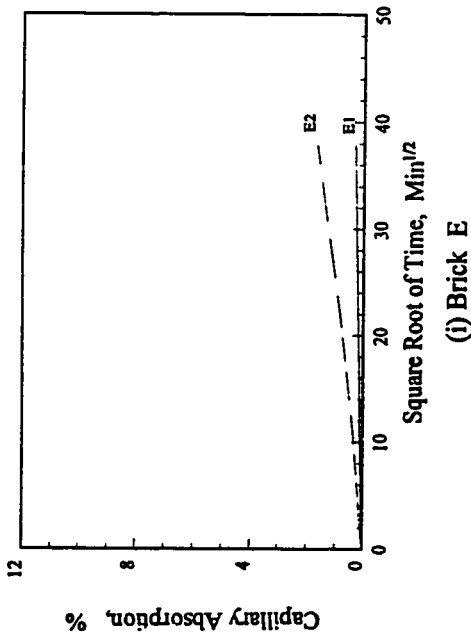


Figure 4.9B Capillary Absorption Curves for bricks E, F, G, H, and J expressed in % of dry weight (S_x)

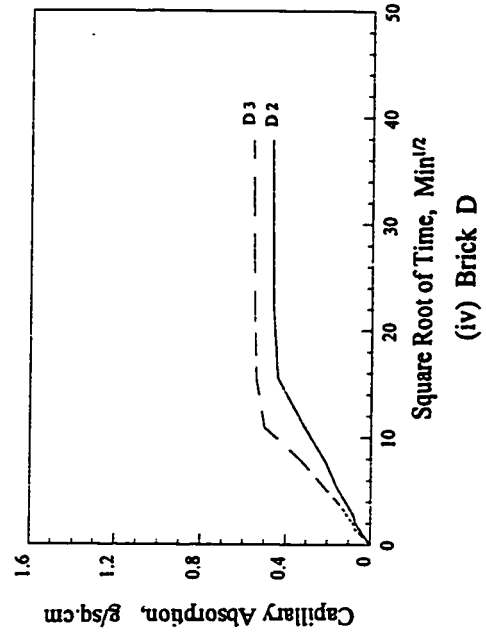
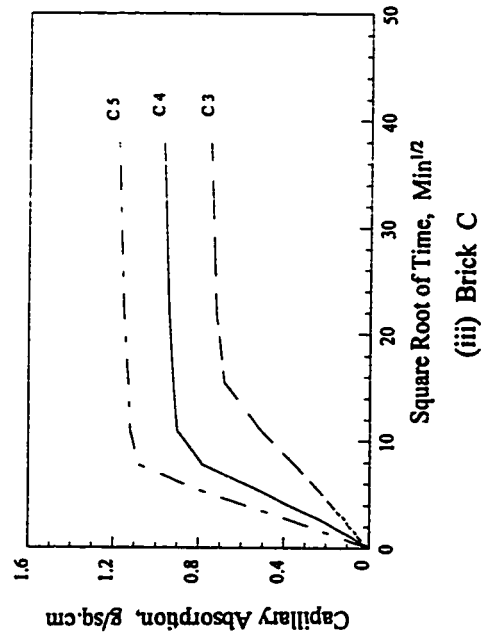
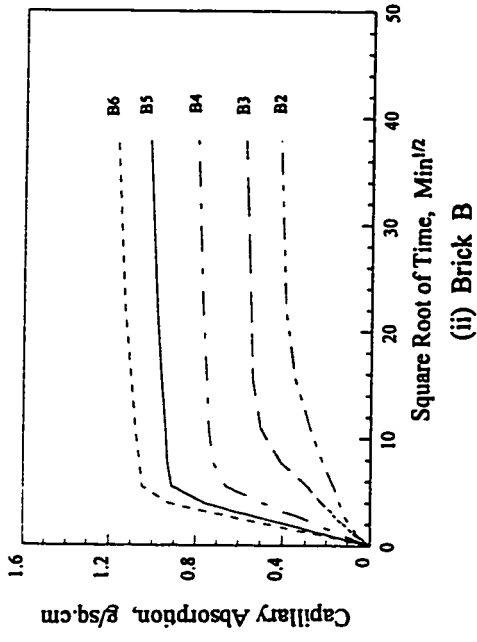
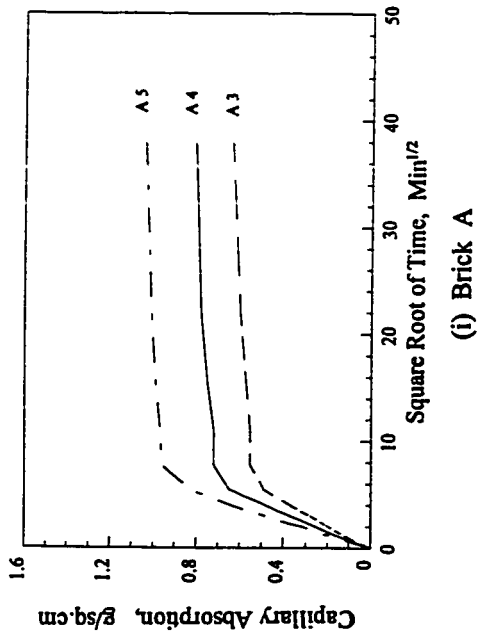


Figure 4.10A Capillary Absorption Curves for bricks A,B,C, and D expressed in absorption per unit area (Sx/A)

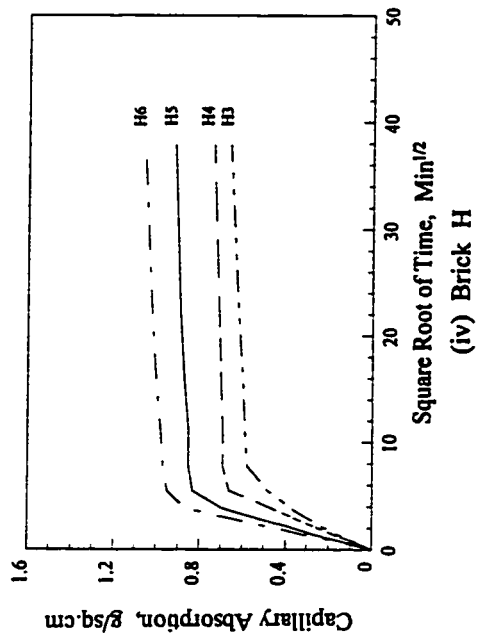
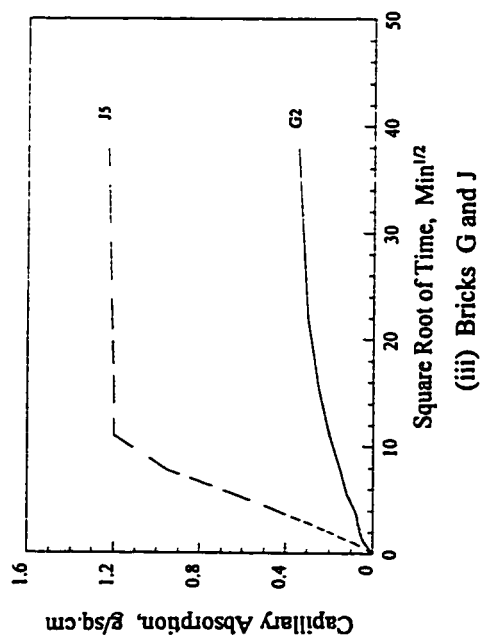
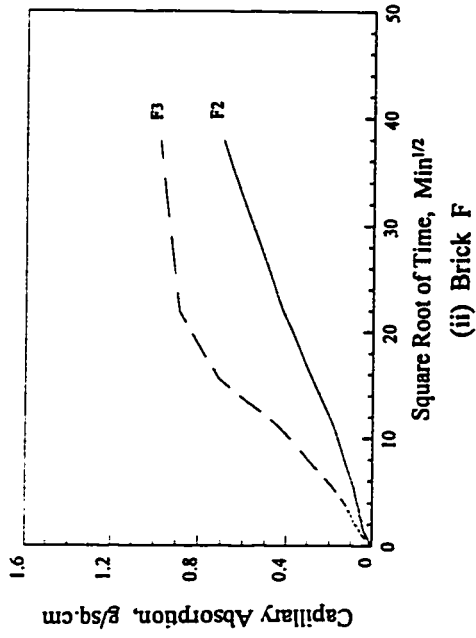
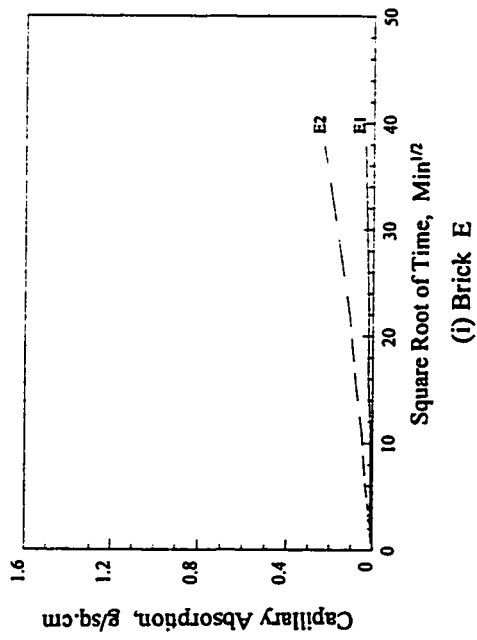


Figure 4.10B Capillary Absorption Curves for bricks E, F, G, H, and J expressed in absorption per unit area (Sx/A)

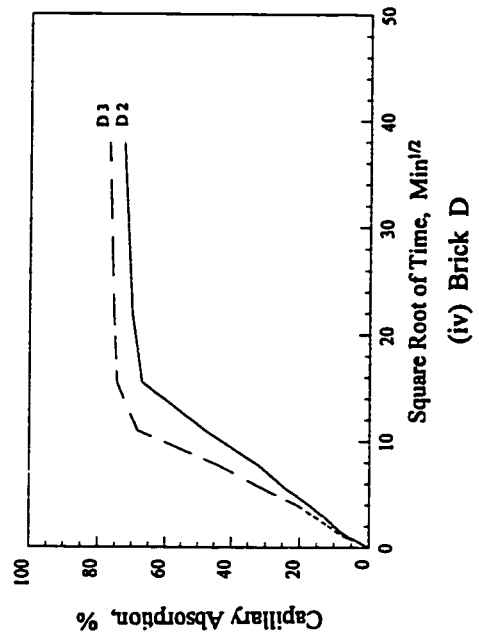
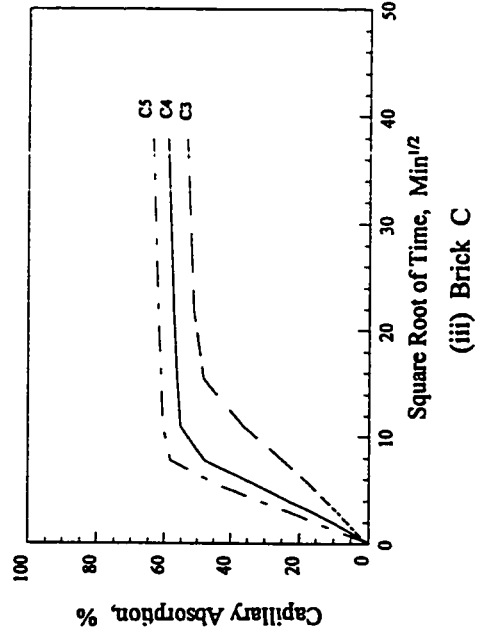
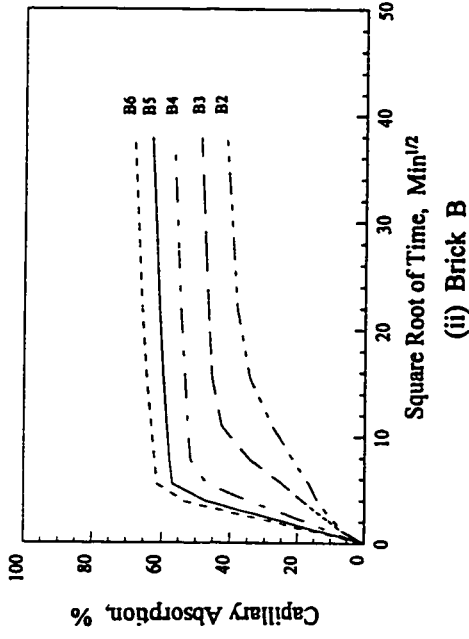
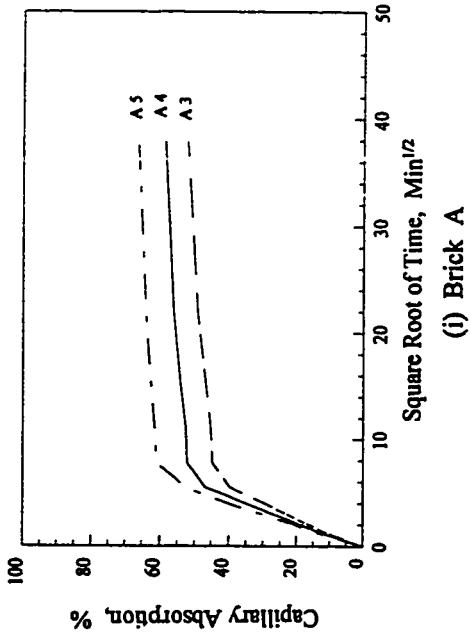


Figure 4.11A Capillary Absorption Curves for bricks A,B,C, and D expressed in % of 5 hr. Boiling Water Absorption (S_x/B)

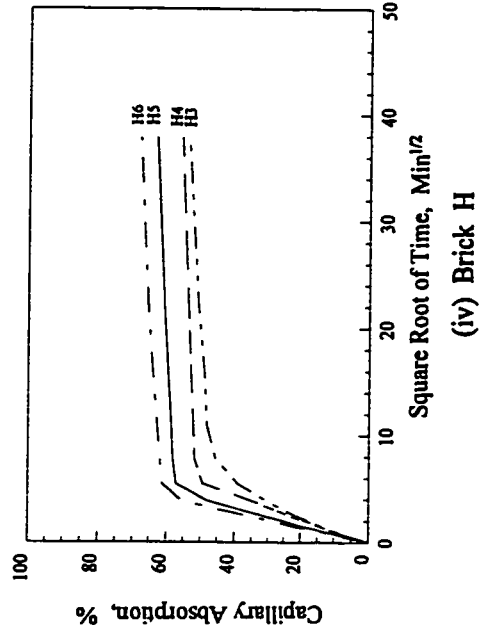
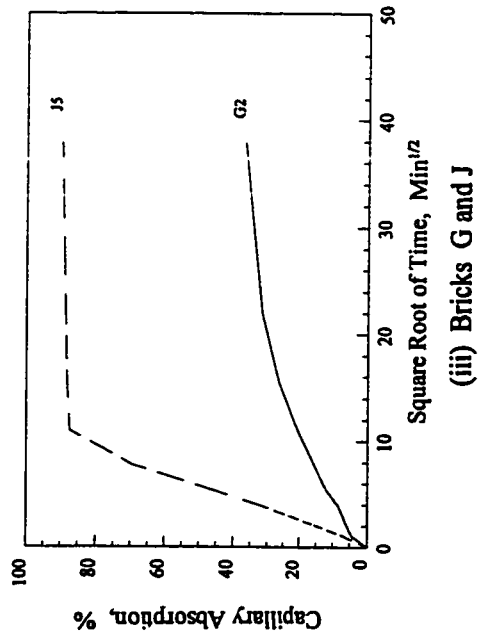
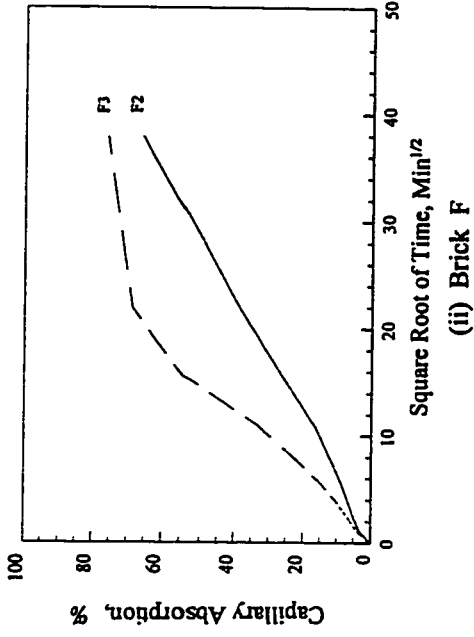
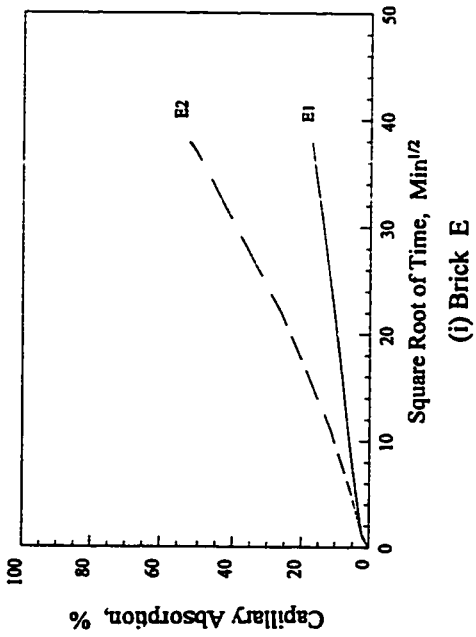


Figure 4.11B Capillary Absorption Curves for bricks E,F,G,H, and J expressed in % of 5 hr. Boiling Water Absorption (S_x/B)

type the rate of absorption was faster for bricks with higher porosity. For brick types A, B, C, D, F, G, and H the total absorption at the end of 24 hours were almost equal in both submersion and capillary absorption. In the case of brick J5 it was observed that the capillary absorption at the end of 24 hours was slightly higher than its submersion absorption value. For brick E there was a huge difference in submersion and capillary absorptions after 24 hours, with submersion absorption values being higher. This huge difference suggests that, in addition to the pore size distribution, the surface characteristics might also affect the water absorption into the bricks. Since the amount of water present inside the brick is the major factor affecting its durability, water absorption properties should be included in the development of durability indices.

4.4 Compressive Strength

The compressive strengths of the brick groups were measured according to the test method specified in ASTM C67. Table 4.5 gives the results from the test. Figure 4.12 shows the gross compressive strengths of the bricks. All the brick groups tested satisfied the ASTM C216 requirement for minimum average compressive strength of 20.7 MPa for severe weathering. Brick types D, E, and F resisted more than 100 MPa before failure. Within a brick type, as expected, the strength decreased with increases in absorption values. Brick J5, which had the highest porosity (27.91 %) amongst the brick types tested, showed much higher strength compared to certain other bricks having lower porosity. This might be due to the fact that majority of pores in J5 were very small (below 1 μm)

Figure 4.13 shows bulk density of the bricks, determined using mercury intrusion porosimeter. The bulk density ranged from 1.9 to 2.4 g/cc and most of the bricks had the density

TABLE 4.5
Density, Strength, and Pulse Velocity of the Bricks

Brick Type	Bulk Density g/cc	Compressive Strength, MPa		Ultrasonic Pulse Velocity m/s
		Gross	Net	
A3	2.1302	43.02	-	3390
A4	2.0793	35.12	-	3161
A5	2.0121	29.60	-	2690
B2	2.1763	74.84	-	3647
B3	2.1456	65.61	-	3396
B4	2.0515	46.75	-	2945
B5	1.9909	32.88	-	2514
B6	1.9540	24.18	-	2280
C3	2.1377	74.53	-	3566
C4	2.0327	54.46	-	3116
C5	2.0052	39.26	-	2842
D2	2.3179	105.18	120.13	4175
D3	2.2847	102.57	117.23	4073
E1	2.4429	143.54	166.49	4383
E2	2.3967	133.94	154.80	4172
F2	2.1178	114.10	130.20	4151
F3	2.0979	109.94	125.35	3806
G2	2.1304	83.18	91.35	3481
H3	2.0935	45.01	-	3133
H4	2.0624	41.08	-	2912
H5	2.0036	32.58	-	2466
H6	1.9589	24.31	-	2201
J5	1.9527	66.48	77.46	3022

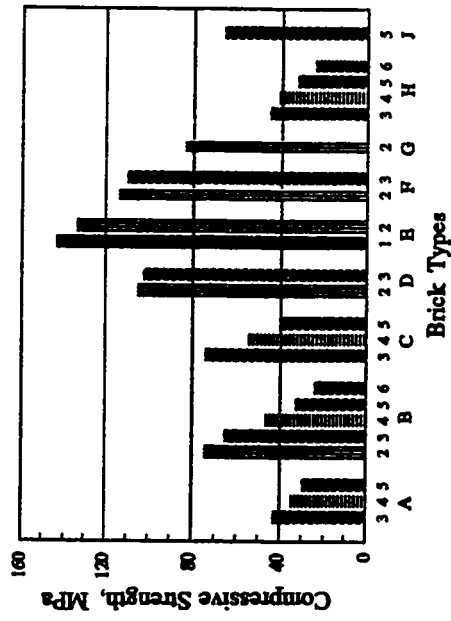


Figure 4.12 Compressive Strength (Gross) of the bricks

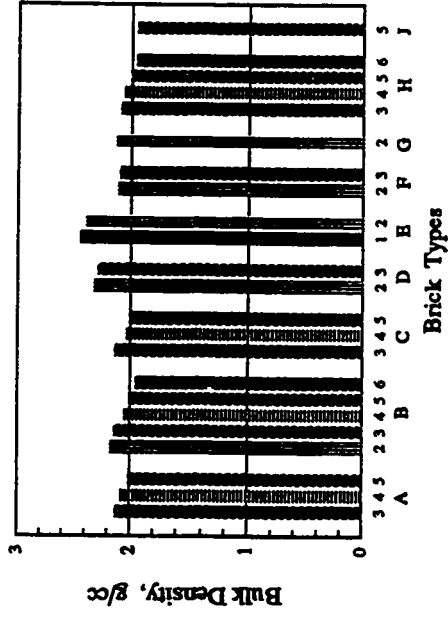


Figure 4.13 Bulk Density of the bricks

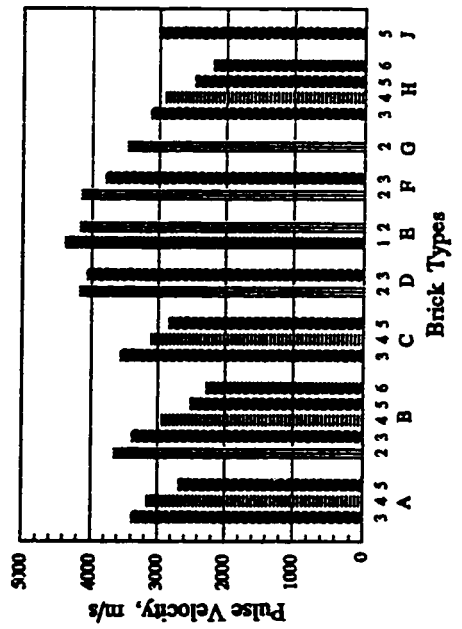


Figure 4.14 Ultrasonic Pulse Velocity of the bricks

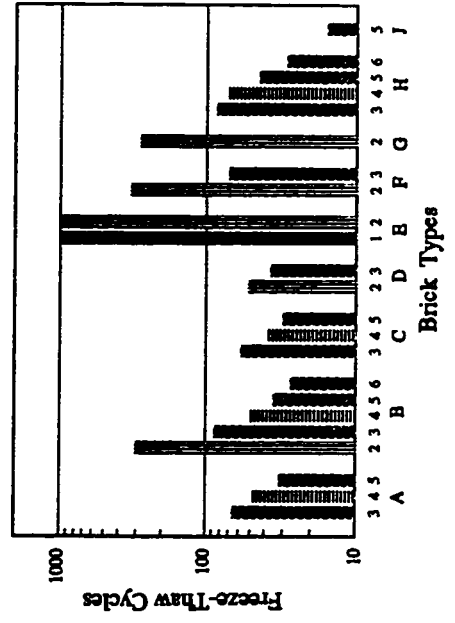


Figure 4.15 Freeze-Thaw cycles resisted by the bricks

around 2 g/cc. Bricks D & E had higher densities as they had lower porosity compared to other bricks.

4.5 Ultrasonic Pulse Velocity

The ultrasonic pulse velocity measurements were taken to study the feasibility of evaluating the durability using nondestructive techniques. The pulse velocity was measured using the test procedures explained in Section 3.5.3. The test results are shown in Table 4.5 and in Figure 4.14. Bricks D, E, and F showed comparatively higher pulse velocity. In general pulse velocity showed an increase with an increase in compressive strength or a decrease in porosity. Within a brick type pulse velocity was found to decrease with increase in absorption values. The relationship between pulse velocity and other properties of the bricks are discussed in detail in Chapter 6.

4.6 Freeze-Thaw Performance

The accelerated freezing and thawing test explained in Section 3.5.4 was used for comparing the relative performance of the bricks. The freeze-thaw performance of the brick groups are given in Table 4.6. It can be seen that failed bricks showed negligible weight loss and none of the bricks had reached a weight loss of 0.5%. The development of visible cracks was observed to be the cause for the failure of all the bricks. The initial saturation level of the bricks were maintained to be almost equal to their corresponding 24 hr. water absorption. During the course of the freeze-thaw test the saturation level of the bricks were found to have increased. The % increase in saturation was more for bricks with lower absorption values compared to bricks with higher absorption values.

TABLE 4.6
Freeze-Thaw Performance of the Bricks

Brick Type	Freeze-thaw Cycles resisted	Initial Saturation	Final Saturation	% Increase in Saturation	Weight Loss
		%	%	%	%
A3	66	5.35	6.46	20.66	0.03
A4	48	6.83	7.81	14.26	0.05
A5	32	8.86	9.77	10.35	0.04
B2	306	3.34	4.65	40.95	0.16
B3	88	4.84	6.04	25.51	0.12
B4	50	6.87	7.85	14.22	0.02
B5	35	8.90	9.81	10.27	0.05
B6	27	10.24	11.08	8.21	0.05
C3	58	5.26	6.45	22.67	0.04
C4	38	6.92	7.71	11.62	0.02
C5	30	8.17	8.95	9.56	0.02
D2	52	3.78	4.28	13.11	0.07
D3	37	4.53	5.01	10.71	0.06
E1	> 1000	0.97	1.74	93.68	0
E2	> 1000	2.42	2.98	23.18	0
F2	331	3.71	5.01	35.61	0.05
F3	71	5.08	5.78	13.49	0.06
G2	286	6.73	8.15	21.10	0.04
H3	86	5.07	6.56	29.39	0.02
H4	72	6.67	8.57	28.49	0.20
H5	44	8.54	10.06	17.80	0.23
H6	29	10.07	10.67	5.96	0.01
J5	16	9.56	10.56	10.46	0.13

Figure 4.15 shows the freeze-thaw cycles resisted by the bricks. Bricks E1 and E2 did not fail even after subjecting to 1000 cycles of freezing and thawing. Therefore, for the sake of comparison in this study, these two bricks were assigned 1000 cycles of freeze-thaw resistance. Brick J5 showed the least resistance with just 16 cycles. Within a brick type, the freeze-thaw cycles resisted decreased with increasing water absorption values.

4.7 Summary

The various properties of the nine different types of bricks used in this research were measured according to the test procedures discussed in Chapter 3. They included pore properties, water absorption properties, compressive strength, pulse velocity, and freeze-thaw resistance. These properties were analyzed in order to characterize the brick types. They were subsequently used for deriving a new durability index (in Chapter 5), for studying the feasibility of nondestructive evaluation of durability (in Chapter 6), and for finding the effect of impregnation on brick properties (in Chapter 7).

Development of Durability Index

The research procedure followed for the development of the durability index was already shown in Figure 3.1. The method to be adopted for deriving the index was decided after carrying out a comparative study of the existing indices and their limitations. This chapter discusses the results of the comparative study and subsequently the derivation of a new index for the evaluation of clay brick durability.

5.1 Comparative Study of Durability Indices

The durability indices developed by various researchers had already been reviewed in Section 2.1.2.3. Equations [2.1] to [2.27] show the different relations developed by Robinson et al [1977], Maage [1984], Nakamura [1988a], and Arnott [1990], defining durability in terms of physical properties of the bricks. Both Nakamura and Arnott gave different sets of equations derived by multivariate regression analysis, with increasing number of variables and regression coefficients. It was found difficult and unnecessary to study all these equations. Therefore it was decided to select the best equation developed by these two researchers for the comparative study. The indices selected are discussed in the following section.

5.1.1 Indices Selected

For the sake of convenience in comparison, the equations for durability developed by the above mentioned researchers would be referred to as Durability Index by Robinson (*DIR*), Durability Index by Maage (*DIM*), Durability Index by Nakamura (*DIN*), and Durability Index by Arnott (*DIA*) respectively. Therefore from equation [2.1], the Durability Index by Robinson (*DIR*) is given by:

$$DIR = \left[\frac{IRA}{10(1 - C/B)} \right] - \left[\frac{145 CS - 6000}{1000} \right] + [C - 10] \quad [5.1]$$

where, *IRA* = initial rate of absorption (g/min.193.55cm²), *C* = 24 hr. cold water absorption (%), *B* = 5 hr. boiling water absorption (%), *CS* = compressive strength (MPa), and *C/B* = saturation coefficient.

From equation [2.2] Durability Index by Maage (*DIM*) is given by:

$$DIM = \frac{3.2}{PV} + 2.4 P3 \quad [5.2]$$

where, *PV* = intruded pore volume (ml/g), and *P3* = % of pores with diameter larger than 3 μm (% of *PV*).

Nakamura [1988a] suggested two sets of equations for indirect evaluation of frost susceptibility, one based on physical characteristic factors of sample (equations [2.3] to [2.7]) and the other based on specific pore volume of sample (equations [2.8] to [2.14]). The equations based on specific pore volume had comparatively higher regression coefficients. Most of the characteristic factors in the equations cannot be easily measured. Also pore size distribution had already been discussed as a major factor affecting durability of bricks. Therefore equation [2.14]

was selected for the comparative study of indices. So Durability Index by Nakamura (*DIN*) is given by:

$$DIN = -0.12 - 0.09(A_p) + 0.15(B_p) + 0.08(C_p) - 0.01(D_p) - 0.01(E_p) - 0.01(F_p) - 0.01(G_p) \quad [5.3]$$

where the variables are specific pore volume (in $10^{-3}\text{cm}^3/\text{g}$) in the following pore size ranges (in pore radius): $A_p = 5\text{-}10\text{ nm}$; $B_p = 10\text{-}50\text{ nm}$; $C_p = 0.05\text{-}0.1\text{ }\mu\text{m}$; $D_p = 0.1\text{-}0.4\text{ }\mu\text{m}$; $E_p = 0.4\text{-}0.7\text{ }\mu\text{m}$; $F_p = 0.7\text{-}1.0\text{ }\mu\text{m}$; $G_p = 1.0\text{-}7.5\text{ }\mu\text{m}$.

Arnott [1990] also suggested two sets of equations for durability indices of bricks, one based on loss of strength during freeze-thaw test (equations [2.15] to [2.19]), and the other based on visual distress during the test (equations [2.20] to [2.27]). The equations based on visual distress had comparatively higher regression coefficients. Also, the field performance is normally assessed through visual appearance and therefore the durability index based on visual distress would better predict the field performance of bricks. After considering these facts, the index based on visual distress was selected for the comparative study. The equations [2.20] to [2.27] had regression coefficients ranging from $R^2=0.76$ to $R^2=0.98$. The variables in the equations ranged from 1 to 12. It could be seen from Table 2.4 that inclusion of more variables did not substantially improve the R^2 value of the equations. Moreover, durability indices should be simple and easy to determine. Therefore in this comparative study equation [2.23] with an R^2 value of 0.95 was selected. So Durability Index by Arnott (*DIA*) is given by:

$$DIA = 9.187A_v - 0.487B_v + 423.8C_v - 2.408D_v - 84.5 \quad [5.4]$$

where, $A_v = \%$ of total sample volume represented by pores greater than $2.8\text{ }\mu\text{m}$, $B_v = 30\text{ minute}$

initial rate of absorption based on net area of sample face exposed to water ($\text{g}/30\text{min}\cdot 193.55\text{cm}^2$), C_v = ratio of 5 hour boiling water absorption to vacuum saturation, and D_v = ratio of 4 hour cold water absorption to 5 hour boiling water absorption expressed as percentage.

5.1.2 Experimental

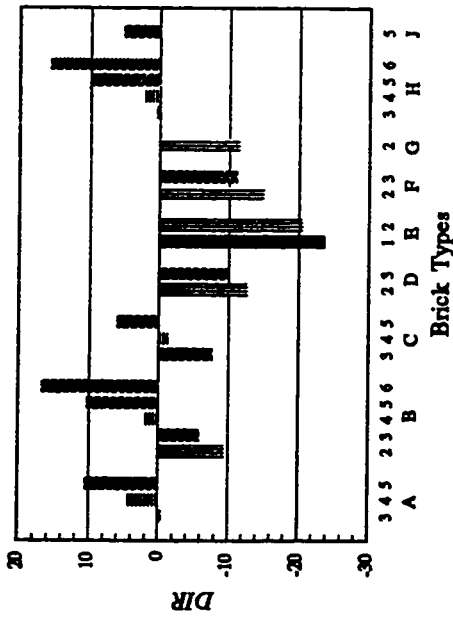
The nine different types of bricks, whose properties were discussed in Chapter 4, were used for the comparative study. The various physical properties of the bricks required for calculating the durability indices were measured using the test procedures explained in Section 3.5. The durability indices of the bricks are given in Table 5.1. Figure 5.1 shows those indices in a graphical form. The physical properties used for calculating the indices are given in tables in Appendix C.

5.1.3 Discussion of Results

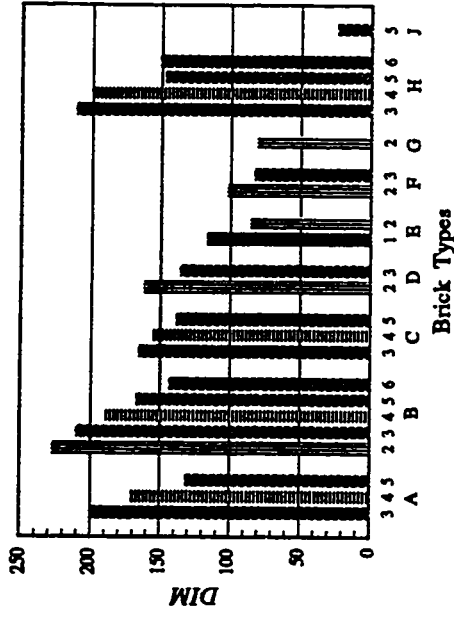
Robinson suggested that a value of 7 or less for *DIR* would mean that less than 10% of the bricks would fail. According to this durability criterion, from Figure 5.1(a), brick types A5, B5, B6, H5, and H6 were considered as nondurable. Bricks D, E, F, and G had very low value of *DIR*, suggesting that they were highly durable. From Table 4.5 it can be seen that bricks D, E, F, and G had comparatively high compressive strength whereas A5, B5, B6, H5, and H6 were among the lowest strength bricks. This suggests that for high strength bricks, *DIR* is primarily governed by the compressive strength. Brick J5, which had the highest pore volume and majority of pores in the 1-0.1 μm range, was found to have a *DIR* value of 5.31, better than some of the other bricks.

TABLE 5.1
Durability Indices of the Bricks

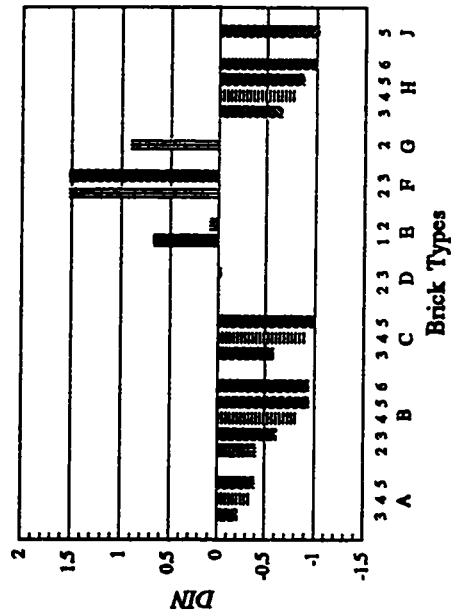
Brick Type	Freeze-thaw Cycles resisted	Durability Indices			
		<i>DIR</i>	<i>DIM</i>	<i>DIN</i>	<i>DIA</i>
A3	66	-0.45	200.22	-0.218	289.28
A4	48	4.36	171.20	-0.358	261.58
A5	32	10.60	131.31	-0.401	210.80
B2	306	-9.38	227.41	-0.413	330.73
B3	88	-5.94	210.60	-0.618	316.40
B4	50	1.97	189.33	-0.813	278.28
B5	35	10.36	167.56	-0.942	243.16
B6	27	16.88	144.02	-0.944	207.14
C3	58	-7.64	166.02	-0.582	279.80
C4	38	-1.21	154.81	-0.917	268.83
C5	30	6.15	138.99	-0.993	231.59
D2	52	-12.67	162.26	-0.009	205.63
D3	37	-9.82	136.10	-0.030	180.76
E1	> 1000	-23.71	117.10	0.676	117.02
E2	> 1000	-20.43	85.85	0.102	102.11
F2	331	-14.96	102.40	1.526	189.07
F3	71	-11.18	82.75	1.530	165.51
G2	286	-11.37	81.11	0.913	299.52
H3	86	0.48	211.49	-0.658	298.48
H4	72	2.34	200.06	-0.797	274.34
H5	44	10.00	147.89	-0.879	225.92
H6	29	15.86	151.09	-1.000	230.73
J5	16	5.31	24.13	-1.025	25.07



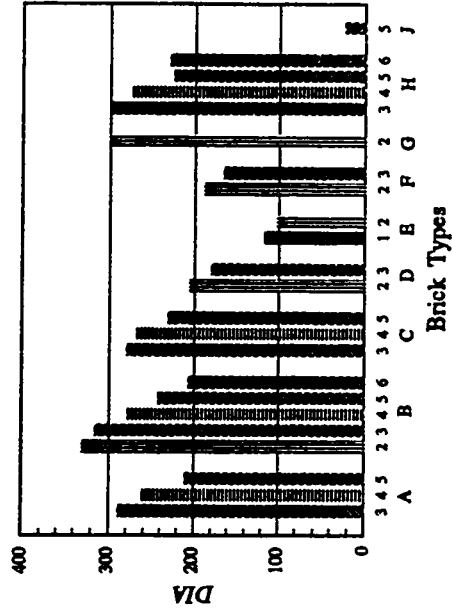
(a) Durability Index by Robinson (*DIR*)



(b) Durability Index by Maage (*DIM*)



(c) Durability Index by Nakamura (*DIN*)



(d) Durability Index by Arnott (*DIA*)

Figure 5.1 The different Durability Indices for the bricks

According to Maage's index, brick J5 was found to have the lowest durability as shown in Figure 5.1(b). Maage recommended a *DIM* value of greater than 70 for qualifying as durable brick and less than 55 for nondurable brick. Based on this criterion, all bricks except J5 qualified as durable brick. Bricks E, F, and G had lower *DIM* values compared to other brick types. But these bricks were found to be comparatively durable than other bricks according to Robinson's method. This difference might be due to the fact that, while *DIR* depended to a large extent on compressive strength, *DIM* depended on pore volume and pore size distribution.

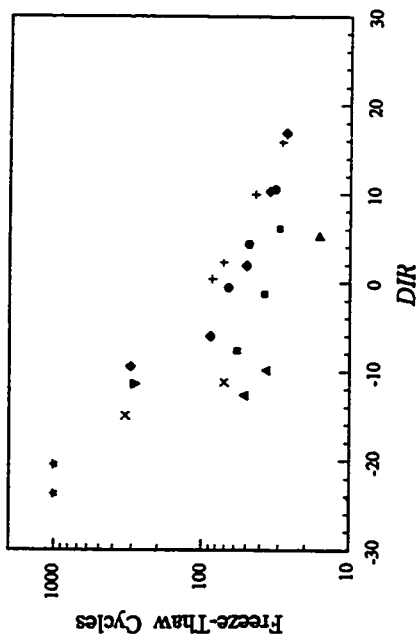
Nakamura found positive high correlations between frost-damage susceptibility and pore volume in the pore diameter range $< 0.2 \mu\text{m}$. Therefore positive values for *DIN* suggests lower durability for bricks. According to Nakamura's method bricks D, E, F, and G were found to have lower durability compared other bricks. This was exactly the opposite to that found by Robinson's method. Both *DIN* and *DIM* identify bricks D, E, F, and G as comparatively less durable. But brick J5, which had the least durability according to *DIM* value, was the most durable brick according to *DIN*. This was because J5 had most of its pores larger than $0.2 \mu\text{m}$ in diameter but less than $1 \mu\text{m}$. From Figure 5.1(c), it can be seen that within a brick type durability increases with increasing water absorption values. This is against what is normally observed in reality.

Figures 5.1(b) and 5.1(d) show that both *DIM* and *DIA* give almost identical assessment of relative durability of bricks. Both these indices employ pore volume larger than $3 \mu\text{m}$ in diameter for assessment. *DIA* also incorporates absorption properties in the evaluation. Accordingly brick G2, which had a comparatively lower *DIM* value, had comparatively higher *DIA* value. Brick J5 had the least *DIA* value among the brick types. Within a brick type, as was expected, the index dropped with increasing absorption values. According to *DIA*, brick E had

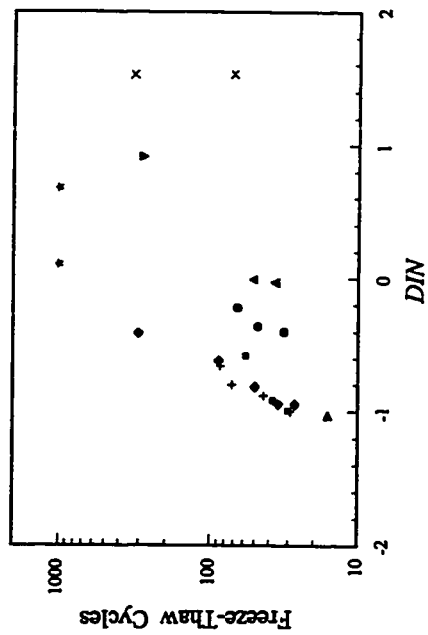
lower durability than brick F whereas *DIR* values put brick E having higher or almost equal durability as brick F.

In order to compare how well these indices could predict the performance of bricks in a freeze-thaw environment, the relationship between indices and frost resistance was studied. For the purpose of comparison it was presumed that a brick which resisted a higher number of cycles in the accelerated freeze-thaw test, was expected to have better durability under natural environment than a brick which resisted a lower number of cycles. Figure 5.2 shows the plots between the respective indices and the freeze-thaw cycles resisted by the bricks. In Figure 5.2(a) *DIR* shows definite trend at higher freeze-thaw cycles, with freeze-thaw resistance increasing as *DIR* value decreases. At lower freeze-thaw cycles (< 100) the data points are rather scattered. Brick D2, D3, and F3, which had high compressive strength and accordingly low index showed much less frost resistance. Also, certain bricks having wide difference in *DIR* values had almost the same frost resistance. The scatter of points might be due to the fact that the distribution of pore size was not considered in *DIR*. Brick J5 which had comparatively better *DIR* value than some of the other bricks was the least frost resistant.

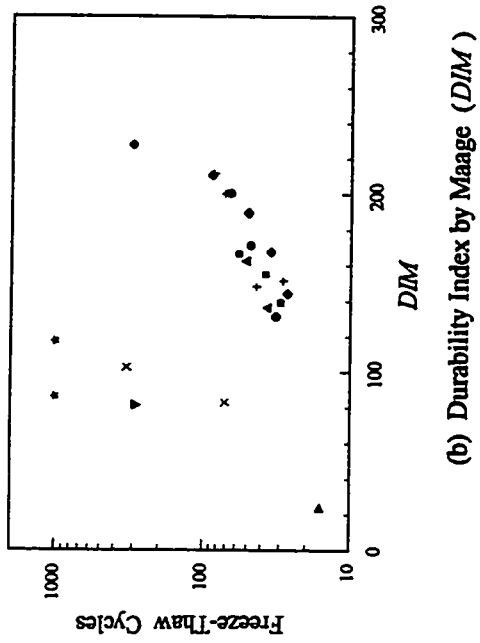
In Figure 5.2(b) the relation between *DIM* and frost resistance is shown. Except for bricks E, F, and G, all other bricks showed an increase in frost resistance with increasing *DIM* values. Bricks E, F, and G had comparatively higher frost resistance. But low *P3* values for these bricks resulted in low *DIM* values. These bricks also had low rate of absorption. The amount of water that is actually present inside the bricks is a critical factor for durability. In addition to porosity and pore size distribution, surface characteristics of bricks may affect the rate and amount of water absorption, which is not taken into consideration by Maage's index. This might be the reason why



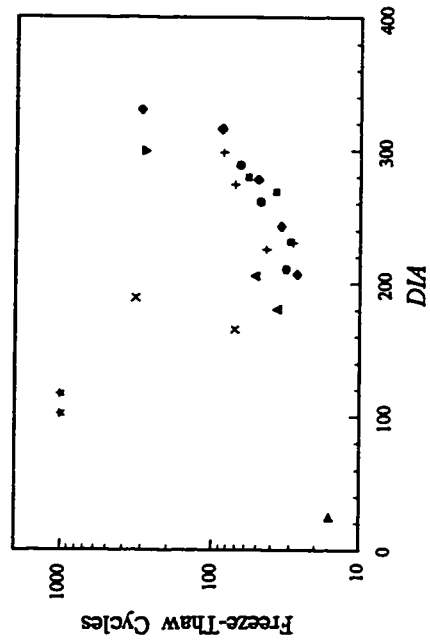
(a) Durability Index by Robinson (DIR)



(c) Durability Index by Nakamura (DIN)



(b) Durability Index by Maage (DIM)



(d) Durability Index by Arnott (DIA)

Brick Types	
●	A
●	B
■	C
■	D
▲	E
▲	F
×	G
▼	H
+	I
▲	J

Figure 5.2 Relation between the different durability indices and frost resistance of the bricks

some of the bricks had low *DIM* values, while they exhibited much better frost resistance.

As seen in Figure 5.2(c), *DIN* showed no relation with frost resistance. The data points were scattered. Bricks, which resisted higher number of cycles, were found to have higher frost susceptibility according to *DIN*. Brick J5, which had the least frost resistance, was evaluated to be the most durable brick as per Nakamura's method.

The relation between *DIA* and frost resistance of the bricks is shown in Figure 5.2(d). *DIA* shows an almost similar trend as *DIM*. But brick G2 had an improved *DIA* value and as a result it showed to follow the general trend, unlike that shown for *DIM* in Figure 5.2(b). Bricks E and F still stayed away from the general trend shown by other bricks, even though brick F showed better *DIA* value. Like *DIM*, *DIA* also needs improvement in defining the durability of low absorption rate bricks.

5.1.4 Summary of the Comparative Study

Robinson's index was found to give emphasis on the compressive strength property of the bricks. The pore size distribution is not a factor in *DIR*. Bricks with large difference in *DIR* values showed almost same frost resistance. Therefore durability evaluation using *DIR* can be misleading. Maage's index (*DIM*) was found to be the better of the four indices studied. *DIM* showed a general trend of increasing frost resistance with increase in index for most of the brick types. In addition, Maage's index specifies limiting values for classifying as durable and nondurable bricks. But *DIM* depends exclusively on pore size distribution and does not consider the amount of water actually absorbed by the bricks. As a result, some bricks had shown higher frost resistance while having low *DIM* values. Therefore Maage's method needs improvement. Nakamura's index

showed no relation to freeze-thaw performance of the bricks. Therefore, based on this comparative study, *DIN* is not recommended for durability evaluation of bricks. Like *DIM*, *DIA* also needs improvement in predicting the durability of low absorption rate bricks. In addition *DIA* is a relative index with no specified limiting values for classifying brick durability. Therefore it can only be used for comparing the durability of bricks.

5.2 Development of Durability Index

In the preceding section the existing durability indices were compared and their performance studied. It was found that those indices had limitations in reliably predicting the durability of bricks. Therefore it was considered necessary to develop a new index to overcome the limitations discussed earlier. This section discusses the method adopted for developing the new durability index and its derivation.

5.2.1 Method Adopted

If an index is developed based on laboratory freeze-thaw test that cannot identify durable and nondurable bricks, then that index will be a relative one, which can only be used for comparing durability. In order to derive an absolute index, either the performance study should involve field test or it should be validated against field performance.

The comparative study showed that *DIM* was better than other existing indices in evaluating durability. *DIM* is also an absolute index which can classify bricks as durable and nondurable. Maage's equation had been found to be correct by other researchers [Smalley et al 1987; Winslow et al 1988]. In addition, it is based on pore characteristics which affect durability

considerably. A drawback with Maage's method is that it requires a mercury porosimeter to evaluate durability, thereby making it a rather expensive test.

But it was found in this study that for certain bricks, *DIM* values might not give a true measure of their frost resistance. The amount of water that is absorbed into a brick normally depends upon the porosity and pore size distribution of bricks. In the case of certain bricks surface characteristics and other unknown factors may affect their water absorption, thereby their frost resistance. Therefore for these bricks, an "apparent pore size distribution" should be used instead of true pore size distribution in Maage's equation, so that *DIM* gives a true measure of frost resistance. The "apparent pore size distribution" may be expressed in terms of the actual absorption characteristics of bricks. Since the amount of water that is actually present in a brick is a major contributing factor to the pressure due to frost action, the absorption characteristics of bricks should be a property to be included in deriving durability index.

So in this study the new durability index was developed by modifying Maage's equation by incorporating absorption properties of bricks. Empirical relations between pore variables *PV* and *P3* in equation [5.2] and the various absorption properties were studied. These relations were used to develop the new durability index based on water absorption properties.

5.2.2 Relation between *PV* and Water Absorption Property

PV represents the total pore volume in the material, measured by the intrusion of mercury into the pores. It also gives the total pore volume that is available for absorbed water. Therefore, the absorption property used for studying the relation with *PV* should give a measure of the total pore volume. The 5 hr. boiling water absorption test is believed to drive out air from pores of

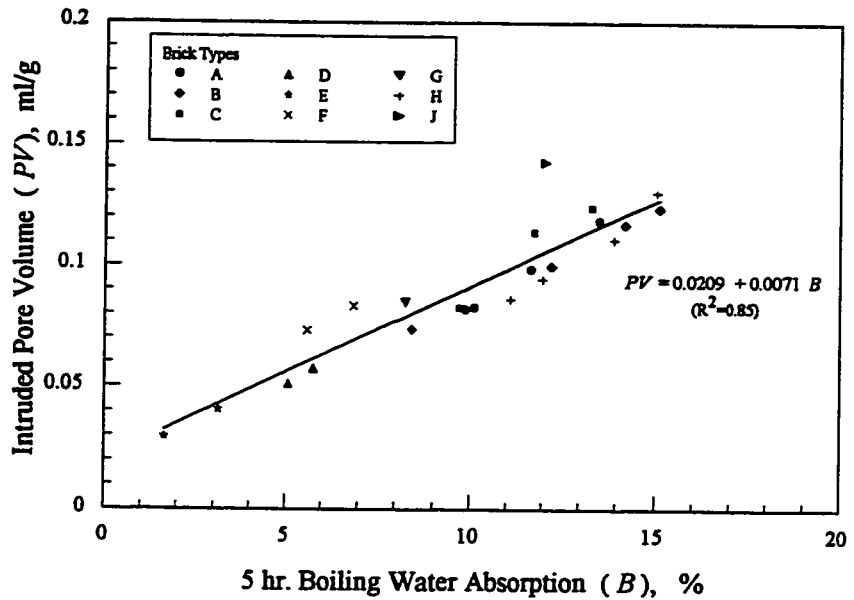


Figure 5.3 Relation between Pore Volume (*PV*) and 5 hr. Boiling Water Absorption (*B*)

specimens and fill them with water. It normally gives the maximum possible absorption and a measure of the total available pore space. The relation between *PV* and *B* is shown in Figure 5.3. It can be seen that *PV* and *B* gives a reasonably good linear relation with a regression coefficient of $R^2=0.85$, using least square method. Brick J5 was observed to be slightly off from the general trend. The empirical equation connecting *PV* and *B* is given by:

$$PV = 0.0209 + 0.0071 B \quad [5.5]$$

5.2.3 Relation between *P3* and Water Absorption Property

It was observed from the properties of the bricks (discussed in Chapter 4) that within a brick type the saturation coefficient (*C/B*) decreased as the *P3* values increased. *C/B* represents

the ratio of amount of water filling the pores in 24 hr. absorption to the total pore volume. Therefore $(1-C/B)$, the ratio of unfilled pores to total pore space, increased with increasing $P3$ values. This observation led to the study of relation between $P3$ and the absorption properties that measure the unfilled pore space. $P3$ values are expressed as % of the total pore volume. Therefore the absorption properties studied were $(1-C_x/B)100$ and $(1-S_x/B)100$, where C_x and S_x were submersion absorption and capillary suction respectively at any time x expressed as % of dry weight, measured according to test procedures explained in Section 3.5. These absorption properties represented the unfilled pore space expressed as % of total pore space (measured in terms of B). Different time intervals were considered and two best relations were identified. Figures 5.4 and 5.5 show the variation of $P3$ with $(1-C1/B)100$ and $(1-S4/B)100$ respectively, where $C1$ is 1 hr. submersion absorption and $S4$ is 4 hr. capillary suction.

A linear relation between $P3$ and absorption property is shown in these Figures. It could be seen that brick types E, F, and G did not follow these linear relations and therefore they were excluded from the regression analysis to develop empirical equations. It was also shown in Figure 5.2b that these brick types did not follow the general trend in the relation between frost resistance and DIM . These bricks had low $P3$ values but relatively high absorption property values. They also showed relatively high frost resistance. The performance of these bricks suggested that they behaved as though they had a much higher $P3$ values, thus justifying the concept of "apparent pore size distribution" suggested in Section 5.2.1.

In Figure 5.4, the relation between $P3$ and $(1-C1/B)100$, with a regression coefficient of $R^2=0.84$, is given by:

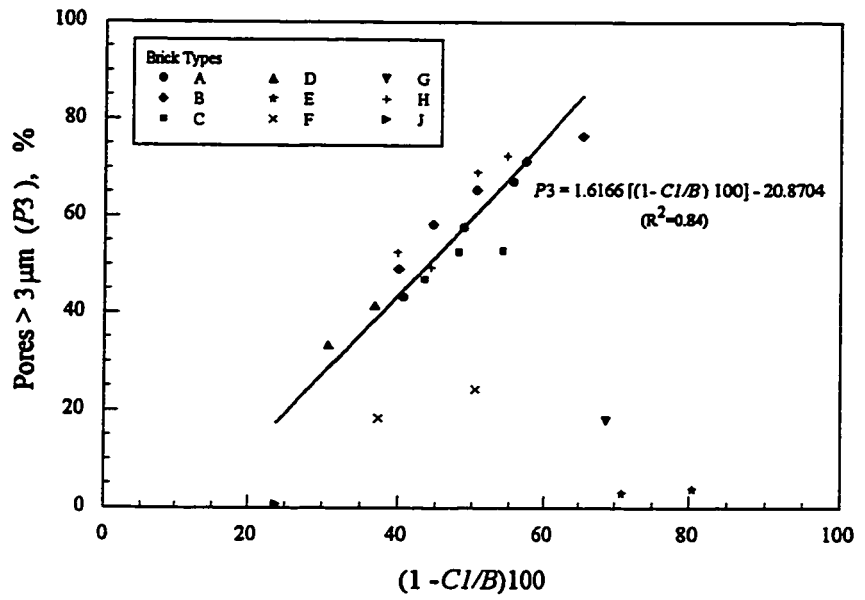


Figure 5.4 Relation between $P3$ and $(1-C1/B)100$

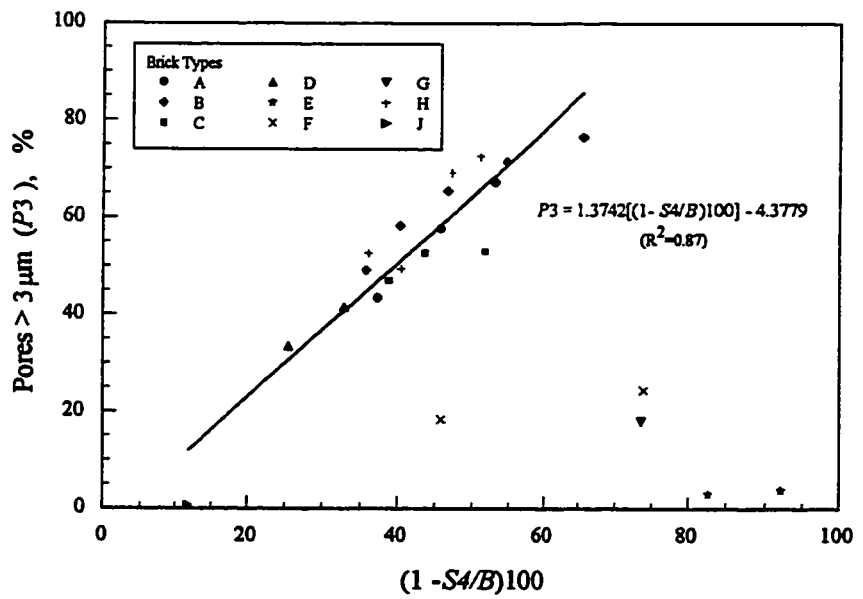


Figure 5.5 Relation between $P3$ and $(1-S4/B)100$

$$P3 = 1.6166 [(1 - C1/B)100] - 20.8704 \quad [5.6]$$

and in Figure 5.5, the relation between $P3$ and $(1-S4/B)100$, with a regression coefficient of $R^2=0.87$, is given by:

$$P3 = 1.3742 [(1 - S4/B)100] - 4.3779 \quad [5.7]$$

Equation [5.7] gave a better relation compared to equation [5.6].

5.2.4 Derivation of New Durability Index

The above empirical equations were used for deriving the new Durability Index based on Absorption Properties ($DIAP$). By substituting equations [5.5] and [5.6] for PV and $P3$ respectively in equation [5.2] and simplifying, $DIAP$ using submersion absorption property is given by:

$$DIAP(C) = \frac{450.70}{(2.94 + B)} + 387.98 (0.87 - \frac{C1}{B}) \quad [5.8]$$

Similarly, by substituting equation [5.5] and [5.7] in equation [5.2] and simplifying, $DIAP$ using capillary suction value is given by:

$$DIAP(S) = \frac{450.70}{(2.94 + B)} + 329.81 (0.97 - \frac{S4}{B}) \quad [5.9]$$

The performance of $DIAP(C)$ and $DIAP(S)$ was studied by observing the relation between these indices and the frost resistance as measured through the accelerated freezing and thawing test explained in Section 3.5. The result of this study is shown in Figures 5.6 and 5.7. These

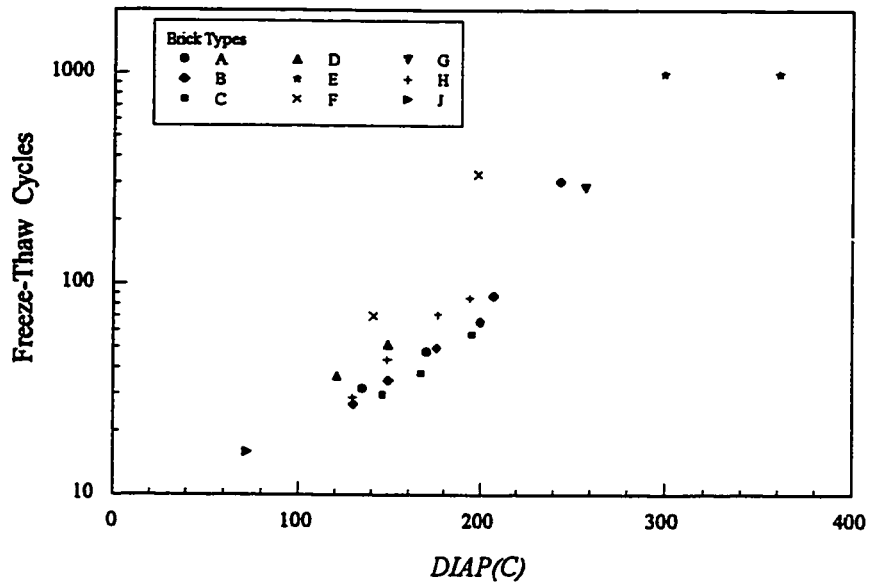


Figure 5.6 Relation between $DIAP(C)$ and frost resistance

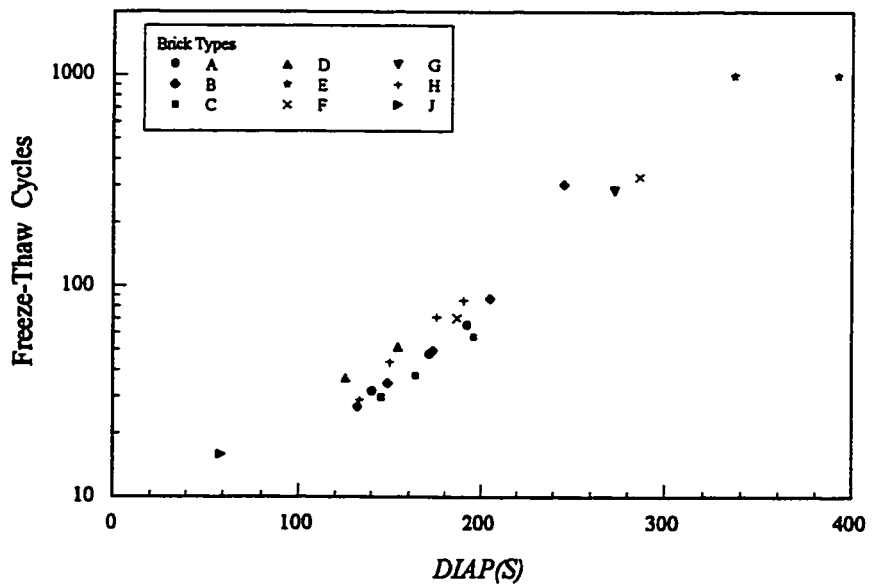


Figure 5.7 Relation between $DIAP(S)$ and frost resistance

indices gave a much better relation with frost resistance than *DIM* (see Figure 5.2b) and unlike for *DIM*, brick types E, F, and G followed the general trend. Comparing Figures 5.6 and 5.7, it can be found that in the case of *DIAP(S)* the scatter of data point is lesser than *DIAP(C)* and therefore *DIAP(S)* is a better index than *DIAP(C)* for defining the frost resistance. Since the freeze-thaw test results were used only for comparing the performance of the bricks, no regression analysis was done between the durability indices developed and the freeze-thaw cycles resisted by the bricks.

In order to find the limiting values for identifying durable and nondurable brick using the new indices, relation between *DIM* and these indices were studied. The results are shown in Figures 5.8 and 5.9. Since *DIM* did not give a true assessment of frost resistance for brick types E, F, and G for reasons discussed in Sections 5.2.1 and 5.2.3, these brick types were excluded from the regression analysis. The equation relating *DIAP(C)* and *DIM* ($R^2=0.83$) is given by:

$$DIAP(C) = 33.0108 + 0.7882 DIM \quad [5.10]$$

and the equation relating *DIAP(S)* and *DIM* ($R^2=0.86$) is given by:

$$DIAP(S) = 27.2385 + 0.8239 DIM \quad [5.11]$$

The limiting values for *DIAP(C)* and *DIAP(S)* were obtained by substituting *DIM* = 70 and *DIM* = 55 in equations [5.10] and [5.11]. These values are given in Table 5.2. In the case of *DIAP(C)* the brick will be durable when *DIAP(C)* > 90 and nondurable when *DIAP(C)* < 75. Similarly, for *DIAP(S)* the limiting values are *DIAP(S)* > 85 for durable and *DIAP(S)* < 70 for nondurable.

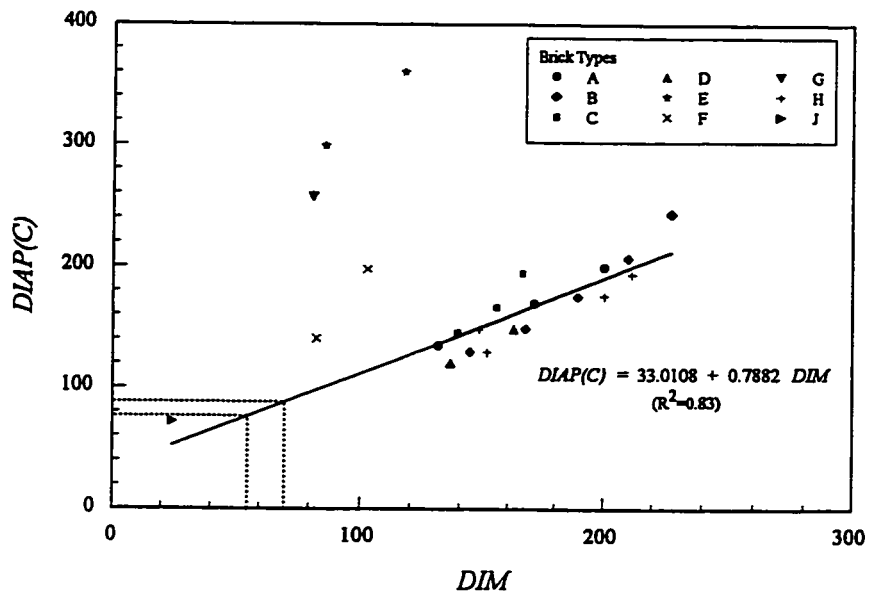


Figure 5.8 Relation between *DIM* and *DIAP(C)*

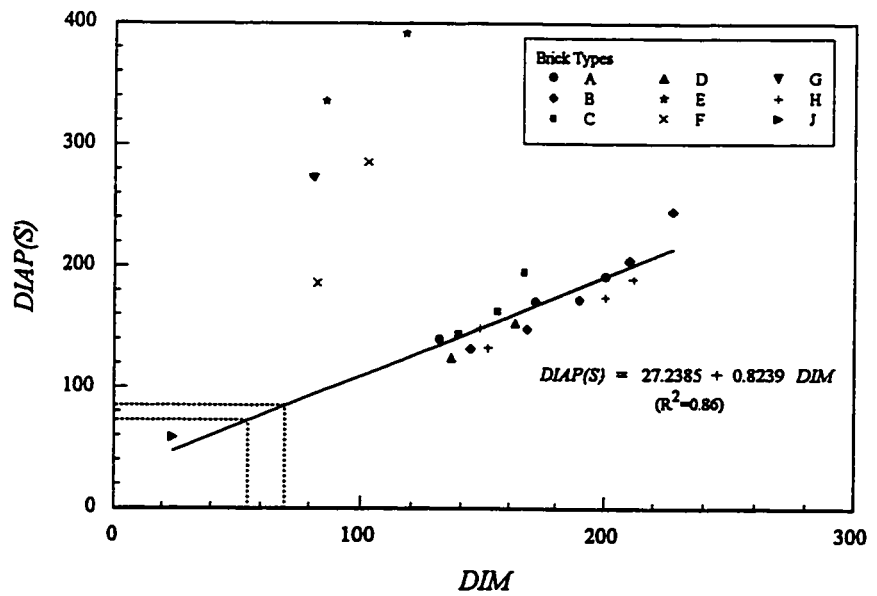


Figure 5.9 Relation between *DIM* and *DIAP(S)*

TABLE 5.2
Limiting Values for the Indices

Index	Limiting Values	
	Durable	Nondurable
<i>DIM</i>	> 70	< 55
<i>DIAP(C)</i>	> 90	< 75
<i>DIAP(S)</i>	> 85	< 70

For brick types E, F, and G, which did not follow the general trend in the relation between *DIM* and frost resistance (see Figure 5.2b), "apparent *P3*" values were calculated by substituting the corresponding $(1-C1/B)100$ and $(1-S4/B)100$ values in equations [5.6] and [5.7]. With these "apparent *P3*" values improved Maage's indices *DIM-I(C)* and *DIM-I(S)* were calculated for bricks E, F, and G using equation [5.2] (when the calculated "apparent *P3*" values exceeded 100, it was equated to 100). The relation between the improved indices and frost resistance is shown in Figures 5.10 and 5.11. Comparing to Figure 5.2b, it can be seen that these improved indices predict the performance of bricks better than *DIM*. *DIM-I(S)* gave a better relation with frost resistance than *DIM-I(C)*.

5.2.5 Validation

In order to validate the new indices developed, their performance in predicting the frost resistance of brick was studied. Three brick types (K, L, and M) were used for this purpose. Of these, K and L were extruded bricks while M was a dry pressed brick. They were classified into

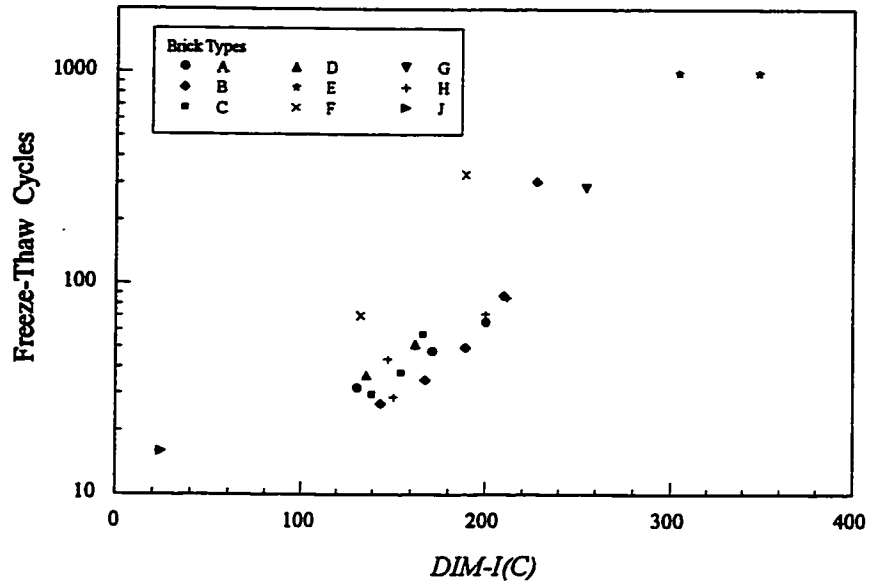


Figure 5.10 Relation between $DIM-I(C)$ and frost resistance

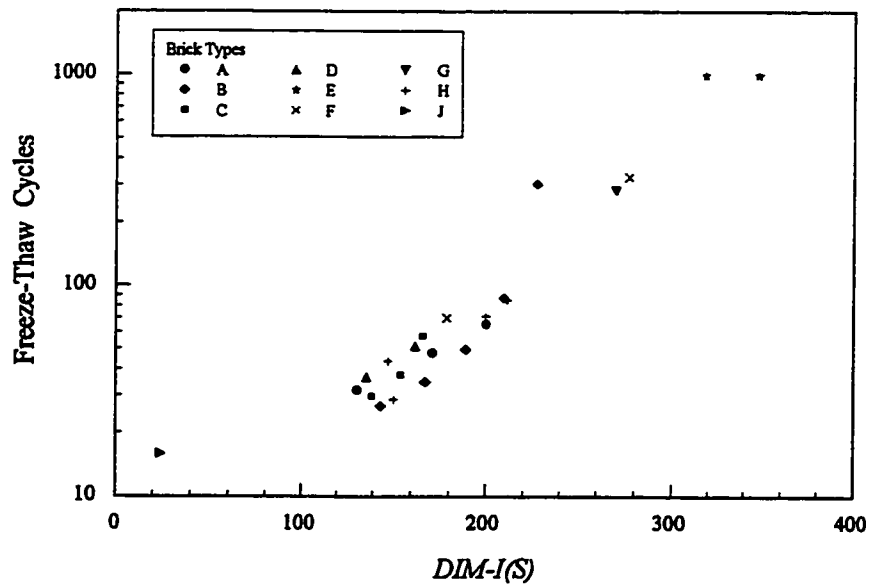


Figure 5.11 Relation between $DIM-I(S)$ and frost resistance

six brick groups as explained in Section 3.4. These brick groups were tested to determine $DIAP(C)$ and $DIAP(S)$ values and the frost resistance using the accelerated freeze-thaw test. In addition, some of the commonly used properties of the bricks were also determined so as to characterize the brick groups. Three specimens were tested from each group and the average values were found. The results are given in Table 5.3

Figures 5.12 and 5.13 show the results of the performance study. For both the indices, the freeze-thaw cycles resisted increases with increasing index values. Thus these indices give a measure of the durability level of bricks.

5.3 Summary

The study carried to compare the performance of existing durability indices showed that they had limitations in reliably assessing durability. The index developed by Maage was found to be better than others in evaluating brick durability. Based on this study, a new durability index was suggested by modifying Maage's index. In fact two indices were developed, one using submersion absorption property, and the other using capillary absorption property. These indices were found to overcome the limitations of Maage's index. They were also validated using a different set of bricks. Out of the two indices, the one based on capillary absorption property, $DIAP(S)$ was found to be better for evaluating clay brick durability and is therefore recommended.

TABLE 5.3
Properties of Brick Types K, L, and M

Property	Brick Types					
	K3	L3	M3	M4	M5	M6
<i>C, %</i>	5.14	5.33	5.24	6.64	8.38	10.71
<i>B, %</i>	7.21	6.85	10.73	12.09	14.87	15.73
<i>C/B</i>	0.71	0.78	0.49	0.55	0.56	0.68
<i>C1/B</i>	0.60	0.74	0.44	0.49	0.53	0.60
<i>S4/B</i>	0.64	0.77	0.46	0.53	0.57	0.64
<i>PV, ml/g</i>	0.0673	0.0653	0.0813	0.0888	0.1172	0.1297
<i>P3, %</i>	39.55	32.09	73.15	61.54	63.36	47.71
Porosity, %	15.10	14.94	17.14	18.22	23.35	25.32
Compressive Strength, MPa	69.69	59.85	48.29	41.77	30.78	21.27
Freeze-Thaw Cycles	62	28	98	72	42	30
<i>DIM</i>	142.47	126.02	214.92	183.73	179.37	139.18
<i>DIAP(C)</i>	148.54	95.58	202.02	176.96	157.23	127.46
<i>DIAP(S)</i>	151.06	110.65	201.73	175.85	156.25	131.09

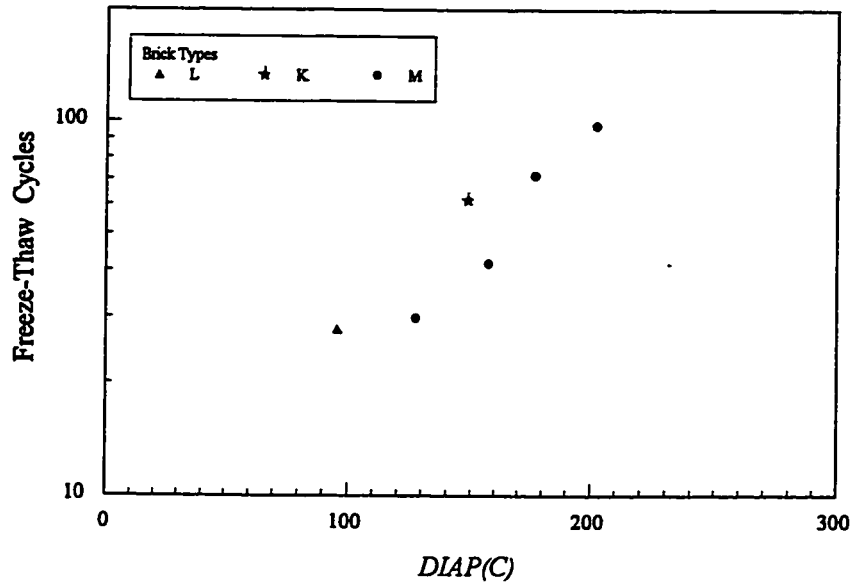


Figure 5.12 Validation of $DIAP(C)$

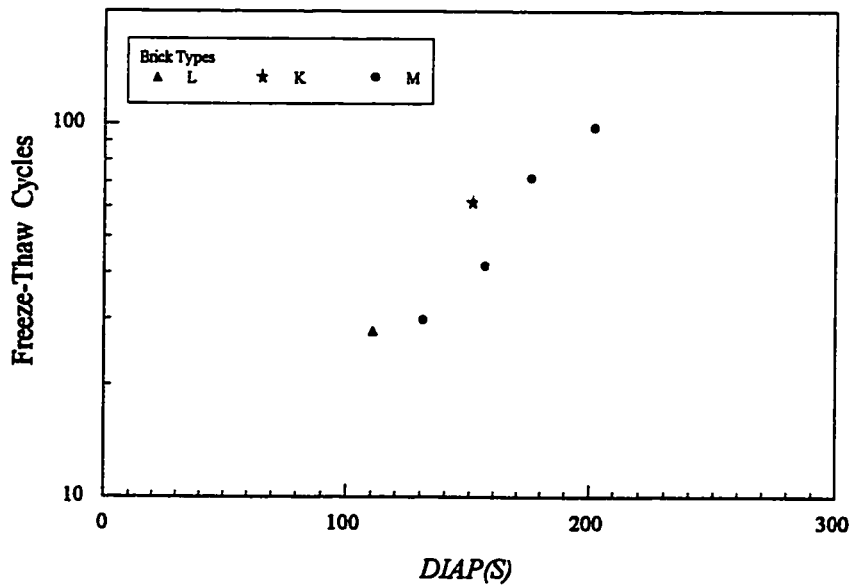


Figure 5.13 Validation of $DIAP(S)$

Nondestructive Evaluation of Durability

As mentioned earlier, not much research work had been done on the use of nondestructive testing (NDT) methods for the evaluation of brick properties. Therefore a study to investigate the feasibility of using NDT methods for evaluating brick durability was undertaken. Based on the review of different NDT methods discussed earlier, ultrasonic pulse velocity was selected for the study. This chapter discusses the research procedure for the feasibility study and the results.

6.1 Research Procedure

The research procedure adopted for the study was already shown in Figure 3.2. The aim of the research was to find whether pulse velocity could be used to identify durable and nondurable brick. In order to achieve this, the durability requirements specified in American standard ASTM C216 (see Table 2.1) were used. This standard provides physical requirements for water absorption and compressive strength to evaluate durability. Therefore relation between these properties and pulse velocity was studied. In addition, relation among the brick properties mentioned in ASTM C216 was also studied. To obtain better relations, test data provided by other researchers were included in the study. These relations were used to develop new provisions for

durability based on pulse velocity. The new provisions provide limiting values for pulse velocity which can be used to identify durable and nondurable brick.

6.2 Pulse Velocity Vs Brick Properties

Relation between pulse velocity and brick properties was studied to find the limiting values, if any, to substitute for the absorption and strength requirements specified in ASTM C216. The results from this study are shown in Figures 6.1 to 6.3.

In Figure 6.1, 5 hr. boiling water absorption shows very good linear relation with pulse velocity, with a regression coefficient of $R^2 = 0.95$ based on least square method. This may be due to the fact that pulse velocity is affected by pores in the material and that 5 hr. absorption gives a measure of the pore space in the brick. As expected, pulse velocity decreased with increasing values of B . Figure 6.2 shows the relation between 24 hr. water absorption and pulse velocity, with a regression coefficient of $R^2 = 0.85$. This relation was studied because ASTM C216 specifies an upper limit of $C = 8\%$, in order to waive the maximum saturation coefficient condition for durability. Since pores are only partially filled with water in a 24 hr. absorption test, a relation as good as that in Figure 6.1 can not be expected in this case.

The minimum compressive strength specified in ASTM C216 is a mandatory requirement to be satisfied to qualify as durable brick. Most of the initial studies involving ultrasonic pulse velocity used compressive strength as a major property being evaluated. In the case of concrete, reasonably good relations were observed between longitudinal pulse velocity and compressive strength [Malhotra 1976]. Figure 6.3 shows the relation between pulse velocity and compressive

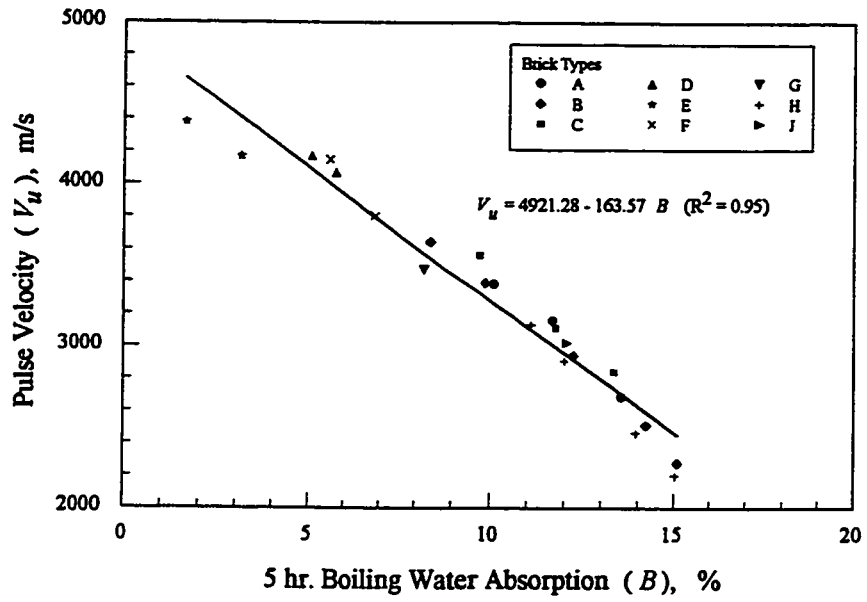


Figure 6.1 Relation between Ultrasonic Pulse Velocity (V_u) and 5 hr. Boiling Water Absorption (B)

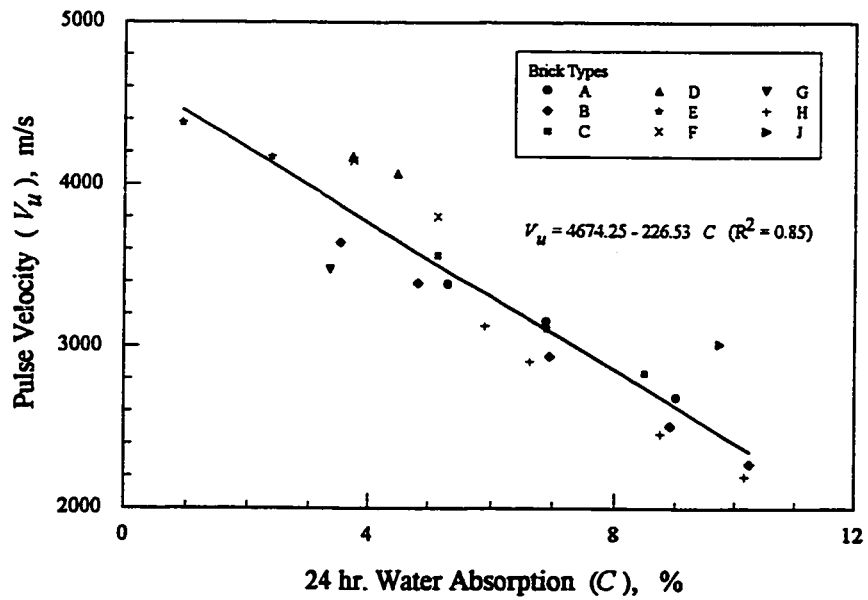


Figure 6.2 Relation between Ultrasonic Pulse Velocity (V_u) and 24 hr. Water Absorption (C)

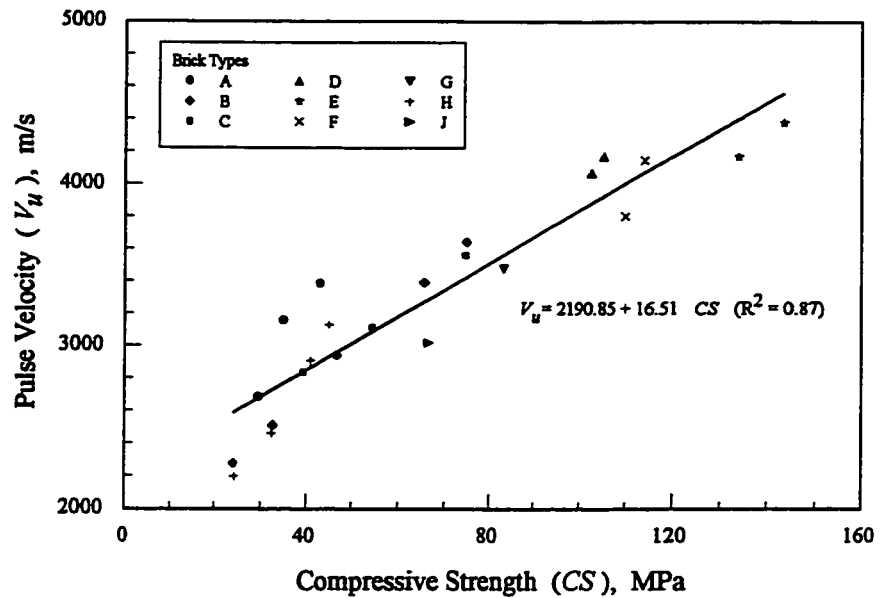


Figure 6.3 Relation between Ultrasonic Pulse Velocity (V_u) and Compressive Strength (CS)

strength for the present study. A linear relation with a $R^2 = 0.87$ was observed. Data points were found to scatter near the low compressive strength region.

6.3 Relation between Brick Properties

In order to derive better limiting values for pulse velocity, it was decided to study the relation between 24 hr. water absorption (C), 5 hr. boiling water absorption (B), and compressive strength for the bricks. An advantage with this is that, as these are common properties, test data provided by other researchers can be included in the study. Table 6.1 shows the details of the data used in this study. Only dry pressed and extruded brick types were used for the analysis.

Arnott [1990] used bricks from five plants across Canada. All bricks were manufactured

TABLE 6.1
Details of Test Data used in this Study

Source of Data	Number of Brick Types	Details of the Brick Types
Present Study		
Derivation:	9	5 Extruded + 4 Dry pressed
Validation:	3	2 Extruded + 1 Dry pressed
Arnott (1990)	5	5 Extruded
Davison (1980)	12	9 Extruded + 3 Dry pressed
Kung (1987c)	8	7 Extruded + 1 Dry pressed
Phillips (1947)	360	280 Extruded + 80 Dry pressed

according to normal production, drying, and firing techniques. The bricks were selected to reflect the normal range of bricks which a plant would produce. Most of the bricks used by Davison [1980] were either manufactured or were used in Atlantic Canada. Kung [1987a, 1987c] used bricks manufactured by six plants in Canada which accounted for 50 % of all the bricks made in Canada. The study by Phillips [1947] included bricks produced by plants throughout Canada.

Figures 6.4 and 6.5 show the results of the study. In Figure 6.4, 5 hr. boiling absorption shows a very good linear relation ($R^2 = 0.90$) with 24 hr. absorption. The continuous line shows the best fit using the least square method of regression analysis. The inclined dashed lines give the lower and upper ranges of the scattered data. For $C = 8 \%$, the best fit line gives $B = 10.53\%$ and the lower and upper ranges give $B = 9 \%$ and $B = 13.5 \%$ respectively. Based on this result, a value of B not exceeding 9% can be used, instead of C not exceeding 8% , as a requirement for waiving the maximum saturation coefficient condition in ASTM C216.

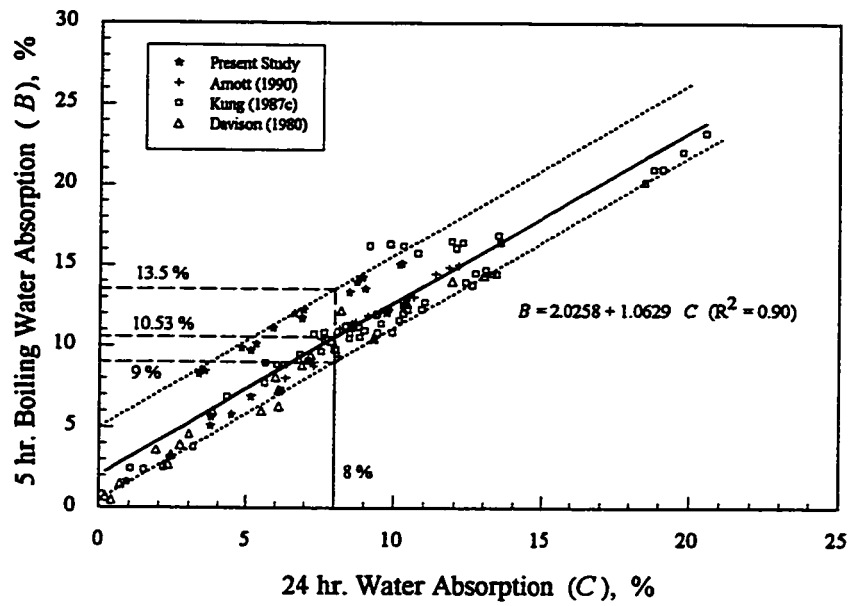


Figure 6.4 Relation between 24 hr. Water Absorption (*C*) and 5 hr. Boiling Water Absorption (*B*)

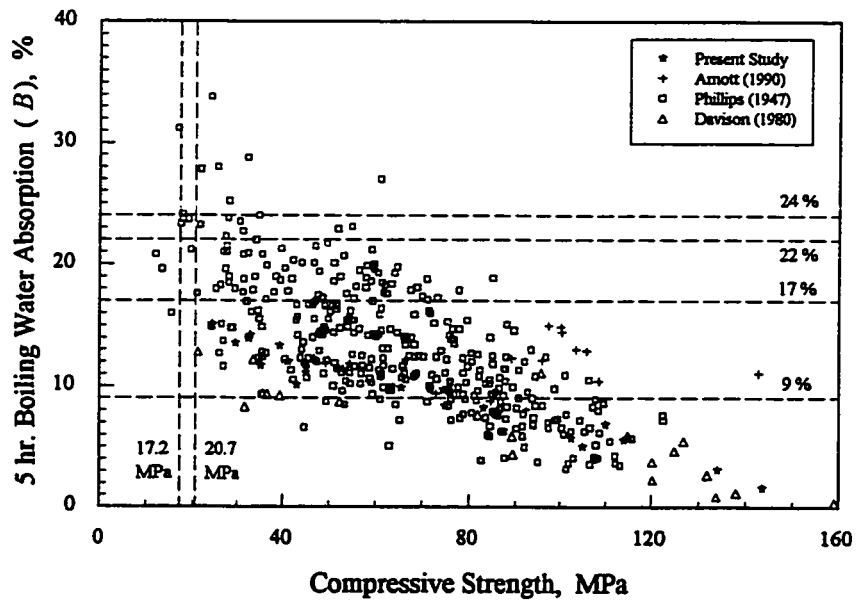


Figure 6.5 Relation between Compressive Strength and 5 hr. Boiling Water Absorption (*B*)

Figure 6.5 shows the relation between 5 hr. boiling absorption and compressive strength. As seen in the figure, the data points were so scattered to suggest any relation, even though the general trend shows, as expected, an increasing strength with decreasing absorption values. The vertical dashed lines set the mandatory minimum compressive strength values for moderate and severe weathering (see Table 2.1). $B = 17\%$ and $B = 22\%$ refer to the maximum values specified in the standard. But this requirement can be waived if the brick passes the 50 cycles freeze-thaw test. Hence it can not be used as mandatory requirement. Based on the test data available, it can be seen from Figure 6.5 that most of the bricks satisfy the ASTM requirement for minimum strength. Very few bricks have compressive strength > 20.7 MPa beyond $B = 24\%$. Therefore it can be suggested that B not exceeding 24% is a reasonable limit to satisfy the strength requirements specified in ASTM for both moderate and severe weathering.

6.4 Derivation of Durability Provisions

The new provisions for evaluating durability using pulse velocity were derived based on the relations between brick properties discussed in Sections 6.2 & 6.3, and the requirements specified in ASTM C216 (see Table 2.1). In Section 6.2, the linear relation between 5 hr. boiling water absorption (B) and pulse velocity (V_u) was found to be very good with a regression coefficient of $R^2 = 0.95$ (see Figure 6.1). So this was used as the basic relation for deriving pulse velocity limiting values. The equation connecting V_u (in m/s) and B (in %) is given by

$$V_u = 4921.28 - 163.57 B \quad [6.1]$$

As mentioned earlier, according to ASTM C216, the saturation coefficient requirement for

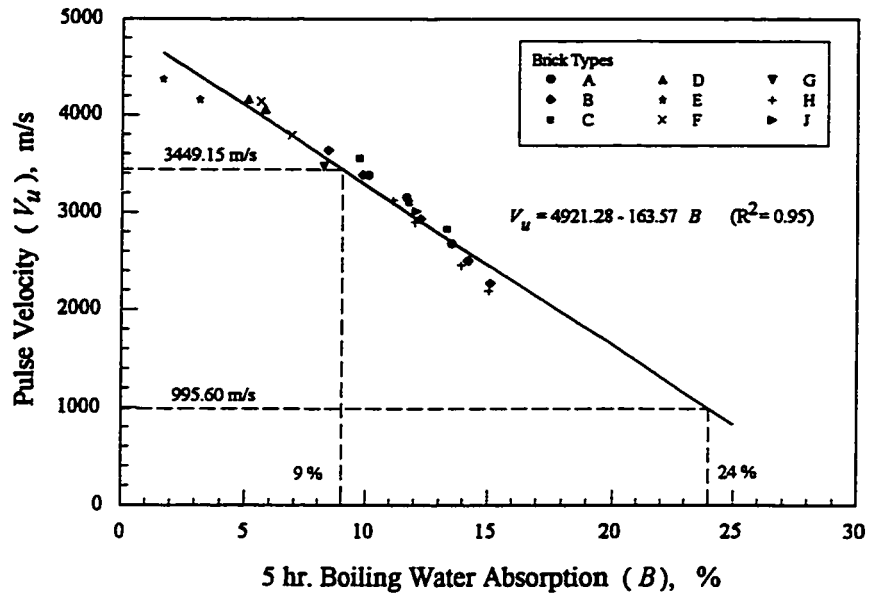


Figure 6.6 Derivation of limiting values for Pulse Velocity to evaluate durability

durability can be waived if the average 24 hr. water absorption does not exceed 8 %. From Figure 6.4, it was already found that B not exceeding 9 % could be used as a condition for waiving the saturation coefficient requirement. This value of B is also less than the maximum specified for severe weathering (17 %). Similarly from Figure 6.5, for B values not exceeding 9 %, the compressive strength values are always above 20.7 MPa (the minimum specified for severe weathering). Therefore bricks, whose B values do not exceed 9 %, can be identified as durable. So by substituting $B = 9 \%$ in equation [6.1], the upper limiting value of pulse velocity was obtained as 3449.15 m/s. This is shown in Figure 6.6. In this figure the linear relation is extrapolated to cover the required range, under the assumption that the linear relation holds good for the entire range. From Figure 6.5, it was already found that bricks might not satisfy the mandatory requirement for compressive strength, if B value exceeded 24 %. Therefore by

substituting $B = 24 \%$ in equation [6.1], the lower limiting value of pulse velocity was obtained as 995.60 m/s. The durability provisions based on pulse velocity are summarised in Table 6.2 below (the limiting values are rounded off to the nearest 100).

TABLE 6.2
Limiting Values for Pulse Velocity (V_u) to Evaluate Durability

When $V_u \geq 3500$ m/s	Brick is durable.
When $V_u < 1000$ m/s	Brick is not durable.
When $1000 \leq V_u < 3500$	Brick can be either durable or not durable. The evaluation of durability in this case should be done using ASTM C216 requirements.

6.5 Validation

The three brick types (K, L, and M) discussed in Section 5.2.5 were used for validating the new durability provisions based on pulse velocity. A total of six brick groups were involved in this study. The properties of these brick groups were already given in Table 5.3. These brick groups were tested to find the pulse velocity using the test procedure explained in Section 3.5.3. Then using the new provisions, the durability of the brick groups were evaluated. The durability was also assessed using the physical requirements specified in ASTM C216. The results are shown in Table 6.3. Comparing the two methods, it can be found that pulse velocity can be used successfully to evaluate the durability of bricks.

TABLE 6.3
Validation of Durability Provisions based on Pulse Velocity

Brick Type	Pulse Velocity m/s	Durability Evaluation using Pulse Velocity	Durability Evaluation using ASTM C216
K3	3315	Durable/nondurable	Durable
L3	3678	Durable	Durable
M3	3158	Durable/nondurable	Durable
M4	3142	Durable/nondurable	Durable
M5	2633	Durable/nondurable	Durable
M6	2114	Durable/nondurable	Durable

6.6 Summary

Based on the feasibility study, new durability provisions were derived using ultrasonic pulse velocity to identify durable and nondurable bricks. These provisions were validated using a different set of bricks. The new provisions give an upper and lower limiting values of 3500 m/s and 1000 m/s respectively for pulse velocity. But the drawback is that when the pulse velocity is between these two values, the new method can not evaluate durability and specifications mentioned in ASTM C216 should be used in such cases. Therefore, at this stage it can only be used along with ASTM method. The new provisions can avoid the time consuming ASTM method when the pulse velocity is above or below the upper and lower limiting values respectively. Being a faster and nondestructive test the new method has a potential for in situ evaluation.

Effect of Impregnation

One of the objectives of this research is to study the effect of impregnation with different materials in improving the frost durability of brick. Impregnation modifies the pore structure of the brick and thereby its absorption characteristics and strength. A modification in these properties affects its frost durability. This chapter discusses the research procedure and the results from the study on the effect of impregnation on brick properties.

7.1 Research Procedure

The research procedure adopted for the study on impregnated bricks was already shown in a block diagram in Figure 3.3. As mentioned in Section 3.2.1, four types of bricks (A, B, C, and F) were used for this study. The brick specimens were prepared according to the procedure and classification described in Section 3.3. A total of seven brick groups (A4, A5, B4, B5, C4, C5, and F3) were involved in this study.

Basically three impregnating materials were chosen in this research, as mentioned in Section 3.2.2, namely methyl methacrylate monomer, paraffin wax, and acrylic sealer. The

properties of MMA monomer were already given in Table 2.5. Two types of processes were adopted for impregnation with polymer, one involving simple soaking of monomer at atmospheric pressure and the other under vacuum. Similarly two types of paraffin waxes were used for the study, namely UNICERE 62 and PARAFINT H1. The properties of these two materials were already discussed in Section 3.2.2 and in Table 3.2. The impregnations using these three materials were carried out according to the procedures explained in Section 3.4.

For convenience in discussing the test results, these different impregnation methods were given designations as shown in Table 7.1. A brief description of the impregnation processes and the different brick groups used for each impregnation type are also given in Table 7.1. All the 5 types of impregnations were studied on bricks A4, B4, C4, and F3. Out of these, T1A and T2B were observed to be comparatively more promising. Therefore these two impregnating types were also used for the relatively more porous bricks A5, B5, and C5.

TABLE 7.1
Impregnation Type Designation and Brick Groups Studied

Impregnation Type Designation	Impregnating Material	Description of Process	Brick Groups Studied
T1A	Methyl methacrylate	Soaking at atmospheric pressure followed by polymerization	A4, B4, C4, F3 A5, B5, C5
T1B	Methyl methacrylate	Impregnation under vacuum followed by polymerization	A4, B4, C4, F3
T2A	Paraffin	Impregnation with UNICERE 62 at 80°C	A4, B4, C4, F3
T2B	Paraffin	Impregnation using PARAFINT H1 at 120°C	A4, B4, C4, F3 A5, B5, C5
T3	Acrylic Sealer	Impregnation by soaking at atmospheric pressure	A4, B4, C4, F3

The effect of impregnation was studied by comparing the properties of control (untreated) and impregnated bricks. Tests were carried out according to the procedures explained in Section 3.5 to determine the various properties. They included pore properties, water absorption properties, compressive strength, pulse velocity, and frost resistance. The test results discussed in Chapter 4 were used for the control bricks. In the case of impregnated bricks, for each type of impregnation, within a brick group, 3 sets of specimens were used. One set was used for water absorption, porosimetry and pulse velocity tests. The second and third sets were used for compressive strength and freeze-thaw tests respectively. For each set, 3 specimens were tested and therefore the test results discussed in this chapter represents the average of 3 test values. In addition to the above mentioned properties, the brick-mortar bond strength was also studied to find whether the impregnation process adversely affected the bonding.

7.2 Loading of Impregnating Materials

The amount of impregnating material that is absorbed into the brick is commonly referred to as loading. It is usually expressed as percentage of dry weight of the specimen. The loading values were determined from the dry weights before and after the impregnation process. The average loading of the impregnating materials for the 3 test sets are given in Table 7.2. It can be seen that T3 gave very low levels of loading. Acrylic sealer is normally used as a surface coating. It forms a water repellent coating as the solvent evaporates. In this study it was used for impregnating the pore space rather than as a surface coating. As the impregnated bricks were air dried, the solvent evaporated leaving low levels of loading. In the case of polymer (T1A and T1B) and paraffin (T2A and T2B) impregnations, the process involved solidification of a liquid material within the pore space and as a result they gave relatively higher loading. Out of the two methods

TABLE 7.2
Loading of Impregnating material

Brick Type	Type of Impregnation	Average Loading of Impregnating Material for different tests, %		
		Water Absorption, Porosimetry, and Pulse Velocity Tests	Compressive Strength Test	Freeze-thaw Test
A4	T1A	3.73	3.46	3.57
	T1B	6.15	6.13	6.86
	T2A	5.62	5.49	5.65
	T2B	6.26	6.26	6.38
	T3	1.74	1.66	1.79
B4	T1A	3.67	3.37	3.88
	T1B	6.80	6.84	6.88
	T2A	5.53	5.42	5.41
	T2B	5.82	5.86	5.85
	T3	1.75	1.49	1.74
C4	T1A	4.25	4.25	4.47
	T1B	7.73	7.93	8.19
	T2A	5.78	5.83	5.86
	T2B	5.69	5.88	5.70
	T3	1.10	1.04	1.05
F3	T1A	4.06	3.81	3.99
	T1B	5.31	5.58	5.32
	T2A	3.97	3.78	3.95
	T2B	3.78	3.71	3.90
	T3	0.52	0.56	0.56
A5	T1A	4.15	-	3.66
	T2B	8.78	-	8.56
B5	T1A	3.55	-	3.37
	T2B	8.13	-	7.35
C5	T1A	4.14	-	4.16
	T2B	7.03	-	7.04

of polymer impregnation, as expected, vacuum impregnation (T1B) gave a much better loading than impregnation at atmospheric pressure (T1A). Comparing T1A with T2A and T2B, it can be seen that paraffin impregnation resulted in better loading. This is due to the fact that some amount of monomer had been lost due to evaporation during the polymerization process in T1A. In the case of T1B also there was monomer loss. It was also observed that the level of loading remained almost the same among the three test sets. For brick types A5, B5, and C5 no compressive strength tests were carried out, because of lack of enough specimens in these groups. Moreover, compressive strength improvement due to impregnation was not a primary issue studied in this research.

7.3 Effect on Pore Properties

The pore properties were determined using mercury intrusion porosimetry, according to the test procedure explained in Section 3.5.2. The properties measured included pore volume, porosity, median and average pore diameters, and the distribution of pore sizes. The effect of impregnation on these properties is discussed in this section.

7.3.1 Pore Volume and Porosity

The pore volume of the impregnated bricks depends upon the loading of the impregnating material in the pores (Figure 7.1). The percentage reductions in pore volume are given in Table 7.3. Since T3 had very low loading, there was no significant reduction in pore volume for these bricks. The percentage reduction for these bricks ranged from 4.78 to 15.02 %. From Figure 7.1 it can be seen that paraffin impregnation normally gives much better reduction in pore volume. In the case of bricks C4 and F3, because of better polymer loading, T1B gave larger reduction in

TABLE 7.3
Pore Properties of Impregnated Bricks

Brick Type	Type of Impregnation	Intruded Pore Volume (PV)		Porosity (P)		Pore Volume > 3 μm (P3) %	Median Pore Diameter μm	Average Pore Diameter μm
		ml/g	% Reduction	%	% Reduction			
A4	Control	0.0986	-	20.49	-	57.81	5.79	1.12
	T1A	0.0594	39.76	12.76	37.73	34.39	1.98	0.31
	T1B	0.0556	43.61	11.89	41.97	54.04	4.30	0.34
	T2A	0.0471	52.23	10.12	50.61	58.31	8.13	0.18
	T2B	0.0370	62.47	8.11	60.42	42.59	1.12	0.12
	T3	0.0914	7.30	19.05	7.03	59.81	7.25	0.32
B4	Control	0.0999	-	20.48	-	65.54	3.92	1.79
	T1A	0.0726	27.33	15.49	24.37	23.50	1.56	0.35
	T1B	0.0572	42.74	12.26	40.14	31.92	2.32	0.37
	T2A	0.0542	45.75	11.63	43.21	28.60	1.33	0.18
	T2B	0.0498	50.15	10.87	46.92	39.94	0.26	0.11
	T3	0.0849	15.02	17.66	13.77	71.30	4.76	0.55
C4	Control	0.1140	-	23.16	-	52.81	3.16	1.56
	T1A	0.0516	54.74	11.32	51.12	40.24	0.81	0.17
	T1B	0.0239	79.04	5.40	76.68	7.18	0.42	0.06
	T2A	0.0552	51.58	11.83	48.92	37.88	1.60	0.17
	T2B	0.0519	54.47	11.69	49.53	45.70	0.21	0.10
	T3	0.0997	12.54	20.65	10.84	58.50	4.80	1.08

TABLE 7.3 (continued)
Pore Properties of Impregnated Bricks

Brick Type	Type of Impregnation	Intruded Pore Volume (PV)		Porosity (P)		Pore Volume > 3 μm (P3) %	Median Pore Diameter μm	Average Pore Diameter μm
		ml/g	% Reduction	%	% Reduction			
F3	Control	0.0836	-	17.54	-	18.53	0.63	0.12
	T1A	0.0248	70.33	5.56	68.30	35.46	0.28	0.04
	T1B	0.0136	83.73	3.12	82.21	5.78	0.08	0.03
	T2A	0.0282	66.27	6.25	64.37	13.11	0.04	0.03
	T2B	0.0409	51.08	6.63	62.20	26.88	0.27	0.04
	T3	0.0796	4.78	16.79	4.28	19.43	0.65	0.14
A5	Control	0.1185	-	23.84	-	43.46	1.84	0.81
	T1A	0.0780	34.18	16.41	31.17	20.74	1.21	0.37
	T2B	0.0314	73.50	6.80	71.48	37.70	0.90	0.07
B5	Control	0.1171	-	23.31	-	58.43	3.46	1.63
	T1A	0.0893	23.74	18.44	20.89	15.29	1.46	0.48
	T2B	0.0539	53.97	11.42	51.01	43.56	2.20	0.11
C5	Control	0.1241	-	24.87	-	47.17	2.91	1.47
	T1A	0.0922	25.71	19.21	22.76	17.99	1.31	0.48
	T2B	0.0546	56.00	11.71	52.92	47.26	2.92	0.10

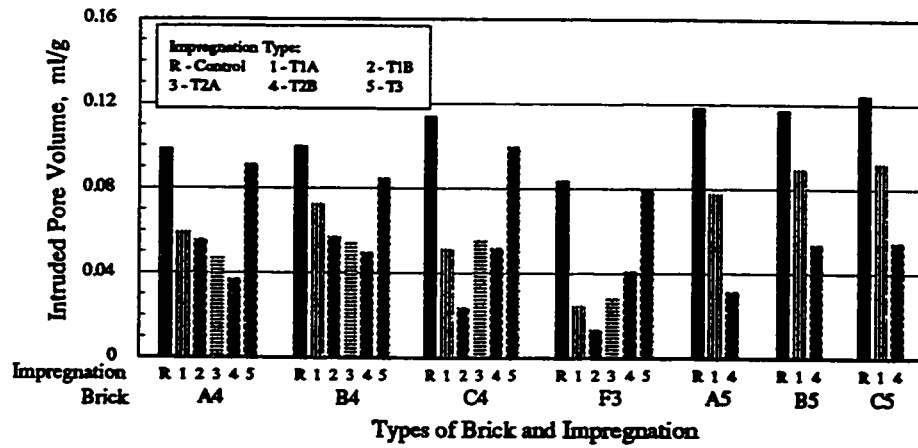


Figure 7.1 Intruded Pore Volume (PV) of the impregnated bricks

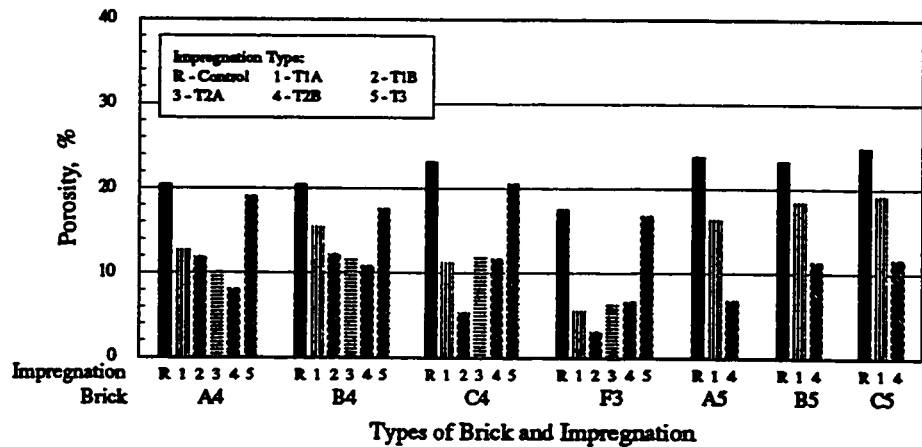


Figure 7.2 Porosity (P) of the impregnated bricks

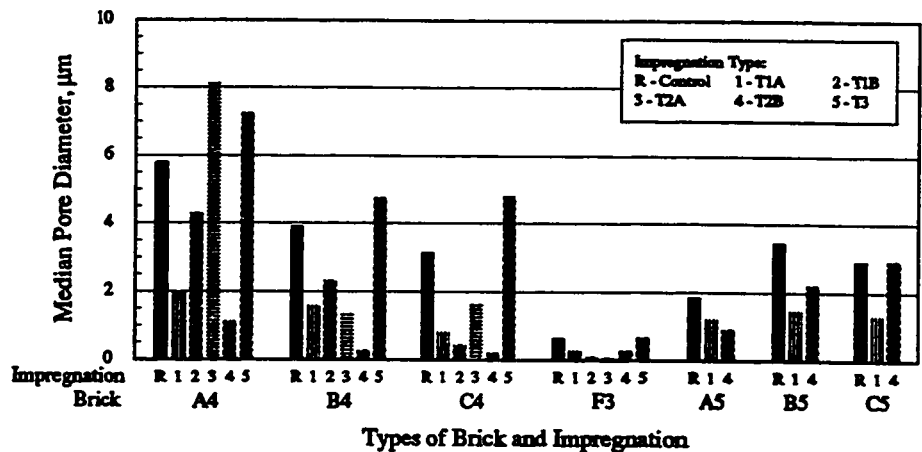


Figure 7.3 Median Pore Diameter of the impregnated bricks

pore volume. From Table 7.3, for bricks A4, B4, and C4, the average reduction in pore volume ranged from about 27 to 55 % for T1A, 40 to 80 % for T1B, 45 to 55 % for T2A and 50 to 62 % for T2B. For the lower porosity brick type F3, the reductions were much higher for polymer impregnation (T1A and T1B). A comparison of polymer (T1A) and paraffin (T2B) impregnations for the higher porosity bricks A5, B5, and C5 shows that T2B gives much better pore volume reduction. The percentage reduction ranged from 23 to 35 % for T1A and 54 to 74 % for T2B. As shown in Table 7.2, there was large variation in the amount of loading for these bricks, which might be the reason for their big difference in pore volume reduction.

Porosity is pore volume expressed as percentage of sample volume. Therefore, as expected, a similar result as for pore volume was observed. Figure 7.2 shows the porosity of control and impregnated bricks. The percentage reduction in porosity is given in Table 7.3.

7.3.2 Median and Average Pore Diameters

In general, except for impregnation type T3, all other impregnations lowered the median pore diameter of the bricks (Figure 7.3 and Table 7.3), which meant that for these impregnations the pore sizes were shifted towards the lower diameter range. As mentioned earlier in Chapter 2, larger diameter pores contribute to brick durability and therefore, the shifting of pore sizes towards lower diameter range may adversely affect the durability. But the total pore volume was found to have reduced and thus the total force exerted due to frost action would be much less, thereby contributing to brick durability. As seen in Figure 7.3 and Table 7.3, the decrease in median pore diameter for bricks A5, B5, and C5 with T1A and T2B were comparatively much less than for other bricks.

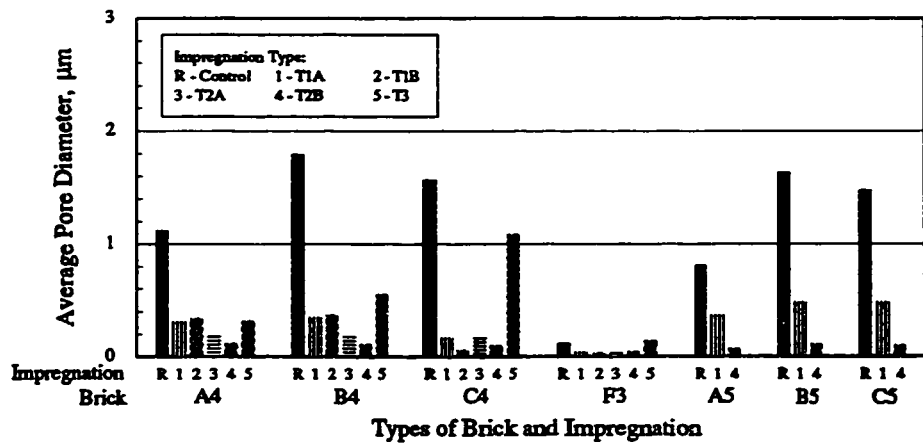


Figure 7.4 Average Pore Diameter of the impregnated bricks

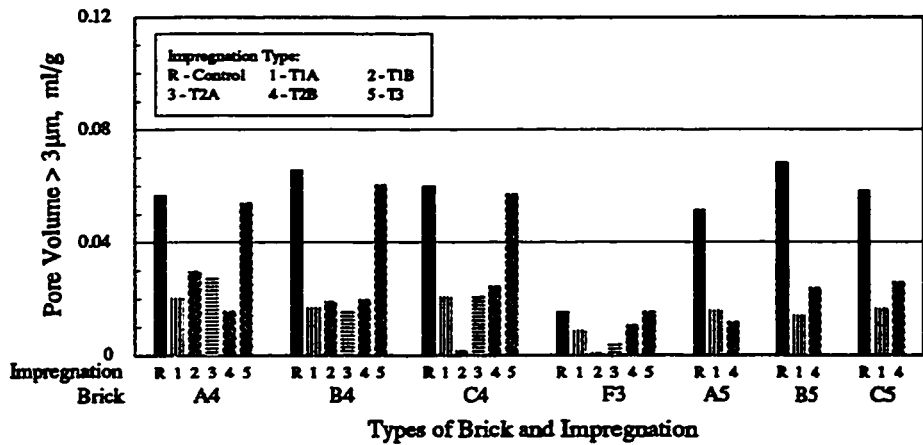


Figure 7.5 Pore Volume of the impregnated bricks > 3 µm in diameter, expressed in ml/g

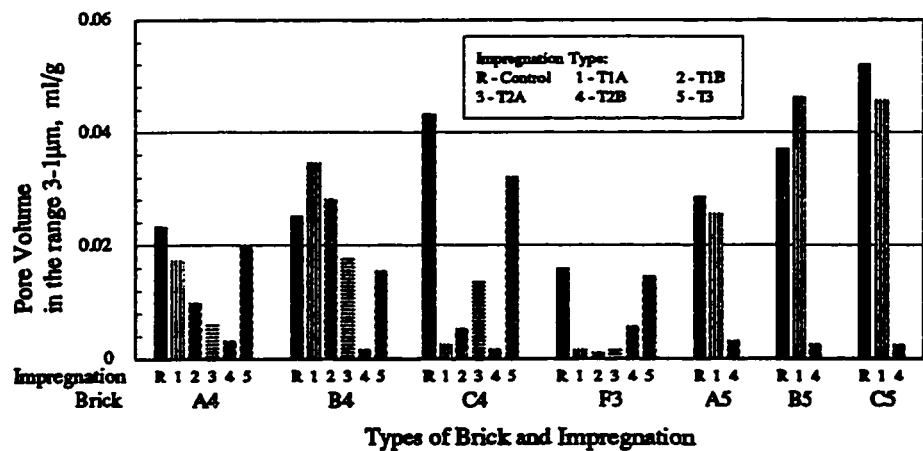


Figure 7.6 Pore Volume of the impregnated bricks in the pore diameter range 3-1 µm, expressed in ml/g

The Average pore diameter for all the impregnated bricks was found to have lowered significantly, thus confirming the shift of pore size distribution towards the lower diameter region (Figure 7.4 and Table 7.3). The decrease was comparatively less for T3. In the case of higher porosity bricks A5, B5, and C5, T2B showed much higher decrease in average diameter compared to T1A.

7.3.3 Pore Size Distribution

The distribution of relevant pore size ranges of control and impregnated bricks, expressed as cumulative intrusion in ml/g, in the pore diameter ranges $> 3 \mu\text{m}$, $3\text{-}1 \mu\text{m}$, $1\text{-}0.1 \mu\text{m}$ and $< 0.1 \mu\text{m}$ are shown respectively in Figures 7.5 to 7.8. Figures 7.9 to 7.12 show the distribution for these ranges, expressed as cumulative intrusion in percentage of total pore volume. Table 7.4 shows the distribution in a tabular form.

From Figures 7.9 to 7.12 it can be seen that bricks impregnated with T3 retained almost the same distribution as the control bricks. For brick type A4, T1A and T2B had much lower percentage of pore volume $> 3 \mu\text{m}$ (P_3) than control bricks. In the case of brick type B4, all impregnations except T3 gave lower than 40 % P_3 values while, for C4 brick, T1B had a very low P_3 value. For the lower porosity F3 brick, T1A and T2B had better pore volume $> 3 \mu\text{m}$ compared to other bricks. For the higher porosity bricks (A5, B5, and C5), T1A had low P_3 values in the range of 15 to 21 % while T2B had much higher values, ranging from 37 to 48 %, which are lower than that for control bricks.

Figure 7.10 shows that T1A had larger distribution of pores, than control bricks, in the range $3\text{-}1 \mu\text{m}$ for all brick types except C4 and F3. The percentage of pore volume in this case

TABLE 7.4
Distribution of Relevant Pore Size Ranges of Impregnated Bricks

Brick Type	Type of Impregnation	Cumulative intrusion in ml/g						Cumulative intrusion in % of total pore volume					
		Pore Diameter Ranges						Pore Diameter Ranges					
		> 3 μm	3-1 μm	1-0.1 μm	< 0.1 μm	> 3 μm	3-1 μm	1-0.1 μm	< 0.1 μm	> 3 μm	3-1 μm	1-0.1 μm	< 0.1 μm
A4	Control	0.0569	0.0234	0.0167	0.0016	57.81	23.79	16.81	1.59	57.81	23.79	16.81	1.59
	T1A	0.0205	0.0174	0.0189	0.0026	34.39	29.38	31.64	4.60	34.39	29.38	31.64	4.60
	T1B	0.0298	0.0099	0.0137	0.0022	54.04	17.67	24.35	3.94	54.04	17.67	24.35	3.94
	T2A	0.0274	0.0060	0.0073	0.0064	58.31	17.36	15.30	13.29	58.31	17.36	15.30	13.29
	T2B	0.0157	0.0031	0.0134	0.0048	42.59	8.46	36.00	12.95	42.59	8.46	36.00	12.95
	T3	0.0541	0.0197	0.0129	0.0047	59.81	21.44	13.57	5.18	59.81	21.44	13.57	5.18
B4	Control	0.0657	0.0252	0.0083	0.0007	65.54	25.44	8.31	0.71	65.54	25.44	8.31	0.71
	T1A	0.0170	0.0347	0.0167	0.0042	23.50	47.70	23.02	5.78	23.50	47.70	23.02	5.78
	T1B	0.0190	0.0282	0.0082	0.0018	31.92	50.18	14.63	3.27	31.92	50.18	14.63	3.27
	T2A	0.0154	0.0176	0.0127	0.0085	28.60	31.38	24.04	15.98	28.60	31.38	24.04	15.98
	T2B	0.0198	0.0017	0.0136	0.0147	39.94	3.25	27.39	29.42	39.94	3.25	27.39	29.42
	T3	0.0605	0.0155	0.0051	0.0038	71.30	18.36	5.89	4.45	71.30	18.36	5.89	4.45
C4	Control	0.0600	0.0433	0.0099	0.0008	52.81	37.79	8.62	0.78	52.81	37.79	8.62	0.78
	T1A	0.0206	0.0026	0.0233	0.0051	40.24	5.04	45.17	9.55	40.24	5.04	45.17	9.55
	T1B	0.0018	0.0053	0.0087	0.0081	7.18	20.24	37.08	35.50	7.18	20.24	37.08	35.50
	T2A	0.0208	0.0135	0.0129	0.0080	37.88	24.32	23.38	14.42	37.88	24.32	23.38	14.42
	T2B	0.0245	0.0017	0.0097	0.0160	45.70	3.05	18.00	33.25	45.70	3.05	18.00	33.25
	T3	0.0572	0.0322	0.0081	0.0022	58.50	31.12	7.95	2.43	58.50	31.12	7.95	2.43

TABLE 7.4 (continued)
Distribution of Relevant Pore Size Ranges of Impregnated Bricks

Brick Type	Type of Impregnation	Cumulative intrusion in ml/g					Cumulative intrusion in % of total pore volume						
		Pore Diameter Ranges					Pore Diameter Ranges						
		> 3 μm	3-1 μm	1-0.1 μm	< 0.1 μm	> 3 μm	3-1 μm	1-0.1 μm	< 0.1 μm	> 3 μm	3-1 μm	1-0.1 μm	< 0.1 μm
F3	Control	0.0155	0.0160	0.0364	0.0157	18.53	19.13	43.53	18.81	18.53	19.13	43.53	18.81
	T1A	0.0088	0.0016	0.0050	0.0094	35.46	6.62	20.11	37.81	35.46	6.62	20.11	37.81
	T1B	0.0008	0.0011	0.0043	0.0074	5.78	7.91	31.95	54.36	5.78	7.91	31.95	54.36
	T2A	0.0037	0.0015	0.0047	0.0183	13.11	5.26	16.57	65.06	13.11	5.26	16.57	65.06
	T2B	0.0106	0.0056	0.0122	0.0125	26.88	12.81	26.08	34.23	26.88	12.81	26.08	34.23
A5	T3	0.0154	0.0146	0.0379	0.0117	19.43	18.20	47.52	14.85	19.43	18.20	47.52	14.85
	Control	0.0515	0.0286	0.0360	0.0024	43.46	24.18	30.31	2.05	43.46	24.18	30.31	2.05
	T1A	0.0160	0.0257	0.0335	0.0028	20.74	32.93	42.78	3.55	20.74	32.93	42.78	3.55
B5	T2B	0.0117	0.0031	0.0097	0.0069	37.70	9.79	29.34	23.17	37.70	9.79	29.34	23.17
	Control	0.0685	0.0371	0.0108	0.0007	58.43	31.73	9.17	0.67	58.43	31.73	9.17	0.67
	T1A	0.0141	0.0463	0.0267	0.0022	15.29	49.57	32.56	2.58	15.29	49.57	32.56	2.58
C5	T2B	0.0240	0.0026	0.0154	0.0119	43.56	4.66	28.95	22.83	43.56	4.66	28.95	22.83
	Control	0.0585	0.0520	0.0126	0.0010	47.17	41.88	10.17	0.78	47.17	41.88	10.17	0.78
	T1A	0.0166	0.0458	0.0277	0.0021	17.99	49.48	30.24	2.29	17.99	49.48	30.24	2.29
	T2B	0.0260	0.0025	0.0098	0.0163	47.26	4.50	18.19	30.05	47.26	4.50	18.19	30.05

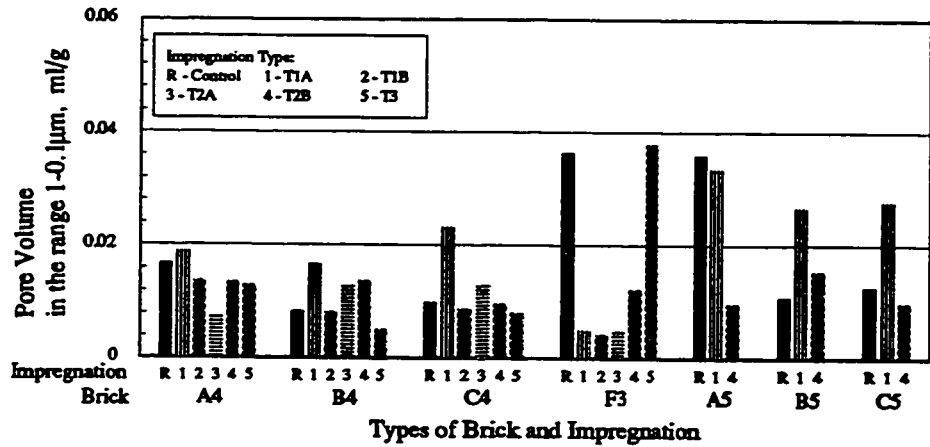


Figure 7.7 Pore Volume of the impregnated bricks in the pore diameter range 1-0.1 μm, expressed in ml/g

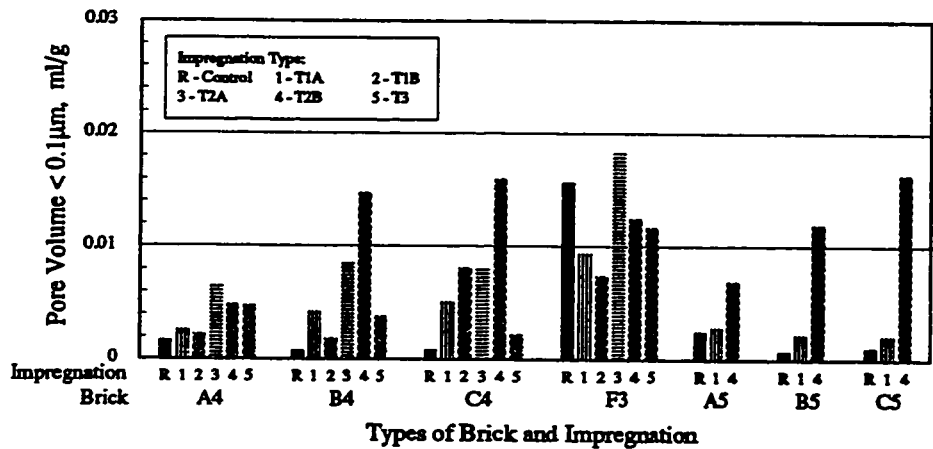


Figure 7.8 Pore Volume of the impregnated bricks < 0.1 μm in diameter, expressed in ml/g

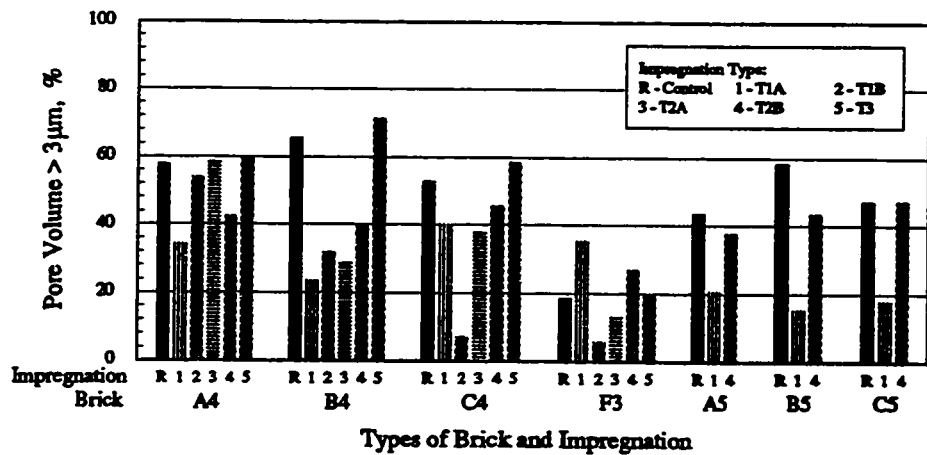


Figure 7.9 Pore Volume of the impregnated bricks > 3 μm in diameter, expressed in % of total pore volume (PV)

varied from about 30 to 50 %. For bricks C4 and F3, T1A showed very low pore volume of around 5 to 7%. T1B had reduced percentage of pore volume in the range 3-1 μm for all brick types except B4. T2A also showed reduced pore volume for all bricks except B4. Brick impregnated with T2B had very low distribution in the 3-1 μm range for all types including the higher porosity bricks. The percentage pore volume in this case ranged from as low as 3 to 13 %.

From Figure 7.11, it can be seen that for all brick types, except the lower porosity F3 type, in general the polymer and paraffin impregnations gave much higher distribution of pores, than control bricks, in the range 1-0.1 μm . For F3, both these impregnations had much lower distributions. T1A was found to have distribution in this range varying from about 20 to 45 % while T2B had the value ranging from 18 to 36 %.

Figure 7.12 shows the distribution of pores < 0.1 μm in diameter. All types of impregnation resulted in an increase in pore volume in this range, except T3 for brick F3. T1A had very low pore volume < 0.1 μm , of less than 5 % except for F3 where it shot up to 38 %. T1B had higher distribution of 36 % and 54 % in this range for bricks C4 and F3 respectively. T2A had around 15 % pore volume < 0.1 μm for brick types A4, B4, and C4, but it went up to 65 % for F3. T2B showed relatively large distribution in the above diameter range, varying from 13 to 34 %.

The pore size distribution curves for the control and impregnated bricks are shown in Figures 7.13A & B and 7.14A & B. The experimental data used for plotting these curves are given in Appendix D.

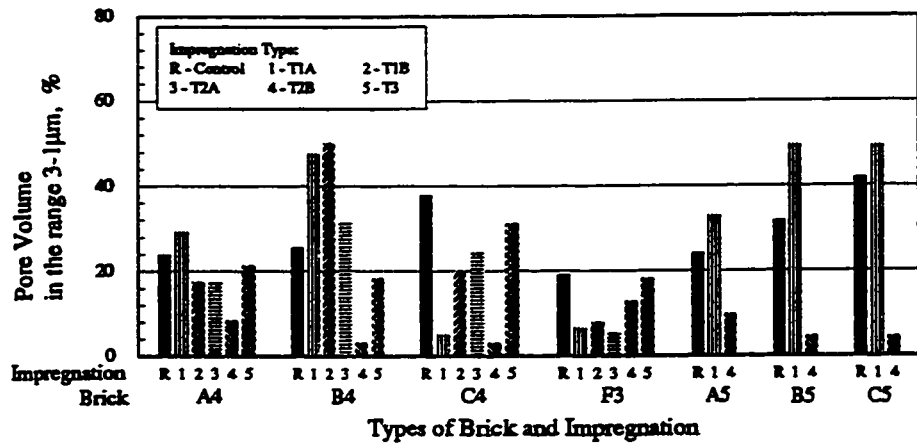


Figure 7.10 Pore Volume of the impregnated bricks in the pore diameter range 3-1 μm, expressed in % of total pore volume (PV)

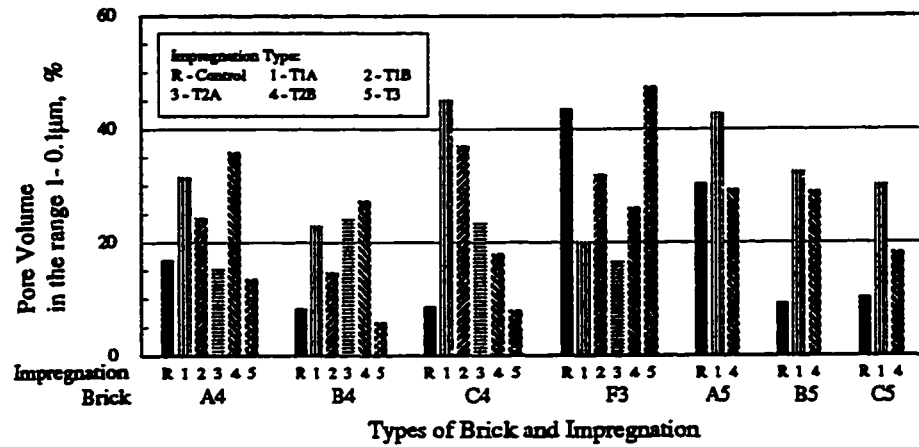


Figure 7.11 Pore Volume of the impregnated bricks in the pore diameter range 1-0.1 μm, expressed in % of total pore volume (PV)

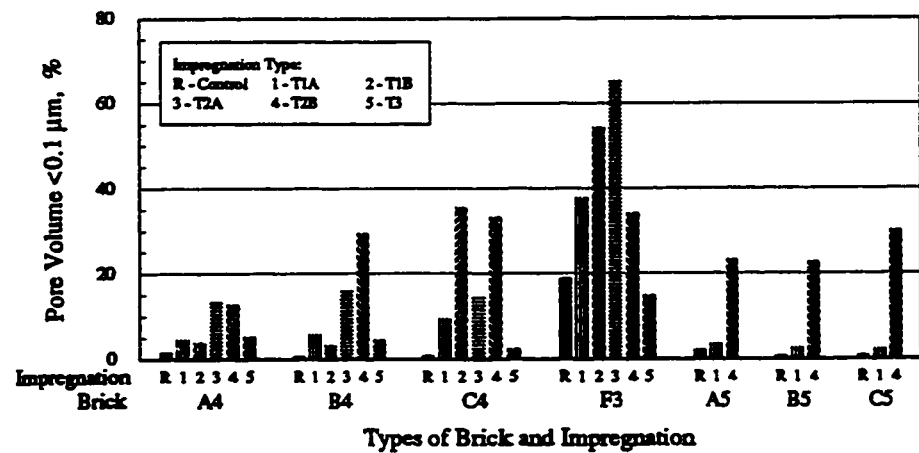


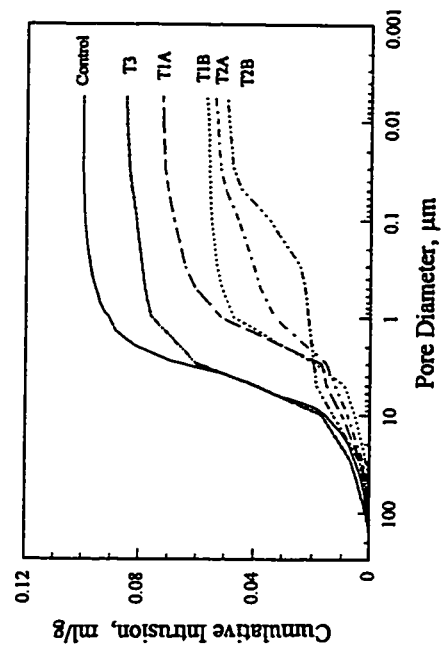
Figure 7.12 Pore Volume of the impregnated bricks <0.1 μm in diameter, expressed in % of total pore volume (PV)

From Figure 7.13A the following observations were made. All impregnations except T3 resulted in large reduction in cumulative intrusion. T3 gave an almost similar distribution curve pattern as control brick, except that it had a lower cumulative intrusion. The pore size distribution for impregnated bricks T1A, T1B, T2A, and T2B were relatively shifted towards lower diameter range. This can be seen from the fact that the curves for impregnated bricks flattened out at lower diameters. Bricks impregnated with T1A had a somewhat similar shape of curves as the control bricks. This fact is more evident in Figure 7.13B. From this Figure it can be suggested that T1A impregnation only slightly shifted the distribution curves towards lower region, with a reduction in the total pore volume. But the paraffin impregnation (T2B) moved the distribution much more to the lower diameter region and also the shapes of the curves were not similar to that of control bricks. The curves flattened out at a much lower diameter. Thus paraffin impregnation (T2B) of porous bricks resulted in better reduction in total pore volume but a larger shifting of pore sizes towards lower diameter region occurred, compared to polymer impregnation (T1A).

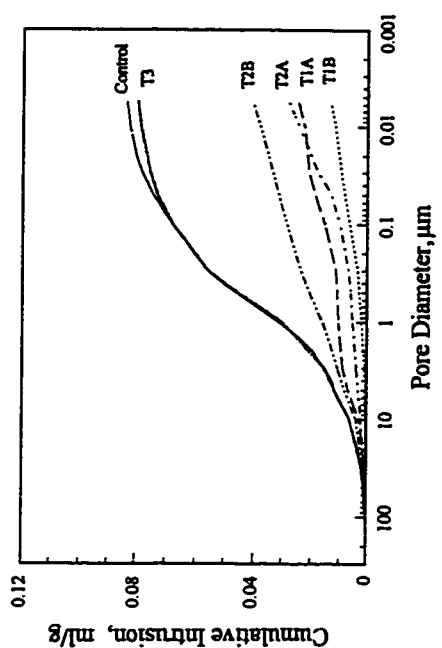
In Figures 7.14A and 7.14B, the distribution of pore sizes is expressed as cumulative intrusion in percentage of total intrusion (or pore volume). These curves clearly show the shifting of impregnated bricks towards the lower region. They can be used to determine the percentage of pore volume within any pore size range. Figure 7.14B shows the similarities between control and polymer impregnation, for the higher porosity bricks. It can be seen that T2B attains 100% intrusion at much lower pore size than T1A and control bricks, thus leaving larger percentage of pore volume with smaller diameter pores.

7.3.4 Summary

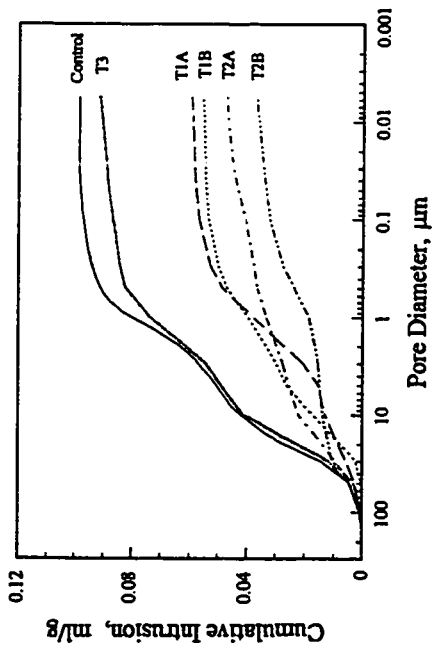
Based on the results discussed above, the following general conclusions were drawn on



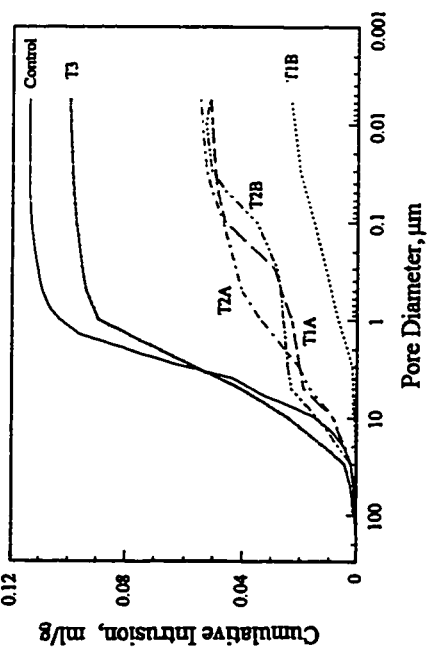
(ii) Brick Type B4



(iv) Brick Type F3



(i) Brick Type A4



(iii) Brick Type C4

Figure 7.13A Pore Size Distribution Curves for the impregnated bricks A4, B4, C4, and F3, expressed as cumulative intrusion in ml/g

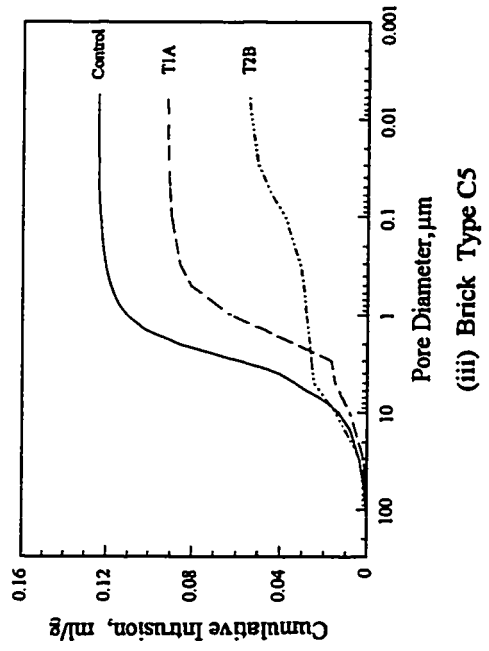
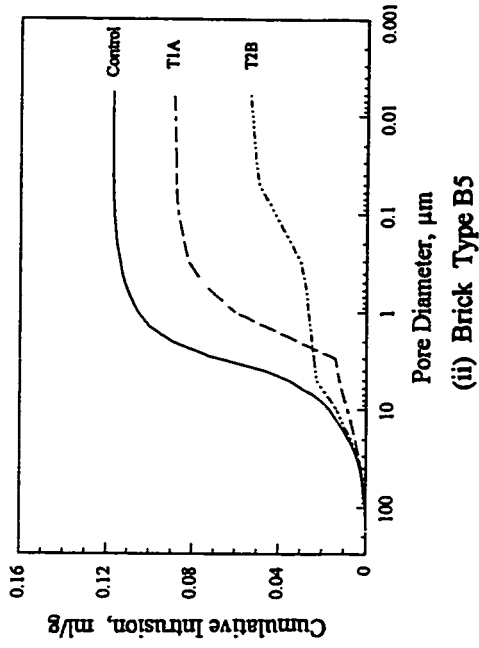
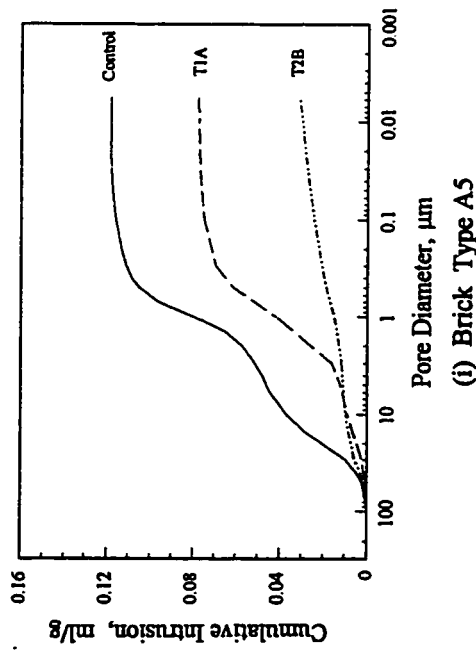


Figure 7.13B Pore Size Distribution Curves for the impregnated bricks A5, B5, and C5, expressed as cumulative intrusion in ml/g

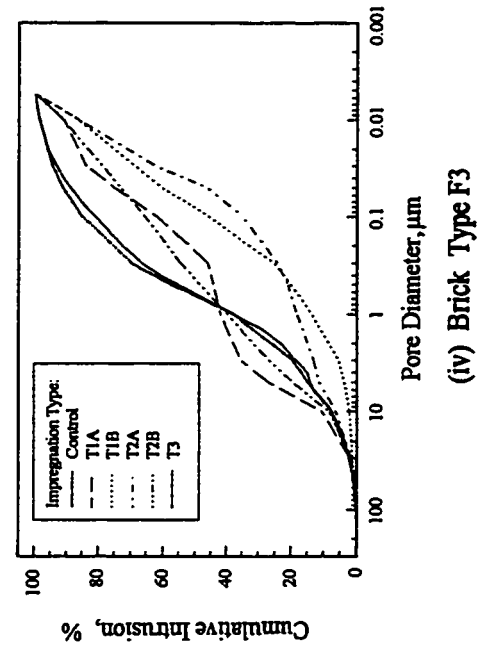
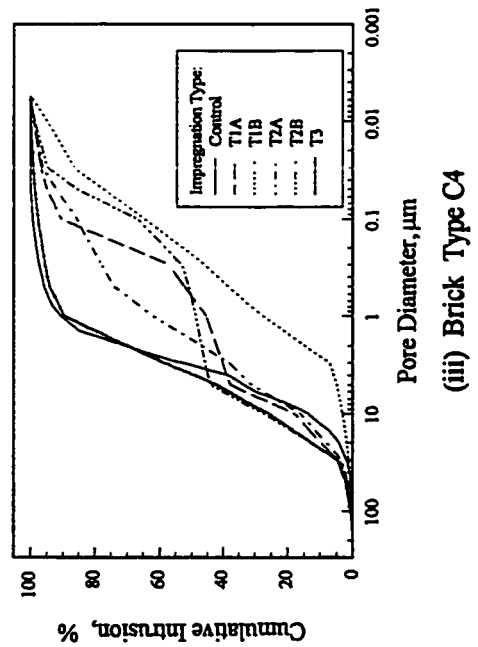
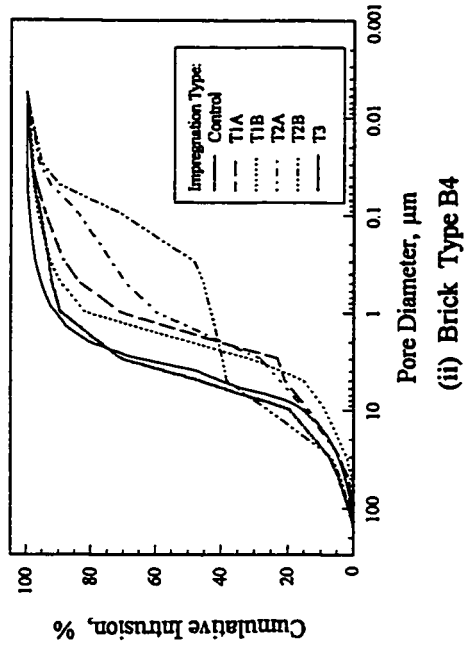
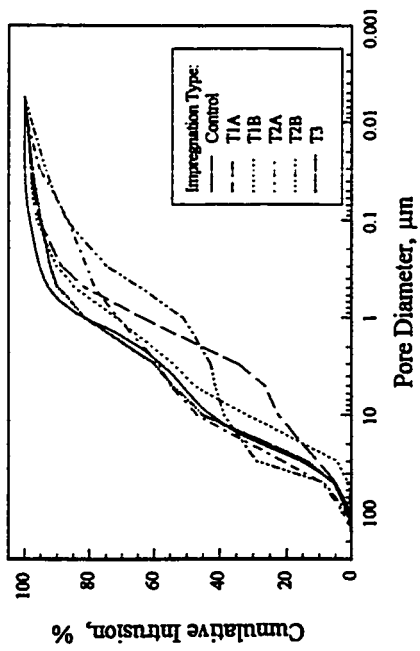


Figure 7.14A Pore Size Distribution Curves for the impregnated bricks A4, B4, C4, and F3, expressed as cumulative intrusion in % of total pore volume (*PV*)

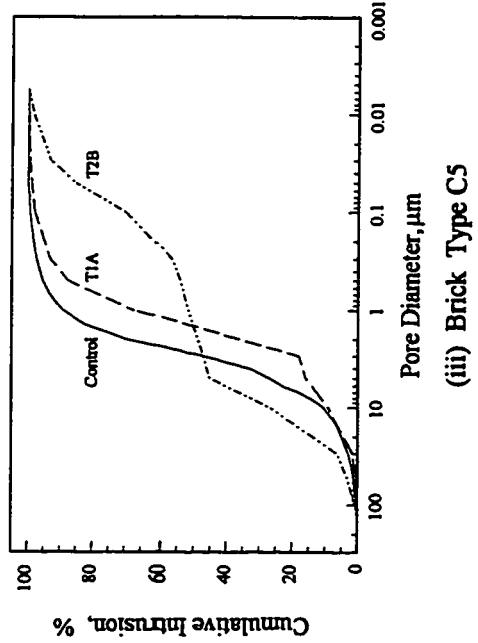
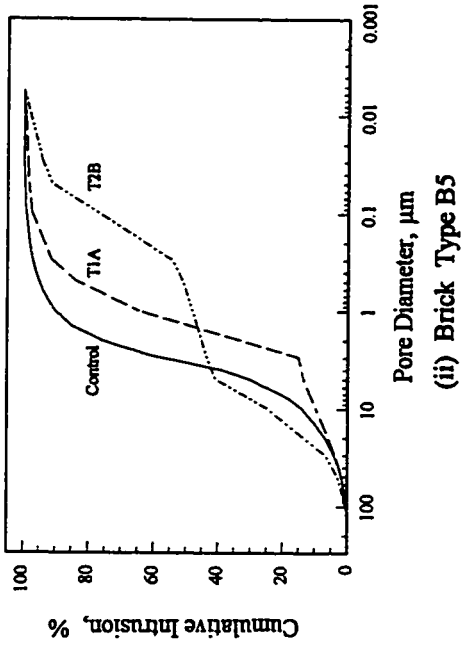
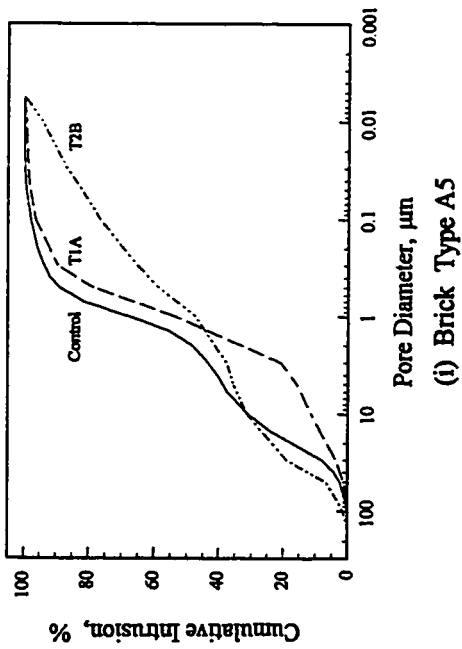


Figure 7.14B Pore Size Distribution Curves for the impregnated bricks A5, B5, and C5, expressed as cumulative intrusion in % of total pore volume (*PV*)

the effect of impregnation on pore properties of bricks. Impregnation with acrylic sealer (T3) did not result in any substantial reduction in porosity or pore volume. Also the distribution of pore sizes was not much affected. All other impregnations reduced the pore volume and porosity, but also shifted the distribution of pore sizes towards lower diameter region. For most of these impregnated bricks the percentage of pores larger than 3 μm in diameter (P_3) was found to have decreased. For higher porosity bricks (A5, B5, & C5) impregnated with polymer and paraffin (T1A & T2B), it was found that paraffin impregnation resulted in relatively larger reduction in pore volume (54 to 74 %) compared to polymer impregnation (23 to 35 %).

7.4 Effect on Water Absorption Properties

The properties studied included 24 hr. water absorption, vacuum saturation, saturation coefficient, submersion absorption, and capillary absorption. The effect of impregnation on these absorption properties is discussed in this Section

7.4.1 Vacuum Saturation

Vacuum saturation was used, as mentioned in Section 3.5.1.4, as a substitute for 5 hr. boiling water absorption test. Vacuum saturation test was expected to give the maximum possible absorption for the bricks and therefore was a measure of the available pore volume. Figure 7.15 shows the vacuum saturation (V) for control and impregnated bricks. Paraffin impregnated bricks (T2A and T2B) had the least absorption values of less than 3 %. From Table 7.5 it can be seen that percentage reduction in V for these bricks were very high, ranging from 74 to 89 %. Impregnation with T3 did not reduce V significantly. The percentage reductions in this case were between 8 to 19 %. T1B was more effective than T1A in reducing vacuum saturation. The

TABLE 7.5
Water Absorption Properties of Impregnated Bricks

Brick Type	Type of Impregnation	24 hr. Water Absorption (C)		Vacuum Saturation (V)		Saturation Coefficient (CV)	
		%	% Reduction	%	% Reduction		% Reduction
A4	Control	6.89	-	11.60	-	0.59	-
	T1A	3.54	48.62	8.24	28.97	0.43	27.11
	T1B	4.06	41.07	6.03	48.02	0.67	-13.56
	T2A	0.11	98.40	2.95	74.57	0.04	93.22
	T2B	0.09	98.69	2.02	82.59	0.05	91.56
	T3	4.31	37.45	9.43	18.71	0.46	22.03
B4	Control	6.95	-	12.39	-	0.56	-
	T1A	3.51	49.50	8.87	28.41	0.39	30.36
	T1B	4.25	38.85	6.17	50.20	0.69	-22.21
	T2A	0.18	97.41	2.28	81.60	0.07	87.50
	T2B	0.18	97.41	2.35	81.03	0.07	87.50
	T3	4.16	40.14	10.04	18.97	0.42	25.00
C4	Control	6.90	-	12.02	-	0.57	-
	T1A	2.62	62.03	7.36	38.77	0.35	38.60
	T1B	3.24	53.04	4.90	59.23	0.66	-15.79
	T2A	0.16	97.68	2.12	82.36	0.08	85.96
	T2B	0.14	97.97	1.75	85.44	0.07	87.72
	T3	4.98	27.83	10.45	13.06	0.47	17.54

TABLE 7.5 (continued)
Water Absorption Properties of Impregnated Bricks

Brick Type	Type of Impregnation	24 hr. Water Absorption (C)		Vacuum Saturation (V)		Saturation Coefficient (C/V)	
		%	% Reduction	%	% Reduction		% Reduction
F3	Control	5.15	-	7.23	-	0.71	-
	T1A	1.45	71.84	2.75	61.96	0.52	26.76
	T1B	1.81	64.85	2.28	68.46	0.79	-11.27
	T2A	0.06	98.83	1.10	84.79	0.05	92.96
	T2B	0.08	98.45	1.36	81.19	0.06	91.55
	T3	4.39	14.76	6.61	8.58	0.66	7.04
A5	Control	9.01	-	13.43	-	0.67	-
	T1A	5.25	41.73	9.47	29.49	0.55	17.91
	T2B	0.15	98.34	1.54	88.53	0.10	85.07
B5	Control	8.92	-	14.37	-	0.62	-
	T1A	5.49	38.45	10.93	23.94	0.50	19.35
	T2B	0.11	98.77	2.08	85.53	0.06	90.32
C5	Control	8.48	-	13.49	-	0.63	-
	T1A	3.52	58.49	9.48	29.73	0.37	41.27
	T2B	0.10	98.82	2.13	84.21	0.05	92.06

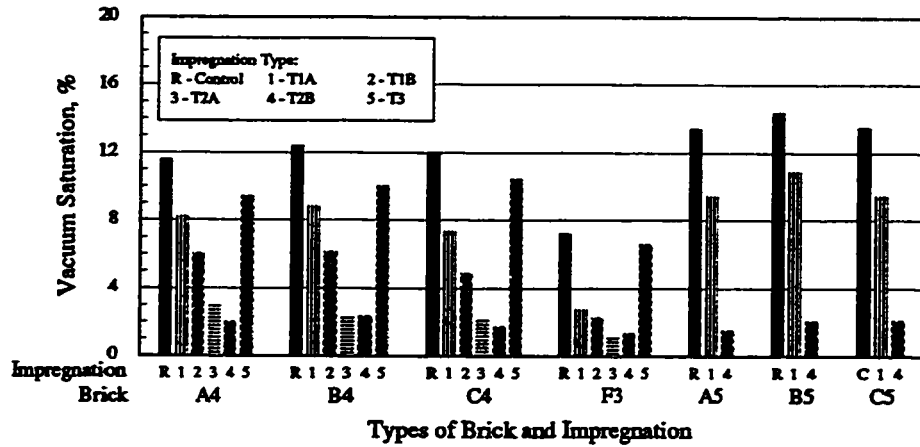


Figure 7.15 Vacuum Saturation (V) of the impregnated bricks

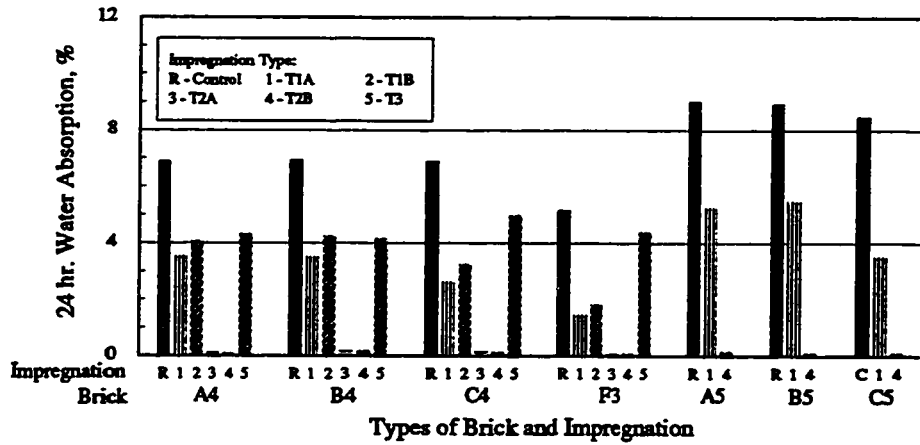


Figure 7.16 24 hr. Water Absorption (C) of the impregnated bricks

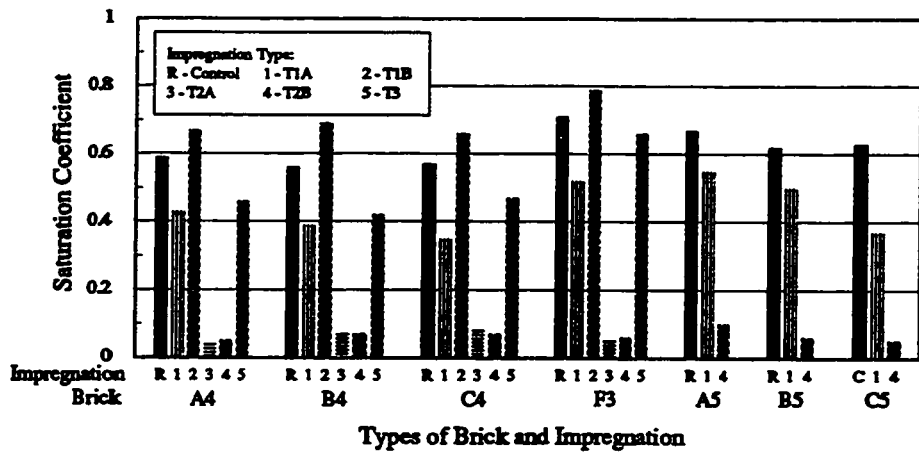


Figure 7.17 Saturation Coefficient (C/V) of the impregnated bricks

percentage reduction for T1A ranged from 28 to 62 %, while that for T1B ranged from 48 to 69 %. Comparing polymer and paraffin impregnations (T1A and T2B) for the higher porosity bricks A5, B5, and C5, it can be found that while T1A provided only about 30 % reduction in V , T2B had about 85 % reduction. The higher reductions in the case of paraffin impregnated bricks may be due to the fact that T2A and T2B had higher impregnant loading (see Table 7.2) in addition to being hydrophobic material.

7.4.2 Submersion Absorption

To determine the effect of impregnation, 10 minute submersion absorption, 1 hr. submersion absorption, and 24 hr. submersion absorption properties were studied. Tables 7.5 and 7.6 give the test results. The submersion absorption properties of control and impregnated bricks are compared in Figures 7.16 to 7.21.

Figure 7.16 shows the 24 hr. water absorption for the bricks. It can be seen that paraffin impregnation was very effective in reducing 24 hr absorption (C). Table 7.5 shows that the percentage reductions in C values for T2A and T2B were very consistent among the different brick types, ranging between 97 to 99 %. The major reason for this large reduction might be due to the fact that paraffin is an hydrophobic material. Polymer impregnations (T1A and T1B) were not as effective, with percentage reduction varying from 38 to 72 %. Acrylic sealer was observed to be very effective against capillary absorption but did not perform as well in retarding absorption under submersion. The percentage reductions in C for T3 ranged from about 15 to 40 %.

The saturation coefficients (C/V) of the bricks were calculated using 24 hr. absorption (C) and vacuum saturation (V) values. Figure 7.17 shows the coefficients for the control and

impregnated bricks. Paraffin impregnated bricks (T2A and T2B) had very low saturation coefficients below 0.1. The percentage reductions for these bricks ranged from 85 to 94 % (Table 7.5). Impregnation with T1A resulted in a reduction in C/V , values ranging between 18 to 42 %. But polymer impregnation under vacuum (T1B) resulted in an increase in C/V values by 11 to 22 %. An increase in C/V value means a decrease in unfilled pore space available. Therefore impregnation with T1B is not recommended from durability point of view. Impregnation with T3 also reduced the saturation coefficient by 7 to 25 %.

Table 7.6 shows the 10 minute and 1 hour submersion absorption properties. Figures 7.18 to 7.21 show these properties in a graphical form. Similar trend as for 24 hr. absorption was obtained in these cases as well. 10 minute and 1 hour absorptions were very low for paraffin impregnated bricks. Absorptions were comparatively high for T1B bricks. It can be seen from Figure 7.21 that 1 hr. absorption as percentage of V in fact increased in the case of T1B bricks. This is due to the fact that vacuum impregnation resulted in sealing of those pores that are normally unfilled during absorption.

7.4.3 Capillary Absorption

Water is normally absorbed into an exposed wall through capillary suction. Therefore it was decided to study also the effect of impregnation on capillary absorption properties of bricks. Absorptions of the bricks after 10 minutes and 1 hour contact with water were measured. The tests were carried out according to the test procedure explained in Section 3.5.1.1. The absorption values were expressed both as percentage of dry weight and percentage of vacuum saturation. Figures 7.22 to 7.25 show these absorption values for the control and impregnated bricks. Table 7.7 shows these properties in a tabular form. It can be seen from these figures that capillary

TABLE 7.6
Submersion Absorption Properties of Impregnated Bricks

Brick Type	Type of Impregnation	Submersion Absorption, % of dry weight				Submersion Absorption, % of Vacuum Saturation (V)			
		10 Minute Absorption		1 Hour Absorption		10 Minute Absorption		1 Hour Absorption	
		%	% Reduction	%	% Reduction	% of V	% Reduction	% of V	% Reduction
A4	Control	5.78	-	5.99	-	49.76	-	51.53	-
	T1A	1.52	73.70	3.02	49.58	18.17	63.48	36.30	29.56
	T1B	2.12	63.32	3.75	37.40	34.25	31.17	61.91	-20.14
	T2A	0.02	99.65	0.06	99.00	0.52	98.95	1.95	96.21
	T2B	0.03	99.48	0.06	99.00	1.28	97.43	2.86	94.45
	T3	1.56	73.01	3.63	60.60	16.63	66.58	38.67	24.96
B4	Control	5.91	-	6.06	-	47.65	-	54.90	-
	T1A	1.37	76.82	2.72	55.12	15.20	68.10	30.38	44.66
	T1B	2.45	58.54	3.95	34.82	39.05	18.04	63.89	-16.38
	T2A	0.03	99.49	0.08	98.68	1.38	97.10	3.40	93.81
	T2B	0.04	99.32	0.09	98.51	1.66	96.52	3.86	92.97
	T3	0.79	86.63	2.11	65.18	7.83	83.57	20.85	62.02
C4	Control	5.44	-	6.12	-	45.15	-	50.86	-
	T1A	0.72	86.76	1.53	75.00	9.43	79.11	20.17	60.34
	T1B	0.92	83.09	2.24	63.40	18.86	58.23	45.63	10.28
	T2A	0.04	99.26	0.07	98.86	1.78	96.06	3.31	93.49
	T2B	0.04	99.26	0.07	98.86	2.19	95.15	3.72	92.69
	T3	1.20	77.94	2.69	56.05	12.16	73.07	26.75	47.40

TABLE 7.6 (continued)
Submersion Absorption Properties of Impregnated Bricks

Brick Type	Type of Impregnation	Submersion Absorption, % of dry weight						Submersion Absorption, % of Vacuum Saturation (V)					
		10 Minute Absorption			1 Hour Absorption			10 Minute Absorption			1 Hour Absorption		
		%	% Reduction	%	% Reduction	%	% Reduction	% of V	% Reduction	% of V	% Reduction	% of V	% Reduction
F3	Control	3.32	-	4.31	-	45.71	-	59.50	-	59.50	-	59.50	-
	T1A	0.69	79.22	1.19	72.39	24.56	46.27	42.75	46.27	28.15	42.75	28.15	
	T1B	0.78	76.51	1.49	65.43	33.08	27.63	63.36	27.63	-6.49	63.36	-6.49	
	T2A	0.02	99.40	0.01	99.77	1.37	97.00	1.20	97.00	97.98	1.20	97.98	
	T2B	0.03	99.10	0.03	99.30	2.34	94.88	2.34	94.88	96.07	2.34	96.07	
T3	0.10	96.99	0.43	90.02	1.52	96.67	6.44	96.67	89.18	6.44	96.67	89.18	
A5	Control	7.69	-	8.04	-	57.20	-	59.81	-	59.81	-	59.81	-
	T1A	3.57	53.58	4.99	37.94	37.53	34.39	52.67	34.39	11.94	52.67	11.94	
	T2B	0.03	99.61	0.07	99.13	2.17	96.21	4.53	96.21	92.43	4.53	92.43	
B5	Control	7.66	-	7.89	-	53.26	-	54.90	-	54.90	-	54.90	-
	T1A	3.40	55.61	4.92	37.64	30.61	42.53	44.76	42.53	18.47	44.76	18.47	
	T2B	0.04	99.48	0.05	99.37	2.05	96.15	2.46	96.15	95.52	2.46	95.52	
C5	Control	7.19	-	7.55	-	53.28	-	55.88	-	55.88	-	55.88	-
	T1A	1.35	81.22	2.58	65.83	14.24	73.27	27.13	73.27	51.45	27.13	51.45	
	T2B	0.05	99.30	0.06	99.21	2.31	95.66	2.73	95.66	95.11	2.73	95.11	

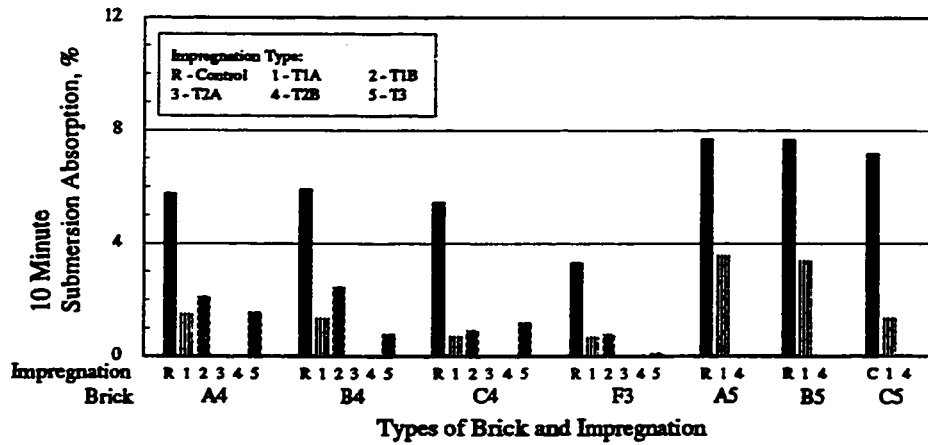


Figure 7.18 10 Minute Submersion Absorption of the impregnated bricks expressed in % of dry weight (CIOM)

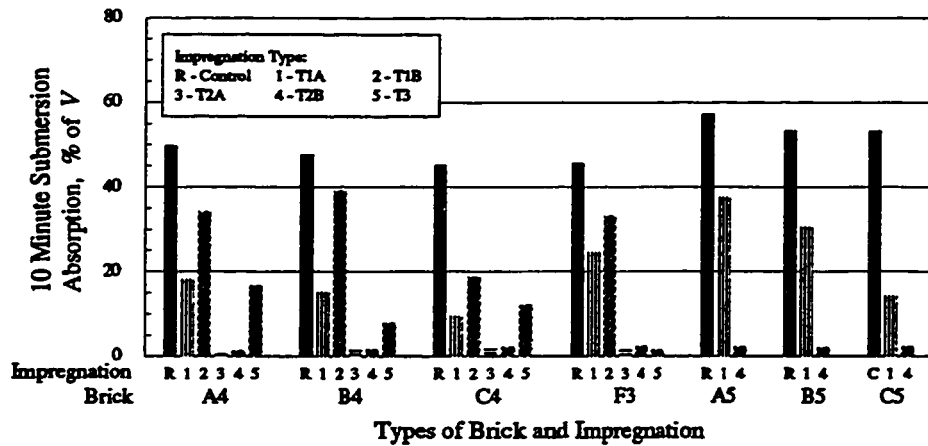


Figure 7.19 10 Minute Submersion Absorption of the impregnated bricks expressed in % of Vacuum Saturation (CIOM/V)

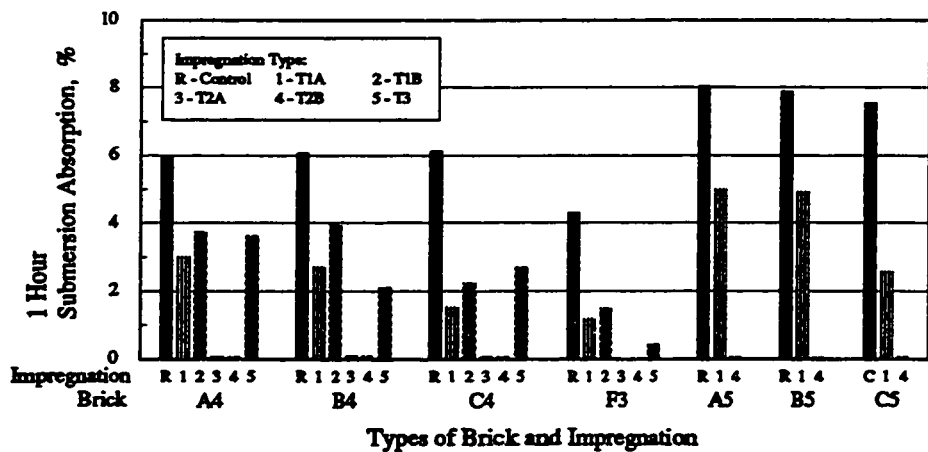


Figure 7.20 1 hour Submersion Absorption of the impregnated bricks expressed in % of dry weight (CI)

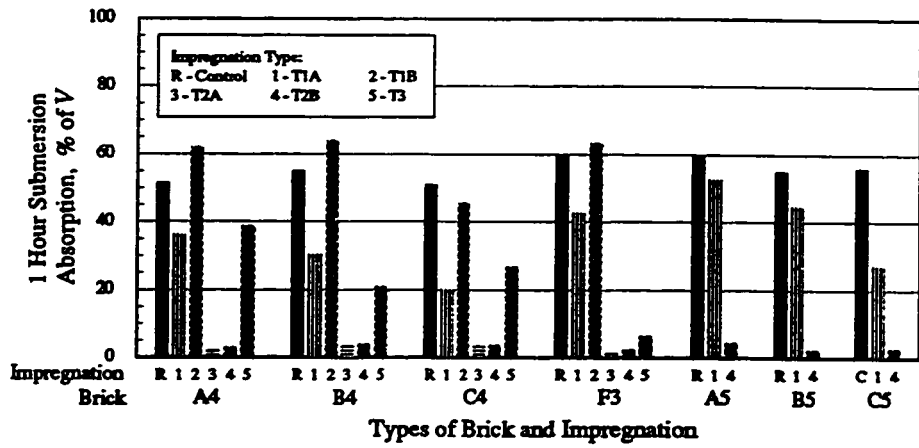


Figure 7.21 1 Hour Submersion Absorption of the impregnated bricks expressed in % of Vacuum Saturation (*CI/V*)

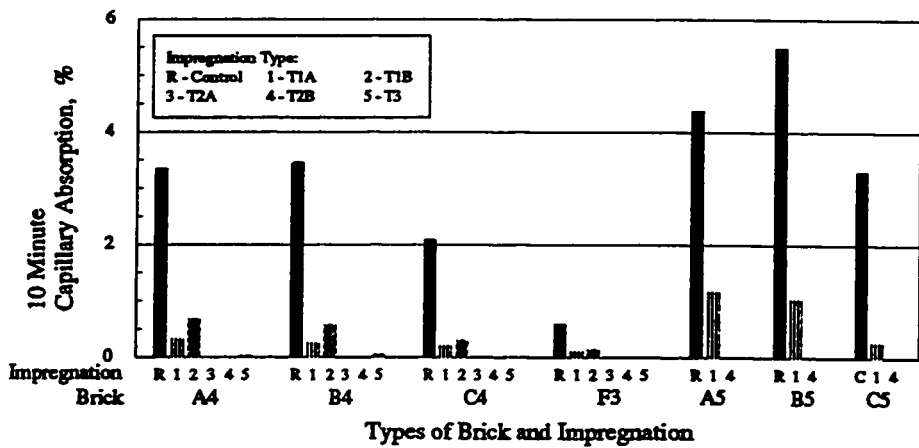


Figure 7.22 10 Minute Capillary Absorption of the impregnated bricks expressed in % of dry weight (*SIOM*)

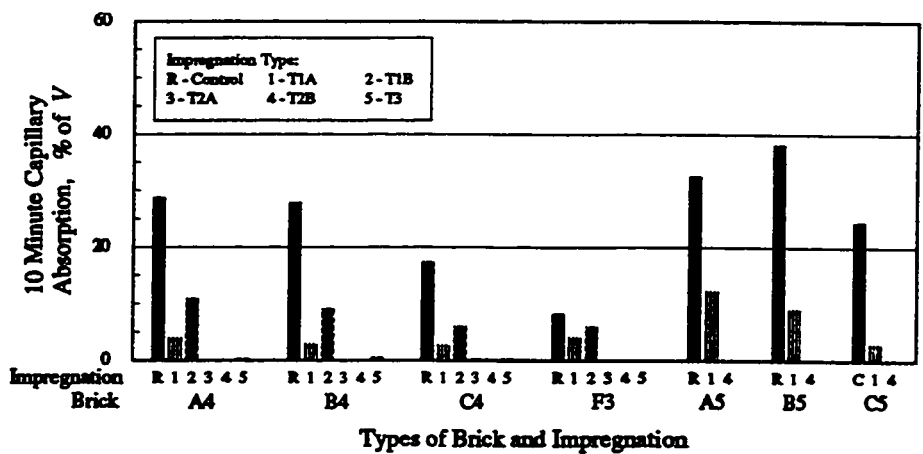


Figure 7.23 10 Minute Capillary Absorption of the impregnated bricks expressed in % of Vacuum Saturation (*SIOM/V*)

TABLE 7.7
Capillary Absorption Properties of Impregnated Bricks

Brick Type	Type of Impregnation	Capillary Absorption, % of dry weight						Capillary Absorption, % of Vacuum Saturation (V)					
		10 Minute Absorption			1 Hour Absorption			10 Minute Absorption			1 Hour Absorption		
		%	% Reduction	%	%	% Reduction	%	% of V	% Reduction	% of V	% Reduction	% of V	% Reduction
A4	Control	3.34	-	6.10	-	28.77	-	52.47	-	-	-	-	-
	T1A	0.33	90.12	1.21	80.16	3.99	86.13	14.56	72.25	86.13	14.56	72.25	
	T1B	0.68	79.64	2.03	66.72	10.93	62.01	32.82	37.45	62.01	32.82	37.45	
	T2A	0	100	0	100	0.03	99.90	0.05	99.90	99.90	0.05	99.90	
	T2B	0	100	0	100	0.09	99.69	0.20	99.62	99.69	0.20	99.62	
	T3	0.03	99.10	0.45	92.62	0.27	99.06	4.64	91.16	99.06	4.64	91.16	
B4	Control	3.46	-	6.31	-	27.83	-	50.93	-	-	-	-	
	T1A	0.26	92.49	1.04	83.52	2.94	89.44	11.46	77.50	89.44	11.46	77.50	
	T1B	0.58	83.24	2.03	67.83	9.08	67.37	32.06	37.05	67.37	32.06	37.05	
	T2A	0	100	0	100	0	100	0.16	99.69	100	0.16	99.69	
	T2B	0	100	0	100	0.04	99.86	0.14	99.73	99.86	0.14	99.73	
	T3	0.05	98.55	0.26	95.88	0.53	98.10	2.58	94.93	98.10	2.58	94.93	
C4	Control	2.09	-	5.65	-	17.34	-	46.88	-	-	-	-	
	T1A	0.21	89.95	0.51	90.97	2.64	84.78	6.47	86.20	84.78	6.47	86.20	
	T1B	0.30	85.65	0.81	85.66	5.95	65.69	16.02	65.83	65.69	16.02	65.83	
	T2A	0	100	0	100	0.21	98.79	0.32	99.32	98.79	0.32	99.32	
	T2B	0	100	0	100	0.12	99.31	0.31	99.34	99.31	0.31	99.34	
	T3	0.02	99.04	0.44	92.21	0.24	98.62	4.42	90.57	98.62	4.42	90.57	

TABLE 7.7 (continued)
Capillary Absorption Properties of Impregnated Bricks

Brick Type	Type of Impregnation	Capillary Absorption, % of dry weight				Capillary Absorption, % of Vacuum Saturation (V)			
		10 Minute Absorption		1 Hour Absorption		10 Minute Absorption		1 Hour Absorption	
		%	% Reduction	%	% Reduction	% of V	% Reduction	% of V	% Reduction
F3	Control	0.59	-	1.53	-	8.19	-	21.06	-
	T1A	0.11	81.36	0.23	84.97	4.03	50.79	8.29	60.64
	T1B	0.14	76.27	0.26	83.01	5.98	26.78	10.71	49.15
	T2A	0	100	0	100	0	100	0.23	98.91
	T2B	0	100	0	100	0.02	99.76	0.24	98.86
T3	0	100	0.01	99.35	0	100	0.16	99.24	
A5	Control	4.37	-	8.28	-	32.46	-	61.56	-
	T1A	1.17	73.23	3.12	62.32	12.27	62.20	32.85	46.64
	T2B	0	100	0	100	0.16	99.51	0.29	99.53
B5	Control	5.49	-	8.2	-	38.12	-	57.18	-
	T1A	1.03	81.24	2.89	64.84	9.12	76.08	25.97	54.58
	T2B	0	100	0.01	99.88	0.07	99.82	0.29	99.49
C5	Control	3.30	-	7.77	-	24.44	-	57.57	-
	T1A	0.27	91.82	0.70	90.99	2.88	88.22	7.46	87.04
	T2B	0	100	0.01	99.87	0.13	99.47	0.46	99.20

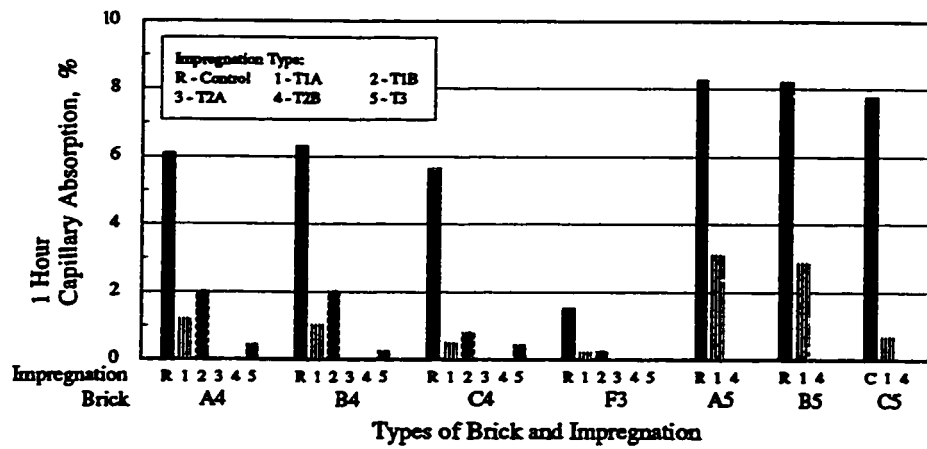


Figure 7.24 1 Hour Capillary Absorption of the impregnated bricks expressed in % of dry weight (*S_I*)

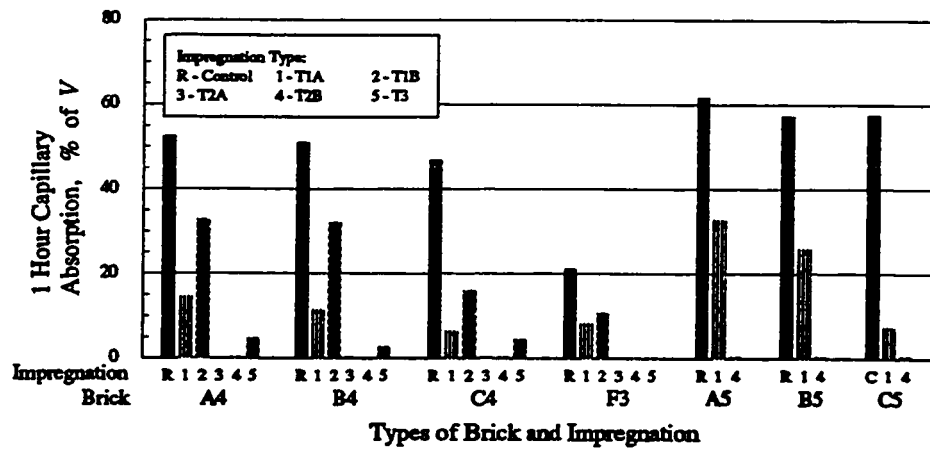


Figure 7.25 1 Hour Capillary Absorption of the impregnated bricks expressed in % of Vacuum Saturation (*S_{I/V}*)

absorptions for paraffin impregnated bricks (T2A and T2B) were almost nil. Polymer impregnated bricks (T1A and T1B) gave better reduction in capillary absorption compared to submersion absorption. Between them, T1A was found to give improved absorption properties than T1B. Bricks impregnated with acrylic sealer (T3) also provided significant reduction in capillary absorption ranging between 90 to 100 %.

7.4.4 Summary

Paraffin impregnation was very effective in reducing submersion absorption, capillary absorption, and vacuum saturation of bricks. The saturation coefficients for these bricks were also found to be very low. The saturation coefficient for all bricks except T1B was decreased due to impregnation. In the case of T1B, an increase in C/V was observed, which might adversely affect durability. This is due to the fact that an increase in C/V shows a decrease in the percentage of unfilled pores that is available for unfrozen water to move during freezing. All the impregnated bricks provided better reduction in capillary absorption compared to submersion absorption. Among polymer impregnated bricks, T1A was found to give improved absorption properties.

7.5 Effect on Compressive Strength

The compressive strength of the impregnated bricks were determined according to the test method specified in ASTM C67. Table 7.8 gives the results from the test. The results are also shown in Figure 7.26. All the impregnated bricks showed an increase in compressive strength. The percentage increases were low for the higher strength brick F3. Polymer impregnated bricks provided higher increase in compressive strength compared to other bricks. T1B improved the strength better than T1A. Among bricks A4, B4, and C4, T1B provided 70 to 80 % increase in

TABLE 7.8
Strength, Density, and Pulse Velocity of Impregnated Bricks

Brick Type	Type of Impregnation	Compressive Strength (Gross)		Bulk Density		Ultrasonic Pulse Velocity	
		MPa	% Increase	g/cc	% Increase	m/s	% Increase
A4	Control	35.12	-	2.0793	-	3161	-
	T1A	52.84	50.46	2.1493	3.37	3477	10.00
	T1B	62.46	77.85	2.1410	2.97	3363	6.39
	T2A	44.97	28.05	2.1500	3.40	3882	22.81
	T2B	50.42	43.56	2.1933	5.48	4164	31.73
	T3	38.49	9.60	2.0874	0.39	3450	9.14
B4	Control	46.75	-	2.0515	-	2945	-
	T1A	64.19	37.30	2.1339	4.02	3484	18.30
	T1B	79.42	69.88	2.1457	4.59	3433	16.57
	T2A	52.83	13.01	2.1520	4.90	4077	38.44
	T2B	57.82	23.68	2.1778	6.16	4212	43.02
	T3	48.78	4.34	2.0795	1.36	3672	24.69
C4	Control	54.46	-	2.0327	-	3116	-
	T1A	73.94	35.77	2.1959	8.03	3846	23.43
	T1B	93.97	72.55	2.2601	11.19	3775	21.15
	T2A	63.99	17.50	2.1450	5.52	4003	28.47
	T2B	66.40	21.92	2.1715	6.83	4114	32.03
	T3	56.15	3.10	2.0734	2.00	3479	11.65

TABLE 7.8 (continued)
Strength, Density, and Pulse Velocity of Impregnated Bricks

Brick Type	Type of Impregnation	Compressive Strength (Gross)		Bulk Density		Ultrasonic Pulse Velocity	
		MPa	% Increase	g/cc	% Increase	m/s	% Increase
F3	Control	109.94	-	2.0979	-	3806	-
	T1A	131.36	19.48	2.2414	6.84	4162	9.35
	T1B	144.78	31.69	2.2946	9.38	4204	10.46
	T2A	114.13	3.81	2.2161	5.63	4264	12.03
	T2B	116.91	6.37	2.1834	4.08	4442	16.71
A5	T3	110.69	0.68	2.1087	0.51	3952	3.84
	Control	-	-	2.0121	-	2690	-
	T1A	-	-	2.1048	4.61	3154	17.25
B5	T2B	-	-	2.1669	7.69	4000	48.70
	Control	-	-	1.9909	-	2514	-
	T1A	-	-	2.0734	4.14	3127	24.38
C5	T2B	-	-	2.1225	6.61	3969	57.88
	Control	-	-	2.0052	-	2842	-
	T1A	-	-	2.0846	3.96	3532	24.28
	T2B	-	-	2.1456	7.00	3956	39.20

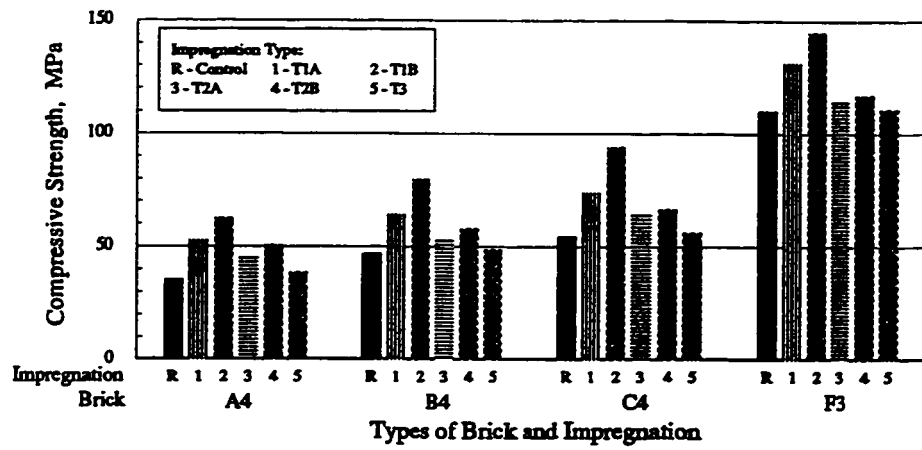


Figure 7.26 Compressive Strength of the impregnated bricks

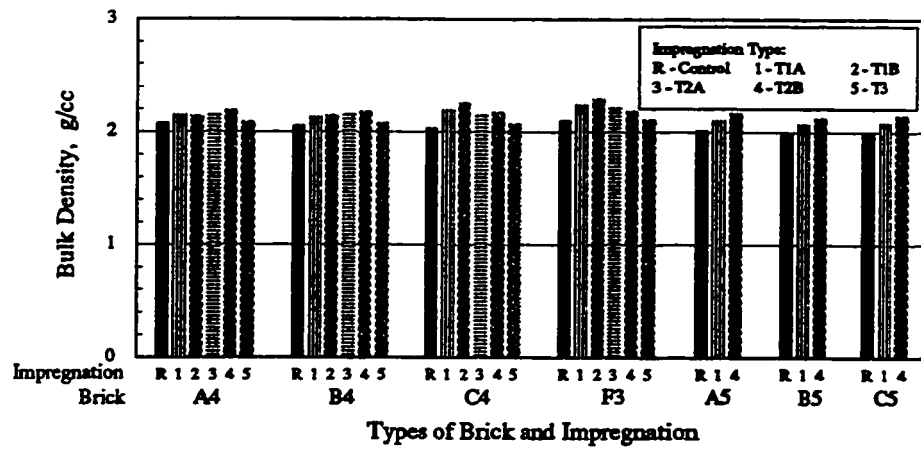


Figure 7.27 Bulk Density of the impregnated bricks

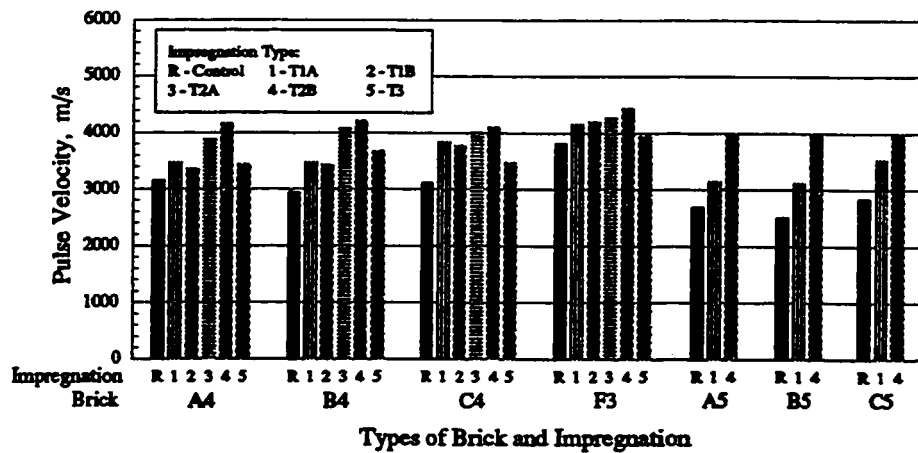


Figure 7.28 Ultrasonic Pulse Velocity of the impregnated bricks

strength whereas T1A provided only 35 to 50 % increase. T2A gave 13 to 28 % increase whereas T2B had 22 to 44 % increase. Bricks impregnated with acrylic sealer had the least improvement in strength of less than 10 %.

The bulk density of the impregnated bricks was measured using mercury intrusion porosimeter. Table 7.8 and Figure 7.27 show the results. The percentage increases in density were very low, less than about 10 %.

7.6 Effect on Pulse Velocity

The pulse velocity depends upon the density and porosity of the material through which it passes. Therefore it can be used as a measure of the effect impregnation in improving the porosity. The pulse velocity of the impregnated bricks were measured using the test procedure explained in Section 3.5.3. The test results are shown in Table 7.8 and in Figure 7.28. Impregnation modified the pore volume and therefore the pulse velocity through brick was observed to have increased. Since the density of the impregnating materials might be different, the percentage increases in pulse velocity were not found to depend upon the amount of loading. In general paraffin impregnated bricks (T2A and T2B) provided larger increases. Among them, T2B had higher values.

7.7 Effect on Freeze-Thaw Performance

The freeze-thaw performance of the impregnated bricks were studied using the accelerated freezing and thawing test explained in Section 3.5.4. This test was used only for comparing the control and impregnated bricks. The test results are given in Table 7.9. Only bricks impregnated

TABLE 7.9
Freeze-Thaw Performance of Impregnated Bricks

Brick Type	Type of Impregnation	Freeze-thaw Cycles resisted		Initial Saturation %	Final Saturation %	% Increase in Saturation %	Weight Loss of brick specimen %
		Number of Cycles	Improvement Factor				
A4	Control	48	-	6.83	7.81	14.26	0.05
	T1A	> 814	> 16.96	3.31	3.50	6.01	0.02
	T1B	95	1.98	4.24	5.18	22.62	0
	T2A	> 1005	> 20.94	0.05	0.12	133.33	0
	T2B	> 1005	> 20.94	0.07	0.19	185.71	0
	T3	214	4.46	4.28	5.93	39.51	0.37
B4	Control	50	-	6.87	7.85	14.22	0.02
	T1A	> 814	> 16.28	3.12	3.37	8.35	0.02
	T1B	80	1.60	4.01	5.04	29.54	0
	T2A	> 1005	> 20.10	0.09	0.21	129.92	0
	T2B	> 1005	> 20.10	0.11	0.18	57.83	0.01
	T3	291	5.82	4.02	6.06	50.73	0.28
C4	Control	38	-	6.92	7.71	11.62	0.02
	T1A	> 814	> 21.42	2.42	3.04	30.92	0
	T1B	113	2.97	3.04	3.63	20.50	0.01
	T2A	> 1005	> 26.45	0.07	0.42	495.24	0
	T2B	> 1005	> 26.45	0.08	0.30	265.61	0
	T3	236	6.21	5.48	6.69	21.96	0.22

TABLE 7.9 (continued)
Freeze-Thaw Performance of Impregnated Bricks

Brick Type	Type of Impregnation	Freeze-thaw Cycles resisted		Initial Saturation %	Final Saturation %	% Increase in Saturation %	Weight Loss of brick specimen %
		Number of Cycles	Improvement Factor				
F3	Control	71	-	5.08	5.78	13.49	0.06
	T1A	> 814	> 11.46	1.38	1.58	15.08	0
	T1B	> 778	> 10.96	1.92	2.14	11.40	0.08
	T2A	> 1005	> 14.15	0.05	0.17	266.67	0
	T2B	> 1005	> 14.15	0.08	0.23	192.13	0
	T3	261	3.68	4.46	5.42	21.44	0.08
A5	Control	32	-	8.86	9.77	10.35	0.04
	T1A	> 814	> 25.44	5.35	4.77	-11.35	0
	T2B	> 1005	> 31.41	0.07	0.07	2.22	0
B5	Control	35	-	8.90	9.81	10.27	0.05
	T1A	> 814	> 23.26	5.50	4.77	-13.37	0
	T2B	> 1005	> 28.71	0.09	0.38	322.59	0
C5	Control	30	-	8.17	8.95	9.56	0.02
	T1A	> 814	> 27.13	4.31	4.10	-4.88	0
	T2B	> 1005	> 33.50	0.10	0.19	93.33	0.02

with T1B and T3 failed. All other impregnated bricks did not fail even after subjecting to about 800 to 1000 cycles of freezing and thawing, giving an improvement factor of more than 10 compared to the control bricks. Bricks showed negligible weight loss during the test and none of the bricks reached a weight loss of 0.5 %. The development of visible cracks was observed to be the cause for the failure of bricks. The saturation level of the bricks was found to increase in almost all the cases. It was observed that, even though the bricks impregnated with acrylic sealer (T3) resisted more than 200 cycles, the surface coating for these brick started to peel off during the course of the test. As seen in Table 7.9, the saturation level for these bricks increased and they had the highest weight loss of all the impregnated bricks. Based on these observations, bricks impregnated with T3 are not recommended for improving durability.

The improvement factor for frost resistance is shown in Table 7.9. It is the ratio of freeze-thaw cycles resisted by the impregnated brick to the corresponding control brick. The frost resistance of the bricks is shown in Figure 7.29. For bricks that did not fail, the maximum number of cycles, to which they were subjected, were used in Figure 7.29 for comparison.

Using the equations mentioned in Chapter 5, durability indices were calculated for the impregnated bricks. It is not clear whether these equations developed for untreated bricks could be extended to impregnated bricks for evaluating durability. The Durability Index by Maage (Equation[5.2]) and the Durability Index based on Absorption Properties (Equation[5.9]) were studied. For calculating $DIAP(S)$, instead of 5hr. boiling water absorption (B), vacuum saturation (V) was used in Equation[5.9]. The results are given in Table 7.10 and Figures 7.30 and 7.31. Comparing Figures 7.29 and 7.30, it can be found that in certain cases, bricks having higher DIM values showed lower frost resistance and vice versa. Figures 7.29 and 7.31 show that $DIAP(S)$

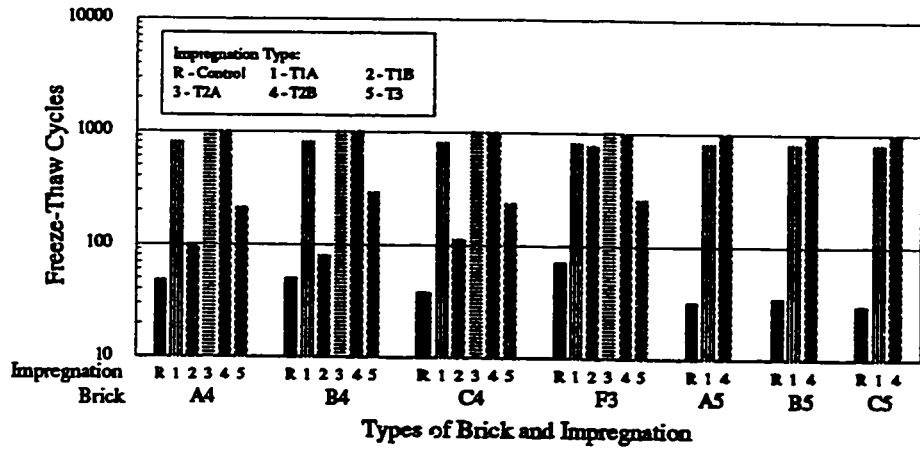


Figure 7.29 Frost Resistance of the impregnated bricks

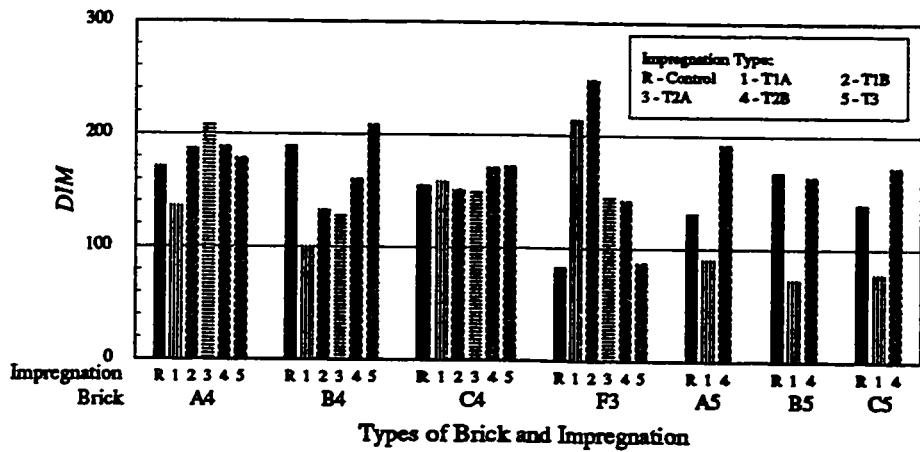


Figure 7.30 Durability Index by Maage (*DIM*) of the impregnated bricks

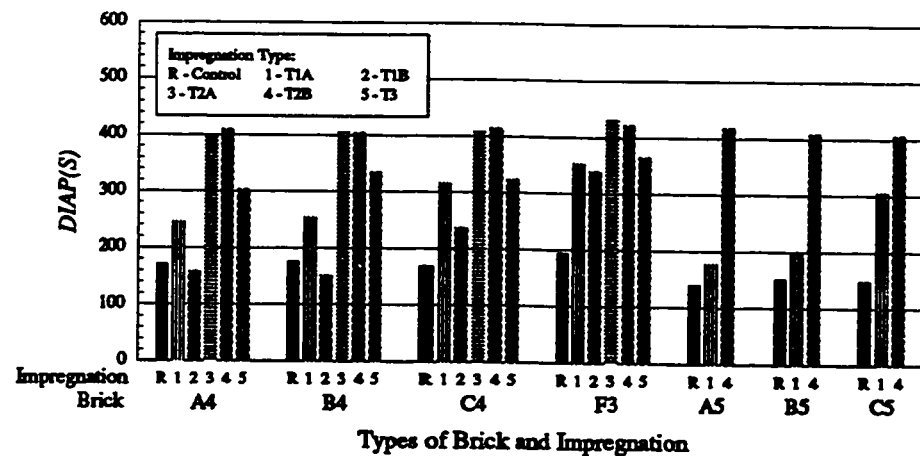


Figure 7.31 Durability Index based on Absorption Properties [*DIAP(S)*] of the impregnated bricks

TABLE 7.10
Durability Indices for Impregnated Bricks

Brick Type	Type of Impregnation	Durability Index by Maage (<i>DIM</i> *)			Durability Index based on Absorption Properties [<i>DIAP(S)</i> **]		
		<i>PV</i> ml/g	<i>P3</i> %	<i>DIM</i>	<i>V</i> %	<i>S4V</i>	<i>DIAP(S)</i>
A4	Control	0.0986	57.81	171.20	11.60	0.5454	171.03
	T1A	0.0594	34.39	136.41	8.24	0.3456	246.25
	T1B	0.0556	54.04	187.25	6.03	0.6439	157.80
	T2A	0.0471	58.31	207.88	2.95	0.0017	395.87
	T2B	0.0370	42.59	188.70	2.02	0.0031	409.76
	T3	0.0914	59.81	178.55	9.43	0.1602	303.52
B4	Control	0.0999	65.54	189.33	12.39	0.5267	175.60
	T1A	0.0726	23.50	100.48	8.87	0.3146	254.32
	T1B	0.0572	31.92	132.55	6.17	0.6602	151.65
	T2A	0.0542	28.60	127.68	2.28	0.0026	405.40
	T2B	0.0498	39.94	160.11	2.35	0.0037	403.89
	T3	0.0849	71.30	208.81	10.04	0.0605	334068
C4	Control	0.1140	52.81	154.81	12.02	0.5518	168.05
	T1A	0.0516	40.24	158.59	7.36	0.1436	316.31
	T1B	0.0239	7.18	151.12	4.90	0.4255	237.07
	T2A	0.0552	37.88	148.88	2.12	0.0057	407.11
	T2B	0.0519	45.70	171.34	1.75	0.0063	413.94
	T3	0.0997	58.50	172.50	10.45	0.0892	324.16

TABLE 7.10 (continued)
Durability Indices for Impregnated Bricks

Brick Type	Type of Impregnation	Durability Index by Maage (DIM)*			Durability Index based on Absorption Properties [DIAP(S)**		
		PV ml/g	P3 %	DIM	V %	S4V	DIAP(S)
F3	Control	0.0836	18.53	82.75	7.23	0.5155	194.22
	T1A	0.0248	35.46	214.14	2.75	0.1380	353.61
	T1B	0.0136	5.78	249.17	2.28	0.2023	339.54
	T2A	0.0282	13.11	144.94	1.10	0.0046	429.96
	T2B	0.0409	26.88	142.75	1.36	0.0063	422.65
A5	T3	0.0796	19.43	86.83	6.61	0.0063	365.03
	Control	0.1185	43.46	131.31	13.43	0.6310	139.34
	T1A	0.0780	20.74	90.80	9.47	0.5413	177.71
B5	T2B	0.0314	37.70	192.39	1.54	0.0055	418.70
	Control	0.1171	58.43	167.56	14.37	0.5906	151.17
	T1A	0.0893	15.29	72.53	10.93	0.4731	196.38
C5	T2B	0.0539	43.56	163.91	2.08	0.0049	408.08
	Control	0.1241	47.17	138.99	13.49	0.6040	148.14
	T1A	0.0922	17.99	77.88	9.48	0.1543	305.31
	T2B	0.0546	47.26	172.03	2.13	0.0081	406.14

* $DIM = \frac{3.2}{PV} + 2.4P3$; ** $DIAP(S) = \frac{450.70}{(2.94 + V)} + 329.81(0.97 - \frac{S4}{V})$

better evaluate the frost resistance of bricks compared to *DIM*.

7.8 Effect on Brick-Mortar Bond Strength

The brick-mortar bond strength test was carried out to determine whether impregnation adversely affected the bond between brick and mortar. The bond test was done using the experimental procedure explained in Section 3.5.6, which was based on American standard test method ASTM C952 [ASTM 1991]. The procedures in this standard are recommended for research into bonding of masonry and not to predict bond strength of commercial masonry construction. Therefore in this study the crossed brick couplet tensile test for evaluating brick-mortar bonding was used only for comparing control and impregnated brick specimens.

Brick types A4, B4, and C4 were used for the experimental study. The results discussed in previous sections showed that polymer impregnation under vacuum was not recommended for improving durability as it resulted in increased saturation coefficient. Also, bricks impregnated with acrylic sealer had a poor freeze-thaw performance due to the impregnating material peeling off during the repeated cycles. Therefore these two impregnation types were not studied for bond strength. Among the paraffin impregnations (T2A and T2B), T2B showed slightly better performance and it had higher melting point around 98°C. Thus only impregnation types T1A and T2B were used for studying the bond strength.

Initially the brick couplets were made using control and impregnated bricks and type N cement-lime mortar with a w/c ratio of 0.5, as per ASTM C270 [ASTM 1992d]. The compressive strength of the mortar specimens were determined using ASTM C109 [ASTM 1993b]. The test

results are given in Table 7.11. It can be seen that the bond strength decreased by about 11 to 13 % for polymer impregnated bricks (except for Brick B4, where it increased by 7.14 %). In the case of paraffin impregnated bricks, the bond strength decreased by 21 to 26 %.

In order to find whether increasing the mortar strength had any effect on bond strength, cement mortar 1:3 without any lime was used for making the brick couplets with impregnated bricks. The w/c ratio was maintained at 0.5. Table 7.11 shows that the tensile bond strength of specimens increased in the case of cement mortar, compared to cement-lime mortar, by about 33 to 60 %. But as with the cement-lime mortar, the bond strength of impregnated specimens with cement mortar decreased compared to the corresponding control bricks. For T1A the reduction was between 8 to 16 % while for T2B it was 23 to 31 %.

There are various reasons for the relatively poor bond strength of impregnated bricks. These are discussed here.

(i) It was observed that all the specimens failed at the upper joint between mortar and brick. According to ASTM C270 [ASTM 1992d], mortar generally bonds best to masonry units having moderate initial rates of absorption (*IRA*) from 5 to 25 g/min/193.55 cm² at the time of laying. The *IRA* values for the control and impregnated bricks are shown in Table 7.11. It can be seen that impregnated bricks have very low suction. The extraction of too much or too little of the available water in the mortar tends to reduce the bond between masonry unit and the mortar. When a very low suction masonry unit is used, the unit tends to float and bond is difficult to accomplish. This is because, water from the mortar rises to the top due to lower density and a layer of water is formed at the joint between mortar and the upper brick, thus affecting bond. This might be the reason why all the specimens failed at the top joint. There is no available means of

TABLE 7.11
Effect of Impregnation on Brick-Mortar Bond Strength

Brick Type	Type of Impregnation	Initial Rate of Absorption (IRA)		TEST 1: Cement-Lime Mortar, Type N			TEST 2: Cement Mortar 1:3 with no lime			TEST 3: Brick couplets impregnated after making		
		IRA g/min./ 193.55cm ²	Reduction %	Loading (Impreg- nation) %	Tensile Bond Strength MPa	Increase %	Loading (Impreg- nation) %	Tensile Bond Strength MPa	Increase %	Loading (Impreg- nation) %	Tensile Bond Strength MPa	Increase %
A4	Control	26.90	-	-	0.35	-	-	0.52	-	-	0.35	-
	T1A	1.89	92.97	3.68	0.31	-11.43	3.73	0.44	-15.38	4.12	0.82	134.29
	T2B	0.01	99.96	5.92	0.26	-25.71	5.88	0.36	-30.77	6.08	0.39	11.43
B4	Control	24.92	-	-	0.28	-	-	0.45	-	-	0.28	-
	T1A	1.40	94.38	3.52	0.30	7.14	3.67	0.40	-11.11	3.97	0.54	92.86
	T2B	0	100	5.78	0.22	-21.43	5.69	0.33	-26.67	5.86	0.30	7.14
C4	Control	15.54	-	-	0.39	-	-	0.57	-	-	0.39	-
	T1A	2.23	85.65	4.07	0.34	-12.82	4.23	0.52	-8.77	4.34	0.84	115.38
	T2B	0	100	5.66	0.30	-23.08	5.77	0.44	-22.81	5.94	0.45	15.38
Compressive Strength of Mortar, MPa				8.83			23.41			8.83		

increasing the suction of a low suction masonry unit, and thus the time lapse between spreading the mortar and placing the unit may have to be increased.

(ii) Mortars having lower water retentivity are desirable for use with masonry units having low suction [ASTM 1992d]. That might be why cement mortar, which has a lower water retentivity compared to cement-lime mortar, gave better bond strength for impregnated bricks.

(iii) In practice the weight of the over laid bricks compresses the mortar joint and may squeeze out the water layer formed at the joint, thus resulting in better bond. This was not the case when specimens were made in the laboratory with crossed brick couplet.

(iv) The specimens used in this study were small and the area of contact between brick and mortar was only around 1500 to 2000 mm². It was observed that, slight displacements of the top brick in the crossed couplet resulted in lack of balance and this might have affected the bond between mortar and upper brick.

Based on the above discussions, it can be suggested that, more studies are required before a final conclusion is drawn on the effect of impregnation on brick-mortar bond. These studies should involve brick walls or prisms rather than brick couplets. This is beyond the scope of this research.

Bond strength tests were also done on brick couplets impregnated after making them. For this, brick couplets were made using untreated bricks and cement-lime mortar with a w/c ratio of 0.5. After curing for about 28 days, these specimens were impregnated with T1A and T2B. The test results are shown in Table 7.11. There was significant increase of about 90 to 135 % in bond strength for polymer impregnated specimens. In the case of paraffin, the increases were small, about 7 to 16 %. These test results suggest that impregnation process can be applied to

prefabricated brick walls or panels with the advantages of improved water absorption and frost resistance, with no concern for reduction in bond strength. More research in this regard is needed.

7.9 Economic Aspects of Impregnation

A detailed economic analysis of impregnation can be carried out only if the additional costs for the impregnation processes are known. The processes used in this research were laboratory based, using existing or newly fabricated facilities. Their application for large scale commercial production was not investigated. Therefore a detailed economic analysis is beyond the scope of this research. Instead, the additional material costs for the impregnation are analyzed and discussed here.

The amount of material required for impregnation will depend upon the porosity of the bricks. The impregnating material consumed by the brick during the impregnation was calculated by assuming a 24 hr. water absorption of about 10 % for the brick and a dry weight of about 2 to 2.2 kg for a full brick and based on the observations made while impregnating the test specimens used in the study. Knowing the amount of material needed for impregnation, the additional material cost of impregnation was then calculated based on the retail price of the impregnating material without taking into account the cost of labour and equipments used for the impregnation. The additional material cost of impregnation is given in Table 7.12 (in Canadian dollars per each full brick). The lower range of current price of clay facing brick is about 300 Canadian dollars per 1000 bricks. Thus even the most cost effective impregnation may almost double the cost of brick (based on the additional material cost of impregnation given in Table 7.12).

TABLE 7.12
Additional Material Cost of Impregnation

Impregnation Type	Additional cost per full brick
T1A and T1B	\$1.50 to \$2.50
T2A	\$0.30 to \$0.40
T2B	\$0.50 to \$0.60
T3	\$0.60 to \$0.70

Polymer impregnation was found to be much more costly compared to other impregnations. Also, polymer impregnation is a rather complicated process involving preparation of monomer, soaking, and polymerization. It is also a risky process when it comes to large scale production with huge quantities of MMA monomer, unless safety precautions are taken to prevent any accidental bulk polymerization. All these add to the production cost of polymer impregnated bricks. Paraffin impregnation was found to be the most cost effective. Also the production cost will be comparatively cheaper for paraffin impregnation, as it involves only melting the wax and soaking the bricks in it. The costs given in Table 7.12 are based on retail prices of the materials and it may decrease in the case of large scale commercial production. The final selection of a material should be based not merely on cost but on a cost-benefit analysis.

7.10 Comparison of Impregnation Types

The effect of impregnation on the properties of bricks were discussed in the preceding sections in this chapter. In this section the five impregnation types used in this research are

compared with respect to their effectiveness in improving the brick properties. The comparison is given in a tabular form in Table 7.13. The properties studied for the comparison included 24 hr. water absorption, saturation coefficient, porosity, compressive strength, freeze-thaw resistance, and brick-mortar bond strength. These properties are expressed in terms of percentage increase or reduction. The additional material cost of impregnation was also used for the purpose of comparison.

TABLE 7.13
Comparison of Impregnation Types

Property	Impregnation Type				
	T1A	T1B	T2A	T2B	T3
% Reduction in 24 hr. Water Absorption, %	38 to 72	38 to 65	97 to 99	97 to 99	15 to 40
% Reduction in Saturation Coefficient, %	18 to 41	-11 to -22	86 to 93	85 to 92	7 to 25
% Reduction in Porosity, %	20 to 68	40 to 82	43 to 64	46 to 71	4 to 11
% Increase in Compressive Strength, %	19 to 50	31 to 78	4 to 28	6 to 44	0.7 to 10
Freeze-thaw Resistance Improvement Factor	>14 to >27	1.6 to >11	>14 to >26	>14 to >34	3 to 6
% Increase in Brick-Mortar Bond Strength, %	-13 to 7	-	-	-21 to -26	-
Additional Material cost of Impregnation (\$ per full brick)	1.5 to 2.5	1.5 to 2.5	0.3 to 0.4	0.5 to 0.6	0.6 to 0.7

From Table 7.13 it can be seen that paraffin impregnation is better than the others in many respects. Paraffin impregnation resulted in significant reduction (above 85 %) in water absorption and saturation coefficient and showed excellent freeze-thaw performance. Also the porosity was reduced considerably (above 40 %). The only drawback with paraffin was the reduction in brick-mortar bond strength (about 25 %). Since bond strength was measured using half brick couplets, more studies are recommended before a final conclusion is drawn about the effect of impregnation on brick-mortar bond.

Conclusion

This research was necessitated by the concerns on premature failure of bricks used for the building envelope. In cold regions like Canada, frost action was found to be the major cause for failure and was, therefore, the primary focus of this research. In an effort to improve the frost durability of bricks, three major objectives were identified for this research. They were:

- to develop an index to evaluate durability,
- to investigate the feasibility of using nondestructive methods to evaluate durability, and
- to study the effect of impregnation towards improving the durability of bricks.

This chapter discusses the conclusions drawn from this study and the recommendations for further study.

8.1 Conclusions from the Study

8.1.1 Conclusions from the Review of Previous Studies

- (i) In addition to porosity, pore size distribution is also an important factor influencing the frost durability of bricks. It can be suggested that pores larger than 3 μm in diameter have no adverse effect on frost resistance of bricks, whereas pores smaller than 1 μm are harmful. The

current American and Canadian standard specifications and test methods for evaluating durability of clay bricks are time consuming and reported to be inadequate in certain cases. The criteria mentioned in the ASTM standard do not take into account the distribution of pore size. Thus the review emphasized the need for developing proper relationships between physical properties of bricks and their frost resistance, so that index could be developed which could be used for reliable assessment of durability in short time. The existing durability indices developed by various researchers were found to have limitations.

(ii) Nondestructive testing (NDT) methods had been extensively used to assess the quality of concrete. Research on the use of these methods for the evaluation of brick masonry had been very limited. More studies were needed on the feasibility of using NDT methods for evaluating the durability of bricks.

(iii) In general, impregnation of ceramic products (concrete, mortar, etc.) resulted in increased strength, reduced absorption, and changes in pore size distribution of such porous materials. Impregnated bricks can be used for locations where high level of saturation and severe weather conditions are expected. In the absence of detailed studies, more research was needed to study the effect of impregnation on the properties and durability of bricks.

8.1.2 Conclusions from the Present Study

(i) In this research a new index based on water absorption properties of bricks was developed for evaluating durability. The method adopted for deriving the index was decided after carrying out a comparative study of the existing indices and their limitations. The comparative study involved the durability indices developed by four researchers, namely Robinson, Maage,

Nakamura, and Arnott. It was found that these indices had limitations in reliably predicting the durability of bricks. Therefore it was considered necessary to develop a new index to overcome the limitations of the existing indices.

Out of the four existing indices studied, the index developed by Maage was found to be simple and relatively fast to determine and has been validated by other researchers. It takes into consideration the effects of porosity and pore size distribution. In addition it specifies limiting values for classifying as durable and nondurable brick. But a drawback with Maage's method is that it is a destructive test and requires an expensive mercury porosimeter to measure the index. It was observed in the comparative study that Maage's method needed improvement as it did not give a true measure of the frost resistance of certain bricks. Maage's method depends exclusively on pore volume and pore size distribution and does not consider the rate of actual absorption of bricks.

Therefore in this study the new durability index was developed by modifying Maage's equation by incorporating absorption properties of bricks. Empirical relation between pore and absorption properties were studied. These relations were used to develop the new durability index based on water absorption properties. In fact two indices were developed, one using submersion absorption property, and the other using capillary absorption property. These indices were found to overcome the limitations of Maage's index. They were also validated using a different set of bricks. Out of these two indices, the one based on capillary absorption property was found to be better and is therefore recommended. In future, results from more brick types can be used to refine these indices.

(ii) As not much research work had been done on the use of NDT methods for the evaluation of brick properties, an investigation of the feasibility of using NDT method for evaluating brick durability was undertaken. Based on the review of different NDT methods, ultrasonic pulse velocity method was selected for the study. The aim of the research was to find whether pulse velocity could be used to identify durable and nondurable brick. In order to achieve this, the durability requirements specified in American standard ASTM C216 were used. This standard provides requirements for water absorption and compressive strength to evaluate durability. Therefore relation between these properties and pulse velocity was studied. To obtain better relation test data provided by other researchers were included in the study. These relations were used to develop new provisions for durability based on pulse velocity.

These new provisions give an upper and lower limiting values for pulse velocity, which can be used to identify durable and nondurable brick. But the drawback is that when the pulse velocity is between these two values, the new method can not evaluate durability and ASTM specifications should be used in such cases. At this stage it can only be used along with ASTM method. The new provisions can avoid the time consuming ASTM method in many cases. Being a faster and nondestructive test it has the potential for in situ evaluation. Results from more brick types can be used in the future to refine these durability provisions. This study was only a feasibility study using pulse velocity as a single parameter. Further studies are required to find relation between pore properties and various pulse characteristics, which can better define durability.

(iii) The following observations were made from the study on the effect of impregnation on brick properties and its durability. All impregnations except acrylic sealer resulted in substantial

reduction in pore volume and porosity, but shifted the distribution of pore sizes towards lower diameter range. Most of these impregnated bricks had large amount of pores smaller than 3 μm in diameter. Paraffin impregnation was very effective in reducing submersion absorption, capillary absorption, and vacuum saturation. The saturation coefficient for all impregnated bricks except polymer impregnation under vacuum was decreased. In the case of vacuum impregnation, saturation coefficient was found to increase, hence it is not recommended for durability improvement. All impregnated bricks provided better reduction in capillary absorption compared to submersion absorption. Impregnation resulted in an increase in compressive strength for all bricks. The freeze-thaw performance of all the impregnated bricks were found to have increased compared to control bricks. In the case of bricks impregnated with acrylic sealer, it was observed that the coating peeled off during the repeated cycles of freezing and thawing. Therefore this sealer is not recommended for improving brick durability. Based on the tests on brick couplets, it was found that, impregnation reduced the bond between brick and mortar. Various reasons were attributed to this reduction in bond. Therefore, more studies are recommended before final conclusions are drawn on the effect of impregnation on bond strength.

(iv) From an analysis of additional material costs, paraffin impregnations were found to be the most cost effective. Polymer impregnations were very expensive (3 to 8 times that of paraffin) because of the price of the monomer. Also, process cost would be higher for polymer impregnation as it involved polymerization step and storing of large quantity of left over monomer containing the initiator. The final selection of a material should be based not merely on cost but also on a cost benefit analysis.

Summarising, this research had resulted in the development of a new durability index for

evaluating clay bricks. Also, new durability provisions using ultrasonic pulse velocity were derived. Studies on impregnated bricks provided the much needed information on the effect of impregnation with different materials on improving the properties and durability of bricks. Thus all the three major objectives of this research were achieved.

8.2 Recommendations for Further Study

No research is an end in itself. There is always avenues for future work. During the course of this research, the following topics were identified and are recommended for further study.

- (i) Study more brick types to refine the durability indices and provisions developed
- (ii) Future work should involve unidirectional freeze-thaw test, as it is found to simulate field conditions better.
- (iii) Study the effect of varying rates of freezing on the freeze-thaw performance of bricks.
- (iv) Study the effect of varying degrees of saturation on the freeze-thaw performance of bricks.
- (v) Future study should involve brick wall component as a whole, instead of individual bricks.
- (vi) Study the ultrasonic pulse characteristics, like attenuation of pulse, using signal processing techniques and try to relate to pore properties.
- (vii) Study the effect of varying the frequency of ultrasonic pulse on its velocity and pulse characteristics.
- (viii) Study the effect of other impregnating materials.
- (ix) Study the properties of impregnated wall components.
- (x) Carry out further study on the bond between impregnated brick and mortar using wall components.
- (xi) Study the rain penetration of impregnated walls.

References

- ACI (1977)**, "State-of-the-art Report: Polymer in Concrete", *American Concrete Institute Committee Report*, ACI, Detroit, Michigan, U.S.A.
- ASTM (1993a)**, "C67-93a: Standard Methods of Sampling and Testing Brick and Structural Clay Tile", American Society for Testing and Materials.
- ASTM (1993b)**, "C109-93: Standard Test Method for Compressive Strength of Hydraulic Cement Mortars (using 2-in. or 50 mm cube specimens)", American Society for Testing and Materials.
- ASTM (1992a)**, "C216-92d: Standard Specifications for Facing Brick (Solid Masonry Units made from Clay or Shale)", American Society for Testing and Materials.
- ASTM (1992b)**, "C666-92: Standard Test Method for Resistance of Concrete to Rapid Freezing and Thawing", American Society for Testing and Materials.
- ASTM (1992c)**, "E494-92: Standard Practice for Measuring Ultrasonic Velocity in Materials", American Society for Testing and Materials.
- ASTM (1992d)**, "C270-92a: Standard Specifications for Mortar for Unit Masonry", American Society for Testing and Materials.
- ASTM (1991)**, "C952-91: Standard Test Method for Bond Strength of Mortar to Masonry Units", American Society for Testing and Materials.
- ASTM (1984)**, "D4404-84: Standard Test Method for Determination of Pore Volume and Pore Volume Distribution of Soil and Rock by Mercury Intrusion Porosimetry", American Society for Testing and Materials.
- ASTM (1983)**, "C597-83: Standard Test Method for Pulse Velocity through Concrete", American Society for Testing and Materials.
- Abrams, D.P., and Matthys, J.H.** (1991), "Present and Future Techniques for Nondestructive Evaluation of Masonry Structures", *The Masonry Society Journal*, Vol. 10, NO. 1, pp. 22-26.

- Al-Hadithi, A.I., Al-Saleem, H.I., and Ikzer, A.G.** (1987), "Evaluation of Properties of Bricks Impregnated with Sulphur", *Materials and Structures*, Vol. 20, pp. 265-269.
- Arnott, M.** (1990), " Investigation of Freeze-thaw Durability", *CBAC/IRC Industrial Research Fellowship Final Report*, NRC-IRC Report No. CR 5680.1, December 1990.
- Bortz, S.A., Marusin, S.L., and Monk Jr., C.B.** (1990), "A Critical Review of Masonry Durability Standards", *Proceedings of the Fifth North American Masonry Conference*, 3-6 June 1990, pp. 1523-1535.
- CNS Electronics** (1993), "PUNDIT Manual for use with the Portable Ultrasonic Nondestructive Digital Indicating Tester", Mark V, C.N.S. Electronics Ltd., London.
- CSA** (1987), "CAN/CSA-A82.1-M87: Burned Clay Brick (Solid Masonry units made from Clay or Shale)", Canadian Standards Association.
- CSA** (1978), "CAN3-82.2-M78: Methods of Sampling and Testing Brick". Canadian Standards Association.
- Chen, W.F., Mehta, H.C., and Slutter, R.G.** (1976), "Sulphur and Polymer Impregnated Brick and Block Prisms", *Journal of Testing and Evaluation*, Vol. 4, No. 4, pp. 283-292.
- Davison, J.I.** (1980), "Linear Expansion due to Freezing and other Properties of Bricks", *Proceedings of Second Canadian Masonry Symposium*, 9-11 June 1980, pp. 13-24.
- De Puy, G.W.** (1975), "Freeze-thaw and Acid Resistance of Polymer Impregnated Concrete", *Durability of Concrete*, SP-47, American Concrete Institute, Detroit, Michigan, pp. 233-257.
- Fowler, D.W., and Fraley, T.J.** (1974), "Investigation of Polymer Impregnated Brick Masonry", *Journal of the Structural Division*, Proceedings of the ASCE, Vol. 100, No. ST1, pp. 1-10.
- Fraley, T.J.** (1971), "An Investigation of the Structural Properties of Polymer Masonry", *Master's Thesis*, University of Texas at Austin, Texas.
- Gabor, T., Becker-Palossy, K., and Bombicz, P.** (1991), "Investigation of Mechanism of Hydrophobic Treatment of Natural and Artificial Building Materials", *Acta Chimica Hungarica*, 128 (2), pp. 163-167.
- Gazzola, E.A.** (1992), "A critical review of durability provisions in Canadian Masonry Materials Standards", *Proceedings of the Sixth Canadian Masonry Symposium*, 15-17 June 1992, Univ. of Saskatchewan, Saskatoon, Saskatchewan, pp. 449-467.
- Hauck, D., Hilker, E., and Ruppik, M.** (1990), "Influence of the Firing Process on Frost Resistance", *Ziegelindustrie International*, ZI 9/90, pp. 501-507.
- Hawes, D.W.** (1991), "Latent Heat Storage in Concrete", *Ph.D. Thesis*, Concordia University, Montreal, p. 339.

- Herget, F.A., Crooks, R.W., and Winslow, D.N.** (1992), "Variability within Single Projects of Physical Properties of Face Brick as Related to Potential Durability", *Sixth Canadian Masonry Symposium*, 15-17 June 1992, University of Saskatchewan, Canada, pp. 417-428.
- Kayyali, O.A.** (1985), "Mercury Intrusion Porosimetry of Concrete Aggregates", *Materials and Structures*, Vol. 18, No. 106, pp. 259-262.
- Kingsley, G.R., Noland, J.L., and Atkinson, R.H.** (1987), "Nondestructive Evaluation of Masonry Structures using Sonic and Ultrasonic Pulse Velocity Techniques", *Proceedings of the Fourth North American Masonry Conference*, August 1987, Los Angeles, California, pp. 67.1 - 67.16.
- Kukacka, L.E., and Romano, A.J.** (1973), "Process Techniques for Producing Polymer Impregnated Concrete", *Polymers in Concrete*, SP-40, ACI, Detroit, pp. 15-31.
- Kung, J.H.** (1987a), "Frost Durability Study on Canadian Clay Bricks: I. Introduction and Sampling", *Durability of Building Materials*, Vol. 5, pp. 103-110.
- Kung, J.H.** (1987b), "Frost Durability Study on Canadian Clay Bricks: II. Thermal Gradient and Quality of Burnt Bricks in Kilns", *Durability of Building Materials*, Vol. 5, pp. 111-124.
- Kung, J.H.** (1987c), "Frost Durability of Canadian Clay Bricks: III. Characterization of Raw Materials and Burnt Bricks", *Durability of Building Materials*, Vol. 5, pp. 125-143.
- Kung, J.H.** (1985), "Frost Durability of Canadian Clay Bricks", *Proceedings of the Seventh International Brick Masonry Conference*, Melbourne, Australia, 17-20 Feb. 1985, pp. 245-252.
- Litvan, G.G.** (1992), "The Effect of Sealers on the Freeze-thaw Resistance of Mortar", *Cement and Concrete Research*, Vol. 22, pp. 1141-1147.
- Maage, M.** (1984), "Frost Resistance and Pore Size Distribution in Bricks", *Materials and Structures*, Vol.17, No. 101, pp. 345-350.
- Mailvaganam, N.P., Deans, J.J., and Cleary, K.** (1990), "Sealing and Water Proofing Materials", *Repair and Protection of Concrete Structures*, Mailvaganam, N.P., Ed., CRC Press, London, pp. 87-116.
- Malhotra, V.M.** (1976), "Testing Hardened Concrete: Nondestructive Methods", *ACI Monograph No. 9*, ACI, Detroit, Michigan, p.188.
- Malhotra, V.M., Carettem G., and Soles, J.A.** (1978), " Long-term Strength and Durability of Sulphur Infiltrated Concrete", *Polymers in Concrete*, SP-58, ACI, Detroit, pp. 367-397.
- Malhotra, V.M., and Sivasundaran, V.** (1991), "Resonant Frequency Methods", *CRC Handbook on Nondestructive Testing of Concrete*, V.M. Malhotra and N.J. Carino, Eds., CRC Press, London, pp. 147-168.

- Marusin, S.L.** (1990), "Failure of Brick with High Compressive Strength, Low Water Absorption, and Saturation Coefficient Higher than 0.8 under Severe Weather Conditions: A Laboratory Report", *Ceramic Bulletin*, Vol. 69, No. 8, pp. 1332-1337.
- Marusin, S.L.** (1989), "Enhancing Concrete Durability by Treatment with Sealers", *Structural Materials, Proceedings of the Session Related to Structural Materials at Structures Congress '89*, San Francisco, CA, May 1-5, 1989, James F. Orofino, Ed., Pub. by ASCE, NY.
- May, J.O. and Butterworth, B.** (1962), "Studies of Pore Size Distribution", *Science of Ceramics*, Vol. 1, Proceedings of a Conference held at Oxford, 26-30 June 1961, G.H. Stewart, Ed., Pub. by Academic Press, pp. 201-221.
- Metz, F., and Knofel, D.** (1992), "Systematic Mercury Porosimetry Investigations on Sand Stones", *Materials and Structures*, Vol. 25, pp. 127-136.
- Micromeritics** (1993), "Pore Sizer 9320 : Operator's Manual", Micromeritics Instrument Corporation, Norcross, GA, U.S.A.
- Muresan, M.** (1973), "Applications of Pressure Porosimetry to Ceramic Products", *Materials and Structures*, Vol. 6, No. 33, pp. 203-207.
- Naik, T.R., and Malhotra, V.M.** (1991), "The Ultrasonic Pulse Velocity Method", *CRC Handbook on Nondestructive Testing of Concrete*, V.M. Malhotra and N.J. Carino, Eds., CRC Press, London, pp. 169-188.
- Nakamura, M.** (1988a), "Indirect Evaluation of Frost Susceptibility of Building Materials", *American Ceramic Society Bulletin*, Vol. 67, No. 12, pp. 1964-1965.
- Nakamura, M.** (1988b), "Automatic Unidirectional Freeze-Thaw Test for Frost Durability of Building Materials", *American Ceramic Society Bulletin*, Vol. 67, No. 12, pp. 1966-1968.
- Nakamura, M., Ohnishi, T., and Kamitani, M.** (1991), "Quantitative Analysis of Pore Structure on Frost Durability of Inorganic Building Materials", *Journal of Ceramic Society Japan*, Vol. 99, No. 11, pp. 1114-1119.
- Noland, J.L., Kingsley, G.R., and Atkinson, R.H.** (1990), "Nondestructive Evaluation of Masonry: An Update", *Masonry: Components to Assemblages*, ASTM STP 1063, John H. Matthys, Ed., American Society for Testing and Materials, Philadelphia, pp. 248-262.
- Phillips, J.G.** (1947), *The Physical Properties of Canadian Building Brick*, Department of Mines and Resources Canada, Ottawa, Canada. p. 99.
- Ramachandran, V.S., Feldman, R.F., and Beaudoin, J.J.** (1981), *Concrete Science*, Pub. by Heydon & Son Ltd., London, p. 427.

- Ravaglioli, A., Balli, M.F., and Negri, G.** (1976), "Sulphur Impregnation of Fired Ceramic Bodies: An Investigation into its Effects on Pore Size Distribution and Frost Resistance", *Proceedings of the Symp.: New Uses of Sulphur and Pyrites*, 17-19 May, Madrid, pp. 132-142.
- Robinson, G.C.** (1984), "The Relationship Between Pore Structure and Durability of Brick", *Ceramic Bulletin*, Vol. 63, No. 2, pp. 295-300.
- Robinson, G.C., Holman, J.R., and Edwards, J.F.** (1977), "Relation Between Physical Properties and Durability of Commercially Marketed Brick", *Ceramic Bulletin*, Vol.56, No.12, pp.1071-75
- Sayers, C.M.** (1981), "Ultrasonic Velocity Dispersion in Porous Materials", *Journal of Physics: D*, Vol. 14, No. 3, pp. 413-420.
- Shah, S.P., Naaman, A.E., and Smith, R.H.** (1978), "Investigation of Concrete Impregnated with Sulphur at Atmospheric Pressure", *Polymers in Concrete*, SP-58, ACI, Detroit, pp. 399-416.
- Smalley, A.R., Aitcin, P.C., and Langlois, J.L.** (1987), "The Correlation between Mercury Porosimetry and the Durability of Burned Clay Brick", *Proceedings of the Fourth North American Masonry Conference*, Vol. II, Aug. 16-17, 1987, pp. 65-1 to 65-13.
- Stochem** (1994), Technical data provided by Stochem Inc., Lachine, Quebec, Canada.
- Stupart, A.W.** (1989), "A Survey of Literature Relating to Frost Damage in Bricks", *Masonry International*, Vol. 5 (2), pp. 42-50.
- Van Der Klugt, L.J.A.R.** (1988), "Frost Testing by Unidirectional Freezing", *British Ceramic Transactions and Journal*, Vol. 87, No. 1, pp. 8-12.
- WACKER-Chemie**, "Silicone Microemulsions: As Aqueous Impregnating Agents for Mineral Building Materials and Surface Coating", *Product Information Brochure*, WACKER-Chemie GmbH, Munich, Germany.
- West, H.W.H., Ford, R.W., and Peake, F.** (1984), "A Panel Freezing Test for Brickwork", *British Ceramic Transactions and Journal*, Vol. 83, pp. 112-115.
- Winslow, D.N.** (1978), "The Validity of High Pressure Mercury Intrusion Porosimetry", *Journal of Colloid and Interface Science*, Vol. 67, No. 1, pp. 42-47.
- Winslow, D.N., and Diamond, S.** (1970), "A Mercury Porosimetry Study of the Evolution of Porosimetry in Portland Cement", *Journal of Materials*, JMLSA, Vol. 5, No. 3, pp. 564-585.
- Winslow, D.N., Kilgour, C.L., and Crooks, R.W.** (1988), "Predicting the Durability of Bricks", *ASTM Journal of Testing & Evaluation*, Vol. 16, No. 6, pp. 527-531.

Appendix **A**

*Pore Size Distribution
Tables & Curves*

TABLE A.1
Pore Size Distribution of Bricks expressed in terms of Cumulative Intrusion in ml/g

Brick Type	Pore Size Distribution : cumulative intrusion in ml/g										
	100 μm	10 μm	5 μm	3 μm	1 μm	0.5 μm	0.3 μm	0.1 μm	0.05 μm	0.03 μm	0.01 μm
A3	0.0009	0.0419	0.0503	0.0557	0.0711	0.0768	0.0787	0.0813	0.0823	0.0827	0.0828
A4	0.0008	0.0419	0.0505	0.0569	0.0803	0.0912	0.0939	0.0970	0.0981	0.0985	0.0986
A5	0.0003	0.0368	0.0461	0.0515	0.0801	0.1055	0.1112	0.1161	0.1177	0.1183	0.1185
B2	0.0006	0.0218	0.0426	0.0567	0.0675	0.0695	0.0706	0.0729	0.0736	0.0739	0.0739
B3	0.0005	0.0129	0.0364	0.0589	0.0758	0.0783	0.0795	0.0814	0.0820	0.0822	0.0822
B4	0.0004	0.0159	0.0406	0.0657	0.0909	0.0956	0.0973	0.0992	0.0997	0.0999	0.0999
B5	0.0004	0.0167	0.0354	0.0685	0.1056	0.1115	0.1139	0.1164	0.1169	0.1171	0.1171
B6	0.0007	0.0180	0.0349	0.0609	0.1087	0.1167	0.1197	0.1228	0.1235	0.1237	0.1237
C3	0.0002	0.0135	0.0299	0.0444	0.0744	0.0783	0.0797	0.0818	0.0826	0.0828	0.0829
C4	0.0001	0.0151	0.0375	0.0600	0.1033	0.1091	0.1109	0.1132	0.1139	0.1140	0.1140
C5	0.0002	0.0133	0.0333	0.0585	0.1105	0.1182	0.1204	0.1231	0.1238	0.1240	0.1241
D2	0.0001	0.0128	0.0194	0.0214	0.0265	0.0341	0.0425	0.0493	0.0506	0.0511	0.0514
D3	0.0000	0.0098	0.0177	0.0193	0.0250	0.0363	0.0476	0.0554	0.0568	0.0573	0.0576
E1	0.0000	0.0007	0.0010	0.0011	0.0052	0.0148	0.0184	0.0241	0.0271	0.0284	0.0287
E2	0.0000	0.0008	0.0011	0.0012	0.0138	0.0302	0.0342	0.0382	0.0399	0.0405	0.0408
F2	0.0001	0.0066	0.0135	0.0180	0.0283	0.0391	0.0465	0.0560	0.0621	0.0660	0.0718
F3	0.0001	0.0064	0.0117	0.0155	0.0315	0.0463	0.0558	0.0679	0.0743	0.0780	0.0824
G2	0.0002	0.0065	0.0126	0.0153	0.0253	0.0514	0.0630	0.0729	0.0770	0.0805	0.0844
H3	0.0005	0.0194	0.0454	0.0628	0.0797	0.0826	0.0838	0.0857	0.0862	0.0863	0.0864
H4	0.0001	0.0120	0.0450	0.0656	0.0867	0.0903	0.0918	0.0939	0.0944	0.0945	0.0946
H5	0.0008	0.0119	0.0293	0.0551	0.0975	0.1041	0.1069	0.1099	0.1106	0.1107	0.1108
H6	0.0003	0.0126	0.0326	0.0688	0.1143	0.1224	0.1255	0.1291	0.1300	0.1302	0.1303
J5	0.0000	0.0005	0.0008	0.0010	0.0061	0.1106	0.1327	0.1416	0.1427	0.1430	0.1430

TABLE A.2
Pore Size Distribution of Bricks expressed as Cumulative Intrusion in % of Total Pore Volume

Brick Type	Pore Size Distribution : cumulative intrusion in % of total pore volume										
	100 μm	10 μm	5 μm	3 μm	1 μm	0.5 μm	0.3 μm	0.1 μm	0.05 μm	0.03 μm	0.01 μm
A3	1.10	50.67	60.80	67.32	85.85	92.73	94.96	98.18	99.39	99.83	100
A4	0.79	42.53	51.35	57.81	81.60	92.54	95.24	98.41	99.49	99.87	100
A5	0.29	31.05	38.89	43.46	67.64	89.03	93.87	97.95	99.31	99.83	100
B2	0.85	29.72	57.81	76.71	91.24	93.89	95.39	98.52	99.53	99.91	100
B3	0.64	15.95	44.56	71.53	92.06	95.14	96.58	98.92	99.72	99.95	100
B4	0.45	15.78	40.69	65.54	90.98	95.67	97.34	99.29	99.84	100	100
B5	0.34	14.30	30.39	58.43	90.16	95.19	97.26	99.33	99.83	99.98	100
B6	0.57	14.50	28.29	49.23	87.88	94.30	96.74	99.24	99.79	99.95	100
C3	0.25	16.56	36.04	53.09	89.66	94.38	96.06	98.67	99.67	99.92	100
C4	0.12	13.43	33.25	52.81	90.60	95.64	97.22	99.22	99.84	100	100
C5	0.18	10.60	26.86	47.17	89.05	95.22	97.01	99.22	99.80	99.95	100
D2	0.12	24.93	37.83	41.67	51.41	66.14	82.40	95.79	98.38	99.37	100
D3	0.04	17.01	30.84	33.60	43.34	62.99	82.54	95.94	98.42	99.36	99.93
E1	0	2.48	3.53	3.90	16.97	46.92	59.65	81.27	93.33	98.61	99.91
E2	0	2.04	2.74	3.09	33.70	73.93	83.85	93.60	97.78	99.26	100
F2	0.14	8.91	18.32	24.50	38.53	53.26	63.28	76.28	84.61	89.94	97.85
F3	0.10	7.74	14.06	18.53	37.66	55.45	66.78	81.19	88.91	93.33	98.61
G2	0.20	7.75	14.96	18.13	29.91	60.57	74.18	85.71	90.53	94.56	99.18
H3	0.50	22.59	52.91	72.69	92.22	95.64	97.05	99.19	99.77	99.89	100
H4	0.07	12.88	47.75	69.28	91.62	95.35	97.01	99.16	99.72	99.79	99.90
H5	0.69	10.70	26.56	49.61	87.82	93.77	96.30	98.99	99.62	99.78	99.87
H6	0.25	9.59	24.96	52.72	87.74	93.91	96.35	99.12	99.77	99.95	100
J5	0.02	0.35	0.54	0.73	4.29	77.35	92.84	99.04	99.81	100	100

TABLE A.3
Pore Size Distribution of Bricks expressed as Cumulative Intrusion in % of Sample Volume

Brick Type	Pore Size Distribution : cumulative intrusion in % of sample volume										
	100 μm	10 μm	5 μm	3 μm	1 μm	0.5 μm	0.3 μm	0.1 μm	0.05 μm	0.03 μm	0.01 μm
A3	0.19	8.93	10.71	11.86	15.14	16.36	16.75	17.31	17.53	17.60	17.63
A4	0.17	8.70	10.50	11.82	16.70	18.95	19.51	20.16	20.38	20.46	20.48
A5	0.07	7.40	9.27	10.36	16.11	21.22	22.38	23.35	23.68	23.80	23.84
B2	0.14	4.75	9.26	12.34	14.68	15.11	15.35	15.85	16.01	16.07	16.08
B3	0.11	2.77	7.82	12.63	16.24	16.78	17.04	17.44	17.58	17.62	17.63
B4	0.09	3.27	8.33	13.48	18.64	19.61	19.94	20.34	20.45	20.48	20.48
B5	0.08	3.31	7.05	13.63	21.01	22.19	22.67	23.15	23.27	23.30	23.31
B6	0.14	3.51	6.82	11.90	21.24	22.79	23.38	23.98	24.11	24.15	24.16
C3	0.04	2.89	6.39	9.49	15.89	16.72	17.02	17.47	17.65	17.69	17.70
C4	0.03	3.06	7.63	12.20	20.98	22.15	22.52	22.98	23.12	23.16	23.16
C5	0.04	2.66	6.69	11.74	22.15	23.68	24.13	24.68	24.82	24.86	24.87
D2	0.01	2.97	4.50	4.97	6.13	7.90	9.84	11.42	11.72	11.84	11.91
D3	0	2.23	4.05	4.42	5.70	8.30	10.88	12.65	12.97	13.09	13.17
E1	0	0.17	0.24	0.27	1.25	3.59	4.47	5.86	6.61	6.91	7.00
E2	0	0.20	0.26	0.30	3.30	7.23	8.20	9.15	9.56	9.70	9.77
F2	0.02	1.39	2.85	3.82	6.00	8.28	9.84	11.86	13.15	13.98	15.21
F3	0.02	1.35	2.46	3.24	6.60	9.72	11.71	14.24	15.60	16.37	17.30
G2	0.04	1.40	2.70	3.28	5.41	10.97	13.44	15.53	16.40	17.14	17.98
H3	0.09	4.05	9.50	13.15	16.68	17.30	17.55	17.93	18.04	18.06	18.08
H4	0.01	2.48	9.29	13.54	17.89	18.62	18.94	19.36	19.47	19.49	19.51
H5	0.15	2.38	5.88	11.04	19.53	20.85	21.42	22.01	22.15	22.18	22.20
H6	0.07	2.47	6.38	13.47	22.39	23.97	24.59	25.29	25.46	25.50	25.52
J5	0.01	0.10	0.15	0.20	1.20	21.60	25.92	27.65	27.86	27.91	27.91

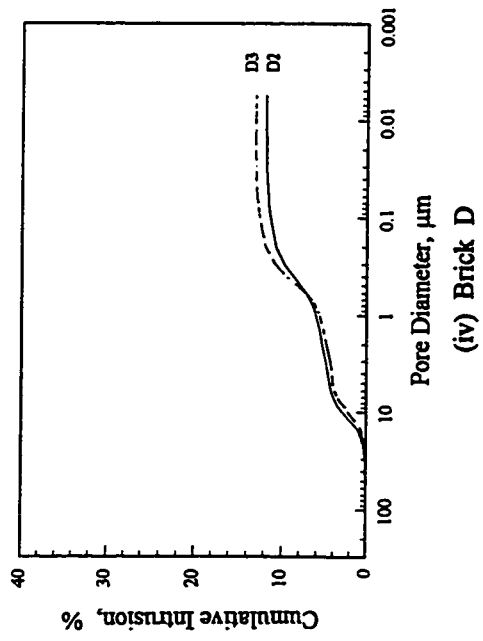
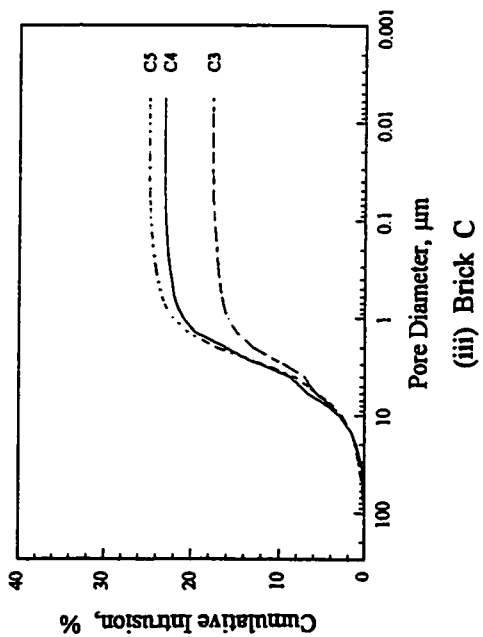
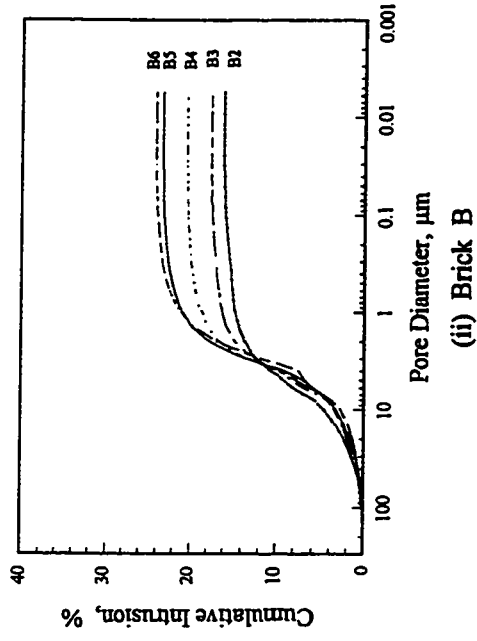
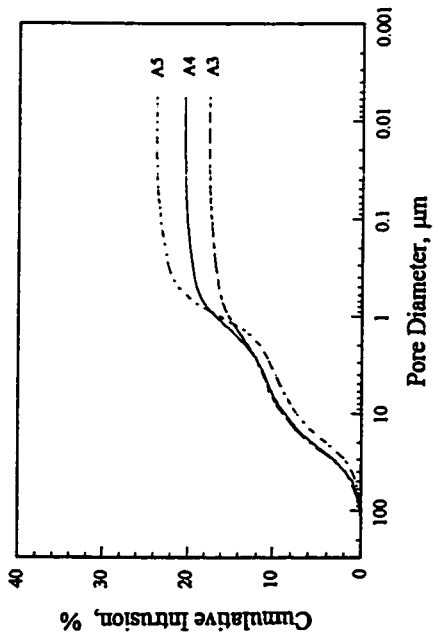


Figure A.1A Pore Size Distribution Curves for bricks A, B, C, and D expressed as cumulative intrusion in % of Sample Volume (% of SV)

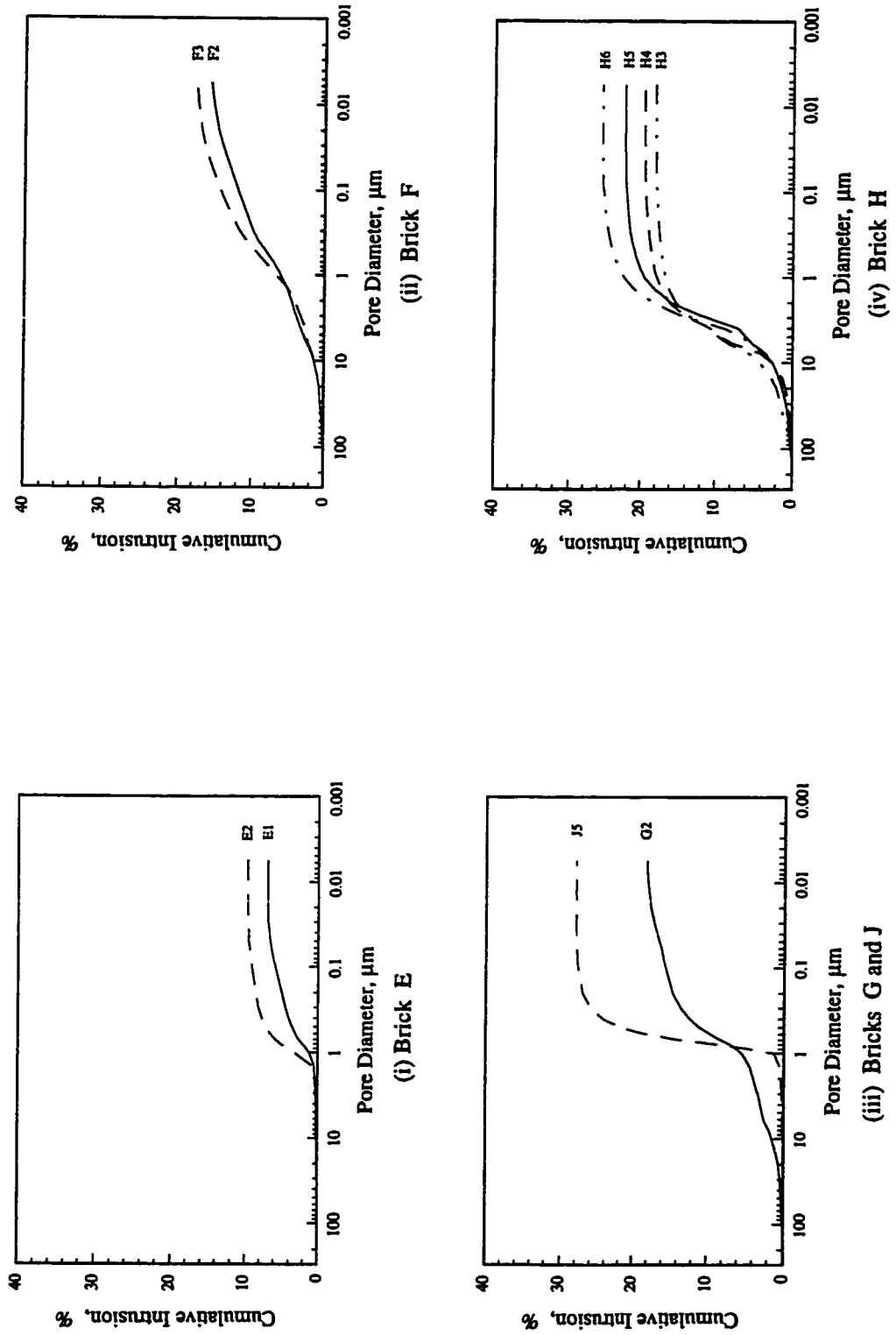


Figure A.1B Pore Size Distribution Curves for bricks E,F,G,H, and J expressed as cumulative intrusion in % of Sample Volume (% of SV)

Appendix **B**

Water Absorption Tables

TABLE B.1
Submersion Absorption of Bricks expressed as % of Dry Weight (Cx)

Brick Type	Submersion Absorption : % of Dry weight (Cx), %												
	1 Minute	2	4	5	8	10	15	30	1 Hour	2	4	8	24
A3	2.74	3.44	4.03	4.22	4.43	4.47	4.47	4.44	4.50	4.63	4.81	5.01	5.32
A4	3.82	4.68	5.39	5.59	5.76	5.78	5.76	5.82	5.99	6.17	6.37	6.58	6.89
A5	5.04	6.19	7.13	7.42	7.66	7.69	7.72	7.88	8.04	8.26	8.49	8.66	9.01
B2	1.20	1.49	1.73	1.84	2.03	2.14	2.31	2.64	2.92	3.10	3.21	3.29	3.53
B3	1.91	2.44	2.93	3.12	3.46	3.63	3.87	4.16	4.22	4.29	4.41	4.55	4.84
B4	3.46	4.42	5.32	5.60	5.87	5.91	5.94	6.01	6.06	6.20	6.37	6.59	6.95
B5	4.99	6.34	7.39	7.56	7.62	7.66	7.69	7.80	7.89	8.04	8.23	8.47	8.92
B6	5.96	7.60	8.65	8.74	8.78	8.81	8.83	8.93	9.07	9.28	9.51	9.79	10.25
C3	1.59	2.05	2.56	2.78	3.20	3.43	3.77	4.22	4.47	4.60	4.74	4.89	5.15
C4	2.25	3.10	4.05	4.42	5.12	5.44	5.85	6.02	6.12	6.29	6.44	6.62	6.90
C5	3.66	4.87	6.00	6.39	6.98	7.19	7.33	7.42	7.55	7.70	7.91	8.13	8.48
D2	1.13	1.44	1.72	1.84	2.07	2.22	2.48	2.92	3.21	3.33	3.48	3.59	3.73
D3	1.38	1.77	2.17	2.35	2.72	2.93	3.29	3.80	3.99	4.15	4.28	4.36	4.48
E1	0.15	0.17	0.19	0.20	0.22	0.23	0.25	0.26	0.32	0.40	0.51	0.64	0.93
E2	0.27	0.33	0.40	0.44	0.50	0.53	0.60	0.70	0.92	1.22	1.61	1.98	2.37
F2	1.08	1.31	1.53	1.63	1.83	1.92	2.12	2.37	2.78	3.11	3.34	3.51	3.75
F3	1.64	2.06	2.49	2.70	3.09	3.32	3.69	4.00	4.31	4.51	4.73	4.89	5.15
G2	1.17	1.34	1.52	1.60	1.77	1.85	1.98	2.38	2.57	2.76	2.91	3.10	3.35
H3	2.93	3.68	4.37	4.59	4.87	4.95	4.99	4.98	5.04	5.17	5.35	5.52	5.90
H4	3.58	4.52	5.35	5.59	5.77	5.78	5.81	5.89	5.94	6.06	6.18	6.35	6.63
H5	5.16	6.46	7.35	7.47	7.53	7.56	7.59	7.64	7.76	7.92	8.14	8.38	8.75
H6	6.32	7.85	8.64	8.67	8.72	8.73	8.77	8.91	9.04	9.26	9.48	9.75	10.17
J5	3.10	4.48	6.06	6.68	7.66	8.04	8.48	8.96	9.19	9.31	9.40	9.53	9.75

TABLE B.2
Submersion Absorption of Bricks expressed as % of Boiling Water Absorption (Cx/B)

Brick Type	Submersion Absorption : % of boiling water absorption (Cx/B), %												
	1 Minute	2	4	5	8	10	15	30	1 Hour	2	4	8	24
A3	27.20	34.14	39.90	41.81	43.88	44.26	44.23	43.94	44.51	45.24	47.55	49.54	52.59
A4	32.80	40.13	46.21	47.91	49.36	49.50	49.29	49.84	51.26	52.85	54.56	56.38	58.96
A5	37.25	45.69	52.60	54.77	56.57	56.77	56.98	58.19	59.36	60.93	62.66	63.94	66.50
B2	14.21	17.57	20.43	21.74	23.92	25.27	27.26	31.11	34.54	36.75	38.12	39.02	41.89
B3	19.31	24.66	29.52	31.43	34.85	36.62	39.08	42.08	42.74	43.42	44.59	46.07	48.93
B4	28.19	36.05	43.34	45.68	47.89	48.24	48.53	49.07	49.51	50.60	52.03	53.78	56.74
B5	35.06	44.50	51.91	53.13	53.55	53.80	54.00	54.78	55.46	56.48	57.80	59.53	62.65
B6	39.41	50.27	57.21	57.79	58.09	58.26	58.41	59.05	60.00	61.37	62.95	64.77	67.84
C3	16.30	21.02	26.16	28.39	32.72	35.06	38.60	43.37	46.02	47.32	48.76	50.37	53.06
C4	19.06	26.24	34.35	37.47	43.42	46.17	49.66	51.18	52.03	53.44	54.73	56.28	58.68
C5	27.55	36.60	45.11	48.05	52.41	54.00	55.01	55.67	56.64	57.80	59.38	61.00	63.64
D2	22.34	28.32	33.80	36.28	40.75	43.79	48.77	57.48	63.22	65.65	68.54	70.75	73.43
D3	24.04	30.70	37.81	40.76	47.21	50.81	57.12	65.94	69.32	72.04	74.21	75.67	77.75
E1	9.67	10.72	12.08	12.63	13.94	14.58	15.38	15.69	19.59	23.35	29.65	36.54	52.83
E2	8.68	10.62	12.87	13.91	15.95	17.02	19.10	22.17	29.07	38.61	51.17	63.07	75.62
F2	19.37	23.32	27.39	29.10	32.56	34.26	37.84	42.17	49.66	55.68	59.71	62.74	67.06
F3	23.75	29.95	36.20	39.19	44.88	48.11	53.54	58.04	62.70	65.56	68.83	71.14	74.99
G2	14.23	16.30	18.49	19.46	21.53	22.51	24.09	28.95	31.27	33.58	35.40	37.71	40.75
H3	26.40	33.15	39.37	41.35	43.87	44.59	44.95	44.86	45.41	46.58	48.20	49.73	53.15
H4	29.83	37.67	44.58	46.58	48.08	48.17	48.42	49.08	49.50	50.50	51.50	52.92	55.25
H5	37.04	46.37	52.76	53.63	54.06	54.27	54.49	54.85	55.71	56.86	58.44	60.16	62.81
H6	42.05	52.23	57.49	57.68	58.02	58.08	58.35	59.28	60.15	61.61	63.07	64.87	67.66
J5	25.73	37.18	50.29	55.44	63.57	66.72	70.37	74.36	76.27	77.26	78.01	79.09	80.91

TABLE B.3
Capillary Absorption of Bricks expressed as % of Dry Weight (Sx)

Brick Type	Capillary Absorption : % of Dry weight (Sx), %												
	1 Minute	2	4	5	8	10	15	30	1 Hour	2	4	8	24
A3	0.89	1.23	1.65	1.84	2.25	2.49	2.95	4.04	4.52	4.58	4.75	4.98	5.29
A4	1.18	1.61	2.18	2.44	3.00	3.34	4.01	5.47	6.10	6.15	6.34	6.59	6.88
A5	1.49	2.05	2.79	3.14	3.92	4.37	5.38	7.17	8.28	8.34	8.48	8.67	8.98
B2	0.48	0.61	0.76	0.82	0.96	1.02	1.18	1.40	1.81	2.36	2.92	3.22	3.51
B3	0.60	0.79	1.03	1.14	1.39	1.53	1.82	2.45	3.40	4.22	4.48	4.60	4.85
B4	1.12	1.58	2.15	2.43	3.07	3.46	4.21	5.72	6.31	6.41	6.53	6.69	6.98
B5	1.73	2.46	3.47	3.91	4.89	5.49	6.67	8.09	8.22	8.34	8.49	8.65	8.99
B6	2.05	3.01	4.16	4.71	5.92	6.63	8.10	9.27	9.36	9.51	9.71	9.91	10.30
C3	0.34	0.45	0.60	0.67	0.85	0.95	1.17	1.66	2.43	3.56	4.70	4.98	5.19
C4	0.58	0.84	1.21	1.40	1.82	2.09	2.66	3.84	5.65	6.51	6.64	6.76	6.97
C5	0.99	1.44	2.04	2.30	2.92	3.30	4.11	5.87	7.77	8.06	8.16	8.28	8.49
D2	0.31	0.40	0.51	0.55	0.65	0.73	0.86	1.22	1.64	2.43	3.41	3.55	3.68
D3	0.41	0.52	0.67	0.74	0.89	0.98	1.18	1.76	2.54	3.94	4.29	4.35	4.44
E1	0.03	0.04	0.04	0.04	0.05	0.05	0.05	0.07	0.08	0.11	0.13	0.18	0.31
E2	0.06	0.07	0.09	0.10	0.11	0.12	0.14	0.19	0.26	0.36	0.55	0.83	1.66
F2	0.16	0.21	0.25	0.27	0.31	0.34	0.38	0.49	0.66	0.94	1.47	2.18	3.68
F3	0.25	0.32	0.41	0.42	0.54	0.59	0.70	1.01	1.53	2.30	3.75	4.72	5.21
G2	0.35	0.41	0.48	0.51	0.57	0.61	0.68	1.00	1.28	1.67	2.17	2.59	3.02
H3	1.12	1.49	1.95	2.16	2.61	2.89	3.41	4.34	5.28	5.35	5.43	5.63	5.98
H4	1.20	1.66	2.24	2.51	3.12	3.50	4.22	5.92	6.21	6.26	6.34	6.45	6.70
H5	1.82	2.56	3.50	3.97	4.97	5.55	6.72	7.97	8.09	8.16	8.29	8.47	8.80
H6	2.11	3.09	4.37	4.88	6.18	6.94	8.36	9.21	9.31	9.42	9.61	9.83	10.20
J5	0.80	1.21	1.78	2.05	2.65	3.10	3.82	5.67	8.37	10.53	10.62	10.68	10.82

TABLE B.4
Capillary Absorption of Bricks expressed as Absorption per Unit Area (Sx/A)

Brick Type	Capillary Absorption : Absorption per unit area (Sx/A), g/cm ²												
	1 Minute	2	4	5	8	10	15	30	1 Hour	2	4	8	24
A3	0.11	0.15	0.20	0.22	0.27	0.30	0.36	0.49	0.55	0.55	0.57	0.60	0.64
A4	0.14	0.19	0.26	0.29	0.35	0.39	0.47	0.65	0.72	0.72	0.75	0.78	0.81
A5	0.17	0.24	0.32	0.37	0.46	0.51	0.63	0.83	0.96	0.97	0.99	1.01	1.04
B2	0.06	0.07	0.09	0.10	0.12	0.12	0.14	0.17	0.22	0.28	0.35	0.39	0.42
B3	0.07	0.09	0.12	0.14	0.17	0.18	0.22	0.29	0.41	0.50	0.54	0.55	0.58
B4	0.13	0.18	0.25	0.28	0.35	0.40	0.48	0.66	0.72	0.74	0.75	0.77	0.80
B5	0.20	0.28	0.39	0.44	0.55	0.62	0.75	0.91	0.93	0.94	0.96	0.98	1.02
B6	0.23	0.34	0.47	0.54	0.67	0.75	0.92	1.05	1.06	1.08	1.10	1.13	1.17
C3	0.05	0.06	0.09	0.10	0.12	0.14	0.17	0.24	0.35	0.51	0.68	0.72	0.75
C4	0.08	0.12	0.17	0.19	0.25	0.29	0.37	0.53	0.78	0.90	0.92	0.94	0.97
C5	0.14	0.20	0.28	0.32	0.41	0.46	0.57	0.81	1.08	1.12	1.13	1.15	1.18
D2	0.04	0.05	0.07	0.07	0.08	0.09	0.11	0.16	0.21	0.31	0.44	0.46	0.47
D3	0.05	0.07	0.08	0.09	0.11	0.12	0.15	0.22	0.32	0.50	0.54	0.55	0.56
E1	0	0.01	0.01	0.01	0.01	0.01	0.01	0.01	0.01	0.01	0.02	0.02	0.04
E2	0.01	0.01	0.01	0.01	0.02	0.02	0.02	0.03	0.04	0.05	0.08	0.11	0.23
F2	0.03	0.04	0.05	0.05	0.06	0.06	0.07	0.09	0.13	0.18	0.28	0.42	0.70
F3	0.05	0.06	0.08	0.09	0.10	0.11	0.13	0.19	0.29	0.43	0.71	0.89	0.98
G2	0.04	0.05	0.06	0.06	0.07	0.07	0.08	0.12	0.15	0.20	0.25	0.30	0.35
H3	0.12	0.16	0.22	0.24	0.29	0.32	0.38	0.48	0.58	0.59	0.60	0.62	0.66
H4	0.13	0.18	0.25	0.28	0.35	0.39	0.47	0.66	0.69	0.69	0.70	0.71	0.74
H5	0.19	0.27	0.37	0.41	0.52	0.58	0.70	0.83	0.85	0.85	0.87	0.89	0.92
H6	0.22	0.32	0.45	0.51	0.64	0.72	0.87	0.95	0.97	0.98	1.00	1.02	1.06
J5	0.09	0.14	0.20	0.23	0.30	0.35	0.43	0.64	0.95	1.20	1.20	1.21	1.23

TABLE B.5
Capillary Absorption of Bricks expressed as % of Boiling Water Absorption (Sx/B)

Brick Type	Capillary Absorption : % of boiling water absorption (Sx/B), %												
	1 Minute	2	4	5	8	10	15	30	1 Hour	2	4	8	24
A3	8.75	12.05	16.20	18.10	22.10	24.47	29.08	39.83	44.73	45.22	46.90	49.25	52.30
A4	10.08	13.80	18.72	20.88	25.76	28.62	34.40	46.85	52.20	52.60	54.25	56.40	58.88
A5	11.03	15.10	20.61	23.20	28.90	32.22	39.69	52.88	61.10	61.55	62.63	64.01	66.28
B2	5.70	7.18	8.91	9.63	11.25	12.03	13.86	16.53	21.27	27.71	34.41	38.14	41.66
B3	6.08	7.93	10.39	11.53	13.95	15.35	18.26	24.60	34.13	42.54	45.33	46.57	49.02
B4	9.15	12.84	17.53	19.73	24.97	28.17	34.31	46.61	51.56	52.39	53.31	54.68	57.04
B5	12.14	17.31	24.34	27.48	34.32	38.50	46.83	56.81	57.76	58.61	59.66	60.77	63.14
B6	13.60	19.93	27.55	31.17	39.15	43.89	53.60	61.30	61.92	62.90	64.23	65.55	68.16
C3	3.47	4.57	6.14	6.83	8.60	9.62	11.87	16.91	24.69	36.30	48.28	51.26	53.48
C4	4.93	7.10	10.28	11.85	15.45	17.71	22.53	32.56	47.93	55.36	56.46	57.46	59.23
C5	7.42	10.86	15.33	17.31	21.94	24.77	30.85	44.05	58.35	60.48	61.22	62.15	63.77
D2	6.08	7.91	10.01	10.81	12.81	14.35	16.95	23.93	32.20	47.71	67.13	69.97	72.59
D3	7.12	9.10	11.60	12.77	15.46	17.08	20.50	30.61	44.11	68.39	74.47	75.43	77.02
E1	1.96	2.32	2.52	2.68	2.91	3.15	3.38	4.18	5.17	6.35	7.88	10.29	17.27
E2	1.78	2.29	2.82	3.08	3.61	3.88	4.52	5.86	8.12	11.36	17.38	26.05	52.41
F2	2.91	3.68	4.46	4.84	5.53	5.99	6.82	8.61	11.77	16.59	26.10	38.70	65.80
F3	3.59	4.67	5.95	6.54	7.80	8.61	10.19	14.58	22.14	33.21	54.21	68.60	75.80
G2	4.26	4.99	5.84	6.20	6.93	7.42	8.27	12.17	15.57	20.32	26.40	31.51	36.74
H3	10.09	13.42	17.57	19.46	23.51	26.04	30.72	39.10	47.57	48.20	48.92	50.72	53.87
H4	10.00	13.83	18.67	20.92	26.00	29.17	35.17	49.33	51.75	52.17	52.83	53.75	55.83
H5	13.07	18.38	25.13	28.50	35.68	39.84	48.24	57.21	58.08	58.58	59.51	60.80	63.17
H6	14.04	20.56	29.08	32.47	41.12	46.17	55.62	61.28	61.94	62.67	63.94	65.40	67.86
J5	6.64	10.04	14.77	17.01	21.99	25.73	31.70	47.05	69.46	87.39	88.13	88.63	89.79

Appendix **C**

***Tables of Properties
for Durability Indices***

TABLE C.1
Physical Properties used for calculating *DIR*

$$DIR = \left[\frac{IRA}{10(1-C/B)} \right] - \left[\frac{145 CS - 6000}{1000} \right] + [C - 10]$$

Brick Type	C %	C/B	IRA g/min./ 193.55cm ²	CS MPa	DIR
A3	5.32	0.53	20.98	43.02	-0.45
A4	6.89	0.59	26.90	35.12	4.36
A5	9.01	0.66	33.61	29.60	10.60
B2	3.53	0.42	11.29	74.84	-9.38
B3	4.84	0.49	13.92	65.61	-5.94
B4	6.95	0.57	24.92	46.75	1.97
B5	8.92	0.63	37.78	32.88	10.36
B6	10.25	0.68	45.22	24.18	16.88
C3	5.15	0.53	9.46	74.53	-7.64
C4	6.90	0.59	15.54	54.46	-1.21
C5	8.48	0.64	26.49	39.26	6.15
D2	3.73	0.73	7.69	105.18	-12.67
D3	4.48	0.78	10.06	102.57	-9.82
E1	0.93	0.53	0.81	143.54	-23.71
E2	2.37	0.76	1.48	133.94	-20.43
F2	3.75	0.67	6.06	114.10	-14.96
F3	5.15	0.75	9.03	109.94	-11.18
G2	3.35	0.41	7.91	83.18	-11.37
H3	5.90	0.53	24.02	45.01	0.48
H4	6.63	0.55	25.70	41.08	2.34
H5	8.75	0.63	36.92	32.58	10.00
H6	10.17	0.68	42.29	24.31	15.86
J5	9.75	0.81	17.48	66.48	5.31

TABLE C.2
Physical Properties used for calculating *DIM*

$$DIM = \frac{3.2}{PV} + 2.4 P3$$

Brick Type	<i>PV</i> ml/g	<i>P3</i> %	<i>DIM</i>
A3	0.0828	67.32	200.22
A4	0.0986	57.81	171.20
A5	0.1185	43.46	131.31
B2	0.0739	76.71	227.41
B3	0.0822	71.53	210.60
B4	0.0999	65.54	189.33
B5	0.1171	58.43	167.56
B6	0.1237	49.23	144.02
C3	0.0829	53.09	166.02
C4	0.1140	52.81	154.81
C5	0.1241	47.17	138.99
D2	0.0514	41.67	162.26
D3	0.0577	33.60	136.10
E1	0.0297	3.90	117.10
E2	0.0408	3.09	85.85
F2	0.0734	24.50	102.40
F3	0.0836	18.53	82.75
G2	0.0851	18.13	81.11
H3	0.0864	72.69	211.49
H4	0.0947	69.28	200.06
H5	0.1110	49.61	147.89
H6	0.1303	52.72	151.09
J5	0.1430	0.73	24.13

TABLE C.3
Physical Properties used for calculating *DIN*

$$DIN = -0.12 - 0.09(A_p) + 0.15(B_p) + 0.08(C_p) - 0.01(D_p) - 0.01(E_p) - 0.01(F_p) - 0.01(G_p)$$

Brick Type	Specific Pore Volume in the specified pore range (in $10^{-3}\text{cm}^3/\text{g}$)							<i>DIN</i>
	A_p	B_p	C_p	D_p	E_p	F_p	G_p	
A3	0	1.50	1.60	6.10	7.30	5.40	26.30	-0.218
A4	0	1.50	1.80	10.00	13.90	8.10	28.70	-0.358
A5	0	2.40	2.60	22.40	25.30	8.40	28.80	-0.401
B2	0	1.10	1.40	3.20	2.40	2.90	48.50	-0.413
B3	0	0.90	1.10	3.50	3.20	4.50	60.90	-0.618
B4	0	0.70	1.00	4.90	5.10	7.10	70.70	-0.813
B5	0	0.80	1.20	7.10	8.00	10.40	78.30	-0.942
B6	0	0.90	1.60	9.10	11.20	14.00	74.40	-0.944
C3	0	1.10	1.30	4.40	6.10	9.00	53.60	-0.582
C4	0	0.90	1.30	5.90	9.20	17.30	71.20	-0.917
C5	0	1.00	1.40	7.80	11.90	16.20	77.60	-0.993
D2	0.01	2.00	2.90	18.30	3.40	1.60	18.70	-0.009
D3	0.01	2.20	3.20	25.10	4.20	1.70	18.50	-0.030
E1	0	4.60	3.80	11.60	6.50	0.80	0.90	0.676
E2	0	2.60	2.30	14.60	17.50	2.00	1.10	0.102
F2	3.10	12.70	6.00	18.80	6.70	3.40	17.10	1.526
F3	2.20	12.30	7.10	24.40	11.90	5.00	15.20	1.530
G2	1.80	9.80	4.60	36.00	11.70	2.70	13.90	0.913
H3	0	0.70	1.00	3.80	3.60	4.60	60.30	-0.658
H4	0	0.70	1.10	4.50	4.70	5.70	72.10	-0.797
H5	0.10	0.90	1.50	8.10	9.50	12.00	70.90	-0.879
H6	0	1.10	1.80	9.60	11.00	13.30	85.00	-1.000
J5	0	1.40	3.30	95.80	40.10	0.80	1.20	-1.025

TABLE C.4
Physical Properties used for calculating *DIA*

$$DIA = 9.187A_v - 0.487B_v + 423.8C_v - 2.408D_v - 84.5$$

Brick Type	A_v %	B_v g/30min./ 193.55cm ²	C_v	D_v %	<i>DIA</i>
A3	12.04	94.73	1.00	47.55	289.28
A4	12.00	124.88	1.01	54.56	261.58
A5	10.53	161.37	1.01	62.66	210.80
B2	12.64	32.75	0.96	38.12	330.73
B3	13.12	56.64	0.98	44.59	316.40
B4	14.18	126.82	0.99	52.03	278.28
B5	14.52	176.82	0.99	57.80	243.16
B6	12.93	204.03	1.00	62.95	207.14
C3	10.13	46.08	0.97	48.76	279.80
C4	13.05	102.86	0.98	54.73	268.83
C5	12.66	157.68	0.99	59.38	231.59
D2	5.02	30.27	1.00	68.54	205.63
D3	4.49	43.31	1.00	74.21	180.76
E1	0.28	1.82	0.64	29.65	117.02
E2	0.31	4.92	0.73	51.17	102.11
F2	3.94	17.95	0.92	59.71	189.07
F3	3.38	36.77	0.95	68.83	165.51
G2	3.38	22.62	1.06	35.40	299.52
H3	13.58	92.97	0.99	48.20	298.48
H4	14.08	126.96	0.98	51.50	274.34
H5	11.99	161.34	0.99	58.44	225.92
H6	14.51	184.81	1.00	63.07	230.73
J5	0.22	124.42	0.84	78.01	25.07

Appendix **D**

*Pore Size Distribution
Tables for
Impregnated Bricks*

TABLE D.1
Pore Size Distribution of Impregnated Bricks expressed as Cumulative Intrusion in ml/g

Brick Type	Type of Impregnation	Pore Size Distribution : cumulative intrusion in ml/g										
		100 μm	10 μm	5 μm	3 μm	1 μm	0.5 μm	0.3 μm	0.1 μm	0.05 μm	0.03 μm	0.01 μm
A4	Control	0.0008	0.0419	0.0505	0.0569	0.0803	0.0912	0.0939	0.0970	0.0981	0.0985	0.0986
	T1A	0.0007	0.0133	0.0157	0.0205	0.0379	0.0485	0.0528	0.0568	0.0578	0.0583	0.0589
	T1B	0.0001	0.0176	0.0264	0.0298	0.0397	0.0470	0.0501	0.0534	0.0543	0.0546	0.0551
	T2A	0.0012	0.0222	0.0257	0.0274	0.0334	0.0366	0.0378	0.0407	0.0431	0.0449	0.0466
	T2B	0.0004	0.0142	0.0153	0.0157	0.0188	0.0237	0.0275	0.0322	0.0336	0.0346	0.0361
	T3	0.0007	0.0409	0.0489	0.0541	0.0738	0.0820	0.0840	0.0867	0.0881	0.0890	0.0905
B4	Control	0.0004	0.0159	0.0406	0.0657	0.0909	0.0956	0.0973	0.0992	0.0997	0.0999	0.0999
	T1A	0.0004	0.0102	0.0153	0.0170	0.0517	0.0608	0.0645	0.0684	0.0704	0.0715	0.0722
	T1B	0	0.0052	0.0091	0.0190	0.0472	0.0515	0.0532	0.0554	0.0559	0.0561	0.0566
	T2A	0.0002	0.0081	0.0123	0.0154	0.0330	0.0382	0.0406	0.0457	0.0502	0.0521	0.0534
	T2B	0.0005	0.0131	0.0191	0.0198	0.0215	0.0227	0.0242	0.0351	0.0447	0.0475	0.0492
	T3	0.0011	0.0170	0.0398	0.0605	0.0760	0.0781	0.0791	0.0811	0.0828	0.0836	0.0847
C4	Control	0.0001	0.0151	0.0375	0.0600	0.1033	0.1091	0.1109	0.1132	0.1139	0.1140	0.1140
	T1A	0.0003	0.0089	0.0191	0.0206	0.0232	0.0269	0.0293	0.0465	0.0490	0.0499	0.0511
	T1B	0	0.0008	0.0012	0.0018	0.0071	0.0097	0.0115	0.0158	0.0187	0.0208	0.0228
	T2A	0.0002	0.0087	0.0170	0.0208	0.0343	0.0408	0.0430	0.0472	0.0509	0.0530	0.0545
	T2B	0.0001	0.0143	0.0235	0.0245	0.0262	0.0273	0.0285	0.0359	0.0461	0.0511	0.0532
	T3	0.0005	0.0244	0.0416	0.0572	0.0894	0.0938	0.0953	0.0975	0.0984	0.0988	0.0995

TABLE D.1 (continued)
Pore Size Distribution of Impregnated Bricks expressed as Cumulative Intrusion in ml/g

Brick Type	Type of Impregnation	Pore Size Distribution : cumulative intrusion in ml/g										
		100 μm	10 μm	5 μm	3 μm	1 μm	0.5 μm	0.3 μm	0.1 μm	0.05 μm	0.03 μm	0.01 μm
F3	Control	0.0001	0.0064	0.0117	0.0155	0.0315	0.0463	0.0558	0.0679	0.0743	0.0780	0.0824
	T1A	0.0001	0.0027	0.0067	0.0088	0.0104	0.0110	0.0114	0.0154	0.0187	0.0209	0.0226
	T1B	0	0.0003	0.0005	0.0008	0.0019	0.0028	0.0034	0.0062	0.0083	0.0094	0.0118
	T2A	0	0.0019	0.0032	0.0037	0.0052	0.0059	0.0068	0.0099	0.0131	0.0177	0.0244
	T2B	0.0001	0.0038	0.0081	0.0106	0.0162	0.0207	0.0237	0.0284	0.0314	0.0334	0.0380
	T3	0.0001	0.0060	0.0117	0.0154	0.0300	0.0458	0.0557	0.0679	0.0728	0.0754	0.0785
A5	Control	0.0003	0.0368	0.0461	0.0515	0.0801	0.1055	0.1112	0.1161	0.1177	0.1183	0.1185
	T1A	0.0002	0.0088	0.0123	0.0160	0.0417	0.0614	0.0699	0.0752	0.0766	0.0770	0.0776
	T2B	0.0004	0.0099	0.0111	0.0117	0.0148	0.0186	0.0208	0.0245	0.0261	0.0275	0.0298
B5	Control	0.0004	0.0167	0.0354	0.0685	0.1056	0.1115	0.1139	0.1164	0.1169	0.1171	0.1171
	T1A	0.0003	0.0090	0.0124	0.0141	0.0604	0.0760	0.0821	0.0871	0.0881	0.0883	0.0888
	T2B	0.0004	0.0136	0.0226	0.0240	0.0266	0.0282	0.0301	0.0420	0.0495	0.0509	0.0529
C5	Control	0.0002	0.0133	0.0333	0.0585	0.1105	0.1182	0.1204	0.1231	0.1238	0.1240	0.1241
	T1A	0.0001	0.0085	0.0147	0.0166	0.0624	0.0810	0.0858	0.0901	0.0911	0.0915	0.0918
	T2B	0.0004	0.0145	0.0249	0.0260	0.0285	0.0299	0.0313	0.0383	0.0466	0.0509	0.0535

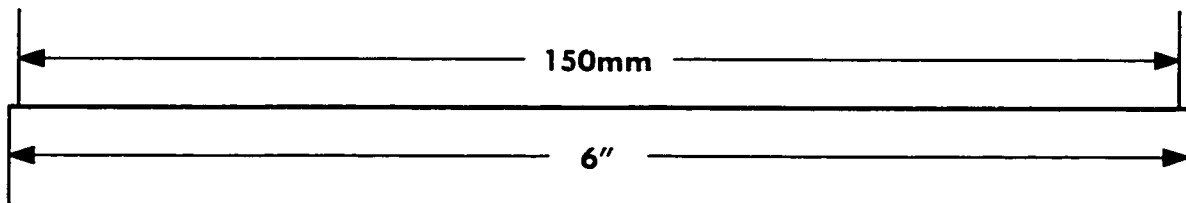
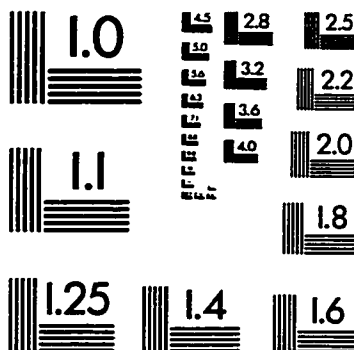
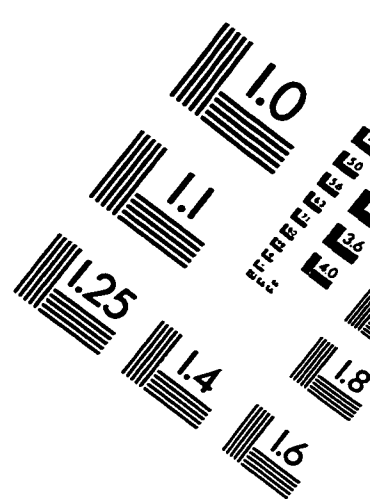
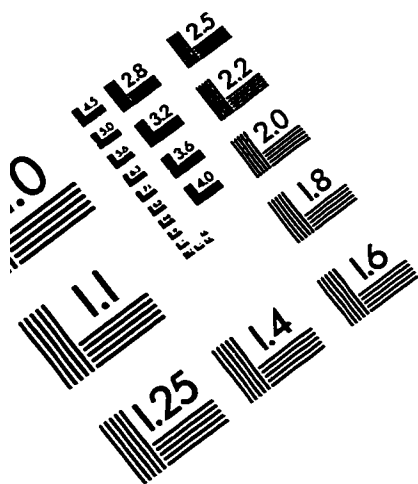
TABLE D.2
Pore Size Distribution of Impregnated Bricks expressed as Cumulative Intrusion in % of Total Pore Volume

Brick Type	Type of Impregnation	Pore Size Distribution : cumulative intrusion in % of total pore volume										
		100 μm	10 μm	5 μm	3 μm	1 μm	0.5 μm	0.3 μm	0.1 μm	0.05 μm	0.03 μm	0.01 μm
A4	Control	0.79	42.53	51.35	57.81	81.60	92.54	95.24	98.41	99.49	99.87	100
	T1A	1.12	22.54	26.43	34.39	63.77	81.40	88.73	95.40	97.12	97.93	99.13
	T1B	0.20	31.96	47.78	54.04	71.71	84.60	90.17	96.06	97.65	98.13	99.15
	T2A	2.57	47.03	54.76	58.31	71.41	78.22	80.78	86.71	91.52	95.34	98.93
	T2B	1.30	38.45	41.41	42.59	51.05	64.15	74.63	87.05	91.06	93.62	97.78
	T3	0.80	45.20	54.11	59.81	81.25	89.83	91.91	94.82	96.34	97.28	98.99
B4	Control	0.45	15.78	40.65	65.54	90.98	95.67	97.34	99.29	99.84	100	100
	T1A	0.49	14.02	21.18	23.50	71.20	83.78	88.88	94.22	96.87	98.51	99.47
	T1B	0	8.97	15.43	31.92	82.10	89.78	92.92	96.73	97.76	98.12	98.99
	T2A	0.49	15.12	22.94	28.60	59.98	69.71	74.22	84.02	92.70	96.26	98.62
	T2B	0.99	26.56	38.42	39.94	43.19	45.55	48.67	70.58	89.90	95.37	98.73
	T3	1.42	19.82	47.06	71.30	89.66	92.15	93.28	95.55	97.55	98.47	99.69
C4	Control	0.12	13.43	33.25	52.81	90.60	95.64	97.22	99.22	99.84	100	100
	T1A	0.52	17.74	37.46	40.24	45.28	52.31	56.94	90.45	95.04	96.80	99.01
	T1B	0.20	3.22	4.99	7.18	27.42	38.37	45.96	64.50	77.39	86.40	95.02
	T2A	0.30	15.84	30.90	37.88	62.20	73.92	77.97	85.58	92.15	96.11	98.86
	T2B	0.20	27.12	43.88	45.70	48.75	50.89	53.13	66.75	85.53	94.82	98.77
	T3	0.52	25.67	43.28	58.50	89.62	93.91	95.40	97.57	98.51	98.96	99.71

TABLE D.2 (continued)
Pore Size Distribution of Impregnated Bricks expressed as Cumulative Intrusion in % of Total Pore Volume

Brick Type	Type of Impregnation	Pore Size Distribution : cumulative intrusion in % of total pore volume										
		100 μm	10 μm	5 μm	3 μm	1 μm	0.5 μm	0.3 μm	0.1 μm	0.05 μm	0.03 μm	0.01 μm
F3	Control	0.10	7.74	14.06	18.53	37.66	55.45	66.78	81.19	88.91	93.33	98.61
	T1A	0.13	10.75	27.09	35.46	42.08	44.31	46.15	62.19	75.12	83.93	91.14
	T1B	0	2.38	3.87	5.78	13.69	20.16	25.31	45.64	60.45	68.97	86.46
	T2A	0	6.58	11.43	13.11	18.37	21.11	24.22	34.94	46.31	62.60	86.40
	T2B	0.10	8.46	19.81	26.88	39.69	48.67	54.75	65.77	73.36	78.99	91.27
A5	T3	0.11	7.62	14.90	19.43	37.63	57.43	69.87	85.15	91.29	94.53	98.74
	Control	0.29	31.05	38.89	43.46	67.64	89.03	93.87	97.95	99.31	99.83	100
	T1A	0.23	11.45	15.77	20.74	53.67	78.80	89.58	96.45	98.17	98.77	99.47
B5	T2B	1.40	31.49	35.51	37.70	47.49	58.87	65.32	76.83	82.16	86.87	94.50
	Control	0.34	14.30	30.39	58.43	90.16	95.19	97.26	99.33	99.83	99.98	100
	T1A	0.40	9.79	13.60	15.29	64.86	83.83	91.44	97.42	98.53	98.89	99.44
C5	T2B	0.60	24.97	40.88	43.56	48.22	51.22	54.68	77.17	91.53	94.24	98.08
	Control	0.18	10.60	26.86	47.17	89.05	95.22	97.01	99.22	99.80	99.95	100
	T1A	0.05	9.20	15.94	17.99	67.47	87.77	93.05	97.71	98.77	99.21	99.61
	T2B	0.76	26.87	45.25	47.26	51.76	54.35	57.00	69.95	85.35	93.17	98.03

IMAGE EVALUATION TEST TARGET (QA-3)



APPLIED IMAGE, Inc
1653 East Main Street
Rochester, NY 14609 USA
Phone: 716/482-0300
Fax: 716/288-5989

© 1993, Applied Image, Inc., All Rights Reserved

